

Development of Selective δ -Opioid Receptor Positive Allosteric Modulators for the Treatment of Depression

by

Shiyuan Zhang

A dissertation submitted in partial fulfillment
of the requirements for the degree of
Doctor of Philosophy
(Medicinal Chemistry)
in the University of Michigan
2023

Doctoral Committee:

Professor John R. Traynor, Co-Chair
Research Professor Andrew White, Co-Chair
Research Assistant Professor Martin Clasby
Professor Peter J. H. Scott

Shiyuan Zhang

sherrice@umich.edu

ORCID iD: 0009-0008-1482-6942

© Shiyuan Zhang 2023

For Grandpa Phil and Grandma Marie

Acknowledgements

I'm grateful for the opportunity to receive my doctoral education from the Department of Medicinal Chemistry at the University of Michigan. Being immersed in an environment filled with experts from diverse scientific backgrounds has truly been a blessing. The faculty members, along with the unwavering support of our dedicated staff, have provided me and my colleagues with a rigorous academic journey, guiding and mentoring us to become proficient researchers. Working alongside this extraordinary group of individuals has been an exceptionally precious experience.

I am immensely grateful to the people who provided invaluable support throughout my academic journey. Above all, I would like to express my gratitude to my co-advisors, Drs. Andrew White and John Traynor, whose guidance has been instrumental in shaping my research. Dr. White has been my mentor since the beginning of my degree, introducing me to the field of drug discovery, specifically in the area of structure-based drug design. His willingness to allow me the freedom to explore various potential solutions during the trial-and-error phase of my research has been invaluable. Furthermore, he has been very gracious during the challenges I faced as a student. As his mentee, I have gained immeasurable experience from his expertise and have grown significantly as a researcher overall. Additionally, this dissertation would also have been impossible without the support of my co-advisor Dr. Traynor. Driven by his passion for opioid receptors, he possesses remarkable insights into our project. He taught me to comprehend the biology and pharmacology behind my chemistry, enhancing my understanding of our project. Furthermore, his dedication to work is exemplary, evident through his prompt email replies and manuscript comments even during his vacation time. His patience and commitment continue to inspire me to work diligently. I am truly grateful for the time, effort, and kindness he invested in training my biological, pharmacological, and writing skills. Furthermore, I want to express my gratitude to Drs. Martin Clasby and Peter Scott, my committee members, for reviewing my dissertation and providing valuable suggestions.

Throughout the years, I have received invaluable assistance from numerous individuals without whom my work would not have been completed. I am immensely grateful to the current

and former senior staff members of the Vahlteich Medicinal Chemistry Core (VMCC): Drs. Kim Hutchings, Mathivanan Packiarajan, Xinmin Gan, Patrick O'Brien, Pil Lee, Mike Wilson, Susan Hagen and Kun Liu. Their guidance and support have not only helped me develop my synthetic and modeling skills but also fostered a warm and encouraging environment during the challenges I encountered. I also extend my thanks to former VMCC director Dr. Scott Larsen for his patient guidance during my early days in the field. I am truly fortunate to have been accepted into this exceptional group of scientists, who have played a significant role in shaping my growth as a researcher.

I am also thankful for the constant encouragement and support of my senior colleagues and colleagues, including Rachel Rowlands, Jake Hitchens and Adam Ard for their constant presence and assistance. They have provided not only laughter and companionship in the lab but also invaluable help with proofreading and sharing their knowledge. Their support has contributed to my growth as a researcher.

I would like to express my gratitude to Kelsey Kochan and Joshua Lawrence West from the Traynor lab. Kelsey devoted a significant amount of time to working on my project, diligently screening compounds and demonstrating the radioactive assay to me. Josh not only screened the compounds, but also took the time to teach me, a chemist, how to conduct the bioassay. I appreciate his assistance in preparing cells for the assays despite my initial mistakes. Their contributions have been invaluable to the progress of my research.

I extend my gratitude to Dr. Andrew Alt, my collaborator from the Center for Chemical Genomics (CCG) lab, as well as to Steve Vander Roest, a member of the research staff. Dr. Alt's contributions and enthusiasm made this project possible, and I am truly thankful for his involvement. Steve played a vital role in teaching me how to conduct high-throughput screening bioassays. Screening hundreds of compounds repeatedly is not fun, and I am grateful for his dedication in carrying out the screening work for my project. His patience in addressing all my questions has been greatly appreciated.

In addition, I would like to express my gratitude to Dr. Larisa Yeomans, the director of the NMR core, whose assistance was vital to the productivity of my research. She provided valuable training and has been incredibly kind and helpful whenever I encountered instrument-related challenges.

Moreover, I am grateful for my undergraduate advisor, Dr. Michael R. Barbachyn. Dr. Barbachyn patiently guided me from my early days as a “baby” in chemistry, teaching me step by step how to conduct reactions. He also provided extensive assistance with my writing. I am profoundly thankful for his mentorship, inspiration, and encouragement to pursue a Ph.D. Without his patience, kindness, and generosity, I would not have grown into the person I am today.

Lastly, and most importantly, I want to express my deepest gratitude to my family. My parents, Chengqiang and Yali Zhang, have provided me with irreplaceable support throughout the years. I owe my accomplishments to their unwavering self-sacrificial love. I am also immensely grateful for the joy and inspiration brought into my life by our beloved daughter, Aravis, and son, Calvin. Aravis's patience during times when my availability is limited has been truly appreciated. Her love for me has served as a source of motivation, encouraging me to persevere through the difficulties I have encountered. Lastly, I would like to thank my husband, Daiwei Zhang. Being student parents has not been easy, yet he willingly took on many household responsibilities and cared for our children, even while managing his own busy workload. I am grateful for his unwavering support and dedication.

Table of Contents

Acknowledgements.....	iii
List of Tables	x
List of Figures.....	xi
List of Schemes.....	xiv
List of Abbreviations	xv
Abstract.....	xvii
Chapter 1 Introduction	1
1.1 The Impact of Major Depression and the Limitations of Current Treatments	1
1.2 Opiates were found to be efficacious antidepressant drugs but are not safe.	2
1.3 Opioid Receptor System and its Activation.....	3
1.4 Concept of Biased Agonism at Opioid Receptors	6
1.4.1 Biased Agonism at MOR.....	6
1.4.2 Biased Agonism at DOR.....	8
1.5 Concept of Allosteric Modulation at Opioid Receptors	9
1.5.1 Phenotypes and Mechanisms of Action of Allosteric Modulators	9
1.5.2 Advantages of PAMs as a Potential Therapeutic Approach.....	11
1.5.3 Allosteric Modulation of Opioid Receptors with PAMs	12
1.5.4 Biased Allosteric Modulation of Opioid Receptors with PAMs	12
1.6 Known Opioid Receptor Allosteric Modulators	13
1.6.1 Known DOR Allosteric Modulators	13
1.6.2 Allosteric Profile of BMS 986187 (1)	14

1.7 Crystal Structures of DOR and current knowledge of the Allosteric Binding Site	18
1.8 Aims	20
1.9 References	22
Chapter 2 Structure-Activity Relationships (SAR) and Improvement of DOR-MOR Selectivity in the Xanthene Series	35
2.1 Summary	35
2.2 Introduction.....	35
2.3 Results and Discussion	38
2.3.1 Exploration of the A-Ring (Benzyl Group)	38
2.3.2 Exploration of B ring and A-B ring attachments	44
2.3.3 DOR selectivity is optimized by a conformation lock in the phenol ring	45
2.3.4 Combined modifications of A- and B-rings.....	50
2.3.5 Confirmation assay, cAMP accumulation assay for selected analogs	50
2.3.6 Synthetic routes to xanthene-dione analogs.....	52
2.4 Conclusion	52
2.5 Methods, Synthesis and Experimental	54
2.5.1 Cell lines	54
2.5.2 β -arrestin2 Recruitment Assay.....	54
2.5.3 Forskolin Stimulated cAMP Inhibition.....	54
2.5.4 Computational Modeling Studies	55
2.5.5 Chemistry	55
2.6 References	96
Chapter 3 Improvement of Druggability of the Xanthene-Dione Series—Solubility	109
3.1 Summary	109
3.2 Introduction.....	110
3.3 Results and Discussion	111

3.3.1 Reduction of lipophilicity at the A-ring.....	111
3.3.2 Reduction of lipophilicity in the B-ring.....	116
3.3.3 Reduction of lipophilicity/molecular weight at the C-rings	118
3.3.4 Combined modifications of B- and C-rings to reduce lipophilicity	121
3.3.5 Attempts to improve solubility by addition of N-alkyl side chains.....	122
3.4 Synthesis of 1,8-dioxo-decahydroacridine derivatives.....	124
3.5 Conclusion	124
3.6 Experimentals	126
3.6.1 Cell culture and biological assays.....	126
3.6.2 Modeling.....	126
3.6.3 Solubility measurements.....	126
3.6.4 Synthesis	126
3.7 References.....	157
Chapter 4 Improvement in the Metabolic Stability of Xanthene-dione Series of DOR PAMs...	159
4.1 Summary.....	159
4.2 Introduction.....	159
4.2.1 The problem of metabolism.....	159
4.3 Results.....	161
4.3.1 Computational prediction of potential sites of metabolism for 1	161
4.3.2 Strategies to reduce metabolism	164
4.4 Synthesis of spiro[2.5]octane and 2-oxaspiro[3.5]nonane xanthene analogs.....	171
4.5 Conclusion	173
4.6 Experimental.....	174
4.6.1 Biological evaluation	174
4.6.2 Prediction of metabolic sites.....	174

4.6.3 Synthesis	174
4.7 References	181
Chapter 5 Future Directions to Optimize the Xanthene-dione Series of DOR-PAMs	185
5.1 Further optimization of the metabolic stability and solubility of the xanthene-diones ..	185
5.1.1 Incorporation of deuterium	185
5.1.2 Expansion and combination of xanthene-dione modifications at the A-ring to further improve metabolic stability and lipophilicity	186
5.1.3 Expansion and combination of xanthene-dione modifications in the B-ring to further improve metabolic stability and lipophilicity while maintaining potency as a DOR and selectivity over MOR.....	187
5.1.4 Combined modifications in B- and C-rings	188
5.1.5 Combined modifications of A-, B-, and C-rings.....	188
5.2 Conclusions.....	190
5.3 References.....	191

List of Tables

Table 1.1: Opioid receptors and effects	5
Table 2.1: SAR table for functionalization of the benzyl group with methyl- and halogen-substituents.....	39
Table 2.2: SAR table for ortho-substitution (R1) of the benzyl group	42
Table 2.3: SAR table for the linker and binding mode of Xanthene series	45
Table 2.4: SAR table for substitution of the B-ring.....	46
Table 2.5: Combined substitutions of A- and B-rings	49
Table 2.6: Confirmation Assay of Selected Analogs.....	50
Table 3.1: 6-membered heterocycle replacements for A-ring	113
Table 3.2: 5-membered heterocycle replacements for A-ring.....	115
Table 3.3: Bioisosteric replacements of phenyl B-ring.....	118
Table 3.4: Modifications at C-rings	120
Table 3.5: Combined modifications of B- and C-rings.....	122
Table 3.6: N-Alkyl substitutions at C-rings to improve aqueous solubility.....	123
Table 4.1 <i>in vitro</i> DMPK profiles of selected analogs ^a	164

List of Figures

Figure 1.1 Activation of opioid receptor and its downstream signaling pathways (Al-Hasani & Bruchas, 2011)	3
Figure 1.2 Examples and structures of common exogenous (A) and endogenous (B) opioid ligands.	4
Figure 1.3 Biased agonism of opioid receptors.....	6
Figure 1.4 Chemical structures of MOR G protein biased agonists: morphine, TRV130, and buprenorphine.	7
Figure 1.5 Chemical structures of selective DOR agonists: SNC80, ARM390, and PN6047.....	8
Figure 1.6 Allosteric modulation of opioid receptors. α is the allosteric effect of the modulators on affinity, and β is the modulators' effect on the efficacy of the agonist. Allosteric modulators may or may not show direct response (intrinsic efficacy).	10
Figure 1.7 PAMs can reinforce while maintain the spatial and temporal activities of the endogenous agonists. A. Effects of endogenous agonists (yellow), effects of PAMs (blue), and effects of synthetic agonists (red and the area under the line). B. Effects of endogenous agonists in brain (center), effects of PAMs in brain (right), and effects of synthetic agonists in brain (left).	11
Figure 1.8 Biased modulation of opioid receptor by PAM.....	13
Figure 1.9 Chemical structures of selected allosteric modulators of opioid receptors.	14
Figure 1.10 Effect of 1mg/kg BMS986187 (1) in the forced swim test in C57BL/6 mice. Left figure shows the action in DOR wild-type mice (+/+) mice compared to heterozygotes (+/-) and knockout (-/-) mice. Thank you to Dr. E Jutkiewicz (Pharmacology, UM for this unpublished figure.	16
Figure 1.11 Effect of BMS-986187 (1) in the tail withdrawal assay in mice (129 strain) and its inhibition by the opioid antagonist naloxone. This is unpublished work from Dr. Traynor, Pharmacology at UM	17
Figure 1.12 (A) DOR PAM, CCG257409 (green) and selective DOR agonist, DPI-287 (yellow) bound to hDOR (PDB: 6PT3). Transmembrane helices are colored from blue to red, Helix I is in dark blue and Helix VII is in dark red. (B) Lipophilicity surface of hDOR (grey) orthosteric and allosteric binding sites is drawn in green (hydrophobic regions) and purple	

(hydrophilic regions). Both DPI-287 (red) and CCG257409 (blue) are embedded in the corresponding binding sites. Important side chain interactions are labeled. 18

Figure 1.13 Overlay of hDOR (grey) (pdb: 6PT3) and hMOR (yellow) (pdb: 6DDF) crystal structures. Major side chain interactions in the allosteric pockets of both receptors are shown. . 19

Figure 2.1 Structure and profile of xanthene series, BMS986187 (1). Three different compartments of 1 for optimization are highlighted in colors: A-ring (pink), B-ring (blue), and C-ring (yellow)..... 38

Figure 2.2 Conformation restrictions are developed on the benzyl group (bond was highlighted in red) with the addition of methyl group (CCG257409) and two methyl groups (CCG363137) in comparison of CCG361257. DOR/MOR activities of each analog were labeled below. The energy-dihedral angle plot of each analog is shown. Energy conformations that are predicted by MOE in the gas phase are in white line, and real crystal structure distribution of conformations is shown in blue bars. Green bar shows where the current conformation of the selected bond is in the plot..... 41

Figure 2.3 Docking pose and structural rationalization of CCG362691 (purple) in hDOR (grey) (pdb: 6PT3) with structural conformation change relative to 1 (blue)..... 43

Figure 2.4 Hairpin-like binding mode of 1 (blue) in MOR (yellow) (PDB: 6DDF). 44

Figure 2.5 A. Structural rationale for low potency of CCG362904 (brown) at hMOR (yellow) (pdb: 6DDF). The 2-methyl group in ring B clashes (orange circles) with His319 (7.36) and conformational change at the benzyl group clashes with Gln124 (2.60). B. Structural rationale for low potency of CCG363081 (green) at hMOR. The 3-methyl group on the B-ring clashes with Trp318 (7.35). Additional conformational change at the benzyl group of CCG363081 clashes with Ile322 (7.39). 48

Figure 2.6 cAMP accumulation data curves of standards, DPDPE (DOR) (Left) and DAMGO (MOR) (Right), 1 (409), CCG362904, or CCG363081 in the presence of appropriate orthosteric agonist. 51

Figure 3.1 Chemical structure of CCG363081 110

Figure 3.2 *in vitro* pharmacological and DMPK profile of 1. Data obtained from Pharmaron. 110

Figure 3.3 Top view of DOR crystal structure (grey) (PDB: 6PT3). 1 (blue with A-ring pointed down to the center of the transmembrane region) was docked in the allosteric site, and orthosteric agonist, DPI-287 (yellow) is bound in orthosteric site. Lipophilicity surface of the binding pockets are shown in green (hydrophobic region) and purple (hydrophilic region). 111

Figure 3.4 Chemical structures of CCG364642 and CCG364641 112

Figure 3.5 Chemical structure of CCG362750..... 114

Figure 3.6 Flexalignment and overlay of CCG362904 (purple) and CCG366793 (pink)..... 117

Figure 4.1 Chemical structure of 1 , and its receptor activities together with the DMPK profile.....	161
Figure 4.2 Predicted potential metabolic soft-spots of 1 with CYP isoforms 3A4 and 2C9 by XenoSite.....	163
Figure 4.3 Chemical structures of compounds listed in Table 4.1	163
Figure 4.4 DOR and MOR activities and <i>LogD_{7.4}</i> values of modified xanthene analogs at A- and B-rings relative to 1	Error! Bookmark not defined.
Figure 4.5 DOR and MOR activities and cLogP values of modified xanthene analogs at C-rings relative to 1	166
Figure 4.6 DOR and MOR activities and cLogP values of CCG367105 relative to 1	167
Figure 4.7 Examples of chemical structures, DOR, and MOR activities of analogs designed to block metabolic sites at A-ring.	168
Figure 4.8 Examples of chemical structures, DOR, and MOR activities of analogs designed to block metabolic sites at B-ring.	169
Figure 4.9 Analogs with combined modifications for reduction of metabolism are listed together with their cLogP and the in vitro data in both DOR and MOR.....	170
Figure 5.1 Blocking site of metabolism of 1 (red) with deuteration.....	185
Figure 5.2 Examples of designed analogues with combined modifications at A-ring to block sites of metabolism and lower lipophilicity while maintain potency against DOR.....	186
Figure 5.3 Examples of designed analogues with combined moieties at the B-ring to address lipophilicity while maintaining potency against DOR and selectivity over MOR	187
Figure 5.4 Examples of combined modifications of both B- and C-rings Examples of combined modifications of both B- and C-rings.....	188
Figure 5.5 Examples of combined moieties on all the parts of the xanthene series.	189
Figure 5.6 Predicted sites of metabolism by CYP3A4 with Xenosite	189
Figure 5.7 Blockage of the site of metabolism with CF ₃ moiety (CCG367105) and new fluorination moiety.....	190

List of Schemes

Scheme 2.2 Synthetic Route and Conditions for 5b	77
Scheme 2.3 Synthetic Route and Conditions for 3b and 5c	79
Scheme 2.4 Synthesis of CCG367211	91
Scheme 2.5 Synthetic route of desired bromide.....	93
Scheme 2.6 Synthetic route of desired chloride.....	94
Scheme 3.1 Synthetic Routes for 1,8-dioxo-decahydroacridine derivatives.....	124
Scheme 3.2 Synthesis for CCG363177	139
Scheme 3.3 Synthetic route for CCG363621 (El-Sepelgy et al., 2014).....	140
Scheme 3.4 Synthetic route for CCG364645 (Mei et al., 2018).....	143
Scheme 3.5 Synthesis of CCG363622	145
Scheme 4.1 Synthesis of spiro[2.5]octane-5,7-dione 2i	172
Scheme 4.2 Synthesis of 2-oxaspiro[3.5]nonane-6,8-dione 2j	172
Scheme 4.3 Synthesis of CCG367105	179

List of Abbreviations

Major Depressive Disorder	MDD
G Protein-Coupled Receptors	GPCRs
δ -Opioid Receptor	DOR
μ -Opioid Receptor	MOR
κ -Opioid Receptor	KOR
Nociception Opioid Receptor	NPOR
Cyclic Adenosine Monophosphate	cAMP
Guanosine-5'-Triphosphate	GTP
Guanosine diphosphate	GDP
G Protein-Gated Inward Rectifying Potassium Channel	K _{ir3}
Mitogen-Activated Protein Kinases	MAPK
Positive Allosteric Modulator	PAM
Negative Allosteric Modulator	NAM
Silent Allosteric Modulator	SAM
Federal Drug Administration	FDA
β -arrestin 2	β arr2
Chinese Hamster Ovary Cell	CHO Cell
Δ^9 -Tetrahydrocannabinol	THC
Cannabidiol	CBD
Enteric Nervous System	ENS
Molecular Dynamic	MD
Molecular Operating Environment	MOE
Cryogenic Electron Microscopy	cryo-EM
Structure Activity Relationship	SAR
Maximum Response of the Drugs/Analog	E _{max}
Calculated Partition Coefficient	cLogP

Distribution Coefficient of n-Octanol/Water at pH 7.4	LogD _{7.4}
Protein Database	PDB
Drug Metabolism and Pharmacokinetics	DMPK
High Throughput Screening	HTS
Molecular Weight	MW

Abstract

Major depressive disorder is one of the three leading causes that reduce quality of life. Due to the comorbidity of major depressive disorder with anxiety and chronic pain, existing antidepressant drugs have limited effectiveness and often lead to adverse effects. There is an urgency for safer and more effective antidepressant therapeutics. The δ -opioid receptor (DOR), a member of the opioid receptor family, has been shown to be involved in mood regulation and chronic pain. In rats and mice, DOR agonists acting at the orthosteric site have antidepressant, anxiolytic, and analgesic effects, without the abuse liability of agonists acting at the μ -opioid receptor (MOR). Although the beneficial effects of DOR activation make it a plausible therapeutic target, activation of DOR leads to pro-convulsive activity; its agonists are also susceptible to profound tolerance.

There is considerable interest in the development of DOR positive allosteric modulators (PAMs). By binding to the distinct location on the receptor, allosteric modulators can alter orthosteric agonist efficacy or affinity, including endogenous opioid peptides, without altering their spatial and temporal release. Thus, the beneficial effects of the peptide ligands are promoted, and adverse effects can be reduced. Consequently, PAMs at DOR could be developed as drugs to treat depression.

A previous high-throughput screening effort identified a series of xanthene-diones as DOR positive allosteric modulators, exemplified by **BMS-986187** (**1**). However, **BMS-986187** is also active as a positive allosteric modulator at MOR with lower activity. The lack of selectivity of **BMS-986187** can be problematic by promoting the adverse effects of MOR agonists. Additionally, **BMS-986187** exhibits a poor pharmacokinetic profile that hinders its druggability.

The work outlined in this dissertation describes a structure-activity study of derivatives of **BMS-986187** to further understand the DOR allosteric binding site and improve the potency and selectivity of BMS-986187. Due to the size, flexibility, and greasiness of the allosteric site, we could not optimize the potency of xanthene-dione series at DOR. However, although DOR and MOR share similarities at their allosteric binding sites I observed differences and have successfully optimized the selectivity of xanthene-dione series for DOR over MOR. By introducing additional conformation restriction and potential steric clashes by synthesizing compounds **CCG363081** and **CCG362904**, the selectivity was improved by more than 1,000-fold while maintaining DOR potency ($EC_{50} = 0.09 \mu\text{M}$).

As the xanthene-dione series shows impressive *in vitro* pharmacological activities, I next attempted to optimize its drug-like characteristics. I first tried improving the solubility profile to reduce its lipophilicity. However, due to the lipophilic nature of the proposed binding site, most of the analogs with exposed electronic effects completely lost DOR activity. Therefore, I shielded the substrates' electronic effects through steric and conformational restriction. Although some loss in potency on DOR was observed, I was able to improve the solubility profile with analogs, **CCG369831** and **CCG363177**.

Additionally, I tried optimizing the metabolic stability of the xanthene-dione series to further improve its druggability. Metabolic soft spots of xanthene series were blocked. However, most of the attempts failed except for the incorporation of halogens. I demonstrated an improvement in metabolic stability profile with **CCG366046** without losing potency at DOR and selectivity over MOR. To date, I have successfully optimized both the selectivity and metabolic stability of the xanthene series with **CCG366046**.

Chapter 1 Introduction

1.1 The Impact of Major Depression and the Limitations of Current Treatments

Major depressive disorder (MDD) is characterized by persistent depressed mood and other symptoms that impair daily life. People who experience the symptoms for more than two weeks are considered to have an episode of MDD. Although MDD is classified as a non-fatal mental disease, it has become one of the most common mental disorders across the world and impacts patients' daily life (James et al., [2018](#)). With a high prevalence rate of 4.4% across the world in 2015 (*Depression and Other Common Mental Disorders*, n.d.), MDD has become one of the top three causes for loss of healthy life due to disability (James et al., 2018). It affects more than one third of the North American population (Khoo et al., 2022; Li, 2015; "Depressive Disorders," 2022). As the prevalence rate of MDD continues to grow, this increasing burden has become a prominent challenge to health care systems and the economy. Various treatments of MDD have been developed, including different generations of antidepressant drugs (first-generation antidepressants: tricyclic antidepressants; second-generation antidepressants: selective serotonin re-uptake inhibitors and selective serotonin noradrenaline re-uptake inhibitors; plus, nonspecific generations of antidepressants: adrenergic alpha-2 receptor antagonists and selective noradrenaline reuptake inhibitors), which are often used in combination with psychotherapy. Unfortunately, the efficacy of the medications is less than satisfactory (Cipriani et al., 2018; Moncrieff & Kirsch, 2005). Nearly half of MDD patients do not respond to their current treatments, and about one fourth of the patients experience a relapse within one to two years (Fava, 2003; *Major Depression*, n.d.; Kasper, 2022). Overall, about 50% of patients prescribed with antidepressant drugs dropout

of the treatment process due to side-effects which worsen the symptoms of MDD (Pradier et al., 2020). A major factor that makes MDD hard to treat and easy to relapse is the comorbidity of MDD with other diseases, including anxiety and chronic pain (such as low back pain and headache disorders) (James et al., 2018).

1.2 Opiates were found to be efficacious antidepressant drugs but are not safe.

Research findings have shown that the opioid receptor system participates a significant role in pain regulation, mood regulation, and brain reward systems. The synthetic opiate, buprenorphine was found to display anti-depressive activity. Patients who suffered from severe MDD and were prescribed low dose buprenorphine have shown reduced MDD symptoms (Serafini et al., 2018). Although synthetic opiates have been found as extremely efficacious at reducing the MDD symptoms and relieving pain, a wide arrange of serious on-target adverse effects are elicited, such as respiratory depression, drowsiness, and constipation (Abuse, 2021). More importantly, euphoria, tolerance and physical dependence that result from the usage of opiates lead to the growing need of higher dosage to maintain the same level of efficacy, which worsens the adverse effects and leads to both addiction and death (DeWire et al., 2013). Therefore, as a synthetic opiate, buprenorphine cannot be considered as a safe drug. However, the participation of opioid receptor family in relieving MDD symptoms and the strong efficacy the synthetic opiate exhibited in treating MDD have drawn our interest for further studies of the opioid receptors as a potential therapeutic target for MDD.

1.3 Opioid Receptor System and its Activation

The opioid receptor family belongs to the superfamily of class A seven transmembrane-spanning G protein-coupled receptors (GPCRs). The opioid receptors were first described in 1973, and later they were further characterized (Charbogne et al., 2014; Filliol et al., 2000). There are four members in the opioid receptor family: μ -opioid receptor (MOR), δ -opioid receptor (DOR), κ -opioid receptor (KOR), and nociceptin opioid receptor (NOPR) (Pathan & Williams, 2012). The first three opioid receptors show a high structural similarities (74%) and share 61% of amino acid

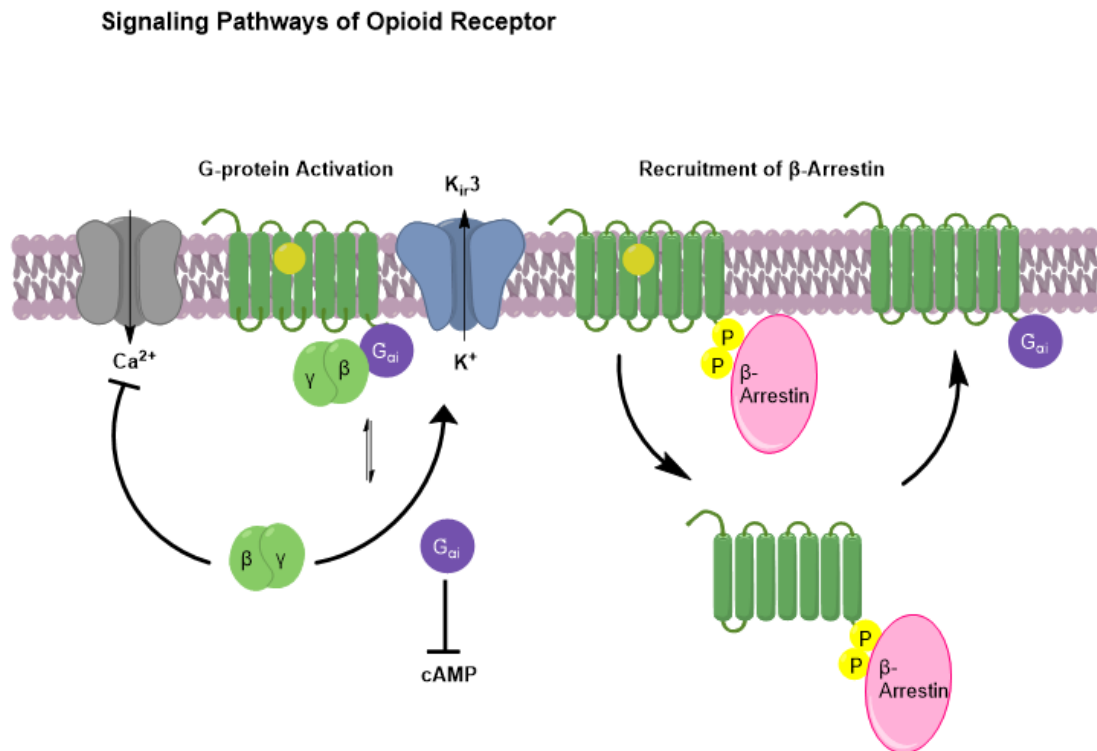


Figure 1.1 Activation of opioid receptor and its downstream signaling pathways (Al-Hasani & Bruchas, 2011)

identity (Stevens et al., 2007). Later, NOPR was found as a fourth member of the opioid receptor family. Unlike other three members of the opioid family, NOPR shows no affinity or little

activation by standard opioid ligands to which MOR, DOR, and KOR bind (**Figure 1.2**) (Toll et al., 2016).

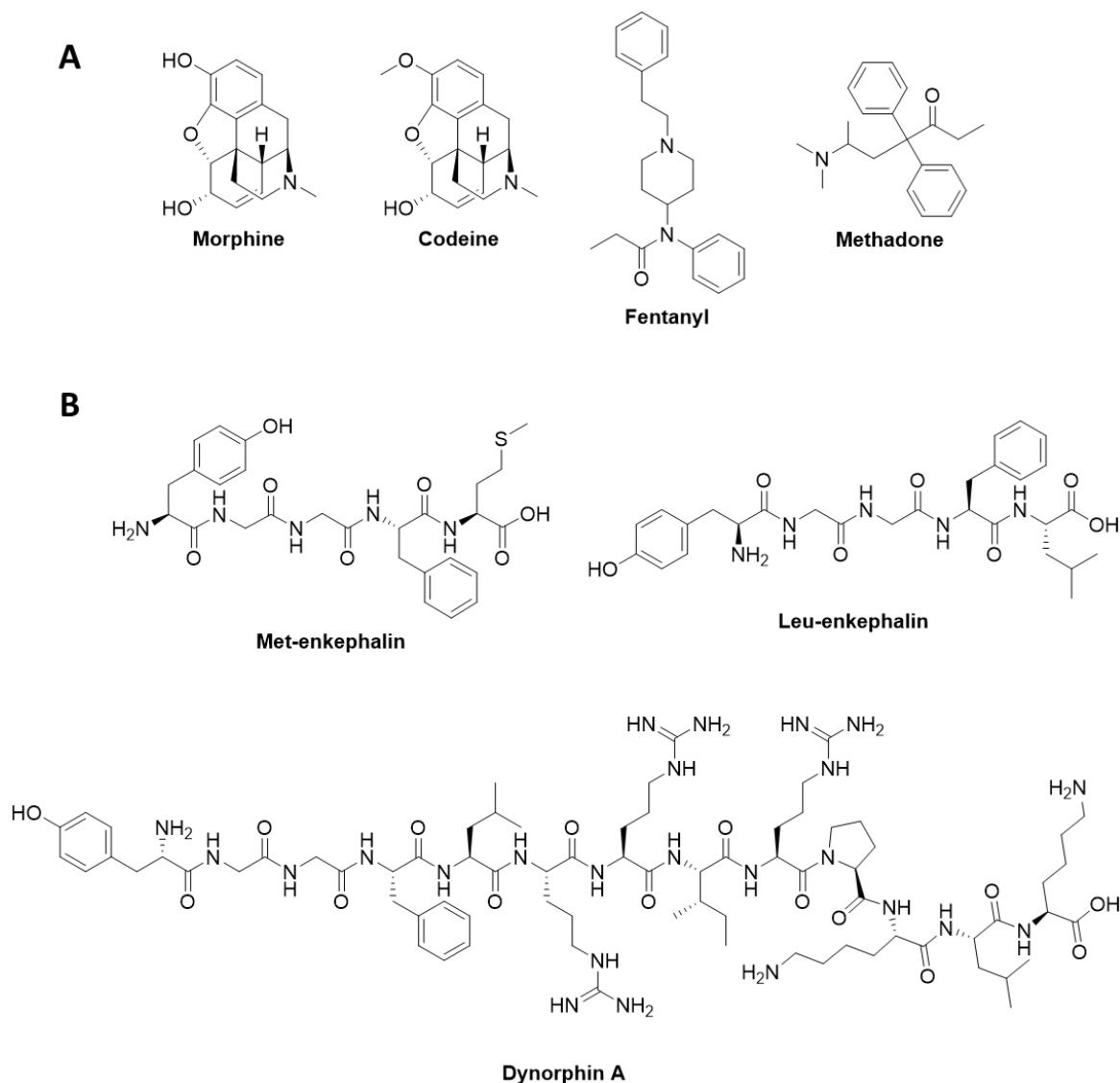


Figure 1.2 Examples and structures of common exogenous (A) and endogenous (B) opioid ligands.

The opioid receptors are predominantly expressed in the central nervous system, including the spinal cord, brain stem, thalamus, and cortex, but are also found in the enteric nervous system (Inturrisi, 2002; DiCello et al., 2022).

Table 1.1: Opioid receptors and effects

MOR (μ)	DOR (δ)	KOR (κ)
Analgesia	Analgesia	Analgesia
Euphoria	Antidepressant	Sedation
Tranquility	Anxiolysis	Dysphoria
Respiratory depression	Physical dependence	Depression
Physical dependence	Convulsion	Diuresis
Constipation		

Altogether, the opioid receptors participate in the regulation of pain, pain transmission, mood, reward and alteration of gastrointestinal motility (**Table 1.1**) (DiCello et al., 2022; Inturrisi, 2002; Stein, 2016).

Activation of the opioid receptors results in the inhibition of the neurons, and thus inhibition of pain transmission (Ahlbeck, 2011). The receptors can be activated by either endogenous opioid peptides, such as enkephalins, β -endorphin, and dynorphins; or synthetic opiates, such as fentanyl and methadone (**Figure 1.2**). Both endogenous and exogenous opioids act at the orthosteric site on the receptors. Occupation of an opioid receptor by an agonist leads to activation of associated heterotrimeric G proteins comprising a $G\alpha$ subunit, and a $G\beta\gamma$ subunit (**Figure 1.1**). There are several classes of G proteins; opioid receptors couple to the $G\alpha_i/o$ family. In the resting state the heterotrimeric $G\alpha_i/o$ protein is occupied by GDP. As an opioid receptor is activated, the GDP dissociates and is replaced by GTP; this leads to separation of the $G\alpha$ and $G\beta\gamma$ subunits. $G\alpha_i$ subunits inhibit the activity of adenylyl cyclase, and thus, inhibit cyclic adenosine monophosphate (cAMP) production (Nestler, 2004). In addition, G protein-gated inward rectifying potassium channel, K_{ir3} is bound to $G\beta\gamma$ subunits which facilitate a K^+ -dependent outward current. The $G\beta\gamma$ subunits also bind to and inhibit a Ca^{2+} -dependent inward current. These effects lead to inhibition of neural excitability and inhibition of neurotransmitter release (**Figure 1.1**) (Ippolito et

al., 2002; Nestler, 2004; Al-Hasani & Bruchas, 2011). Activated opioid receptors are also phosphorylated at the C-terminal tail by G protein-coupled receptor kinases 2 (GRK2) which leads to recruitment of β -arrestins (β -arrestin 1 and β -arrestin 2) to the receptor. These processes lead to desensitization of the receptor. The β -arrestin-bound receptor undergoes internalization (Cahill et al., 2017). During internalization, some of the receptor complexes can continue to signal. Internalized receptors may be recycled back to cell surface (e.g. MOR), while other receptors types (e.g. DOR) are degraded. (**Figure 1.1**) (Cahill et al., 2017; Trapaidze et al., 1996). β -arrestins recruited to the opioid receptors can also signal, for example to the mitogen-activated protein kinases (MAPK) which can lead to changes in gene transcription (Al-Hasani & Bruchas, 2011).

1.4 Concept of Biased Agonism at Opioid Receptors

1.4.1 Biased Agonism at MOR

As mentioned earlier, research findings have shown that different downstream signaling pathways of the activated opioid receptors are induced by conformational changes in the receptors and lead to various outcomes (Wootten et al., 2018). The ability of ligands to selectively activate a specific

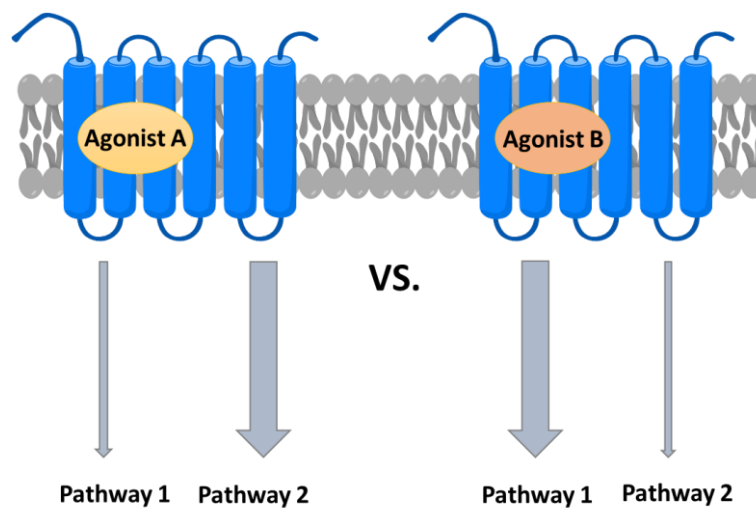


Figure 1.3 Biased agonism of opioid receptors.

downstream signaling pathway over others is known as biased agonism (**Figure 1.3**). Some biased ligands can distinguish between G protein, and β -arrestin. Older findings using mice lacking β -arrestin 2 (β arr2^{-/-} mice) suggest that recruitment and signaling downstream of β -arrestin 2 contributes to adverse effects, including constipation and respiratory depression (Bohn et al., 1999, 2000; DeWire et al., 2013; Manglik et al., 2016). However, more extensive research with different strains of mice suggest that recruitment of β -arrestins might not contribute to the development of the adverse effects (Kliwer et al., 2019). More research and deeper understanding of the development of adverse effects are needed for further therapeutic development.

Although the mechanisms of downstream signaling and their relationships to the development of the adverse effects remains controversial, therapeutic approaches continue to work on the concept of biased agonism of opioid receptors. Research studies show that some MOR agonists, such as, morphine, TRV130, and buprenorphine (**Figure 1.4**) are G protein biased agonists (Pedersen et al., 2020; DeWire et al., 2013; McPherson et al., 2010) in comparison to DAMGO, a full agonist of MOR for both G protein and β -arrestin activation. TRV130, which is structurally different from morphine, was found to be a selective and more potent MOR agonist (**Figure 1.4**), TRV130 exhibits a 6-fold increase in potency in comparison with morphine (DeWire et al., 2013). MOR activation by TRV130 shows greatly reduced receptor phosphorylation at the

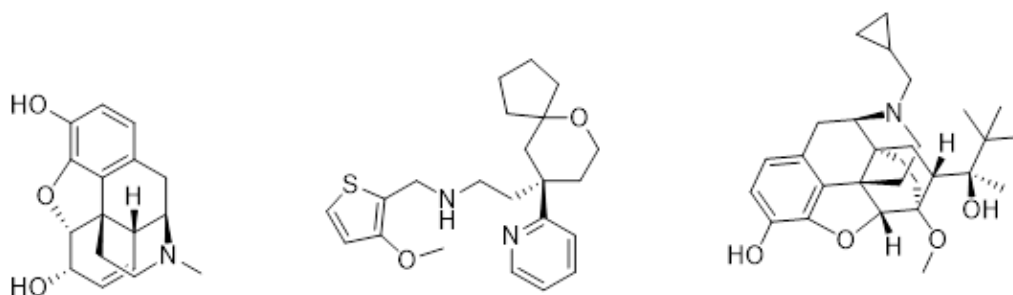


Figure 1.4 Chemical structures of MOR G protein biased agonists: morphine, TRV130, and buprenorphine.

C-terminal tail, and thus, significantly reduces the β -arrestin recruitment level. TRV130 only

exhibits 14% of the efficacy of morphine in β -arrestin recruitment assay and shows about 3-fold bias toward G protein (DeWire et al., 2013). In recent research, Pedersen's research group showed that buprenorphine shares similar bias profile and potency in G protein as TRV130 (Pedersen et al., 2020). Recently, TRV130 has been approved by FDA as the first biased MOR receptor agonist for hospital use as a short-term severe pain reliever (Lambert & Calo, 2020). Although laboratory data has exhibited exciting results on the compounds, and both TRV130 and buprenorphine have been approved by FDA, the translation of the drug effects (reduction of the adverse effects) of the compounds remained questionable (Lambert & Calo, 2020) and more data are needed.

1.4.2 Biased Agonism at DOR

Since most of the biased-related research was studied with MOR, the concept of biased agonism at DOR is less well understood. Research studies on DOR suggested that G protein-biased agonists can reduce and separate the adverse effects (e.g. tolerance) from the beneficial antidepressant, anxiolytic, and analgesic properties (A. A. Pradhan et al., 2011; A. A. Pradhan et al., 2009, 2010). *In vivo* studies in mice show that the DOR selective agonist, SNC80 (**Figure 1.5**), which results in high receptor internalization and desensitization, strongly downregulates DOR in the

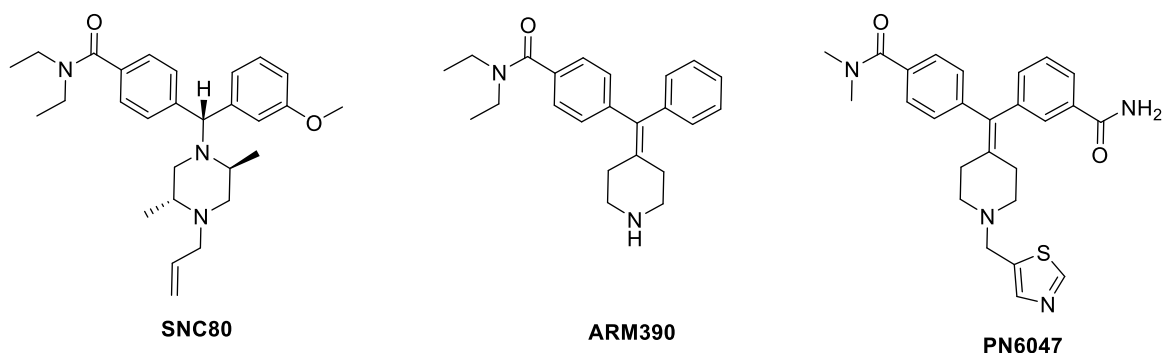


Figure 1.5 Chemical structures of selective DOR agonists: SNC80, ARM390, and PN6047.

nervous system which completely abolishes DOR-mediated beneficial effects (A. A. Pradhan et al., 2010). In contrast, the DOR agonist, ARM390 (**Figure 1.5**), which does not internalize the

receptors, also shows analgesic tolerance; however, it retains the anxiolytic/antidepressant and locomotor properties of DOR (A. A. A. Pradhan et al., 2010; A. A. Pradhan et al., 2011). The underlying mechanisms of this internalization-independent analgesic tolerance remain unclear. Recently, PN6047 (**Figure 1.5**), a derivative of SNC80, was reported as a G protein-biased selective DOR agonist which exhibits reduced adverse effects (Conibear et al., 2020). *In vitro* studies suggest that PN6047 has a similar β -arrestin recruitment potency profile as SNC80 and ARM390, but is a partial agonist compared to SNC80 (Conibear et al., 2020). In comparison with SNC80 and ARM390, PN6047 also has a 10-fold higher potency to stimulate G protein activation. Additionally, no receptor desensitization was observed with PN6047 even after 48 h of treatment at 1 μ M and no analgesic tolerance developed in mice after 16 days of treatment at a dose level of 3 mg/kg. Moreover, no convulsions, a significant side-effect of SNC80, developed at a high dosage of 80 mg/kg (Conibear et al., 2020). However, more research is needed to confirm these interesting properties of PN6047.

1.5 Concept of Allosteric Modulation at Opioid Receptors

1.5.1 Phenotypes and Mechanisms of Action of Allosteric Modulators

In the last decade, the concept of allosteric modulation of orthosteric ligands acting at GPCRs has emerged and become a novel therapeutic approach for developing selective and potentially safe compounds to treat a variety of diseases. Allosteric modulators are small molecules that bind to receptors at so-called “allosteric sites” that are geographically distinct from the orthosteric binding site where endogenous ligands bind. On their own, allosteric modulators remain silent and do not show intrinsic efficacy, but they create a conformational change that can alter receptor signaling by modulating the affinity and/or efficacy of the orthosteric ligand in the orthosteric site (**Figure 1.6**). Allosteric modulators can show different cooperativities with orthosteric ligands. Positive allosteric modulators (PAMs) (enhance the potency and/or efficacy of the orthosteric agonists), negative allosteric modulators (NAMs) (inhibit the activation of the receptor by reducing the potency and/or efficacy of the agonists), and silent allosteric modulators (SAMs) (bring no change to the potency and/or efficacy of the agonists). Additionally, there is a phenotype of PAM that shows intrinsic efficacy without the presence of a orthosteric agonist; such compounds are known as Ago-PAMs (May et al., 2007; Foster & Conn, 2017; Kenakin, 2014). Throughout the years,

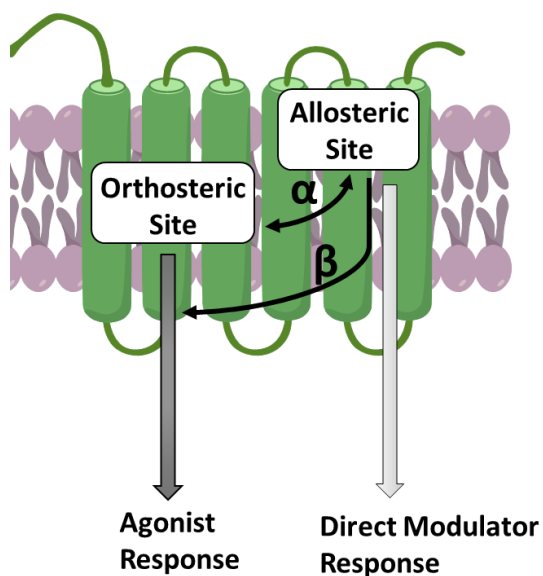


Figure 1.6 Allosteric modulation of opioid receptors. α is the allosteric effect of the modulators on affinity, and β is the modulators' effect on the efficacy of the agonist. Allosteric modulators may or may not show direct response (intrinsic efficacy).

allosteric ligands of opioid receptors have been discovered. Such compounds have potential use as treatments for pain, opioid use disorder and anxiety and depression. Allosteric sites on the opioid receptors have been putatively identified through molecular dynamic and mutagenic studies. However, at the time of writing there are no crystal or cryo-EM structures of opioid receptors bound to an allosteric modulator (Bartuzi et al., 2015, 2020; Olson et al., 2021; Shang et al., 2016).

1.5.2 Advantages of PAMs as a Potential Therapeutic Approach

In contrast to orthosteric agonists, PAMs have more benefits and advantages as a potential therapeutic approach. First, allosteric sites are often believed to be less conserved relative to orthosteric site. Targeting the allosteric site can increase the likelihood of developing selective

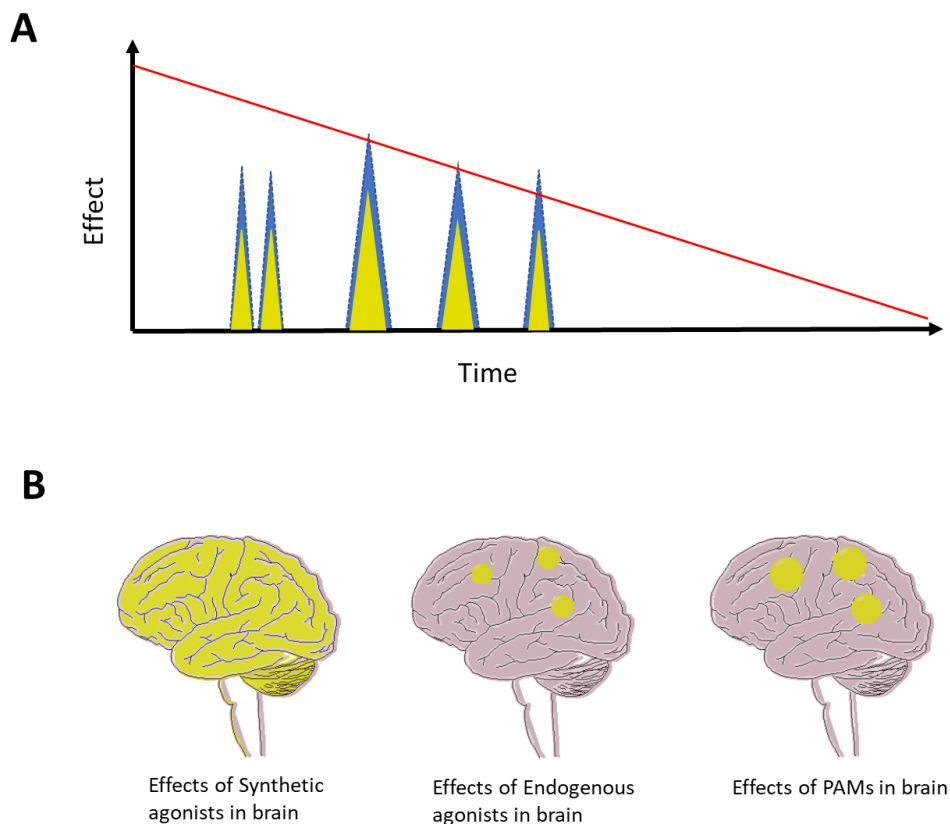


Figure 1.7 PAMs can reinforce while maintain the spatial and temporal activities of the endogenous agonists. A. Effects of endogenous agonists (yellow), effects of PAMs (blue), and effects of synthetic agonists (red and the area under the line). B. Effects of endogenous agonists in brain (center), effects of PAMs in brain (right), and effects of synthetic agonists in brain (left).

compounds among the subtypes of the receptor family (Conn et al., 2014; May et al., 2007) and thus may avoid off-target adverse effects (Burford et al., 2013; Livingston & Traynor, 2018; Melancon et al., 2012). Second, as mentioned earlier, PAMs, unlike orthosteric agonists, remain silent and do not show intrinsic efficacy without the occupancy of an orthosteric ligand (endogenous peptides or synthetic agonists) (Melancon et al., 2012; Reyes-Alcaraz et al., 2020; Wootten et al., 2013). Therefore, PAMs only modulate the affinity and/or efficacy of the orthosteric ligand. Third, PAMs preserve both the temporal and spatial activities of endogenous neurotransmitters and so potentially show reduced the on-target adverse effects (**Figure 1.7**) (Livingston & Traynor, 2018; Melancon et al., 2012; Rasmussen & Farr, 2009). Fourth, PAMs only reinforce the effects of the endogenous agonists and thus enhance the signal and efficacy, without overstimulation. Fifth, PAMs' degree of cooperativity with the orthosteric agonists has a "ceiling effect" (Gao & Jacobson, 2013; Stanczyk et al., 2019), because once the allosteric sites are filled with PAMs, the effects are saturated. Additionally, probe dependence is exhibited in PAMs, which means the effects of PAMs are dependent on the orthosteric ligands.

1.5.3 Allosteric Modulation of Opioid Receptors with PAMs

Endogenous opioid peptides are released temporarily at specific locations in the brain when needed. PAMs only enhance the affinity and/or efficacy while the peptides remain binding to the receptors in their specified locations. However, since synthetic agonists activate all the opioid receptors in the brain, this overstimulation of the receptors for a long period of time can lead to the development of serious adverse effects, such as tolerance (**Figure 1.7**) (Burford, Traynor, et al., 2015; Kenakin, 2012; Remesic et al., 2017).

1.5.4 Biased Allosteric Modulation of Opioid Receptors with PAMs

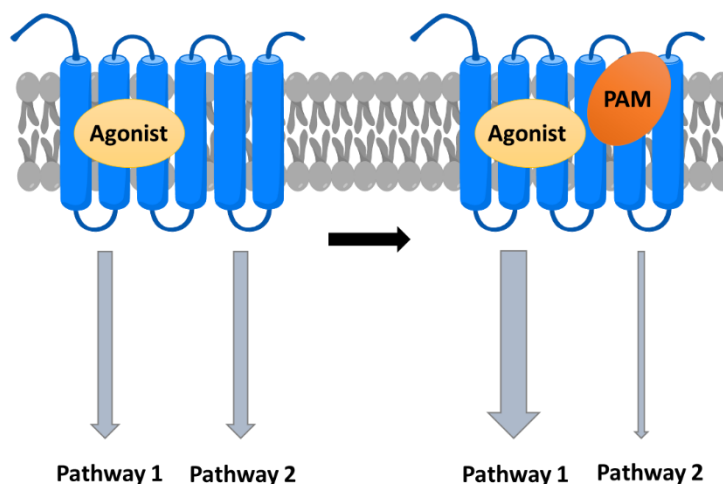


Figure 1.8 Biased modulation of opioid receptor by PAM.

In addition to the therapeutic advantages, PAMs can biasedly modulate orthosteric agonist activity towards different downstream signaling pathways (**Figure 1.8**). Different from orthosteric biased agonism which is achieved by using orthosteric agonists that selectively activate a specific signaling pathway (**Figure 1.3**), PAMs can potentially stabilize a new conformation of the receptor that allows an unbiased endogenous agonist to selectively activate a specific signaling pathway or enhance the action of a biased agonist towards or away from its preferred signaling pathway (Kenakin, 2012; Keov et al., 2011; Khajehali et al., 2015; Smith et al., 2018).

1.6 Known Opioid Receptor Allosteric Modulators

1.6.1 Known DOR Allosteric Modulators

Several DOR allosteric modulators have been identified. These include Δ^9 -tetrahydrocannabinol (THC) and cannabidiol (CBD), which are natural products and are claimed to be NAMs of both MOR and DOR (**Figure 1.9**) (Livingston & Traynor, 2018). Additionally, BMS 986187 (**1**) was discovered recently by high-throughput screening as a selective DOR PAM with low activity at MOR (**Figure 1.8**) (Burford, Livingston, et al., 2015).

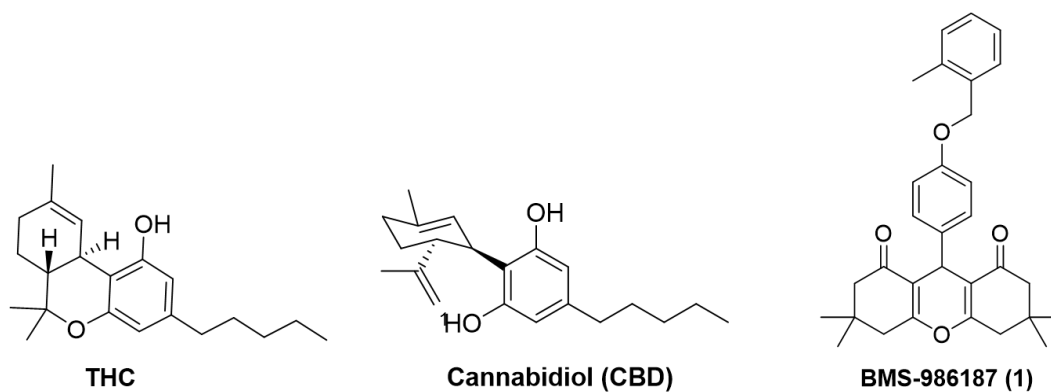


Figure 1.9 Chemical structures of selected allosteric modulators of opioid receptors.

1.6.2 Allosteric Profile of BMS 986187 (1)

1.6.2.1 **1** was discovered as a somewhat selective DOR PAM

As a representative of the xanthene-dione series, **1** was first identified as a potent and moderately selective DOR PAM, since it has no intrinsic activity on its own, exhibits DOR potency at $EC_{50} = 30$ nM / $E_{max} = 124\%$ in the β -arrestin recruitment assay, and shows a 100-fold selectivity over MOR (Burford, Livingston, et al., 2015). Additionally, this PAM gave an 18-fold increase in potency of the endogenous opioid peptide Leucine-enkephalin in the β -arrestin recruitment assay, a 32-fold shift in affinity with respect to the $GTP\gamma^{35}S$ assay (from 221 nM to 7 nM), and a 56-fold shift to the left in potency with the forskolin-stimulated cAMP assay (Burford, Livingston, et al., 2015; Livingston et al., 2018). Further studies showed that **1** may be less selective for DOR over MOR with about a 20-30-fold affinity selectivity between the two receptors (Livingston et al., 2018). Furthermore, **1** still retained activity in the $GTP\gamma^{35}S$ assay in brain membranes from mice lacking DOR (Stanczyk et al., 2019). As **1** shows about a 50-fold selectivity on DOR over MOR, it suggests that both receptors might share somewhat conserved allosteric sites.

1.6.2.2 Compound 1 exhibits ago-PAM properties that biasedly activate downstream signaling pathways

However, different from the results of the β -arrestin recruitment assay, **1** exhibits ago-PAM properties in the cAMP assay by fully inhibiting cAMP accumulation at a concentration of 3 μ M and activating GTP γ ³⁵S with an EC₅₀ of 323 nM and Emax of 92 % (Emax is normalized to 100 % with SNC80) (Stanczyk et al., 2019). Furthermore, **1** is a G protein-biased ago-PAM which, on its own, exhibits a >1,700-fold potency shift between the activation of GTP γ ³⁵S (EC₅₀ = 323 nM) and the recruitment of β -arrestin (EC₅₀ = >550 μ M), in addition to a suboptimal maximal response to the recruitment of β -arrestin in comparison to the response of GTP γ ³⁵S (Stanczyk et al., 2019). Moreover, a low level of DOR internalization was observed with **1** (7%) relative to SNC80 (33%) over a 2 h time frame, and low levels of both DOR phosphorylation and desensitization were seen relative to SNC80 (Stanczyk et al., 2019).

In the enteric nervous system (ENS) *in vitro*, **1** was found to inhibit the electrically evoked colon contraction at a high concentration (10 μ M), which confirmed its ago-PAM properties (DiCello et al., 2022). Although in DiCello's work, **1** shows a low level of DOR internalization (control = 22.3 \pm 1.1% vs. **1** = 20.0 \pm 0.79%) (confirming Stanczyk's work), it also enhances DOR internalization caused by ARM390 (without **1**, EC₅₀ = 2.6 μ M / Emax = 49.6%; with 300 nM of **1**, EC₅₀ = 30 nM / 58 %) to the level of the full agonist SNC80 (EC₅₀ = 18.2 nM / 52.9%) (DiCello et al., 2022). This result suggests that **1** can biasedly modulate agonists toward a specific pathway. However, the exact mechanism of its biased modulation requires further studies.

1.6.2.3 in vivo studies of 1 in mice

- Effects on the Gut

1 did not disturb the GI mobility or have any effect on fecal output under normal conditions but reduced castor oil-induced diarrhea and stress-induced hypermotility with a treatment of **1** at 1 mg/kg (DiCello et al., 2022). These findings suggest that **1** does not lead to the GI side effects as most opioid receptor agonists do and could be a good therapeutic approach with reduced adverse effects compared to traditional synthetic opioid receptor agonists.

- Antidepressant-like effects at DOR

Drugs with antidepressant like activity can be identified using “learned helplessness” assays such as the forced swim test. In this 6 min test rodents swim and/or climb to escape but then give up becoming immobile and float. Compounds with antidepressant-like activity increase swimming and climbing responses and decrease immobility. **Figure 1.10** shows the effect of **1** in the forced swim test. The antidepressant-like effect is lost in mice lacking DOR and is prevented by pretreatment with the DOR antagonist naltrindole (Dripps, Traynor, Jutkiewicz, unpublished). Importantly BMS-986178 does not cause convulsions and so is potentially safer than orthosteric DOR agonists such as SNC80.

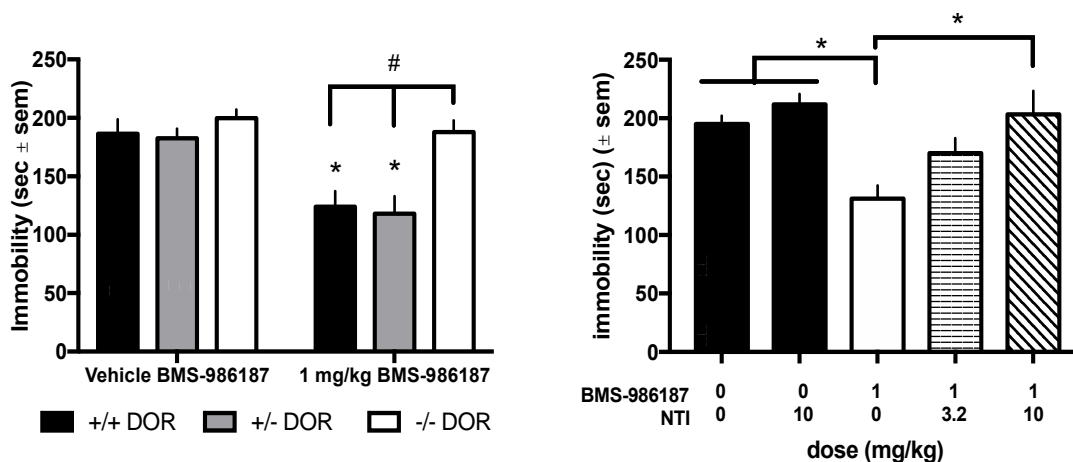


Figure 1.10 Effect of 1mg/kg BMS986187 (**1**) in the forced swim test in C57BL/6 mice. Left figure shows the action in DOR wild-type mice (+/+) mice compared to heterozygotes (+/-) and knockout (-/-) mice. Thank you to Dr. E Jutkiewicz (Pharmacology, UM for this unpublished figure).

- Antinociceptive effects at MOR

Although **1** shows 20-fold to 100-fold selectivity for DOR, it does show activity attributable to MOR agonism *in vivo*. **Figure 1.11** shows the effect of **1** in the warm-water tail-withdrawal assay in mice. This effect is blocked by naloxone showing it is opioid receptor mediated. DOR agonists, such as SNC80, do not work in this assay suggesting this is a MOR-mediated effect.

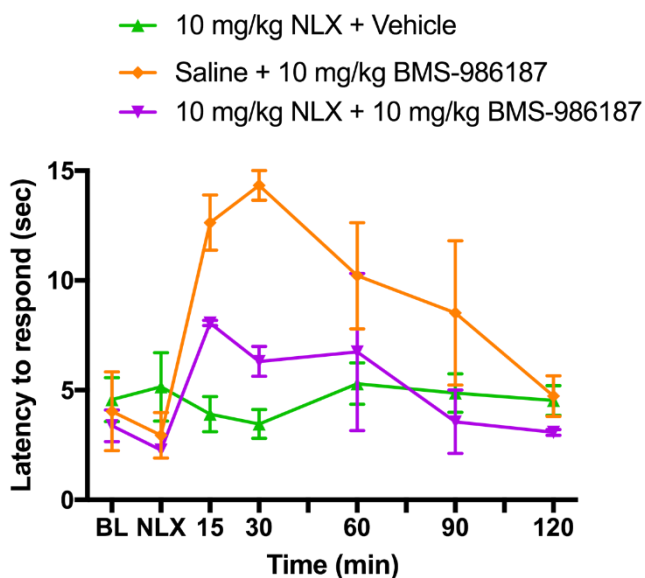


Figure 1.11 Effect of BMS-986187 (**1**) in the tail withdrawal assay in mice (129 strain) and its inhibition by the opioid antagonist naloxone. This is unpublished work from Dr. Traynor, Pharmacology at UM

The *in vivo* MOR activity of **1** is problematic because it could mean that the compound has the potential for abuse (**Figure 1.11**). Therefore, because the compound has DOR-mediated antidepressant-like activity but also MOR activity *in vivo*, in this thesis, I report further exploration of compound **1** to optimize its selectivity on DOR over MOR and improve druggability.

1.7 Crystal Structures of DOR and current knowledge of the Allosteric Binding Site

To explore and further understand more about the DOR allosteric binding site and its differences from MOR, we studied the crystal structures of both DOR and MOR. We used the structures of activated human DOR, in the presence of selective DOR agonist **DPI-287**, and human MOR, in the presence of selective agonist DAMGO (PDB: 6PT3-DOR, 6DDF-MOR) (Claff et al., 2019; Koehl et al., 2018; Stevens, 2004). Unfortunately, there are no DOR or MOR crystal or cryo-EM structures bound to both orthosteric agonist and allosteric modulator, which hindered us from knowing the exact binding interactions between BMS-986187 and the receptors (Foster & Conn, 2017). However, molecular dynamic (MD) and mutagenesis studies have been performed with **1** at DOR and MD studies of a MOR-PAM (**BMS986122**) at MOR (Bartuzi et al., 2015; Shang et

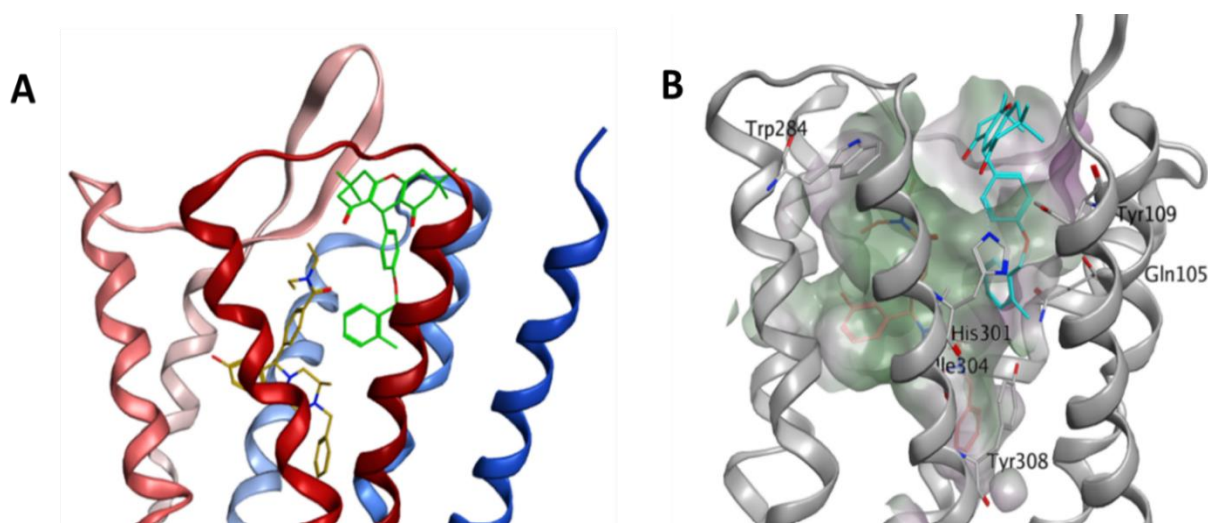


Figure 1.12 (A) DOR PAM, CCG257409 (green) and selective DOR agonist, DPI-287 (yellow) bound to hDOR (PDB: 6PT3). Transmembrane helices are colored from blue to red, Helix I is in dark blue and Helix VII is in dark red. (B) Lipophilicity surface of hDOR (grey) orthosteric and allosteric binding sites is drawn in green (hydrophobic regions) and purple (hydrophilic regions). Both DPI-287 (red) and CCG257409 (blue) are embedded in the corresponding binding sites. Important side chain interactions are labeled.

al., 2016). In opioid receptors, the allosteric site of the modulators is commonly found in the vestibule of the orthosteric site (**Figure 1.12A**) (Melancon et al., 2012; Wootten et al., 2013;

Bartuzi et al., 2015; Shang et al., 2016; Livingston & Traynor, 2018; Olson et al., 2021). This location for allosteric binding was also suggested in the above studies at MOR and DOR.

The shown docking orientation of **1** (blue) in DOR (**Figure 1.12A**) indicates that the DOR PAM was binding in the extracellular region, the vestibule of the receptor which appears to be a highly hydrophobic region (**Figure 1.12B**), while the agonist DPI-287 was binding in the expected orthosteric site, located in the center of the transmembrane domain of DOR. **1** was predicted to bind in the conformation with the benzyl group pointing toward the center of the receptor. The major side chain interactions with **1** were located on the transmembrane helices II and VII. The major H-bonding interaction was with His301 (7.36), which had an edge-to-face interaction with the B-ring of **1** and served as a hydrogen-bond donor for one of the dione carbonyl moieties of the xanthene-dione. Major hydrophobic interactions between **1** and the side chains were Gln105 (2.60), Tyr109 (2.64), Val297 (7.32), Leu300 (7.35), Ile304 (7.39), and Tyr308 (7.43) (**Figure**

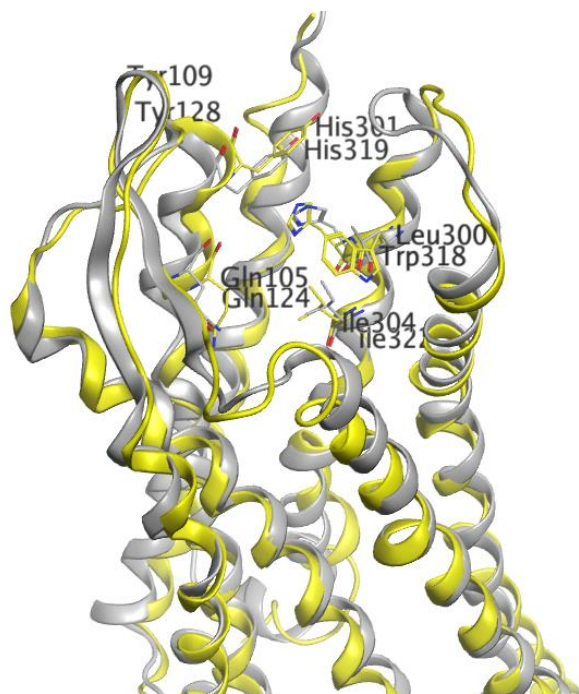


Figure 1.13 Overlay of hDOR (grey) (pdb: 6PT3) and hMOR (yellow) (pdb: 6DDF) crystal structures. Major side chain interactions in the allosteric pockets of both receptors are shown.

1.12B). The allosteric pocket of MOR was similar to DOR with minor differences. The MOR PAM (**BMS986122**) was predicted to interact with side-chains of MOR at Asn127 (2.63), Trp128 (2.64), Trp318 (7.35), His319 (7.36), and Ile322 (7.39) (Bartuzi et al., 2015).

I was not able to dock **1** into the analogous situation to DOR in MOR due to clashes formed between **1** and the amino-acid side chains of MOR (**Figure 1.13**). These differences between DOR and MOR at the potential allosteric binding site provide a rationale for the DOR selectivity of **1** and suggest that selectivity of **1** could be improved.

1.8 Aims

The purpose of this thesis is to further explore the different requirements for allosteric binding to DOR and MOR using the discovered xanthene-dione series, as exemplified by BMS-986187 (**1**). As **1** has been identified as a DOR-PAM and has been studied both *in vitro* and *in vivo*, further optimization of its selectivity over MOR remains unchallenged. Moreover, optimization of the druggability of this series of compounds is necessary for future *in vivo* preclinical studies.

Chapter 2: Structure-Activity Relationship (SAR) and Optimization of Xanthene Series for Selectivity over MOR

Chapter two investigates the SAR of the xanthene-dione series of PAMs at DOR and MOR to further understand the requirements for optimal binding to allosteric binding pockets of the receptors. It was found that the binding sites of the receptors are large and flexible. Thus, the potency of the series is hard to optimize. However, it was discovered that conformational restriction in the molecule greatly improved the selectivity for DOR over MOR.

Chapter 3: SAR of Xanthene-dione Series and Improvement of Distribution, Metabolism and Pharmacokinetics (DMPK) properties by Enhancing Solubility

The work described in Chapter 3 attempts to improve the solubility of xanthene-dione series through bioisosteric exercises and adding basic side chains. The solubility profile of xanthene-diones series is low due to its high lipophilicity and high molecular weight. This poor solubility profile hinders the druggability of xanthene series. Attempts to improve the solubility **of 1** remained challenging while maintaining activity as a DOR-PAM and selectivity over MOR.

Chapter 4: SAR of Xanthene-dione Series and Improvement of Distribution, Metabolism and Pharmacokinetics (DMPK) properties by Enhancing Metabolic Stability

As an essential property of druggability, it is important for a drug to be metabolically stable. However, the xanthene-dione series likely has a low metabolic stability due its high lipophilicity and high number of metabolic soft-spots. Attempts to improve the stability by blocking the metabolic soft-spots were somewhat successful, but further optimization needs to be carried out in the future in order to maintain high potency.

1.9 References

- Abuse, N. I. on D. (2021, June 1). *Prescription Opioids DrugFacts*. National Institute on Drug Abuse. <https://nida.nih.gov/publications/drugfacts/prescription-opioids>
- Ahlbeck, K. (2011). Opioids: A two-faced Janus. *Current Medical Research and Opinion*, 27(2), 439–448. <https://doi.org/10.1185/03007995.2010.545379>
- Al-Hasani, R., & Bruchas, M. R. (2011). Molecular Mechanisms of Opioid Receptor-Dependent Signaling and Behavior. *Anesthesiology*, 115(6), 1363–1381. <https://doi.org/10.1097/ALN.0b013e318238bba6>
- Almond, L. M., Yang, J., Jamei, M., Tucker, G. T., & Rostami-Hodjegan, A. (2009). Towards a quantitative framework for the prediction of DDIs arising from cytochrome P450 induction. *Current Drug Metabolism*, 10(4), 420–432. <https://doi.org/10.2174/138920009788498978>
- Baillie, T. A. (2008). Metabolism and Toxicity of Drugs. Two Decades of Progress in Industrial Drug Metabolism. *Chemical Research in Toxicology*, 21(1), 129–137. <https://doi.org/10.1021/tx7002273>
- Banks, W. A. (2009). Characteristics of compounds that cross the blood-brain barrier. *BMC Neurology*, 9(1), S3. <https://doi.org/10.1186/1471-2377-9-S1-S3>
- Bartuzi, D., Kaczor, A. A., & Matosiuk, D. (2015). Activation and Allosteric Modulation of Human μ Opioid Receptor in Molecular Dynamics. *Journal of Chemical Information and Modeling*, 55(11), 2421–2434. <https://doi.org/10.1021/acs.jcim.5b00280>
- Bartuzi, D., Kędzierska, E., Kaczor, A. A., Schmidhammer, H., & Matosiuk, D. (2020). Novel Positive Allosteric Modulators of μ Opioid Receptor—Insight from In Silico and In Vivo Studies. *International Journal of Molecular Sciences*, 21(22), 8463. <https://doi.org/10.3390/ijms21228463>
- Bassoni, D. L., Raab, W. J., Achacoso, P. L., Loh, C. Y., & Wehrman, T. S. (2012). Measurements of β -Arrestin Recruitment to Activated Seven Transmembrane Receptors Using Enzyme Complementation. In A. P. Davenport (Ed.), *Receptor Binding Techniques* (pp. 181–203). Humana Press. https://doi.org/10.1007/978-1-61779-909-9_9
- Bellettato, C. M., & Scarpa, M. (2018). Possible strategies to cross the blood–brain barrier. *Italian Journal of Pediatrics*, 44(2), 131. <https://doi.org/10.1186/s13052-018-0563-0>
- Bioisosteres in Medicinal Chemistry* (1st ed.). (2012). John Wiley & Sons, Ltd. <https://doi.org/10.1002/9783527654307>
- Bohn, L. M., Gainetdinov, R. R., Lin, F.-T., Lefkowitz, R. J., & Caron, M. G. (2000). μ -Opioid receptor desensitization by β -arrestin-2 determines morphine tolerance but not dependence. *Nature*, 408(6813), Article 6813. <https://doi.org/10.1038/35047086>

- Bohn, L. M., Lefkowitz, R. J., Gainetdinov, R. R., Peppel, K., Caron, M. G., & Lin, F.-T. (1999). Enhanced Morphine Analgesia in Mice Lacking β -Arrestin 2. *Science*, 286(5449), 2495–2498. <https://doi.org/10.1126/science.286.5449.2495>
- Bourdonnec, B. L., Windh, R. T., Ajello, C. W., Leister, L. K., Gu, M., Chu, G.-H., Tuthill, P. A., Barker, W. M., Koblish, M., Wiant, D. D., Graczyk, T. M., Belanger, S., Cassel, J. A., Feschenko, M. S., Brogdon, B. L., Smith, S. A., Christ, D. D., Derelanko, M. J., Kutz, S., ... Dolle, R. E. (2008). Potent, Orally Bioavailable Delta Opioid Receptor Agonists for the Treatment of Pain: Discovery of N,N-Diethyl-4-(5-hydroxyspiro[chromene-2,4'-piperidine]-4-yl)benzamide (ADL5859). *Journal of Medicinal Chemistry*, 51(19), 5893–5896. <https://doi.org/10.1021/jm8008986>
- Burford, N. T., Clark, M. J., Wehrman, T. S., Gerritz, S. W., Banks, M., O'Connell, J., Traynor, J. R., & Alt, A. (2013). Discovery of positive allosteric modulators and silent allosteric modulators of the μ -opioid receptor. *Proceedings of the National Academy of Sciences*, 110(26), 10830–10835. <https://doi.org/10.1073/pnas.1300393110>
- Burford, N. T., Livingston, K. E., Canals, M., Ryan, M. R., Budenholzer, L. M. L., Han, Y., Shang, Y., Herbst, J. J., O'Connell, J., Banks, M., Zhang, L., Filizola, M., Bassoni, D. L., Wehrman, T. S., Christopoulos, A., Traynor, J. R., Gerritz, S. W., & Alt, A. (2015). Discovery, Synthesis, and Molecular Pharmacology of Selective Positive Allosteric Modulators of the δ -Opioid Receptor. *Journal of Medicinal Chemistry*, 58(10), 4220–4229. <https://doi.org/10.1021/acs.jmedchem.5b00007>
- Burford, N. T., Traynor, J. R., & Alt, A. (2015). Positive allosteric modulators of the μ -opioid receptor: A novel approach for future pain medications. *British Journal of Pharmacology*, 172(2), 277–286. <https://doi.org/10.1111/bph.12599>
- Cahill, T. J., Thomsen, A. R. B., Tarrasch, J. T., Plouffe, B., Nguyen, A. H., Yang, F., Huang, L.-Y., Kahsai, A. W., Bassoni, D. L., Gavino, B. J., Lamerdin, J. E., Triest, S., Shukla, A. K., Berger, B., Little, J., Antar, A., Blanc, A., Qu, C.-X., Chen, X., ... Lefkowitz, R. J. (2017). Distinct conformations of GPCR- β -arrestin complexes mediate desensitization, signaling, and endocytosis. *Proceedings of the National Academy of Sciences*, 114(10), 2562–2567. <https://doi.org/10.1073/pnas.1701529114>
- Charbogne, P., Kieffer, B. L., & Befort, K. (2014). 15 years of genetic approaches in vivo for addiction research: Opioid receptor and peptide gene knockout in mouse models of drug abuse. *Neuropharmacology*, 76, 204–217. <https://doi.org/10.1016/j.neuropharm.2013.08.028>
- Chen, C.-M., Ding, H., Mabry, K. M., & Ko, M.-C. (2022). Enhanced antidepressant-like effects of a delta opioid receptor agonist, SNC80, in rats under inflammatory pain. *Pharmacology Biochemistry and Behavior*, 214, 173341. <https://doi.org/10.1016/j.pbb.2022.173341>
- Chung, P. C. S., & Kieffer, B. L. (2013). Delta opioid receptors in brain function and diseases. *Pharmacology & Therapeutics*, 140(1), 112–120. <https://doi.org/10.1016/j.pharmthera.2013.06.003>

- Cipriani, A., Furukawa, T. A., Salanti, G., Chaimani, A., Atkinson, L. Z., Ogawa, Y., Leucht, S., Ruhe, H. G., Turner, E. H., Higgins, J. P. T., Egger, M., Takeshima, N., Hayasaka, Y., Imai, H., Shinohara, K., Tajika, A., Ioannidis, J. P. A., & Geddes, J. R. (2018). Comparative efficacy and acceptability of 21 antidepressant drugs for the acute treatment of adults with major depressive disorder: A systematic review and network meta-analysis. *The Lancet*, *391*(10128), 1357–1366. [https://doi.org/10.1016/S0140-6736\(17\)32802-7](https://doi.org/10.1016/S0140-6736(17)32802-7)
- Claff, T., Yu, J., Blais, V., Patel, N., Martin, C., Wu, L., Han, G. W., Holleran, B. J., Van der Poorten, O., White, K. L., Hanson, M. A., Sarret, P., Gendron, L., Cherezov, V., Katritch, V., Ballet, S., Liu, Z.-J., Müller, C. E., & Stevens, R. C. (2019). Elucidating the active δ -opioid receptor crystal structure with peptide and small-molecule agonists. *Science Advances*, *5*(11), eaax9115. <https://doi.org/10.1126/sciadv.aax9115>
- Congreve, M., Carr, R., Murray, C., & Jhoti, H. (2003). A ‘Rule of Three’ for fragment-based lead discovery? *Drug Discovery Today*, *8*(19), 876–877. [https://doi.org/10.1016/S1359-6446\(03\)02831-9](https://doi.org/10.1016/S1359-6446(03)02831-9)
- Conibear, A. E., Asghar, J., Hill, R., Henderson, G., Borbely, E., Tekus, V., Helyes, Z., Palandri, J., Bailey, C., Starke, I., von Mentzer, B., Kendall, D., & Kelly, E. (2020). A Novel G Protein-Biased Agonist at the δ Opioid Receptor with Analgesic Efficacy in Models of Chronic Pain. *The Journal of Pharmacology and Experimental Therapeutics*, *372*(2), 224–236. <https://doi.org/10.1124/jpet.119.258640>
- Conn, P. J., Lindsley, C. W., Meiler, J., & Niswender, C. M. (2014). Opportunities and challenges in the discovery of allosteric modulators of GPCRs for treating CNS disorders. *Nature Reviews. Drug Discovery*, *13*(9), 692–708. <https://doi.org/10.1038/nrd4308>
- Dahal, U. P., Joswig-Jones, C., & Jones, J. P. (2012). Comparative study of the affinity and metabolism of type I and type II binding quinoline carboxamide analogs by cytochrome P450 3A4. *Journal of Medicinal Chemistry*, *55*(1), 280–290. <https://doi.org/10.1021/jm201207h>
- Depression and Other Common Mental Disorders*. (n.d.). Retrieved July 26, 2022, from <https://www.who.int/publications-detail-redirect/depression-global-health-estimates>
- Depressive Disorders. (2022). In *Diagnostic and Statistical Manual of Mental Disorders*. American Psychiatric Association Publishing. https://doi.org/10.1176/appi.books.9780890425787.x04_Depressive_Disorders
- DeWire, S. M., Yamashita, D. S., Rominger, D. H., Liu, G., Cowan, C. L., Graczyk, T. M., Chen, X.-T., Pitis, P. M., Gotchev, D., Yuan, C., Koblish, M., Lark, M. W., & Violin, J. D. (2013). A G Protein-Biased Ligand at the μ -Opioid Receptor Is Potently Analgesic with Reduced Gastrointestinal and Respiratory Dysfunction Compared with Morphine. *Journal of Pharmacology and Experimental Therapeutics*, *344*(3), 708–717. <https://doi.org/10.1124/jpet.112.201616>

- Di, L., Fish, P. V., & Mano, T. (2012). Bridging solubility between drug discovery and development. *Drug Discovery Today*, 17(9), 486–495. <https://doi.org/10.1016/j.drudis.2011.11.007>
- DiCello, J. J., Carbone, S. E., Saito, A., Pham, V., Szymaszkiwicz, A., Gondin, A. B., Alvi, S., Marique, K., Shenoy, P., Veldhuis, N. A., Fichna, J., Canals, M., Christopoulos, A., Valant, C., & Poole, D. P. (2022). Positive allosteric modulation of endogenous delta opioid receptor signaling in the enteric nervous system is a potential treatment for gastrointestinal motility disorders. *American Journal of Physiology. Gastrointestinal and Liver Physiology*, 322(1), G66–G78. <https://doi.org/10.1152/ajpgi.00297.2021>
- Drug Bioavailability: Estimation of Solubility, Permeability, Absorption and Bioavailability, Volume 18.* (n.d.). Retrieved November 22, 2022
- Fava, M. (2003). Diagnosis and definition of treatment-resistant depression. *Biological Psychiatry*, 53(8), 649–659. [https://doi.org/10.1016/S0006-3223\(03\)00231-2](https://doi.org/10.1016/S0006-3223(03)00231-2)
- Filliol, D., Ghozland, S., Chluba, J., Martin, M., Matthes, H. W. D., Simonin, F., Befort, K., Gavériaux-Ruff, C., Dierich, A., LeMeur, M., Valverde, O., Maldonado, R., & Kieffer, B. L. (2000). Mice deficient for δ - and μ -opioid receptors exhibit opposing alterations of emotional responses. *Nature Genetics*, 25(2), Article 2. <https://doi.org/10.1038/76061>
- Foster, D. J., & Conn, P. J. (2017). Allosteric modulation of GPCRs: New insights and potential utility for treatment of schizophrenia and other CNS disorders. *Neuron*, 94(3), 431–446. <https://doi.org/10.1016/j.neuron.2017.03.016>
- Gallantine, E. L., & Meert, T. F. (2005). A Comparison of the Antinociceptive and Adverse Effects of the μ -Opioid Agonist Morphine and the δ -Opioid Agonist SNC80. *Basic & Clinical Pharmacology & Toxicology*, 97(1), 39–51. https://doi.org/10.1111/j.1742-7843.2005.pto_97107.x
- Ganesan, S. S., Kothandapani, J., & Ganesan, A. (n.d.). Zinc Chloride Catalyzed Collective Synthesis of Arylmethylene Bis(3- hydroxy-2-cyclohexene-1-ones) and 1,8-Dioxo-octahydroxanthene/acridine Derivatives. *Letters in Organic Chemistry*, 11(9), 682–687.
- Gao, Z.-G., & Jacobson, K. A. (2013). Allosteric modulation and functional selectivity of G protein-coupled receptors. *Drug Discovery Today: Technologies*, 10(2), e237–e243. <https://doi.org/10.1016/j.ddtec.2012.08.004>
- Gaskin, D. J., & Richard, P. (2012). The Economic Costs of Pain in the United States. *The Journal of Pain*, 13(8), 715–724. <https://doi.org/10.1016/j.jpain.2012.03.009>
- Guengerich, F. P. (2006). Cytochrome P450s and other enzymes in drug metabolism and toxicity. *The AAPS Journal*, 8(1), E101–E111. <https://doi.org/10.1208/aapsj080112>
- Guengerich, F. P., & MacDonald, J. S. (2007). Applying Mechanisms of Chemical Toxicity to Predict Drug Safety. *Chemical Research in Toxicology*, 20(3), 344–369. <https://doi.org/10.1021/tx600260a>

- Hong, S., Yuan, Y., Yang, Q., Chen, L., Deng, J., Chen, W., Lian, H., Mota-Morales, J. D., & Liimatainen, H. (2019). Choline chloride-zinc chloride deep eutectic solvent mediated preparation of partial O-acetylation of chitin nanocrystal in one step reaction. *Carbohydrate Polymers*, 220, 211–218. <https://doi.org/10.1016/j.carbpol.2019.05.075>
- Inturrisi, C. E. (2002). Clinical Pharmacology of Opioids for Pain. *The Clinical Journal of Pain*, 18(4), S3.
- Ippolito, D. L., Temkin, P. A., Rogalski, S. L., & Chavkin, C. (2002). N-terminal Tyrosine Residues within the Potassium Channel Kir3 Modulate GTPase Activity of Gai. *Journal of Biological Chemistry*, 277(36), 32692–32696. <https://doi.org/10.1074/jbc.M204407200>
- Issa, N. T., Wathieu, H., Ojo, A., Byers, S. W., & Dakshnamurthy, S. (2017). Drug Metabolism in Preclinical Drug Development: A Survey of the Discovery Process, Toxicology, and Computational Tools. *Current Drug Metabolism*, 18(6), 556–565. <https://doi.org/10.2174/1389200218666170316093301>
- James, S. L., Abate, D., Abate, K. H., Abay, S. M., Abbafati, C., Abbasi, N., Abbastabar, H., Abd-Allah, F., Abdela, J., Abdelalim, A., Abdollahpour, I., Abdulkader, R. S., Abebe, Z., Abera, S. F., Abil, O. Z., Abraha, H. N., Abu-Raddad, L. J., Abu-Rmeileh, N. M. E., Accrombessi, M. M. K., ... Murray, C. J. L. (2018). Global, regional, and national incidence, prevalence, and years lived with disability for 354 diseases and injuries for 195 countries and territories, 1990–2017: A systematic analysis for the Global Burden of Disease Study 2017. *The Lancet*, 392(10159), 1789–1858. [https://doi.org/10.1016/S0140-6736\(18\)32279-7](https://doi.org/10.1016/S0140-6736(18)32279-7)
- Jones, P. J. H., & Leatherdale, S. T. (1991). Stable isotopes in clinical research: Safety reaffirmed. *Clinical Science*, 80(4), 277–280. <https://doi.org/10.1042/cs0800277>
- Kalgutkar, A. S., & Soglia, J. R. (2005). Minimising the potential for metabolic activation in drug discovery. *Expert Opinion on Drug Metabolism & Toxicology*, 1(1), 91–142. <https://doi.org/10.1517/17425255.1.1.91>
- Kasper, S. (2022). Initiating Antidepressant Medication: What is the Most Important Factor? *Advances in Therapy*, 39(1), 5–12. <https://doi.org/10.1007/s12325-021-02028-7>
- Katz, J. J., & Crespi, H. L. (1966). Deuterated Organisms: Cultivation and Uses. *Science*, 151(3715), 1187–1194. <https://doi.org/10.1126/science.151.3715.1187>
- Kaushik, P., Kumar, A., Kumar, P., Kumar, S., Singh, B. K., & Bahadur, V. (2020). Cu-catalyzed one-pot multicomponent approach for the synthesis of symmetric and asymmetric 1,4-dihydropyridine (1,4-DHP) linked 1,2,3-triazole derivatives. *Synthetic Communications*, 50(13), 2033–2042. <https://doi.org/10.1080/00397911.2020.1762222>
- Kaya, M., Yıldırım, Y., & Çelik, G. Y. (2015). Synthesis, Characterization, and In Vitro Antimicrobial and Antifungal Activity of Novel Acridines. *Pharmaceutical Chemistry Journal*, 48(11), 722–726. <https://doi.org/10.1007/s11094-015-1181-4>

- Kenakin, T. P. (2012). Biased signalling and allosteric machines: New vistas and challenges for drug discovery. *British Journal of Pharmacology*, *165*(6), 1659–1669. <https://doi.org/10.1111/j.1476-5381.2011.01749.x>
- Kenakin, T. P. (Ed.). (2014). Front-matter. In *A Pharmacology Primer (Fourth Edition)* (pp. i–iii). Academic Press. <https://doi.org/10.1016/B978-0-12-407663-1.00015-6>
- Keov, P., Sexton, P. M., & Christopoulos, A. (2011). Allosteric modulation of G protein-coupled receptors: A pharmacological perspective. *Neuropharmacology*, *60*(1), 24–35. <https://doi.org/10.1016/j.neuropharm.2010.07.010>
- Kerns, E. H., & Di, L. (2008). *Drug-like properties: Concepts, structure design and methods: from ADME to toxicity optimization*. Academic Press.
- Khajehali, E., Malone, D., Glass, M., Sexton, P., Christopoulos, A., & Leach, K. (2015). Biased Agonism and Biased Allosteric Modulation at the CB1 Cannabinoid Receptor. *Molecular Pharmacology*, *88*. <https://doi.org/10.1124/mol.115.099192>
- Khoo, Y., Demchenko, I., Frey, B. N., Milev, R. V., Ravindran, A. V., Parikh, S. V., Ho, K., Rotzinger, S., Lou, W., Lam, R. W., Kennedy, S. H., & Bhat, V. (2022). Baseline anxiety, and early anxiety/depression improvement in anxious depression predicts treatment outcomes with escitalopram: A CAN-BIND-1 study report. *Journal of Affective Disorders*, *300*, 50–58. <https://doi.org/10.1016/j.jad.2021.12.027>
- Kirchmair, J., Williamson, M. J., Tyzack, J. D., Tan, L., Bond, P. J., Bender, A., & Glen, R. C. (2012). Computational Prediction of Metabolism: Sites, Products, SAR, P450 Enzyme Dynamics, and Mechanisms. *Journal of Chemical Information and Modeling*, *52*(3), 617–648. <https://doi.org/10.1021/ci200542m>
- Kliwer, A., Schmiedel, F., Sianati, S., Bailey, A., Bateman, J. T., Levitt, E. S., Williams, J. T., Christie, M. J., & Schulz, S. (2019). Phosphorylation-deficient G-protein-biased μ -opioid receptors improve analgesia and diminish tolerance but worsen opioid side effects. *Nature Communications*, *10*, 367. <https://doi.org/10.1038/s41467-018-08162-1>
- Koehl, A., Hu, H., Maeda, S., Zhang, Y., Qu, Q., Paggi, J. M., Latorraca, N. R., Hilger, D., Dawson, R., Matile, H., Schertler, G. F. X., Granier, S., Weis, W. I., Dror, R. O., Manglik, A., Skinnotis, G., & Kobilka, B. K. (2018). Structure of the μ -opioid receptor–Gi protein complex. *Nature*, *558*(7711), Article 7711. <https://doi.org/10.1038/s41586-018-0219-7>
- Kola, I., & Landis, J. (2004). Can the pharmaceutical industry reduce attrition rates? *Nature Reviews Drug Discovery*, *3*(8), Article 8. <https://doi.org/10.1038/nrd1470>
- Krapcho, A. P., Weimaster, J. F., Eldridge, J. M., Jahngen, E. G. E., Lovey, A. J., & Stephens, W. P. (1978). Synthetic applications and mechanism studies of the decarboxylations of geminal diesters and related systems effected in dimethyl sulfoxide by water and/or by water with added salts. *The Journal of Organic Chemistry*, *43*(1), 138–147. <https://doi.org/10.1021/jo00395a032>

- Kushner, D. J., Baker, A., & Dunstall, T. G. (1999). Pharmacological uses and perspectives of heavy water and deuterated compounds. *Canadian Journal of Physiology and Pharmacology*, 77(2), 79–88.
- Lambert, D., & Calo, G. (2020). Approval of oliceridine (TRV130) for intravenous use in moderate to severe pain in adults. *BJA: British Journal of Anaesthesia*, 125(6), e473–e474. <https://doi.org/10.1016/j.bja.2020.09.021>
- Le Bourdonnec, B., Windh, R. T., Leister, L. K., Zhou, Q. J., Ajello, C. W., Gu, M., Chu, G.-H., Tuthill, P. A., Barker, W. M., Koblish, M., Wiant, D. D., Graczyk, T. M., Belanger, S., Cassel, J. A., Feschenko, M. S., Brogdon, B. L., Smith, S. A., Derelanko, M. J., Kutz, S., ... Dolle, R. E. (2009). Spirocyclic Delta Opioid Receptor Agonists for the Treatment of Pain: Discovery of N,N-Diethyl-3-hydroxy-4-(spiro[chromene-2,4'-piperidine]-4-yl) Benzamide (ADL5747). *Journal of Medicinal Chemistry*, 52(18), 5685–5702. <https://doi.org/10.1021/jm900773n>
- Lewis, D. F. V., & Dickins, M. (2002). Substrate SARs in human P450s. *Drug Discovery Today*, 7(17), 918–925. [https://doi.org/10.1016/S1359-6446\(02\)02412-1](https://doi.org/10.1016/S1359-6446(02)02412-1)
- Lewis, D. F. V., Jacobs, M. N., & Dickins, M. (2004). Compound lipophilicity for substrate binding to human P450s in drug metabolism. *Drug Discovery Today*, 9(12), 530–537. [https://doi.org/10.1016/S1359-6446\(04\)03115-0](https://doi.org/10.1016/S1359-6446(04)03115-0)
- Li, J.-X. (2015). Pain and depression comorbidity: A preclinical perspective. *Behavioural Brain Research*, 276, 92–98. <https://doi.org/10.1016/j.bbr.2014.04.042>
- Lindsley, C. W., Emmitte, K. A., Hopkins, C. R., Bridges, T. M., Gregory, K. J., Niswender, C. M., & Conn, P. J. (2016). Practical Strategies and Concepts in GPCR Allosteric Modulator Discovery: Recent Advances with Metabotropic Glutamate Receptors. *Chemical Reviews*, 116(11), 6707–6741. <https://doi.org/10.1021/acs.chemrev.5b00656>
- Lipinski, C. A. (2000). Drug-like properties and the causes of poor solubility and poor permeability. *Journal of Pharmacological and Toxicological Methods*, 44(1), 235–249. [https://doi.org/10.1016/S1056-8719\(00\)00107-6](https://doi.org/10.1016/S1056-8719(00)00107-6)
- Lipinski, C., & Hopkins, A. (2004). Navigating chemical space for biology and medicine. *Nature*, 432(7019), Article 7019. <https://doi.org/10.1038/nature03193>
- Livingston, K. E., Stanczyk, M. A., Burford, N. T., Alt, A., Canals, M., & Traynor, J. R. (2018). Pharmacologic Evidence for a Putative Conserved Allosteric Site on Opioid Receptors. *Molecular Pharmacology*, 93(2), 157–167. <https://doi.org/10.1124/mol.117.109561>
- Livingston, K. E., & Traynor, J. R. (2018). Allostery at opioid receptors: Modulation with small molecule ligands. *British Journal of Pharmacology*, 175(14), 2846–2856. <https://doi.org/10.1111/bph.13823>
- Major Depression*. (n.d.). National Institute of Mental Health (NIMH). Retrieved July 10, 2022, from <https://www.nimh.nih.gov/health/statistics/major-depression>

- Manglik, A., Lin, H., Aryal, D. K., McCorvy, J. D., Dengler, D., Corder, G., Levit, A., Kling, R. C., Bernat, V., Hübner, H., Huang, X.-P., Sassano, M. F., Giguère, P. M., Löber, S., Da Duan, Scherrer, G., Kobilka, B. K., Gmeiner, P., Roth, B. L., & Shoichet, B. K. (2016). Structure-based discovery of opioid analgesics with reduced side effects. *Nature*, 537(7619), Article 7619. <https://doi.org/10.1038/nature19112>
- May, L. T., Leach, K., Sexton, P. M., & Christopoulos, A. (2007). Allosteric Modulation of G Protein–Coupled Receptors. *Annual Review of Pharmacology and Toxicology*, 47(1), 1–51. <https://doi.org/10.1146/annurev.pharmtox.47.120505.105159>
- MCKIBBEN, B. P., MEYERS, K. M., Zhang, Y., Marshall, D. R., Cogan, D., Lord, J., Chen, Z., Burke, J., & Balestra, M. (2018). *Bicyclic imidazole derivatives useful for the treatment of renal disease, cardiovascular diseases and fibrotic disorders* (World Intellectual Property Organization Patent WO2018005177A1). <https://patents.google.com/patent/WO2018005177A1/en>
- McPherson, J., Rivero, G., Baptist, M., Llorente, J., Al-Sabah, S., Krasel, C., Dewey, W. L., Bailey, C. P., Rosethorne, E. M., Charlton, S. J., Henderson, G., & Kelly, E. (2010). μ -Opioid Receptors: Correlation of Agonist Efficacy for Signalling with Ability to Activate Internalization. *Molecular Pharmacology*, 78(4), 756–766. <https://doi.org/10.1124/mol.110.066613>
- Meanwell, N. A. (2011). Synopsis of Some Recent Tactical Application of Bioisosteres in Drug Design. *Journal of Medicinal Chemistry*, 54(8), 2529–2591. <https://doi.org/10.1021/jm1013693>
- Meanwell, N. A. (2015). The Influence of Bioisosteres in Drug Design: Tactical Applications to Address Developability Problems. In N. A. Meanwell (Ed.), *Tactics in Contemporary Drug Design* (pp. 283–381). Springer. https://doi.org/10.1007/7355_2013_29
- Melancon, B. J., Hopkins, C. R., Wood, M. R., Emmitte, K. A., Niswender, C. M., Christopoulos, A., Conn, P. J., & Lindsley, C. W. (2012). Allosteric Modulation of Seven Transmembrane Spanning Receptors: Theory, Practice, and Opportunities for Central Nervous System Drug Discovery. *Journal of Medicinal Chemistry*, 55(4), 1445–1464. <https://doi.org/10.1021/jm201139r>
- Moncrieff, J., & Kirsch, I. (2005). Efficacy of antidepressants in adults. *BMJ: British Medical Journal*, 331(7509), 155–157.
- Murray, M. R., & Benitez, H. H. (1967). Deuterium Oxide: Direct Action on Sympathetic Ganglia Isolated in Culture. *Science*, 155(3765), 1021–1024. <https://doi.org/10.1126/science.155.3765.1021>
- Mutlib, A. E., Gerson, R. J., Meunier, P. C., Haley, P. J., Chen, H., Gan, L. S., Davies, M. H., Gemzik, B., Christ, D. D., Krahn, D. F., Markwalder, J. A., Seitz, S. P., Robertson, R. T., & Miwa, G. T. (2000). The Species-Dependent Metabolism of Efavirenz Produces a Nephrotoxic Glutathione Conjugate in Rats. *Toxicology and Applied Pharmacology*, 169(1), 102–113. <https://doi.org/10.1006/taap.2000.9055>

- Nagase, H., & Saitoh, A. (2020). Research and development of κ opioid receptor agonists and δ opioid receptor agonists. *Pharmacology & Therapeutics*, 205, 107427. <https://doi.org/10.1016/j.pharmthera.2019.107427>
- Nebert, D. W., & Russell, D. W. (2002). Clinical importance of the cytochromes P450. *The Lancet*, 360(9340), 1155–1162. [https://doi.org/10.1016/S0140-6736\(02\)11203-7](https://doi.org/10.1016/S0140-6736(02)11203-7)
- Nestler, E. J. (2004). Historical review: Molecular and cellular mechanisms of opiate and cocaine addiction. *Trends in Pharmacological Sciences*, 25(4), 210–218. <https://doi.org/10.1016/j.tips.2004.02.005>
- Olson, K. M., Traynor, J. R., & Alt, A. (2021). Allosteric Modulator Leads Hiding in Plain Site: Developing Peptide and Peptidomimetics as GPCR Allosteric Modulators. *Frontiers in Chemistry*, 9. <https://www.frontiersin.org/articles/10.3389/fchem.2021.671483>
- Pathan, H., & Williams, J. (2012). Basic opioid pharmacology: An update. *British Journal of Pain*, 6(1), 11–16. <https://doi.org/10.1177/2049463712438493>
- Pedersen, M. F., Wróbel, T. M., Märcher-Rørsted, E., Pedersen, D. S., Møller, T. C., Gabriele, F., Pedersen, H., Matusiuk, D., Foster, S. R., Bouvier, M., & Bräuner-Osborne, H. (2020). Biased agonism of clinically approved μ -opioid receptor agonists and TRV130 is not controlled by binding and signaling kinetics. *Neuropharmacology*, 166, 107718. <https://doi.org/10.1016/j.neuropharm.2019.107718>
- Perrine, S. A., Hoshaw, B. A., & Unterwald, E. M. (2006). Delta opioid receptor ligands modulate anxiety-like behaviors in the rat. *British Journal of Pharmacology*, 147(8), 864–872. <https://doi.org/10.1038/sj.bjp.0706686>
- Phang-Lyn, S., & Llerena, V. A. (2021). Biochemistry, Biotransformation. In *StatPearls [Internet]*. StatPearls Publishing. <https://www.ncbi.nlm.nih.gov/books/NBK544353/>
- Pradhan, A. A. A., Becker, J. A. J., Scherrer, G., Tryoen-Toth, P., Filliol, D., Matifas, A., Massotte, D., Gavériaux-Ruff, C., & Kieffer, B. L. (2009). In Vivo Delta Opioid Receptor Internalization Controls Behavioral Effects of Agonists. *PLOS ONE*, 4(5), e5425. <https://doi.org/10.1371/journal.pone.0005425>
- Pradhan, A. A. A., Walwyn, W., Nozaki, C., Filliol, D., Erbs, E., Matifas, A., Evans, C., & Kieffer, B. L. (2010). Ligand-Directed Trafficking of the δ -Opioid Receptor In Vivo: Two Paths Toward Analgesic Tolerance. *Journal of Neuroscience*, 30(49), 16459–16468. <https://doi.org/10.1523/JNEUROSCI.3748-10.2010>
- Pradhan, A. A., Befort, K., Nozaki, C., Gavériaux-Ruff, C., & Kieffer, B. L. (2011). The delta opioid receptor: An evolving target for the treatment of brain disorders. *Trends in Pharmacological Sciences*, 32(10), 581–590. <https://doi.org/10.1016/j.tips.2011.06.008>
- Pradier, M. F., McCoy Jr, T. H., Hughes, M., Perlis, R. H., & Doshi-Velez, F. (2020). Predicting treatment dropout after antidepressant initiation. *Translational Psychiatry*, 10(1), Article 1. <https://doi.org/10.1038/s41398-020-0716-y>

- Prentis, R. A., Lis, Y., & Walker, S. R. (1988). Pharmaceutical innovation by the seven UK-owned pharmaceutical companies (1964-1985). *British Journal of Clinical Pharmacology*, 25(3), 387–396.
- Prueksaritanont, T., & Tang, C. (2012). ADME of Biologics—What Have We Learned from Small Molecules? *The AAPS Journal*, 14(3), 410–419. <https://doi.org/10.1208/s12248-012-9353-6>
- Rasmussen, N. A., & Farr, L. A. (2009). Beta-endorphin response to an acute pain stimulus. *Journal of Neuroscience Methods*, 177(2), 285–288. <https://doi.org/10.1016/j.jneumeth.2008.10.013>
- Remesic, M., Hruby, V. J., Porreca, F., & Lee, Y. S. (2017). Recent Advances in the Realm of Allosteric Modulators for Opioid Receptors for Future Therapeutics. *ACS Chemical Neuroscience*, 8(6), 1147–1158. <https://doi.org/10.1021/acscchemneuro.7b00090>
- Research and Development in the Pharmaceutical Industry | Congressional Budget Office*. (2021, April 8). <https://www.cbo.gov/publication/57126>
- Reyes-Alcaraz, A., Garcia-Rojas, E. Y. L., Bond, R. A., & McConnell, B. K. (2020). Allosteric Modulators for GPCRs as a Therapeutic Alternative with High Potential in Drug Discovery. In *Molecular Pharmacology*. IntechOpen. <https://doi.org/10.5772/intechopen.91838>
- Saitoh, A., Kimura, Y., Suzuki, T., Kawai, K., Nagase, H., & Kamei, J. (2004). Potential Anxiolytic and Antidepressant-Like Activities of SNC80, a Selective δ -Opioid Agonist, in Behavioral Models in Rodents. *Journal of Pharmacological Sciences*, 95(3), 374–380. <https://doi.org/10.1254/jphs.FPJ04014X>
- Serafini, G., Adavastro, G., Canepa, G., De Berardis, D., Valchera, A., Pompili, M., Nasrallah, H., & Amore, M. (2018). The Efficacy of Buprenorphine in Major Depression, Treatment-Resistant Depression and Suicidal Behavior: A Systematic Review. *International Journal of Molecular Sciences*, 19(8), 2410. <https://doi.org/10.3390/ijms19082410>
- Shang, Y., Yeatman, H. R., Provasi, D., Alt, A., Christopoulos, A., Canals, M., & Filizola, M. (2016). Proposed Mode of Binding and Action of Positive Allosteric Modulators at Opioid Receptors. *ACS Chemical Biology*, 11(5), 1220–1229. <https://doi.org/10.1021/acscchembio.5b00712>
- Sharma, D., Soni, M., Kumar, S., & Gupta, G. (2009). *Solubility Enhancement – Eminent Role in Poorly Soluble Drugs*. 5.
- Smith, J. S., Lefkowitz, R. J., & Rajagopal, S. (2018). Biased Signalling: From Simple Switches to Allosteric Microprocessors. *Nature Reviews. Drug Discovery*, 17(4), 243–260. <https://doi.org/10.1038/nrd.2017.229>

- St. Jean, D. J., & Fotsch, C. (2012). Mitigating Heterocycle Metabolism in Drug Discovery. *Journal of Medicinal Chemistry*, 55(13), 6002–6020. <https://doi.org/10.1021/jm300343m>
- Stanczyk, M. A., Livingston, K. E., Chang, L., Weinberg, Z. Y., Puthenveedu, M. A., & Traynor, J. R. (2019). The δ -opioid receptor positive allosteric modulator BMS 986187 is a G-protein-biased allosteric agonist. *British Journal of Pharmacology*, 176(11), 1649–1663. <https://doi.org/10.1111/bph.14602>
- Stein, C. (2016). Opioid Receptors. *Annual Review of Medicine*, 67(1), 433–451. <https://doi.org/10.1146/annurev-med-062613-093100>
- Stepan, A. F., Karki, K., McDonald, W. S., Dorff, P. H., Dutra, J. K., DiRico, K. J., Won, A., Subramanyam, C., Efremov, I. V., O'Donnell, C. J., Nolan, C. E., Becker, S. L., Pustilnik, L. R., Sneed, B., Sun, H., Lu, Y., Robshaw, A. E., Riddell, D., O'Sullivan, T. J., ... Obach, R. S. (2011). Metabolism-Directed Design of Oxetane-Containing Arylsulfonamide Derivatives as γ -Secretase Inhibitors. *Journal of Medicinal Chemistry*, 54(22), 7772–7783. <https://doi.org/10.1021/jm200893p>
- Stepan, A. F., Mascitti, V., Beaumont, K., & Kalgutkar, A. S. (2013). Metabolism-guided drug design. *MedChemComm*, 4(4), 631. <https://doi.org/10.1039/c2md20317k>
- Stevens, C. W. (2004). Opioid research in amphibians: An alternative pain model yielding insights on the evolution of opioid receptors. *Brain Research. Brain Research Reviews*, 46(2), 204–215. <https://doi.org/10.1016/j.brainresrev.2004.07.003>
- Stevens, C. W., Brasel, C. M., & Mohan, S. (2007). Cloning and bioinformatics of amphibian mu, delta, kappa, and nociceptin opioid receptors expressed in brain tissue: Evidence for opioid receptor divergence in mammals. *Neuroscience Letters*, 419(3), 189–194. <https://doi.org/10.1016/j.neulet.2007.04.014>
- Sun, D., Gao, W., Hu, H., & Zhou, S. (2022). Why 90% of clinical drug development fails and how to improve it? *Acta Pharmaceutica Sinica B*, 12(7), 3049–3062. <https://doi.org/10.1016/j.apsb.2022.02.002>
- Thompson, T. N. (2001). Optimization of metabolic stability as a goal of modern drug design. *Medicinal Research Reviews*, 21(5), 412–449. <https://doi.org/10.1002/med.1017>
- Toll, L., Bruchas, M. R., Calo', G., Cox, B. M., & Zaveri, N. T. (2016). Nociceptin/Orphanin FQ Receptor Structure, Signaling, Ligands, Functions, and Interactions with Opioid Systems. *Pharmacological Reviews*, 68(2), 419–457. <https://doi.org/10.1124/pr.114.009209>
- Trapaidze, N., Keith, D. E., Cvejic, S., Evans, C. J., & Devi, L. A. (1996). Sequestration of the δ Opioid Receptor. *Journal of Biological Chemistry*, 271(46), 29279–29285. <https://doi.org/10.1074/jbc.271.46.29279>
- Wang, C. W., & Chen, J. (2018). *N*-(phenylsulfonyl)benzamides and related compounds as bcl-2 inhibitors (World Intellectual Property Organization Patent WO2018027097A1). <https://patents.google.com/patent/WO2018027097A1/en?q=WO2018027097A1>

- Wang, J., Sánchez-Roselló, M., Aceña, J. L., del Pozo, C., Sorochinsky, A. E., Fustero, S., Soloshonok, V. A., & Liu, H. (2014). Fluorine in Pharmaceutical Industry: Fluorine-Containing Drugs Introduced to the Market in the Last Decade (2001–2011). *Chemical Reviews*, *114*(4), 2432–2506. <https://doi.org/10.1021/cr4002879>
- Waring, M. J. (2010). Lipophilicity in drug discovery. *Expert Opinion on Drug Discovery*, *5*(3), 235–248. <https://doi.org/10.1517/17460441003605098>
- Waterhouse, R. N. (2003). Determination of lipophilicity and its use as a predictor of blood–brain barrier penetration of molecular imaging agents. *Molecular Imaging & Biology*, *5*(6), 376–389. <https://doi.org/10.1016/j.mibio.2003.09.014>
- Wenthur, C. J., Gentry, P. R., Mathews, T. P., & Lindsley, C. W. (2014). Drugs for Allosteric Sites on Receptors. *Annual Review of Pharmacology and Toxicology*, *54*, 165–184. <https://doi.org/10.1146/annurev-pharmtox-010611-134525>
- Wester, M. R., Yano, J. K., Schoch, G. A., Yang, C., Griffin, K. J., Stout, C. D., & Johnson, E. F. (2004). The Structure of Human Cytochrome P450 2C9 Complexed with Flurbiprofen at 2.0-Å Resolution*. *Journal of Biological Chemistry*, *279*(34), 35630–35637. <https://doi.org/10.1074/jbc.M405427200>
- Williams, P. A., Cosme, J., Vinković, D. M., Ward, A., Angove, H. C., Day, P. J., Vonnrhein, C., Tickle, I. J., & Jhoti, H. (2004). Crystal Structures of Human Cytochrome P450 3A4 Bound to Metyrapone and Progesterone. *Science*, *305*(5684), 683–686. <https://doi.org/10.1126/science.1099736>
- Wootten, D., Christopoulos, A., Marti-Solano, M., Babu, M. M., & Sexton, P. M. (2018). Mechanisms of signalling and biased agonism in G protein-coupled receptors. *Nature Reviews Molecular Cell Biology*, *19*(10), Article 10. <https://doi.org/10.1038/s41580-018-0049-3>
- Wootten, D., Christopoulos, A., & Sexton, P. M. (2013). Emerging paradigms in GPCR allostery: Implications for drug discovery. *Nature Reviews Drug Discovery*, *12*(8), Article 8. <https://doi.org/10.1038/nrd4052>
- Wuitschik, G., Carreira, E. M., Wagner, B., Fischer, H., Parrilla, I., Schuler, F., Rogers-Evans, M., & Müller, K. (2010). Oxetanes in Drug Discovery: Structural and Synthetic Insights. *Journal of Medicinal Chemistry*, *53*(8), 3227–3246. <https://doi.org/10.1021/jm9018788>
- Yano, J. K., Wester, M. R., Schoch, G. A., Griffin, K. J., Stout, C. D., & Johnson, E. F. (2004). The Structure of Human Microsomal Cytochrome P450 3A4 Determined by X-ray Crystallography to 2.05-Å Resolution*. *Journal of Biological Chemistry*, *279*(37), 38091–38094. <https://doi.org/10.1074/jbc.C400293200>
- Yeung, C. K., Fujioka, Y., Hachad, H., Levy, R. H., & Isoherranen, N. (2011). Are circulating metabolites important in drug–drug interactions?: Quantitative analysis of risk prediction and inhibitory potency. *Clinical Pharmacology and Therapeutics*, *89*(1), 105–113. <https://doi.org/10.1038/clpt.2010.252>

- Zafrani, Y., Yeffet, D., Sod-Moriah, G., Berliner, A., Amir, D., Marciano, D., Gershonov, E., & Saphier, S. (2017). Difluoromethyl Bioisostere: Examining the “Lipophilic Hydrogen Bond Donor” Concept. *Journal of Medicinal Chemistry*, *60*(2), 797–804. <https://doi.org/10.1021/acs.jmedchem.6b01691>
- Zaretzki, J., Matlock, M., & Swamidass, S. J. (2013). XenoSite: Accurately Predicting CYP-Mediated Sites of Metabolism with Neural Networks. *Journal of Chemical Information and Modeling*, *53*(12), 3373–3383. <https://doi.org/10.1021/ci400518g>
- Zhang, Z., Zhu, M., & Tang, W. (2009). Metabolite Identification and Profiling in Drug Design: Current Practice and Future Directions. *Current Pharmaceutical Design*, *15*(19), 2220–2235. <https://doi.org/10.2174/138161209788682460>

Chapter 2 Structure-Activity Relationships (SAR) and Improvement of DOR-MOR Selectivity in the Xanthene Series

2.1 Summary

Major depressive disorder (MDD) has become one of the most prevalent mental disorders across the world. Yet, the effectiveness of current anti-depressant drugs remains questionable due to the complexity and comorbidity of MDD with other diseases, such as chronic pain. Recent research findings have shown that the δ -opioid receptor (DOR) plays a significant role in mood regulation, in addition to affording analgesia. Targeting DOR with positive allosteric modulation has been investigated with a series of xanthene-diones. BMS986187 (**1**) is a xanthene-dione and a potent DOR positive allosteric modulator (PAM). In this chapter, a structure-activity-relationship study of **1** is described. This was conducted to further optimize the DOR activity and improve selectivity over μ -opioid receptors (MOR) since compounds acting at MOR have abuse liability and safety issues.

2.2 Introduction

Major depressive disorder (MDD) is one of the top three causes reducing quality of life due to disability (James et al., 2018). Although several types of antidepressant drugs with different mechanisms of action are available clinically, approximately 50-60% of the patients do not respond to current treatments and fall into unproductive trial-and-change cycles (Fava, 2003; *Major Depression*, n.d.; Kasper, 2022). Overall, approximately 50% of the patients prescribed with antidepressant drugs drop out of treatment (Pradier et al., 2020). Furthermore, the comorbidity

of MDD with anxiety and chronic pain, which affects more than one third of the North American population, makes MDD difficult to diagnose and manage (Khoo et al., 2022; Li, 2015; Gaskin & Richard, 2012; “Depressive Disorders,” 2022).

The δ -opioid receptor (DOR), a member of the opioid receptor family and a class A G protein-coupled receptor (GPCR), together with its endogenous ligands, the enkephalins has been implicated in mood regulation and chronic pain (Chung & Kieffer, 2013; Filliol et al., 2000). Consequently, DOR agonists have antidepressant, anxiolytic, and analgesic effects in rats and mice (Saitoh et al., 2004; Perrine et al., 2006; Chung & Kieffer, 2013; Chen et al., 2022; Gallantine & Meert, 2005), without the abuse liability of agonists acting at the mu-opioid receptor (MOR). Although the beneficial effects of DOR activation make it a plausible therapeutic target, activation of DOR can lead to pro-convulsive activity; DOR agonists are also susceptible to profound tolerance (Gallantine & Meert, 2005; Charbogne et al., 2014; Burford, Livingston, et al., 2015; Chung & Kieffer, 2013; Chen et al., 2022; Bourdonnec et al., 2008; Le Bourdonnec et al., 2009; Nagase & Saitoh, 2020). However, despite these issues, several DOR agonists have been studied for their therapeutic potential and one compound, AZD2327, has been evaluated in Phase 2 clinical trials for antidepressant and anxiolytic activity, although dosing was adjusted to account for potential convulsant activity (Richards et al., 2016).

There is considerable interest in the development of allosteric modulators of GPCRs (Foster and Conn, 2017) including DOR (Livingston and Traynor, 2018). Such compounds bind to a site on the receptor that is topographically distinct from the orthosteric site which is defined as the binding site for the native ligand of a particular GPCR. By binding to a distinct site, allosteric modulators can promote (positive allosteric modulators or PAMs) or inhibit (negative allosteric modulators or NAMs) the action of agonists, endogenous or exogenous, acting at the

orthosteric site. In the case of an endogenous hormone or neurotransmitter a PAM would promote activity at its cognate receptor, without altering its spatial or temporal release pattern. Thus, PAMs of DOR (DOR-PAMs) are predicted to enhance the action of endogenous DOR peptides released in mood disorders and thereby promote their antidepressant and anti-anxiety effects. Additionally, since DOR-PAMs do not alter the spatial and temporal release of peptide ligands for DOR, side-effects, in particular pro-convulsant activity and tolerance development, will be reduced (Melancon et al., 2012; Livingston & Traynor, 2018; Olson et al., 2021; Rasmussen & Farr, 2009). Moreover, an ideal DOR-PAM would not show activity in the absence of an orthosteric ligand (Reyes-Alcaraz et al., 2020; Melancon et al., 2012; Livingston & Traynor, 2018; Wootten et al., 2013) and exhibit a ceiling to its action when the allosteric site is saturated, thereby further reducing the potential for side-effects (Gao & Jacobson, 2013; Melancon et al., 2012; Stanczyk et al., 2019).

A previous high-throughput screening (HTS) effort, identified a series of xanthene-diones as DOR-PAMs, exemplified by, BMS986187 (**1**) (**Figure 2.1**). BMS-986187 is also active as a PAM at MOR, albeit with lower activity (Livingston et al., 2018) which could be problematic in promoting the actions of MOR agonists, for example their abuse liability.

In this chapter I describe the synthesis and evaluation of derivatives of **1** to enhance

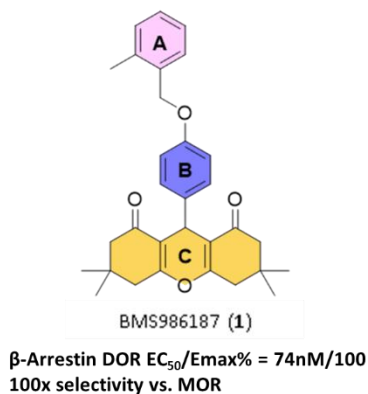


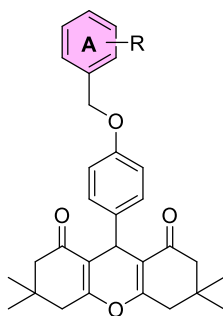
Figure 2.1 Structure and profile of xanthene series, BMS986187 (**1**). Three different compartments of **1** for optimization are highlighted in colors: A-ring (pink), B-ring (blue), and C-ring (yellow).

selectivity for DOR over MOR. Optimization strategies focused on adding substituents to the benzyl moiety (A-ring) and substitutions in the phenol (B-ring). One action downstream of an agonist occupied GPCR is the recruitment of the protein β -arrestin to the receptor (see chapter 1). Therefore, to evaluate the synthesized derivatives for DOR-PAM activity and selectivity over MOR the level of recruitment of β -arrestin2 to DOR or MOR was evaluated using the PathHunter® β -arrestin assay in CHO cells, as described (Burford, Livingston, et al., 2015; Bassoni et al., 2012). In this assay the ability of each new derivative to enhance the activity of an effective concentration 20-40 (EC_{20} - EC_{40}) of the DOR and MOR endogenous opioid peptide methionine enkephalin was determined. This provided a potency measure (EC_{50}) for each derivative. Furthermore, as activated opioid receptors lead to the inhibition of adenylyl cyclase activity, which in turn lowers cAMP abundance, selected analogs were evaluated with the cAMP-Glo accumulation assay (Promega Corporation).

2.3 Results and Discussion

2.3.1 Exploration of the A-Ring (Benzyl Group)

Table 2.1: SAR table for functionalization of the benzyl group with methyl- and halogen-substituents



β-Arrestin Recruitment ^a

Compound (CCG)	R	DOR EC ₅₀ (μM)/E _{max}	MOR EC ₅₀ (μM)/E _{max}	Selectivity MOR/DOR ^b
1	2-Methyl	0.074/100	7.57/100	102
361257	H	0.50/80	>10/ N/A	>20
363240	3-Methyl	0.72/113	N/A	N/A
362683	4-Methyl	2.83/100	>10/ N/A	>3
364644	2-Methoxy	1.88/100	>10/ N/A	>5
363237	3-Methoxy	2.75/76	>10/ N/A	>3
363238	4-Methoxy	0.88/84	>10/ N/A	>11
361196	2-Fluoro	0.71/74	>10/ N/A	>14
257408	3-Fluoro	0.49/80	>10/ N/A	>20
361195	4-Fluoro	0.54/80	>10/ N/A	>18
364641	2-Chloro	0.047/88*	>10/ N/A	>212
365668	3-Chloro	0.41/76	>10/ N/A	>24
364642	4-Chloro	0.60/96	>10/ N/A	>16
362911	2-Bromo	1.89/87	>10/ N/A	>5
362912	3-Bromo	>10/ N/A	>10/ N/A	N/A
362913	4-Bromo	2.87/53	>10/ N/A	>3
362939	2-Iodo	0.15/81	10/82	>66
362974	3-Iodo	1.25/86	>10/ N/A	>8
362934	4-Iodo	>10/ N/A	>10/ N/A	N/A
361375	2,3-Difluoro	0.58/69	>10/ N/A	>17
361256	2,4-Difluoro	0.30/101	>10/ N/A	>33
361337	2,5-Difluoro	0.73/91	>10/ N/A	>13
361318	2,6-Difluoro	0.50/92	>10/ N/A	>20
361255	3,4-Difluoro	0.33/88	>10/ N/A	>30
361355	3,5-Difluoro	0.38/103	>10/ N/A	>30
361319	2-Fluoro-5-chloro	1.09/85	>10/ N/A	>9
361335	2-Fluoro-4-chloro	0.32/97	>10/ N/A	>31
362686	2-Fluoro-6-chloro	1.25/82	>10/ N/A	>8
362731	2-Fluoro-3-chloro	2.01/77	>10/ N/A	>4
364647	3-Fluoro-2-chloro	2.64/103	10/73	>3
362685	3-Fluoro-4-chloro	1.73/62	>10/ N/A	>5
362730	3-Fluoro-5-chloro	0.99/97	>10/ N/A	>10
362732	3-Fluoro-6-chloro	3.72/91	>10/ N/A	>2
362733	4-Fluoro-2-chloro	0.33/91	>10/ N/A	>30

362734	4-Fluoro-3-chloro	0.47/57	>10/ N/A	>21
364646	2,3-Dichloro	1.40/91	>10/ N/A	>7
365857	3,4-Dichloro	1.42/83	>10/ N/A	>7
366790	2,6-Dichloro	0.081/97	6/65	74
366794	2,4-Dichloro	0.58/111	>10/ N/A	>17
362684	2,3-Dimethyl	3.10/85	>10/ N/A	>3
363138	2,4-Dimethyl	0.34/75	>10/ N/A	>29
363239	2,5-Dimethyl	0.32/114	>10/ N/A	>31
363241	3,4-Dimethyl	0.33/101	>10/ N/A	>30
362687	3,5-Dimethyl	2.62/91	>10/ N/A	>4
363137	2,6-Dimethyl	0.048/100*	2.3/100	8
364643	2-Methyl-4-fluoro	0.22/100	>10/ N/A	>45
364648	2-Methyl-4-chloro	0.26/76	>10/ N/A	>38
362935	3-Bromo-5-methyl	0.99/80	>10/ N/A	>10
362936	3-Bromo-2-methyl	>10/ N/A	>10/ N/A	N/A
362937	3-Bromo-4-methyl	0.55/60	>10/ N/A	>18
362938	2-Bromo-6-methyl	0.035/91	>10/ N/A	>285
362975	4-Bromo-3-methyl	3.28/84	>10/ N/A	>3
363011	3-Bromo-6-methyl	0.24/79	>10/ N/A	>41
363012	2-Bromo-3-methyl	>10/N/A	>10/ N/A	N/A
363013	2-Bromo-4-methyl	1.40/71	>10/ N/A	>7
363014	4-Bromo-2-methyl	0.58/100	>10/ N/A	>17
363015	2,4-Dibromo	0.60/100	>10/ N/A	>16
363016	3,4-Dibromo	0.36/87	>10/ N/A	>27
365920	2-Methoxy-4-chloro	0.19/90	>10/ N/A	>52
362680	2-Naphthalene	1.1/77	>10/ N/A	>9

a. All the analogs were tested in “PAM mode” in the presence of an EC₂₀ concentration of Met-enkephalin for both DOR and MOR. Mean values of EC₅₀ (potency) and maximal effect (Emax) are reported in the table (n = ≥2). Emax values of **1** for both DOR and MOR were normalized to 100%, and other analogs are adjusted relative to **1**. *b.* potency ratios of MOR over DOR were calculated from the EC₅₀ values. *Analog was tested in PAM mode in the presence of an EC₄₀ of the DOR agonist DPDPE (n = ≥3).

2.3.1.1. Methyl and halogen substitutions

In a small, reported structure–activity relationship (SAR) study within the xanthene-dione series, the 2-methyl derivative **1** emerged as the most potent and selective analog amongst mono-substituted benzyl congeners with a reported DOR potency of 0.03 μM (Burford, Livingston, et al., 2015). In our hands **1** had similar properties with an EC₅₀ to recruit β-arrestin to DOR of 0.07 μM compared to 7.6 μM at MOR. Removal of the 2-methyl to release a conformation lock on the A-

ring and reduce hydrophobic interactions provided **CCG361257** (Figure 2.2).

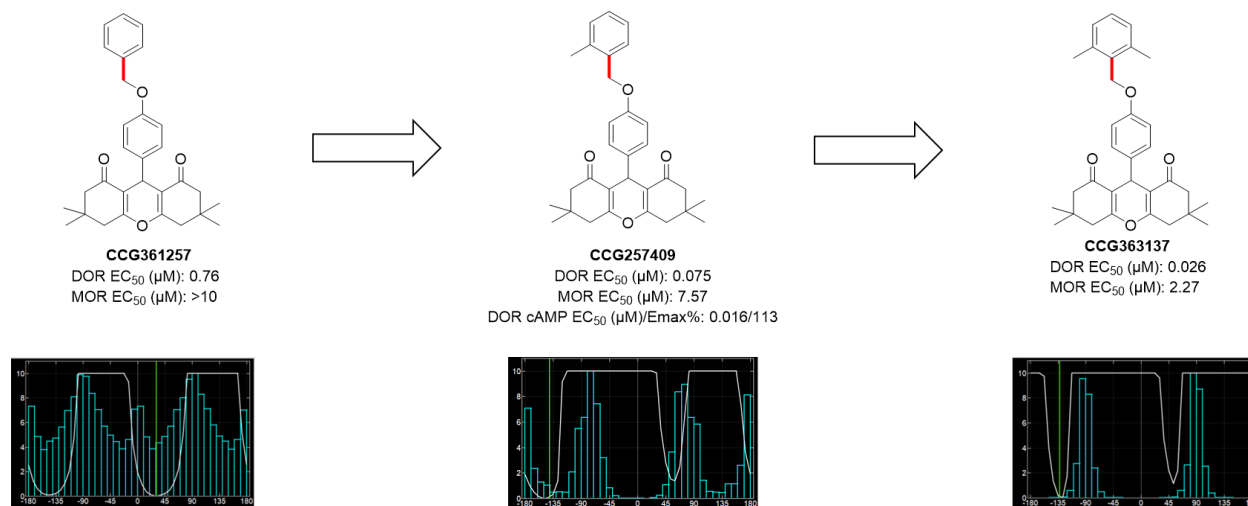


Figure 2.2 Conformation restrictions developed on the benzyl group (bond highlighted in red) with the addition of one methyl group (**CCG257409**) or two methyl groups (**CCG363137**) in comparison to **CCG361257**. DOR/MOR-PAM activities of each analog are given below the structures. The energy-dihedral angle plot of each analog is shown. Energy conformations that are predicted by MOE (Molecular Operating Environment) in the gas phase are shown by the white line, and real crystal structure distribution of conformations is shown by the blue bars. The green shows where the current conformation of the selected bond is in the plot.

This compound exhibited a 6-fold drop in potency towards DOR ($EC_{50} = 0.5 \mu\text{M}$). Moving the methyl substituent to the 3- or especially the 4- position also resulted in a considerable loss of activity as did di-substitution with the 3,4- and 3,5- substitutions being particularly unfavorable (**Table 2.1**).

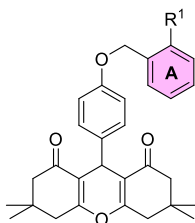
A 2-Cl > 2-Iodo group efficiently substituted for 2-methyl, although the 2-Br did not. Again, both 3- and especially 4-substitutions were less favored, maintaining a moderate level of potency or complete loss of activity in DOR, with EC_{50} s in the range of 0.4 - >10 μM . Fluorinated derivatives showed a reduction in potency of 8-10-fold compared to the parent **1**, but the activity of the fluoro compounds, unlike other substituents, was not dependent on its position in the ring.

In the di-halogenated series, the 2,6-dichloro substituted analogue (**CCG366790**) ($EC_{50} = 0.081 \mu\text{M}$) (**Table 2.1**), was particularly favored over the other di-halo derivatives presumably because this substitution pattern provided a conformational lock. The 2,6-dimethyl moiety

(**CCG363137**) which also generated the same conformation restriction as the 2,6-dichloro (**CCG366790**) showed a similar result ($EC_{50} = 0.026 \mu\text{M}$; **Figure 2.2**). Dihalogenated 2,3- and 2,5-derivatives were disfavored by DOR, with a 50-fold or more loss in potency relative to **1**. In contrast, the 2,4-dihalo analogs maintained some DOR activity levels in the 0.3-0.6 μM range. Of the halogenated derivatives only the 2,6-dichloro derivative (**CCG366790**) showed any improvement in activity at MOR (6 μM , **Table 2.1**).

We also examined combinations of halogens with methyl substitutions. Of these compounds only the 2-Bromo-6-methyl retained DOR activity of the parent again likely due to the created conformation lock, all other combinations lost activity.

Table 2.2: SAR table for ortho-substitution (R1) of the benzyl group



Compound	R ¹	<u>β-Arrestin Recruitment^a</u>		Selectivity MOR/DOR ^b
		DOR EC ₅₀ (μM)/E _{max}	MOR EC ₅₀ (μM)/E _{max}	
1	Methyl	0.074/100	7.57/100	102
362688	CF ₃	2.78/100	>10/ N/A	>3
367264	CF ₂ H	0.29/103	>10/ N/A	>34
369551	CFH ₂	0.29/94	>10/ N/A	>34
365669	OCF ₃	0.19/82	>10/ N/A	
365670	OCF ₂ H	0.21/80	>10/ N/A	
366697	Ethyl	0.16/98	6.4/100	40
362750	Isopropyl	0.14/98	>10/ N/A	>71
362691	<i>tert</i> -butyl	0.059/96	>10/ N/A	>169
362751	cyclopropyl	0.11/96	>10/ N/A	>90
367265	Cyano	2.93/111	>10/ N/A	>3
369832	Morpholin-4-yle	0.36/88*	>10/ N/A	>10

a-b. Same as **Table 2.1**. * Analog was tested in the presence of an EC₄₀ of DPDPE (n = \geq 3)

2.3.1.2. Exploration of Electrostatic effects

Since the requirements for PAM activity at DOR strongly favored a 2-substitution in the benzyl group, we explored electron-withdrawing groups at this position (J. Wang et al., 2014). Replacement of the 2-methyl with 2-OMe (**CCG-364644**) afforded a drastic loss of potency as did 2-trifluoromethyl (**CCG362688**), and 2-cyano (**CCG367265**). The reduction in DOR-PAM activity with a 2-morpholin-4-yle substituent (**CCG369832**) was less severe. Replacing the trifluoromethyl (**CCG362688**) with difluoromethyl moiety (**CCG367264**) or fluoromethyl (**CCG369551**) recovered activity by approximately 10-fold, possibly because the protons can serve as lipophilic donors and stabilize the conformation of the phenyl ring (Zafrani et al., 2017; Wang et al., 2014). Both trifluoromethoxy (**CCG365669**) and difluoromethoxy (**CCG365670**) moieties exhibited about a 10-fold increase in potency compared to the 2-methoxy derivative (**CCG364644**).

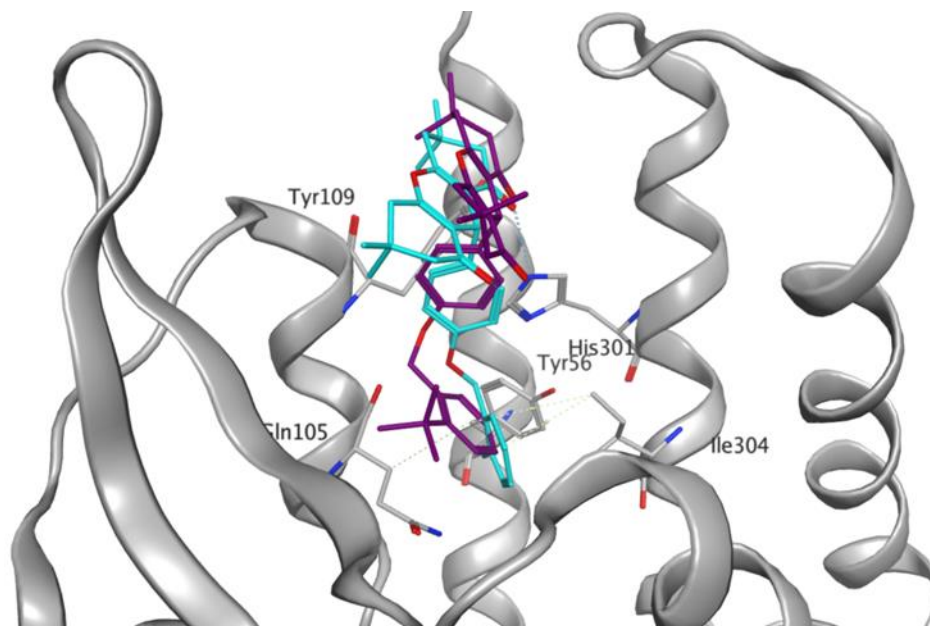


Figure 2.3 Docking pose and structural rationalization of CCG362691 (purple) in hDOR (grey) (pdb: 6PT3) with structural conformation change relative to 1 (blue).

2.3.1.2. Exploration of steric effects

To probe the space-limiting size of the binding site, sterically larger lipophilic functional groups were systematically incorporated into 2-position of the A ring. The starting 2-methyl of **1** was replaced by ethyl, cyclopropyl, isopropyl or butyl (**Table 2.2**). All substituents were within 2-fold of the activity of **1**, and the ethyl-derivative showed a similar MOR activity as **1**. (**Table 2.6**). This suggests that the DOR binding site at this position must be rather large and flexible, easily accommodating 2-substituents of increasing size and lipophilicity.

Furthermore, docking of t-butyl derivative into the orthosteric site of the active DOR structure (PDB: 6PT3) suggested a change in binding mode compared to **1**. (**Figure 2.2**). This change without a corresponding change in potency suggests that it will be difficult to gain DOR potency by modifying the 2-position of the benzyl group.

2.3.2 Exploration of B ring and A-B ring attachments

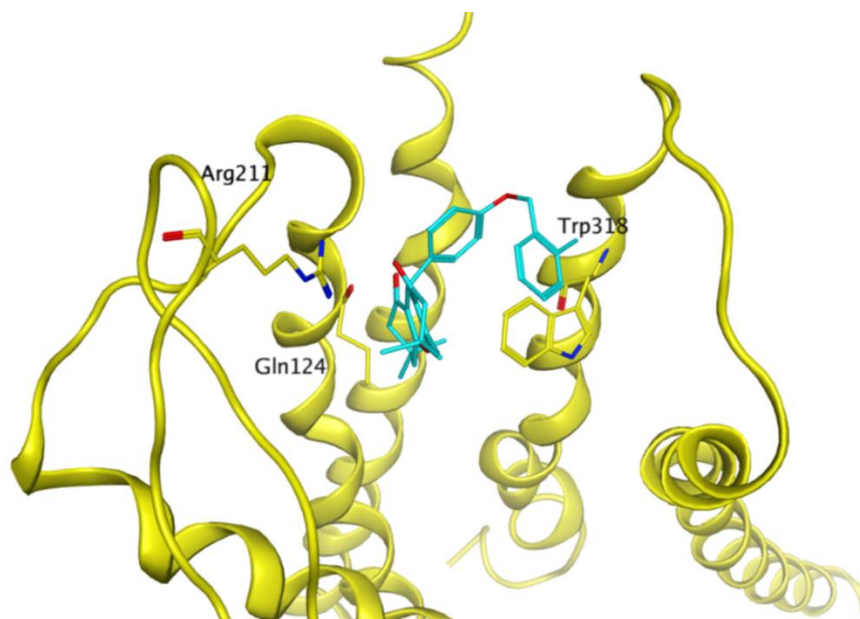
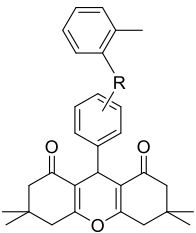
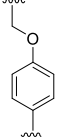
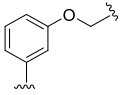
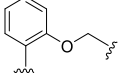
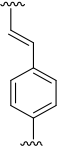


Figure 2.4 Hairpin-like binding mode of **1** (blue) to MOR (yellow) (PDB: 6DDF).

It was observed that **1** could potentially bind to DOR and especially MOR (PDB: 6DDF) in a hairpin shape. (**Figure 2.3**). To test this hypothesis, analogs **CCG362910**, **CCG363017**, and **CCG362711** which have natural hairpin-like folding conformations of different angles were synthesized. None of the three analogs exhibited MOR activity and had only weak potency at DOR (**CCG362910** and **CCG362711**) or lost potency (**CCG363017**) (**Table 2.3**). These results suggest that xanthene-dione series compounds do not bind in a hairpin-like conformation.

Table 2.3: SAR table for the linker and binding mode of Xanthene series

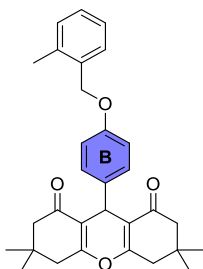


Compound	R	<u>β-Arrestin Recruitment^a</u>		Selectivity MOR/DOR ^b
		DOR EC ₅₀ (μ M)/E _{max}	MOR EC ₅₀ (μ M)/E _{max}	
1		0.074/100	7.57/100	102
362910		5.33/87	>10/ N/A	>2
363017		>10/ N/A	>10/ N/A	N/A
362711		3.32/100	>10/ N/A	>3

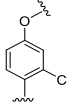
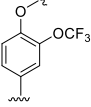
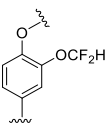
a-b. Same as **Table 2.1**.

2.3.3 DOR selectivity is optimized by a conformation lock in the phenol ring

Table 2.4: SAR table for substitution of the B-ring



Compound	B	<u>β-Arrestin Recruitment^a</u>		Selectivity ^b
		DOR EC ₅₀ (μ M)/E _{max}	MOR EC ₅₀ (μ M)/E _{max}	
362904		0.24/95*	>10/ N/A**	>416
363081		0.087/85*	>10/ N/A**	>1,100
366165		>10/ N/A	>10/ N/A	N/A
366204		>10/ N/A	>10/ N/A	N/A
366695		>10/ N/A	>10/ N/A	N/A
366696		>10/ N/A	>10/ N/A	N/A
362897		0.54/105	6.66/48	12
366047		0.42/95	>10/ N/A***	>24

367065		0.78/78	>10/ N/A***	>13
366126		0.86/100	>10/ N/A	>12
366128		0.32/90	>10/ N/A	>116

a-b. Same as Table 2.1. *Analog was tested in PAM mode in the presence of an EC₄₀ of DPDPE (n = 3) for the detection of signal. **No activity was observed at 100 μM. ***No MOR activity was observed at 30 μM.

Despite the high structural similarity between DOR and MOR and the evidence for a conserved allosteric binding site (Livingston et al., 2018), conformations of the side-chain residues in the putative allosteric site of MOR are different from DOR. The binding mode of **1** to DOR is incompatible with a similar binding mode in MOR. Hence, we hypothesized that enhanced activity and selectivity for DOR could be achieved by locking the conformation of **1** at its linking B-ring, thereby hindering rotation (Wenthur et al., 2014). Strategically located methyl substituents on the B ring of **1** were investigated (Table 2.4). Both 3-methyl-4-((2-methylbenzyl)oxy)phenyl (CCG362904), which locks the rotatable bond of the phenyl and 2-methyl-4-((2-methylbenzyl)oxy)phenyl (CCG363081), which locks the rotatable bond of the C-ring, were synthesized. CCG363081 (EC₅₀ = 0.087 μM) retained the DOR PAM activity of the parent, whereas CCG363081 showed a 3-fold loss in potency (EC₅₀ = 0.24 μM). Moreover, these two compounds were not active at MOR even at 100 μM in the β-arrestin recruitment assay, with no MOR activity detected in the more sensitive cAMP accumulation assay at 10 μM (Table 2.6). Only CCG362897, incorporating a 3-fluoro-4-((2-methylbenzyl)oxy)phenyl fragment, showed appreciable activity as a MOR PAM, although this compound lost potency as a DOR PAM. The

Cl derivatives were similarly less active at DOR as was incorporation of electron-withdrawing groups.

In addition to conformational restriction that was formed by the methyl groups in the B-ring, I hypothesized that the loss of MOR activity might also be due to the clashes created by both 2-methyl and 3-methyl of the B-ring with side chains His319 (7.36) and Trp318 (7.35), respectively in the putative MOR allosteric site (**Figure 2.5**). Moreover, methyl substitutions in the B-ring changed the conformation of ring A. Our docking poses showed the methyl group of **CCG362904** generated a mild intramolecular steric repulsion on ring A such that it clashes with the side-chain of Gln124 (2.60) in MOR (**Figure 2.5A**). The methyl group of **CCG363081** is further away from ring A and clashed with Ile322 (7.39) (**Figure 2.5B**). The postulated clashes created by the methyl groups could explain the complete loss of MOR activity.

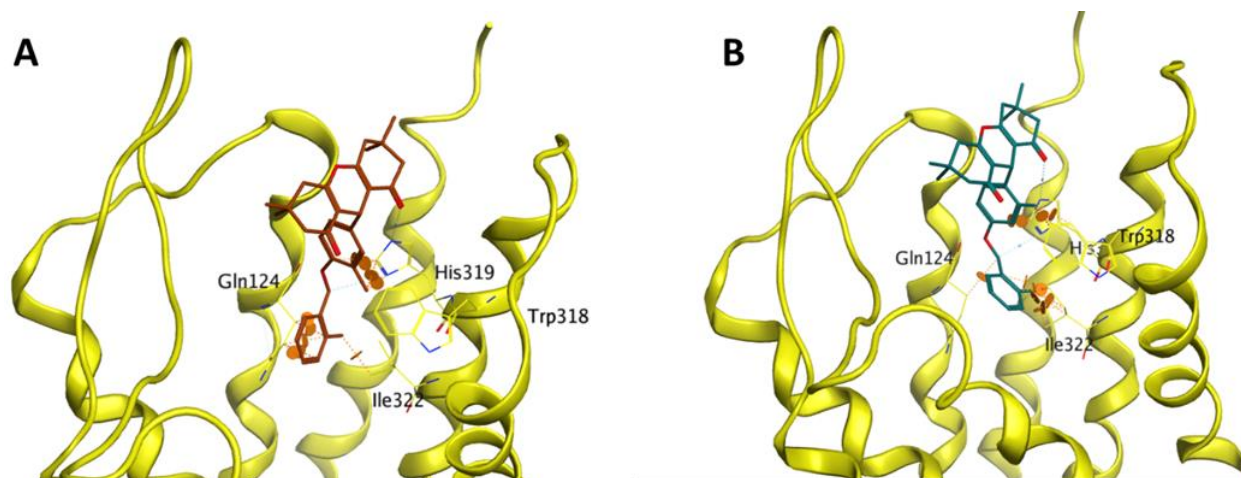
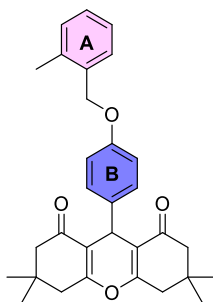
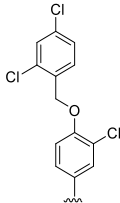
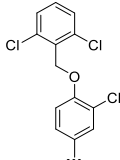


Figure 2.5 A. Structural rationale for low potency of CCG362904 (brown) at hMOR (yellow) (pdb: 6DDF). The 2-methyl group in ring B clashes (orange circles) with His319 (7.36) and conformational change at the benzyl group clashes with Gln124 (2.60). B. Structural rationale for low potency of CCG363081 (green) at hMOR. The 3-methyl group on the B-ring clashes with Trp318 (7.35). Additional conformational change at the benzyl group of **CCG363081** clashes with Ile322 (7.39).

Table 2.5: Combined substitutions of A- and B-rings



Compound	B	<u>β-Arrestin Recruitment</u> ^a		Selectivity ^b
		DOR EC ₅₀ (μM)/Emax	MOR EC ₅₀ (μM)/Emax	
366027		0.86/82	>10/ N/A	>11
366026		0.43/70	>10/ N/A	>23
366046		0.40/85	>10/ N/A*	>75
366127		0.32/130	>10/ N/A	>31
366129		0.70/70	10/ N/A	>14
366162		1.61/73	>10/ N/A	>6

366792		0.88/79	>10/ N/A	>11
366791		1.37/79	>10/ N/A	>7

a-b. Same as **Table 2.1**. *No MOR activity was observed at >30 μM .

2.3.4 Combined modifications of A- and B-rings

After studying changes separately on both the A- and B-rings, combinations were examined (**Table 2.5**). Unfortunately, analogs with combined modifications did not maintain nanomolar potency in DOR. Most of the analogs had moderate DOR activity between 0.3-1.6 μM .

2.3.5 Confirmation assay, cAMP accumulation assay for selected analogs

To further verify the activities of selected analogs, the cAMP accumulation assay which measures opioid-mediated inhibition of the enzyme adenylyl cyclase was used. This assay is more sensitive than the β -arrestin recruitment assay due to amplified downstream signaling. For instance, **1** exhibited an EC_{50} at DOR of 0.074 μM in β -arrestin recruitment assay but an EC_{50} of 0.016 μM in the cAMP assay (**Figure 2.5**). This increase of signal sensitivity was also seen at MOR where **1** exhibited an EC_{50} of 0.32 μM , compared to 7.6 μM in the β -arrestin assay. Thus, the selectivity of **I** for DOR compared to MOR as measured in this assay is only 20-fold, which may explain why the compound shows MOR activity in vivo (see thesis introduction).

Table 2.6: Confirmation Assay of Selected Analogs

Compound	DOR EC_{50} (μM)/ E_{max}	cAMP Accumulation ^a	
		MOR EC_{50} (μM)/ E_{max}	

1	0.016/100	0.32/100
366790	0.028/98 ^b	
362688	0.068/96	
367264	0.0076/130	
365920	0.033/116	
368551	0.012/116	
362691	0.032/93	
362904	0.11/97	>10/ N/A
363081	0.092/86	>10/ N/A
366047	0.095/89	

a. Selected analogs were tested in PAM mode to measure cAMP accumulation level in the presence of an EC40 of DPDPE in DOR cells and an EC40 of DAMGO in MOR cells, n = 3. b. Analog was tested with n = 2.

Most of the selected analogs in **Table 2.6** showed similar DOR potency in the range 0.01-0.03 μM which further confirmed the data from our primary assay. We also observed that the 2-trifluoro moiety (**CCG362688**) exhibited a high potency as a DOR PAM in this assay (cAMP EC₅₀ = 0.068 μM) in stark contrast to its activity in the vs. β -arrestin assay (EC₅₀ = 2.78 μM). Since adenylyl cyclase is downstream of G protein activation, this suggests the compound enhances activity in a G protein biased manner. Among all the selected analogs listed in **Table 2.6**, the 2-difluoro moiety (**CCG367264**) was the most potent DOR PAM with an EC₅₀ of 0.008 μM (8 nM). Furthermore, methyl substitutions in B-ring, to give **CCG362904** and **CCG363081** exhibited a high level of DOR activity (DOR cAMP EC₅₀ = ~0.10 μM) and improved selectivity over MOR (MOR cAMP EC₅₀ = >10 μM) confirming the selectivity from the β -arrestin assay (**Figure 2.5**).

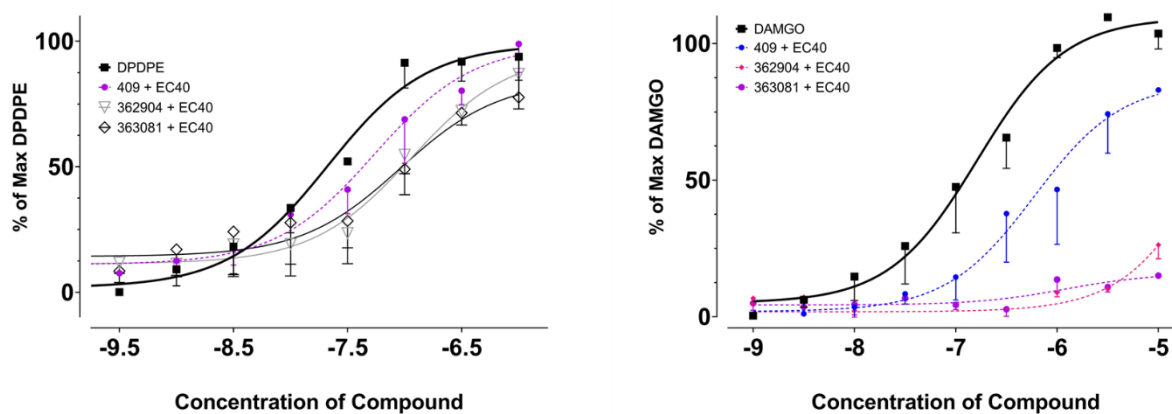
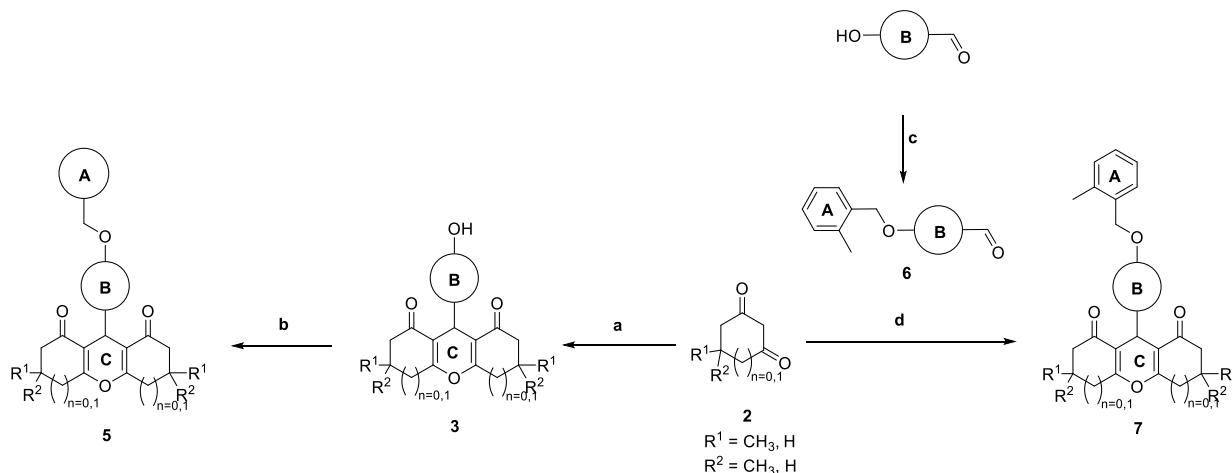


Figure 2.6 cAMP accumulation data curves of standards, DPDPE (DOR) (Left) and DAMGO (MOR) (Right), **1** (409), **CCG362904**, or **CCG363081** in the presence of appropriate orthosteric agonist.

2.3.6 Synthetic routes to xanthene-dione analogs

The synthesis of analogs **5a-6e** started from two different routes (**Scheme 2.1**). In the first route, commercially available diones **2** underwent Knoevenagel condensation with the desired 4-hydroxycarbaldehyde to yield intermediate **3**, and further substitution with the desired halides to obtain the final compounds **5** (Burford, Livingston, et al., 2015). In the second route, the desired carbaldehyde was protected with desired benzyl halides to form intermediate **6**, and further

Scheme 2.1 Synthetic routes for generating xanthene analogs



Reagents and Condition: (a) desired 4-hydroxycarbaldehyde, H_2SO_4 , 70% IPA, reflux, 16h (50-80%); (b) desired halides, Cs_2CO_3 , DMF, RT, 16h; (c) 2-methylbenzyl bromide, Cs_2CO_3 , DMF, RT, 16h, (60-80%); (d) ZnCl_2 , 70% IPA, reflux, 16h (50-80%)

condensed with desired dione **2** to form the final compounds **7** (Ganesan et al., n.d.).

2.4 Conclusion

In summary, we have explored requirements for the binding of the xanthene-dione PAMs to the allosteric site on DOR. The results suggest the allosteric pocket is large. In addition, docking studies suggest that **1** might not bind in the same conformation and position in MOR as in DOR. Thus, by introducing an extra-conformation lock at the center aromatic ring (B-ring) with methyl groups we were able to maintain DOR activity and enhance selectivity over MOR. In particular,

CCG363081 is especially promising as a DOR PAM that lacks MOR activity with a potency as a DOR PAM of 0.09 μM in the cAMP and β -arrestin assays and $> 100 \mu\text{M}$ at MOR in the β -arrestin assay and $>10\mu\text{M}$ in the cAMP assay.

One caveat to the findings is that I have only tested the PAMs using the peptides Met-enkephalin and (in a few assays) its DOR preferring derivative DPDPE as the orthosteric ligand. No other DOR peptides or small molecule DOR ligands were used. Similarly at MOR only Met-enkephalin and its close synthetic analogue DAMGO were used. Due to the phenomenon of probe dependence, it is possible we could see different sensitivities at DOR and MOR using a more diverse set of orthosteric agonists.

2.5 Methods, Synthesis and Experimental

2.5.1 *Cell lines*

PathHunter® eXpress β -Arrestin GPCR cells are engineered to co-express the ProLink™ (PK) tagged GPCR and the Enzyme Acceptor (EA) tagged β -Arrestin. Activation of the GPCR-PK induces β -Arrestin-EA recruitment, forcing complementation of the two β -galactosidase enzyme fragments (EA and PK). These cells have been modified to express the MOR, and the DOR in 2 distinct cell lines.

2.5.2 *β -arrestin2 Recruitment Assay*

The PathHunter® β -galactosidase enzyme complementation assay (DiscoverRx, Fremont, CA) was used to measure β -arrestin 2 recruitment to hDOR or hMOR expressed in CHO cells as described (Burford et al., 2013). In this assay one part of the β -galactosidase enzyme is attached to the receptor and one part to β -arrestin2. When β -arrestin 2 is recruited to DOR or MOR the two parts form an active enzyme. Cells expressing either DOR or MOR were incubated with varying concentrations of test compounds for 60 min at 37°C in the presence of a concentration of standard opioid (Met-enkephalin/DPDPE/DAMGO) causing a 20 or 40% response (EC20/40). Concentration curves for the standards were determined in each assay and the lead compound was included in each assay to ensure consistency. β -galactosidase activity following enzyme complementation was detected by luminescence using a Synergy 2 plate reader (Biotech, Winooski, VT). All assays were done in quadruplicate, repeated 2-3x.

2.5.3 *Forskolin Stimulated cAMP Inhibition*

Forskolin-stimulated cAMP inhibition was measured using the cAMP-Glo™ assay (Promega, WI), following the manufacturer's instructions. MOR, and DOR (DiscoverRx, Fremont, CA) cells were treated with agonist for 10 mins, followed by addition of 1 μ M forskolin (Cayman Chemicals) treated for an additional 15 minutes. Luminescence was read on a MicroBeta (PerkinElmer, Waltham, MA). All assays were done in quadruplicate and repeated 2-3x.

2.5.4 Computational Modeling Studies

a. DOR-MOR Overlay Model

DOR (6PT3) and MOR (6DDF) were loaded into Molecular Operating Environment 2023 (Molecular Operating Environment (MOE), 2023; Chemical Computing Group ULC, 910-1010 Sherbrooke St. West, Suite #910, Montreal, QC H3A 2R7, Canada, 2023), and the QuickPrep function was used to prepare the protein structures. After the preparation was complete, alignment of the protein sequences was performed, and a super-position of the proteins was then created into the 3D space which is referred to as an overlay model.

b. Docking at Allosteric Binding Site

To determine the allosteric binding sites of DOR/MOR and binding poses of the DOR PAMs, general MOE docking protocol was followed. The orthosteric agonists of the receptors were selected as the placement. Other used parameters include: Amber 10:EHT for force field, rigid receptor refinement, and London dG, GBVI/WSA dG for the scoring method. All the docking results underwent refinement through visual inspection and comparison with literature values. Compounds with desired binding poses were further examined in both receptors.

2.5.5 Chemistry

Unless explicitly specified otherwise, the experimental procedures were conducted under the following conditions. All operations took place at room temperature (approximately 18°C to 25°C), 90°C, 120°C with reflux, or within a pressure vessel under a nitrogen atmosphere. Solvent evaporation was carried out using a rotary evaporator under reduced pressure. The progress of the reaction was monitored either by thin layer chromatography (TLC) or liquid chromatography (LC), and the provided reaction times are for illustrative purposes only. Silica gel chromatography was performed using a CombiFlash® system (Teledyne Isco, Inc., Lincoln, NE, USA) with pre-packed silica gel cartridges or on Merck silica gel 60 (230-400 mesh) (Merck KGaA, Darmstadt, Germany). The structure and purity of all final products were verified using at least one of the following analytical methods: nuclear magnetic resonance (NMR) and LC-MS.

a. NMR

NMR data was acquired at the Biochemical NMR Core Laboratory, College of Pharmacy, University of Michigan, using an Agilent 400MHz and 500MHz MR spectrometer equipped with

analysis was performed using MestreNova 14.1.0 by Mestrelab Research S.L. Chemical shift (δ) values are reported in parts per million (ppm) relative to tetramethyl silane (TMS), which served as the internal standard. Coupling constants (J) are expressed in hertz (Hz), and standard abbreviations for signal shape include: s for singlet, d for doublet, t for triplet, m for multiplet, br for broad, etc.

b. ESI-MS

Unless explicitly stated otherwise, the electrospray ionization-mass spectrometric (ESI-MS) procedures were conducted using electrospray ionization (ESI) in positive mode on a Waters LCT time-of-flight (TOF) mass spectrometer from Waters Corp. (Milford, MA, USA). A solvent carrier gradient of 100% to 85% solvent A (water with 0.1% trifluoroacetic acid) and 0% to 15% solvent B (acetonitrile with 0.1% trifluoroacetic acid and methanol with 0.1% trifluoroacetic acid) was employed. The reported ion forms are (M+H)⁺, (M+Na)⁺, or (M+K)⁺, obtained from the mass spectra. Retention times in minutes (RT) are reported based on the chromatographic spectra acquired.

c. HPLC

Unless explicitly stated otherwise, the liquid chromatographic analysis was conducted using an Agilent LAB CDS Chemstation Edition for LC and LC/MS system. The chromatograms were analyzed using Agilent Open LAB Intelligent Reporting A.01.06.111 software. Samples were prepared at a concentration of 1 mg/mL, and the injection volume was set to 5-10 μ L. For elution, a gradient of mobile phase consisting of water:acetonitrile (90:10) to acetonitrile:water (90:10) over a duration of 13 minutes was utilized. Both water and acetonitrile were supplemented with 0.1% trifluoroacetic acid (TFA) (Method-1), and an Agilent Eclipse C-18 column was employed. The compounds were assayed at a UV wavelength of 250 nm, and the retention times (RT) are reported in minutes.

Intermediate 3 Procedure

9-(4-hydroxyphenyl)-3,3,6,6-tetramethyl-3,4,5,6,7,9-hexahydro-1*H*-xanthene-1,8(2*H*)-dione (**3**)
To a solution of 4-hydroxybenzaldehyde (500 mg, 1 Eq, 4.09 mmol) and 5,5-dimethylcyclohexane-1,3-dione (1.18 g, 2.05 Eq, 8.39 mmol) in 70% IPA (13mL) was treated with H₂SO₄ (80.3 mg, 43.6 μ L, 0.2 Eq, 819 μ mol). The yellow reaction mixture was refluxed for 5 h and cooled to room temperature. Precipitates formed overnight. The solids were filtered and

washed with cold 70% IPA. White solids formed (0.57g, 38% yield). ¹H NMR (499 MHz, dmsO) δ 9.13 (s, 1H), 7.00 – 6.83 (m, 2H), 6.62 – 6.49 (m, 2H), 4.39 (s, 1H), 3.30 (s, 2H), 2.53 (d, *J* = 18.1 Hz, 2H), 2.23 (d, *J* = 16.1 Hz, 2H), 2.05 (d, *J* = 16.2 Hz, 2H), 1.01 (s, 6H), 0.88 (s, 6H).

Compound 5a General Procedures

To a solution of 9-(4-hydroxyphenyl)-3,3,6,6-tetramethyl-3,4,5,6,7,9-hexahydro-1*H*-xanthene-1,8(2*H*)-dione (80 mg, 1 Eq, 0.22 mmol) and benzyl halide (52 mg, 1.2 Eq, 0.26 mmol) in DMF (1mL) was treated with Cs₂CO₃ (0.14 g, 2 Eq, 0.44 mmol). The reaction mixture was stirred at room temperature for 16 h. The reaction was diluted with water, and the solids were filtered. The crude material was chromatographed over silica gel, eluting with 0-40% EtOAc/Hex. Compounds were isolated above 95% pure.

9-(4-((2,3-dimethylbenzyl)oxy)phenyl)-3,3,6,6-tetramethyl-3,4,5,6,7,9-hexahydro-1H-xanthene-1,8(2H)-dione (CCG362684) [sz-08-06]

Following the general procedure on a scale of 60mg (0.16mmol) 9-(4-hydroxyphenyl)-3,3,6,6-tetramethyl-3,4,5,6,7,9-hexahydro-1*H*-xanthene-1,8(2*H*)-dione (**3**), 1-(bromomethyl)-2,3-dimethylbenzene (52 mg, 1.2 Eq, 0.26 mmol) was used and isolated 0.1g (96% yield) of the desired product. ¹H NMR (499 MHz, cdcl₃) δ 7.22 (dd, *J* = 9.2, 2.7 Hz, 3H), 7.17 – 7.12 (m, 1H), 7.09 (t, *J* = 7.5 Hz, 1H), 6.90 – 6.80 (m, 2H), 4.95 (s, 2H), 4.72 (s, 1H), 2.46 (s, 4H), 2.31 (s, 3H), 2.28 – 2.11 (m, 7H), 1.10 (s, 6H), 1.01 (s, 6H). ¹³C NMR (126 MHz, cdcl₃) δ 196.51, 162.07, 157.45, 137.12, 136.69, 135.60, 134.81, 130.01, 129.32, 127.03, 125.49, 115.79, 114.28, 69.09, 50.78, 40.87, 32.20, 31.00, 29.25, 27.40, 20.33, 14.87. ESI MS *m/z* 485.26 (M + H)⁺

3,3,6,6-tetramethyl-9-(4-((4-methylbenzyl)oxy)phenyl)-3,4,5,6,7,9-hexahydro-1H-xanthene-1,8(2H)-dione (CCG363683) [sz-08-07]

Following the general procedure on a scale of 70mg (0.19mmol) 9-(4-hydroxyphenyl)-3,3,6,6-tetramethyl-3,4,5,6,7,9-hexahydro-1*H*-xanthene-1,8(2*H*)-dione (**3**), 1-(bromomethyl)-4-methylbenzene (61 mg, 2 Eq, 0.33 mmol) was used and isolated 0.05g (64% yield) of the desired product. ¹H NMR (499 MHz, cdcl₃) δ 7.34 – 7.24 (m, 2H), 7.23 – 7.09 (m, 4H), 6.91 – 6.72 (m, 2H), 4.92 (s, 2H), 4.70 (s, 1H), 2.45 (s, 4H), 2.35 (s, 3H), 2.29 – 2.09 (m, 4H), 1.10 (s, 6H), 0.99 (s, 6H). ¹³C NMR (126 MHz, cdcl₃) δ 196.45, 162.03, 157.39, 137.60, 136.63, 134.16, 129.30, 129.17, 127.69, 115.79, 114.31, 69.85, 50.76, 40.86, 32.19, 30.95, 29.24, 27.37, 21.17. ESI MS *m/z* 471.25 (M + H)⁺

9-(4-(benzyloxy)phenyl)-3,3,6,6-tetramethyl-3,4,5,6,7,9-hexahydro-1H-xanthene-1,8(2H)-dione (CCG361257) [SEH-07-078]

White solids isolated 0.07 g (60% yield). ¹H NMR (400 MHz, Chloroform-d) δ 7.45 – 7.27 (m, 5H), 7.20 (d, J = 8.7 Hz, 2H), 6.83 (d, J = 8.7 Hz, 2H), 4.97 (s, 2H), 4.70 (s, 1H), 2.45 (s, 4H), 2.27 – 1.93 (m, 4H), 1.09 (s, 6H), 0.99 (s, 6H). HPLC: 99.4% (retention time, 7.90 min)

9-(4-((2-fluorobenzyl)oxy)phenyl)-3,3,6,6-tetramethyl-3,4,5,6,7,9-hexahydro-1H-xanthene-1,8(2H)-dione (CCG361196) [SEH-07-075]

White solids isolated 0.09 g (71% yield). ¹H NMR (400 MHz, Chloroform-d) δ 7.47 (d, J = 1.8 Hz, 1H), 7.28 (d, J = 7.3 Hz, 1H), 7.22 – 7.14 (m, 2H), 7.14 – 7.07 (m, 1H), 7.06 – 6.98 (m, 1H), 6.87 – 6.75 (m, 2H), 5.04 (s, 2H), 4.70 (s, 1H), 2.45 (s, 4H), 2.30 – 2.08 (m, 4H), 1.09 (s, 6H), 0.99 (s, 6H). HPLC: 96.0% (retention time, 7.90 min).

9-(4-((4-fluorobenzyl)oxy)phenyl)-3,3,6,6-tetramethyl-3,4,5,6,7,9-hexahydro-1H-xanthene-1,8(2H)-dione (CCG361195) [SEH-07-074A]

White solids isolated 0.08 g (63% yield). ¹H NMR (400 MHz, Chloroform-d) δ 7.40 – 7.29 (m, 2H), 7.22 – 7.11 (m, 2H), 7.07 – 6.91 (m, 2H), 6.89 – 6.59 (m, 2H), 4.92 (s, 2H), 4.70 (s, 1H), 2.45 (s, 4H), 2.26 – 2.03 (m, 4H), 1.09 (s, 6H), 0.99 (s, 6H). HPLC: 100% (retention time, 7.88 min).

9-(4-((2,3-difluorobenzyl)oxy)phenyl)-3,3,6,6-tetramethyl-3,4,5,6,7,9-hexahydro-1H-xanthene-1,8(2H)-dione (CCG361375) [SEH-07-085]

White solids isolated 0.08 g (62% yield). ¹H NMR (400 MHz, Chloroform-d) δ 7.25 – 7.14 (m, 3H), 7.13 – 6.98 (m, 2H), 6.90 – 6.67 (m, 2H), 5.06 (d, J = 1.4 Hz, 2H), 4.70 (s, 1H), 2.45 (s, 4H), 2.28 – 2.01 (m, 4H), 1.10 (s, 6H), 0.99 (s, 6H). HPLC: 99.3% (retention time, 7.95 min)

9-(4-((2,4-difluorobenzyl)oxy)phenyl)-3,3,6,6-tetramethyl-3,4,5,6,7,9-hexahydro-1H-xanthene-1,8(2H)-dione (CCG361256) [SEH-07-077]

White solids isolated 0.1 g (77% yield). ¹H NMR (400 MHz, Chloroform-d) δ 7.48 – 7.37 (m, 1H), 7.28 – 7.17 (m, 2H), 6.92 – 6.76 (m, 4H), 4.98 (s, 2H), 4.70 (s, 1H), 2.45 (s, 4H), 2.28 – 2.12 (m, 4H), 1.09 (s, 6H), 0.99 (s, 6H). HPLC: 99.4% (retention time, 7.88 min)

9-(4-((2,5-difluorobenzyl)oxy)phenyl)-3,3,6,6-tetramethyl-3,4,5,6,7,9-hexahydro-1H-xanthene-1,8(2H)-dione (CCG361337) [SEH-07-083]

White solids isolated 0.07 g (55% yield). ¹H NMR (400 MHz, Chloroform-d) δ 7.28 – 7.15 (m, 3H), 6.98 (dtt, J = 23.8, 8.3, 4.0 Hz, 2H), 6.87 – 6.78 (m, 2H), 5.02 (s, 2H), 4.70 (s, 1H), 2.45 (s, 4H), 2.28 – 2.07 (m, 4H), 1.10 (s, 6H), 0.99 (s, 6H). HPLC: 94.9% (retention time, 7.96 min)

9-(4-((2,6-difluorobenzyl)oxy)phenyl)-3,3,6,6-tetramethyl-3,4,5,6,7,9-hexahydro-1H-xanthene-1,8(2H)-dione (CCG361318) [SEH-07-080]

White solids isolated 0.9 g (70% yield). ¹H NMR (400 MHz, Chloroform-d) δ 7.35 – 7.24 (m, 2H), 7.24 – 7.16 (m, 2H), 6.96 – 6.80 (m, 3H), 5.03 (s, 2H), 4.70 (s, 1H), 2.45 (s, 4H), 2.28 – 2.12 (m, 4H), 1.10 (s, 6H), 0.99 (s, 6H). HPLC: 100% (retention time, 7.85 min)

9-(4-((3,4-difluorobenzyl)oxy)phenyl)-3,3,6,6-tetramethyl-3,4,5,6,7,9-hexahydro-1H-xanthene-1,8(2H)-dione (CCG361255) [SEH-07-076]

White solids isolated 0.09 g (68% yield). ¹H NMR (400 MHz, Chloroform-d) δ 7.25 – 7.14 (m, 3H), 7.13 – 6.98 (m, 2H), 6.86 – 6.66 (m, 2H), 4.91 (s, 2H), 4.69 (s, 1H), 2.45 (s, 4H), 2.32 – 2.07 (m, 4H), 1.10 (s, 6H), 0.99 (s, 6H). HPLC: 100% (retention time, 7.99 min)

9-(4-((3,5-difluorobenzyl)oxy)phenyl)-3,3,6,6-tetramethyl-3,4,5,6,7,9-hexahydro-1H-xanthene-1,8(2H)-dione (CCG361355) [SEH-07-084]

White solids isolated 0.1 g (78% yield). ¹H NMR (400 MHz, Chloroform-d) δ 7.29 – 7.17 (m, 2H), 6.96 – 6.88 (m, 2H), 6.83 – 6.75 (m, 2H), 6.78 – 6.68 (m, 1H), 4.95 (s, 2H), 4.70 (s, 1H), 2.45 (s, 4H), 2.30 – 1.95 (m, 4H), 1.10 (s, 6H), 0.99 (s, 6H). HPLC: 98.9% (retention time, 8.04 min)

9-(4-((5-chloro-2-fluorobenzyl)oxy)phenyl)-3,3,6,6-tetramethyl-3,4,5,6,7,9-hexahydro-1H-xanthene-1,8(2H)-dione (CCG361319) [SEH-07-081]

White solids isolated 0.1 g (81% yield). ¹H NMR (400 MHz, Chloroform-d) δ 7.47 (dd, J = 6.2, 2.7 Hz, 1H), 7.28 – 7.18 (m, 3H), 7.00 (t, J = 9.0 Hz, 1H), 6.87 – 6.79 (m, 2H), 5.00 (s, 2H), 4.70 (s, 1H), 2.45 (s, 4H), 2.23 – 2.17 (m, 4H), 1.26 (s, 0H), 1.10 (s, 6H), 0.99 (s, 6H). HPLC: 98.9% (retention time, 8.28 min)

9-(4-((4-chloro-2-fluorobenzyl)oxy)phenyl)-3,3,6,6-tetramethyl-3,4,5,6,7,9-hexahydro-1H-xanthene-1,8(2H)-dione (CCG361335) [SEH-07-082]

White solids isolated 0.11 g (84% yield). ¹H NMR (400 MHz, Chloroform-d) δ 7.41 (t, J = 8.0 Hz, 1H), 7.21 (d, J = 8.6 Hz, 2H), 7.17 – 7.06 (m, 2H), 6.81 (d, J = 8.6 Hz, 2H), 5.00 (s, 2H), 4.70 (s, 1H), 2.45 (s, 4H), 2.29 – 2.07 (m, 4H), 1.10 (s, 6H), 0.99 (s, 6H). HPLC: 94.7% (retention time, 8.32 min)

9-(4-((2-isopropylbenzyl)oxy)phenyl)-3,3,6,6-tetramethyl-3,4,5,6,7,9-hexahydro-1H-xanthene-1,8(2H)-dione (CCG362750) [SEH-07-088]

White solids isolated 0.08 g (61% yield). ¹H NMR (400 MHz, Chloroform-d) δ 7.38 – 7.28 (m, 3H), 7.26 – 7.13 (m, 3H), 6.88 – 6.80 (m, 2H), 4.97 (s, 2H), 4.71 (s, 1H), 3.16 (p, J = 6.9 Hz, 1H),

2.46 (s, 4H), 2.29 – 2.13 (m, 4H), 1.24 (d, J = 6.8 Hz, 6H), 1.10 (s, 6H), 1.00 (s, 6H). HPLC: 99.3% (retention time, 8.55 min)

9-(4-((2-(tert-butyl)benzyl)oxy)phenyl)-3,3,6,6-tetramethyl-3,4,5,6,7,9-hexahydro-1H-xanthene-1,8(2H)-dione (CCG362691) [SEH-07-087A]

White solids isolated 0.04 g (29% yield). ¹H NMR (400 MHz, Chloroform-d) δ 7.51 – 7.39 (m, 2H), 7.31 – 7.18 (m, 4H), 6.89 – 6.81 (m, 2H), 5.15 (s, 2H), 4.71 (s, 1H), 2.46 (d, J = 1.0 Hz, 4H), 2.29 – 2.12 (m, 4H), 1.41 (s, 9H), 1.10 (s, 6H), 1.01 (s, 6H). HPLC: 96.5% (retention time, 8.71 min)

9-(4-((2-cyclopropylbenzyl)oxy)phenyl)-3,3,6,6-tetramethyl-3,4,5,6,7,9-hexahydro-1H-xanthene-1,8(2H)dione (CCG362751) [SEH-07-089]

White solids isolated 0.1 g (75% yield). ¹H NMR (400 MHz, Chloroform-d) δ 7.38 (dd, J = 7.2, 1.4 Hz, 1H), 7.29 – 7.13 (m, 4H), 7.07 – 7.00 (m, 1H), 6.90 – 6.83 (m, 2H), 5.14 (s, 2H), 4.71 (s, 1H), 2.45 (s, 4H), 2.28 – 2.13 (m, 4H), 1.97 (ddd, J = 13.9, 8.6, 5.4 Hz, 1H), 1.10 (s, 6H), 1.00 (s, 6H), 0.96 – 0.87 (m, 2H), 0.72 – 0.63 (m, 2H). HPLC: 97.4% (retention time, 8.39 min)

3,3,6,6-tetramethyl-9-(4-((2-(trifluoromethyl)benzyl)oxy)phenyl)-3,4,5,6,7,9-hexahydro-1H-xanthene-1,8(2H)-dione (CCG362688) [sz-08-10]

Following the general procedure on a scale of 70mg (0.19mmol) 9-(4-hydroxyphenyl)-3,3,6,6-tetramethyl-3,4,5,6,7,9-hexahydro-1H-xanthene-1,8(2H)-dione (**3**), 1-(bromomethyl)-2-(trifluoromethyl)benzene (91 mg, 58 μL, 2 Eq, 0.38 mmol) was used and isolated 0.07g (70% yield) of the desired product. ¹H NMR (499 MHz, cdcl₃) δ 7.71 (d, J = 7.8 Hz, 1H), 7.65 (d, J = 7.9 Hz, 1H), 7.57 – 7.47 (m, 1H), 7.38 (t, J = 7.6 Hz, 1H), 7.23 – 7.17 (m, 2H), 6.87 – 6.76 (m, 2H), 5.18 (s, 2H), 4.70 (s, 1H), 2.44 (d, J = 1.1 Hz, 4H), 2.28 – 2.12 (m, 4H), 1.09 (s, 6H), 0.99 (s, 6H). ¹³C NMR (126 MHz, cdcl₃) δ 196.46, 162.08, 156.82, 137.13, 132.08, 129.41, 128.62, 127.48, 115.72, 114.39, 65.97, 50.75, 40.85, 40.85, 32.18, 30.97, 29.21, 27.38. ¹⁹F NMR (470 MHz, cdcl₃) δ -113.30 (dd, J = 8.9, 6.1 Hz). ESI MS m/z 525.22 (M + H)⁺

9-(4-((3,5-dimethylbenzyl)oxy)phenyl)-3,3,6,6-tetramethyl-3,4,5,6,7,9-hexahydro-1H-xanthene-1,8(2H)-dione (CCG362687) [sz-08-11]

Following the general procedure on a scale of 70mg (0.19mmol) 9-(4-hydroxyphenyl)-3,3,6,6-tetramethyl-3,4,5,6,7,9-hexahydro-1H-xanthene-1,8(2H)-dione (**3**), 1-(bromomethyl)-3,5-dimethylbenzene (76 mg, 2 Eq, 0.38 mmol) was used and isolated 0.07g (72% yield) of the desired product. ¹H NMR (499 MHz, cdcl₃) δ 7.23 – 7.16 (m, 2H), 7.00 (d, J = 1.7 Hz, 2H), 6.93 (s, 1H),

6.89 – 6.78 (m, 2H), 4.88 (s, 2H), 4.70 (s, 1H), 2.45 (s, 4H), 2.33 (s, 6H), 2.26 – 2.11 (m, 4H), 1.09 (s, 6H), 0.99 (s, 6H). ¹³C NMR (126 MHz, cdcl₃) δ 196.44, 162.05, 157.44, 138.06, 137.02, 136.65, 129.52, 125.46, 115.78, 114.32, 70.06, 50.77, 40.85, 32.18, 32.18, 29.25, 27.35, 21.25. ESI MS m/z 485.27 (M + H)⁺

3,3,6,6-tetramethyl-9-(4-((2-methylbenzyl)oxy)phenyl)-3,4,5,6,7,9-hexahydro-1H-xanthene-1,8(2H)-dione (CCG257409) [sz-08-12]

Following the general procedure on a scale of 70mg (0.19mmol) 9-(4-hydroxyphenyl)-3,3,6,6-tetramethyl-3,4,5,6,7,9-hexahydro-1H-xanthene-1,8(2H)-dione (**3**), 1-(bromomethyl)-2-methylbenzene (42 mg, 30 μL, 1.2 Eq, 0.23 mmol) was used and isolated 0.05g (50% yield) of the desired product. ¹H NMR (499 MHz, cdcl₃) δ 7.36 (dd, J = 6.7, 2.4 Hz, 1H), 7.25 – 7.14 (m, 5H), 6.86 – 6.80 (m, 2H), 4.93 (s, 2H), 4.70 (s, 1H), 2.45 (s, 4H), 2.33 (s, 3H), 2.28 – 2.11 (m, 4H), 1.09 (s, 6H), 0.99 (s, 6H). ¹³C NMR (126 MHz, cdcl₃) δ 196.48, 162.04, 157.42, 136.72, 135.00, 130.30, 129.31, 128.76, 125.96, 115.78, 114.28, 68.47, 50.77, 40.86, 32.18, 30.99, 29.23, 27.38, 18.87. ESI MS m/z 471.25 (M + H)⁺

9-(4-((2-chloro-6-fluorobenzyl)oxy)phenyl)-3,3,6,6-tetramethyl-3,4,5,6,7,9-hexahydro-1H-xanthene-1,8(2H)-dione (CCG362686) [sz-08-13]

Following the general procedure on a scale of 70mg (0.19mmol) 9-(4-hydroxyphenyl)-3,3,6,6-tetramethyl-3,4,5,6,7,9-hexahydro-1H-xanthene-1,8(2H)-dione (**3**), 2-(bromomethyl)-1-chloro-3-fluorobenzene (85 mg, 52 μL, 2 Eq, 0.38 mmol) was used and isolated 0.06g (66% yield) of the desired product. ¹H NMR (499 MHz, cdcl₃) δ 7.29 – 7.19 (m, 4H), 7.01 (ddd, J = 9.3, 8.1, 1.4 Hz, 1H), 6.92 – 6.77 (m, 2H), 5.08 (d, J = 1.9 Hz, 2H), 4.71 (s, 1H), 2.45 (d, J = 1.0 Hz, 4H), 2.26 – 2.11 (m, 4H), 1.09 (s, 6H), 1.00 (s, 6H). ¹³C NMR (126 MHz, cdcl₃) δ 196.46, 162.05, 157.14, 137.01, 130.56, 130.48, 129.34, 125.48, 125.45, 122.70, 115.75, 114.35, 60.91, 50.75, 40.86, 32.19, 31.01, 29.23, 27.39. ¹⁹F NMR (470 MHz, cdcl₃) δ -60.40. ESI MS m/z 509.19 (M + H)⁺

9-(4-((4-chloro-3-fluorobenzyl)oxy)phenyl)-3,3,6,6-tetramethyl-3,4,5,6,7,9-hexahydro-1H-xanthene-1,8(2H)-dione (CCG362685) [sz-08-14]

Following the general procedure on a scale of 70mg (0.19mmol) 9-(4-hydroxyphenyl)-3,3,6,6-tetramethyl-3,4,5,6,7,9-hexahydro-1H-xanthene-1,8(2H)-dione (**3**), 4-(bromomethyl)-1-chloro-2-fluorobenzene (85 mg, 2 Eq, 0.38 mmol) was used and isolated 0.08g (80% yield) of the desired product. ¹H NMR (499 MHz, cdcl₃) δ 7.36 (dd, J = 8.2, 7.5 Hz, 1H), 7.23 – 7.15 (m, 3H), 7.09 (ddd, J = 8.3, 2.0, 0.9 Hz, 1H), 6.86 – 6.73 (m, 2H), 4.93 (s, 2H), 4.69 (s, 1H), 2.44 (d, J = 1.1 Hz,

4H), 2.19 (q, J = 16.3 Hz, 4H), 1.09 (s, 6H), 0.98 (s, 6H). ¹³C NMR (126 MHz, cdcl₃) δ 196.45, 162.10, 159.11, 157.12, 156.77, 138.32, 137.23, 130.59, 129.44, 123.44, 123.41, 120.21, 115.68, 115.53, 115.36, 114.32, 68.55, 50.74, 40.84, 32.18, 31.01, 29.24, 27.32. ¹⁹F NMR (470 MHz, cdcl₃) δ -115.16 (dd, J = 9.7, 7.5 Hz). ESI MS m/z 509.18 (M + H)⁺

9-(4-((2-chloro-5-fluorobenzyl)oxy)phenyl)-3,3,6,6-tetramethyl-3,4,5,6,7,9-hexahydro-1H-xanthene-1,8(2H)-dione (CCG362732) [sz-08-15]

Following the general procedure on a scale of 70mg (0.19mmol) 9-(4-hydroxyphenyl)-3,3,6,6-tetramethyl-3,4,5,6,7,9-hexahydro-1H-xanthene-1,8(2H)-dione (**3**), 2-(bromomethyl)-1-chloro-4-fluorobenzene (85 mg, 52 μL, 2 Eq, 0.38 mmol) was used and isolated 0.07g (67% yield) of the desired product. ¹H NMR (400 MHz, cdcl₃) δ 7.30 (td, J = 8.9, 4.0 Hz, 2H), 7.25 – 7.20 (m, 2H), 6.94 (ddd, J = 8.8, 7.8, 3.0 Hz, 1H), 6.87 – 6.77 (m, 2H), 5.04 (s, 2H), 4.71 (s, 1H), 2.46 (s, 4H), 2.27 – 2.12 (m, 4H), 1.10 (s, 6H), 0.99 (s, 6H). ¹³C NMR (101 MHz, cdcl₃) δ 196.52, 162.79, 162.15, 160.34, 156.64, 137.36, 137.34, 137.28, 130.39, 129.51, 129.43, 126.71, 126.68, 115.68, 115.48, 115.42, 115.31, 114.40, 66.55, 50.80, 50.74, 50.68, 40.93, 40.84, 32.20, 31.05, 30.95, 29.30, 29.24, 27.37, 27.32. ¹⁹F NMR (376 MHz, cdcl₃) δ -114.68 (ddd, J = 9.0, 7.6, 4.9 Hz). ESI MS m/z 531.17 (M + Na)⁺

9-(4-((3-chloro-4-fluorobenzyl)oxy)phenyl)-3,3,6,6-tetramethyl-3,4,5,6,7,9-hexahydro-1H-xanthene-1,8(2H)-dione (CCG362734) [sz-08-16]

Following the general procedure on a scale of 70mg (0.19mmol) 9-(4-hydroxyphenyl)-3,3,6,6-tetramethyl-3,4,5,6,7,9-hexahydro-1H-xanthene-1,8(2H)-dione (**3**), 4-(bromomethyl)-2-chloro-1-fluorobenzene (85 mg, 51 μL, 2 Eq, 0.38 mmol) was used and isolated 0.08g (79% yield) of the desired product. ¹H NMR (499 MHz, cdcl₃) δ 7.44 (dd, J = 7.0, 2.1 Hz, 1H), 7.30 – 7.17 (m, 3H), 7.11 (t, J = 8.7 Hz, 1H), 6.86 – 6.75 (m, 2H), 4.90 (s, 2H), 4.70 (s, 1H), 2.45 (s, 4H), 2.19 (q, J = 16.3 Hz, 4H), 1.09 (s, 6H), 0.99 (s, 6H). ¹³C NMR (126 MHz, cdcl₃) δ 196.45, 162.13, 158.63, 156.85, 156.65, 137.22, 134.34, 129.67, 129.44, 127.19, 127.13, 121.11, 120.97, 116.65, 116.48, 115.68, 114.33, 68.58, 50.76, 40.84, 32.18, 31.02, 29.25, 27.31. ¹⁹F NMR (470 MHz, cdcl₃) δ -116.83 (q, J = 7.0 Hz). ESI MS m/z 509.18 (M + H)⁺

9-(4-((2-chloro-4-fluorobenzyl)oxy)phenyl)-3,3,6,6-tetramethyl-3,4,5,6,7,9-hexahydro-1H-xanthene-1,8(2H)-dione (CCG362733) [sz-08-17]

Following the general procedure on a scale of 70mg (0.19mmol) 9-(4-hydroxyphenyl)-3,3,6,6-tetramethyl-3,4,5,6,7,9-hexahydro-1H-xanthene-1,8(2H)-dione (**3**), 1-(bromomethyl)-2-chloro-4-

fluorobenzene (85 mg, 2 Eq, 0.38 mmol) was used and isolated 0.08g (78% yield) of the desired product. ¹H NMR (400 MHz, cdcl₃) δ 7.49 (dd, J = 8.7, 6.1 Hz, 1H), 7.24 – 7.17 (m, 2H), 7.13 (dd, J = 8.5, 2.6 Hz, 1H), 6.98 (td, J = 8.4, 2.6 Hz, 1H), 6.89 – 6.74 (m, 2H), 5.02 (s, 2H), 4.70 (s, 1H), 2.45 (d, J = 1.1 Hz, 4H), 2.30 – 2.10 (m, 4H), 1.10 (s, 6H), 0.99 (s, 6H). ¹³C NMR (101 MHz, cdcl₃) δ 196.53, 163.21, 162.13, 160.72, 156.83, 137.18, 133.34, 130.92, 130.89, 130.20, 129.46, 116.87, 115.70, 114.36, 66.55, 50.75, 40.91, 40.84, 40.76, 32.20, 31.05, 29.29, 29.24, 27.37, 27.32. ¹⁹F NMR (376 MHz, cdcl₃) δ -112.71 (q, J = 7.7 Hz). ESI MS m/z 509.19 (M + H)⁺

9-(4-((3-chloro-5-fluorobenzyl)oxy)phenyl)-3,3,6,6-tetramethyl-3,4,5,6,7,9-hexahydro-1H-xanthene-1,8(2H)-dione (CCG362730) [sz-08-18]

Following the general procedure on a scale of 70mg (0.19mmol) 9-(4-hydroxyphenyl)-3,3,6,6-tetramethyl-3,4,5,6,7,9-hexahydro-1H-xanthene-1,8(2H)-dione (**3**), 1-(bromomethyl)-3-chloro-5-fluorobenzene (85 mg, 2 Eq, 0.38 mmol) was used and isolated 0.09g (87% yield) of the desired product. ¹H NMR (400 MHz, cdcl₃) δ 7.24 – 7.14 (m, 3H), 7.09 – 6.95 (m, 2H), 6.86 – 6.70 (m, 2H), 4.97 – 4.85 (m, 2H), 4.70 (s, 1H), 2.52 – 2.35 (m, 4H), 2.31 – 2.10 (m, 4H), 1.09 (s, 6H), 0.99 (s, 6H). ¹³C NMR (101 MHz, cdcl₃) δ 196.52, 163.98, 162.15, 161.50, 156.69, 141.21, 141.13, 137.32, 135.14, 129.47, 122.95, 115.66, 115.61, 115.36, 114.33, 112.65, 112.44, 68.49, 50.74, 40.83, 32.20, 31.05, 30.97, 29.28, 27.32. ¹⁹F NMR (376 MHz, cdcl₃) δ -110.73 (td, J = 8.6, 1.6 Hz). ESI MS m/z 509.19 (M + H)⁺

9-(4-((3-chloro-2-fluorobenzyl)oxy)phenyl)-3,3,6,6-tetramethyl-3,4,5,6,7,9-hexahydro-1H-xanthene-1,8(2H)-dione (CG362731) [sz-08-19]

Following the general procedure on a scale of 70mg (0.19mmol) 9-(4-hydroxyphenyl)-3,3,6,6-tetramethyl-3,4,5,6,7,9-hexahydro-1H-xanthene-1,8(2H)-dione (**3**), 1-(bromomethyl)-3-chloro-2-fluorobenzene (85 mg, 2 Eq, 0.38 mmol) was used and isolated 0.1g (93% yield) of the desired product. ¹H NMR (400 MHz, cdcl₃) δ 7.35 (dddd, J = 13.8, 8.5, 6.7, 1.7 Hz, 2H), 7.24 – 7.18 (m, 2H), 7.08 (td, J = 7.9, 1.2 Hz, 1H), 6.88 – 6.76 (m, 2H), 5.09 – 4.99 (m, 2H), 4.70 (s, 1H), 2.45 (s, 4H), 2.31 – 2.08 (m, 4H), 1.09 (s, 6H), 0.99 (s, 6H). ¹³C NMR (101 MHz, cdcl₃) δ 196.52, 162.14, 156.79, 137.24, 130.04, 129.45, 127.88, 126.25, 126.11, 124.67, 124.62, 121.01, 120.84, 115.69, 114.29, , 63.40, 50.74, 40.83, 32.20, 31.03, 29.27, 27.34. ¹⁹F NMR (376 MHz, cdcl₃) δ -120.73 (t, J = 6.6 Hz). ESI MS m/z 509.18 (M + H)⁺

9-(4-((2-bromobenzyl)oxy)phenyl)-3,3,6,6-tetramethyl-3,4,5,6,7,9-hexahydro-1H-xanthene-1,8(2H)-dione (CCG362911) [sz-08-41]

Following the general procedure on a scale of 50mg (0.14mmol) 9-(4-hydroxyphenyl)-3,3,6,6-tetramethyl-3,4,5,6,7,9-hexahydro-1*H*-xanthene-1,8(2*H*)-dione (3), 1-bromo-2-(bromomethyl)benzene (68 mg, 37 μ L, 2 Eq, 0.27 mmol) was used and isolated 0.07g (96% yield) of the desired product. ¹H NMR (499 MHz, Chloroform-*d*) δ 7.55 (dd, *J* = 8.1, 1.2 Hz, 1H), 7.51 (dd, *J* = 7.7, 1.7 Hz, 1H), 7.30 (td, *J* = 7.5, 1.2 Hz, 1H), 7.25 – 7.19 (m, 2H), 7.15 (td, *J* = 7.7, 1.7 Hz, 1H), 6.92 – 6.76 (m, 2H), 5.05 (s, 2H), 4.71 (s, 1H), 2.45 (s, 4H), 2.30 – 2.09 (m, 4H), 1.10 (s, 6H), 0.99 (s, 6H). ¹³C NMR (126 MHz, Chloroform-*d*) δ 196.46, 162.11, 156.97, 137.08, 136.55, 132.49, 129.39, 129.08, 128.97, 127.52, 122.19, 115.74, 114.45, 69.37, 50.77, 40.86, 32.19, 30.98, 29.25, 27.38. ESI MS *m/z* 557.12 (M + Na)⁺

9-(4-((3-bromobenzyl)oxy)phenyl)-3,3,6,6-tetramethyl-3,4,5,6,7,9-hexahydro-1H-xanthene-1,8(2H)-dione (CCG362912) [sz-08-42]

Following the general procedure on a scale of 50mg (0.14mmol) 9-(4-hydroxyphenyl)-3,3,6,6-tetramethyl-3,4,5,6,7,9-hexahydro-1*H*-xanthene-1,8(2*H*)-dione (3), 1-bromo-3-(bromomethyl)benzene (68 mg, 2 Eq, 0.27 mmol) was used and isolated 0.05g (72% yield) of the desired product. ¹H NMR (499 MHz, Chloroform-*d*) δ 7.55 (d, *J* = 1.8 Hz, 1H), 7.42 (dt, *J* = 8.0, 1.5 Hz, 1H), 7.31 (dd, *J* = 7.8, 1.5 Hz, 1H), 7.22 (dd, *J* = 8.2, 6.3 Hz, 3H), 6.84 – 6.78 (m, 2H), 4.94 (s, 2H), 4.71 (s, 1H), 2.45 (s, 4H), 2.20 (q, *J* = 16.3 Hz, 4H), 1.10 (s, 6H), 0.99 (s, 6H). ¹³C NMR (126 MHz, Chloroform-*d*) δ 196.45, 162.11, 156.99, 139.61, 137.09, 130.88, 130.35, 130.07, 129.41, 125.90, 122.58, 115.72, 114.35, 69.04, 50.76, 40.85, 32.19, 30.99, 29.26, 27.35. ESI MS *m/z* 557.12 (M + Na)⁺

9-(4-((4-bromobenzyl)oxy)phenyl)-3,3,6,6-tetramethyl-3,4,5,6,7,9-hexahydro-1H-xanthene-1,8(2H)-dione (CCG362913) [sz-08-43]

Following the general procedure on a scale of 50mg (0.14mmol) 9-(4-hydroxyphenyl)-3,3,6,6-tetramethyl-3,4,5,6,7,9-hexahydro-1*H*-xanthene-1,8(2*H*)-dione (3), 1-bromo-4-(bromomethyl)benzene (68 mg, 2 Eq, 0.27 mmol) was used and isolated 0.05g (74% yield) of the desired product. ¹H NMR (499 MHz, Chloroform-*d*) δ 7.52 – 7.42 (m, 2H), 7.26 (d, *J* = 8.3 Hz, 2H), 7.23 – 7.18 (m, 2H), 6.87 – 6.77 (m, 2H), 4.92 (s, 2H), 4.70 (s, 1H), 2.45 (s, 4H), 2.20 (q, *J* = 16.3 Hz, 4H), 1.10 (s, 6H), 0.99 (s, 6H). ¹³C NMR (126 MHz, Chloroform-*d*) δ 196.44, 162.08, 157.03, 137.02, 136.29, 131.61, 129.40, 129.12, 121.71, 115.72, 114.33, 69.17, 50.77, 40.86, 32.19, 31.00, 29.25, 27.35. ESI MS *m/z* 573.10 (M + K)⁺

9-(4-((3-bromo-5-methylbenzyl)oxy)phenyl)-3,3,6,6-tetramethyl-3,4,5,6,7,9-hexahydro-1H-xanthene-1,8(2H)-dione (CCG362935) [sz-08-46]

Following the general procedure on a scale of 50mg (0.14mmol) 9-(4-hydroxyphenyl)-3,3,6,6-tetramethyl-3,4,5,6,7,9-hexahydro-1H-xanthene-1,8(2H)-dione (**3**), 1-bromo-3-(bromomethyl)-5-methylbenzene (43 mg, 1.2 Eq, 0.16 mmol) was used and isolated 0.07g (90% yield) of the desired product. ¹H NMR (499 MHz, cdcl₃) δ 7.34 (d, J = 2.0 Hz, 1H), 7.26 (s, 1H), 7.24 – 7.16 (m, 2H), 7.15 – 7.07 (m, 1H), 6.87 – 6.74 (m, 2H), 4.89 (s, 2H), 4.71 (s, 1H), 2.32 (s, 3H), 2.20 (q, J = 16.3 Hz, 4H), 1.10 (s, 6H), 0.99 (s, 6H). ¹³C NMR (126 MHz, cdcl₃) δ 196.44, 162.09, 157.06, 140.32, 139.28, 137.02, 131.48, 129.38, 127.44, 126.78, 122.34, 115.73, 114.34, 69.14, 50.77, 40.86, 32.19, 30.99, 29.25, 27.34, 21.11. ESI MS m/z 571.14 (M + Na)⁺

9-(4-((3-bromo-2-methylbenzyl)oxy)phenyl)-3,3,6,6-tetramethyl-3,4,5,6,7,9-hexahydro-1H-xanthene-1,8(2H)-dione (CCG362936) [sz-08-47]

Following the general procedure on a scale of 60mg (0.16mmol) 9-(4-hydroxyphenyl)-3,3,6,6-tetramethyl-3,4,5,6,7,9-hexahydro-1H-xanthene-1,8(2H)-dione (**3**), 1-bromo-3-(bromomethyl)-2-methylbenzene (52 mg, 1.2 Eq, 0.20 mmol) was used and isolated 0.08g (92% yield) of the desired product. ¹H NMR (499 MHz, cdcl₃) δ 7.53 (dd, J = 8.0, 1.3 Hz, 1H), 7.32 (d, J = 7.6 Hz, 1H), 7.25 – 7.17 (m, 2H), 7.04 (t, J = 7.8 Hz, 1H), 6.87 – 6.76 (m, 2H), 4.95 (s, 2H), 4.71 (s, 1H), 2.46 (s, 4H), 2.41 (s, 3H), 2.21 (q, J = 16.3 Hz, 4H), 1.10 (s, 6H), 1.00 (s, 6H). ¹³C NMR (126 MHz, cdcl₃) δ 196.48, 162.09, 157.10, 137.05, 137.02, 136.54, 132.46, 129.40, 128.02, 127.08, 126.13, 115.73, 114.29, 68.98, 50.77, 40.86, 32.19, 31.04, 29.25, 27.38, 18.69. ESI MS m/z 571.14 (M + Na)⁺

9-(4-((3-bromo-4-methylbenzyl)oxy)phenyl)-3,3,6,6-tetramethyl-3,4,5,6,7,9-hexahydro-1H-xanthene-1,8(2H)-dione (CCG362937) [sz-08-48]

Following the general procedure on a scale of 50mg (0.14mmol) 9-(4-hydroxyphenyl)-3,3,6,6-tetramethyl-3,4,5,6,7,9-hexahydro-1H-xanthene-1,8(2H)-dione (**3**), 2-bromo-4-(bromomethyl)-1-methylbenzene (43 mg, 1.2 Eq, 0.16 mmol) was used and isolated 0.06g (76% yield) of the desired product. ¹H NMR (499 MHz, cdcl₃) δ 7.57 (s, 1H), 7.24 – 7.14 (m, 4H), 6.87 – 6.76 (m, 2H), 4.90 (s, 2H), 4.71 (s, 1H), 2.45 (s, 4H), 2.38 (s, 3H), 2.20 (q, J = 16.3 Hz, 4H), 1.10 (s, 6H), 0.99 (s, 6H). ¹³C NMR (126 MHz, cdcl₃) δ 196.43, 162.08, 157.09, 137.37, 136.96, 136.69, 131.31, 130.81, 129.37, 126.40, 124.91, 115.74, 114.34, 68.91, 50.77, 40.86, 32.19, 30.98, 29.26, 27.35, 22.62. ESI MS m/z 571.14 (M + Na)⁺

9-(4-((2-bromo-6-methylbenzyl)oxy)phenyl)-3,3,6,6-tetramethyl-3,4,5,6,7,9-hexahydro-1H-xanthene-1,8(2H)-dione (CCG362938) [sz-08-49]

Following the general procedure on a scale of 55mg (0.15mmol) 9-(4-hydroxyphenyl)-3,3,6,6-tetramethyl-3,4,5,6,7,9-hexahydro-1H-xanthene-1,8(2H)-dione (**3**), 1-bromo-2-(bromomethyl)-3-methylbenzene (48 mg, 1.2 Eq, 0.18 mmol) was used and isolated 0.08g (96% yield) of the desired product. ¹H NMR (499 MHz, cdcl₃) δ 7.43 (dd, J = 8.0, 1.3 Hz, 1H), 7.25 – 7.20 (m, 2H), 7.17 – 7.11 (m, 1H), 7.08 (t, J = 7.7 Hz, 1H), 6.93 – 6.80 (m, 2H), 5.12 (s, 2H), 4.72 (s, 1H), 2.46 (s, 4H), 2.41 (s, 3H), 2.29 – 2.13 (m, 4H), 1.10 (s, 6H), 1.01 (s, 6H). ¹³C NMR (126 MHz, cdcl₃) δ 196.53, 162.08, 157.36, 140.88, 136.89, 133.98, 130.72, 129.84, 129.79, 129.33, 126.17, 115.77, 114.29, 67.45, 50.79, 40.87, 32.20, 31.05, 29.22, 27.47, 20.14. ESI MS m/z 571.14 (M + Na)⁺

9-(4-((3-fluorobenzyl)oxy)phenyl)-3,3,6,6-tetramethyl-3,4,5,6,7,9-hexahydro-1H-xanthene-1,8(2H)-dione (CCG257408) [sz-08-52]

Following the general procedure on a scale of 50mg (0.14mmol) 9-(4-hydroxyphenyl)-3,3,6,6-tetramethyl-3,4,5,6,7,9-hexahydro-1H-xanthene-1,8(2H)-dione (**3**), 1-(bromomethyl)-3-fluorobenzene (31 mg, 20 μL, 1.2 Eq, 0.16 mmol) was used and isolated 0.06g (93% yield) of the desired product. ¹H NMR (499 MHz, cdcl₃) δ 7.31 (td, J = 7.9, 5.8 Hz, 1H), 7.24 – 7.19 (m, 2H), 7.18 – 7.14 (m, 1H), 7.12 (dt, J = 9.7, 2.1 Hz, 1H), 6.98 (td, J = 8.5, 2.6 Hz, 1H), 6.88 – 6.77 (m, 2H), 4.97 (s, 2H), 4.71 (s, 1H), 2.46 (s, 4H), 2.20 (q, J = 16.3 Hz, 4H), 1.10 (s, 6H), 0.99 (s, 6H). ¹³C NMR (126 MHz, cdcl₃) δ 196.44, 163.92, 162.09, 157.02, 139.91, 137.04, 129.40, 122.76, 115.73, 114.73, 114.56, 114.35, 114.15, 69.13, 50.76, 40.86, 32.19, 30.99, 29.25, 27.34. ¹⁹F NMR (470 MHz, cdcl₃) δ -113.03 (td, J = 9.1, 5.8 Hz). ESI MS m/z 497.21 (M + Na)⁺

9-(4-((4-bromo-3-methylbenzyl)oxy)phenyl)-3,3,6,6-tetramethyl-3,4,5,6,7,9-hexahydro-1H-xanthene-1,8(2H)-dione (CCG362975) [sz-08-53]

Following the general procedure on a scale of 50mg (0.14mmol) 9-(4-hydroxyphenyl)-3,3,6,6-tetramethyl-3,4,5,6,7,9-hexahydro-1H-xanthene-1,8(2H)-dione (**3**), 1-bromo-4-(bromomethyl)-2-methylbenzene (43 mg, 1.2 Eq, 0.16 mmol) was used and isolated 0.07g (92% yield) of the desired product. ¹H NMR (499 MHz, cdcl₃) δ 7.50 (d, J = 8.1 Hz, 1H), 7.26 (d, J = 2.9 Hz, 1H), 7.25 – 7.16 (m, 2H), 7.11 – 6.99 (m, 1H), 6.89 – 6.74 (m, 2H), 4.89 (s, 2H), 4.71 (s, 1H), 2.45 (s, 4H), 2.39 (s, 3H), 2.20 (q, J = 16.3 Hz, 4H), 1.10 (s, 6H), 0.99 (s, 6H). ¹³C NMR (126 MHz, cdcl₃) δ 196.44, 162.07, 157.12, 138.03, 136.95, 136.49, 132.41, 129.93, 129.38, 126.47, 124.21, 115.74, 114.33, 69.26, 50.77, 40.86, 32.19, 30.99, 29.25, 27.35, 22.89. ESI MS m/z 571.14 (M + Na)⁺

9-(4-((2-bromo-3-methylbenzyl)oxy)phenyl)-3,3,6,6-tetramethyl-3,4,5,6,7,9-hexahydro-1H-xanthene-1,8(2H)-dione (CCG363012) [sz-08-54]

Following the general procedure on a scale of 50mg (0.14mmol) 9-(4-hydroxyphenyl)-3,3,6,6-tetramethyl-3,4,5,6,7,9-hexahydro-1H-xanthene-1,8(2H)-dione (**3**), 2-bromo-1-(bromomethyl)-3-methylbenzene (40 mg, 1.1 Eq, 0.15 mmol) was used and isolated 0.07g (99% yield) of the desired product. ¹H NMR (499 MHz, cdcl₃) δ 7.38 – 7.31 (m, 1H), 7.25 – 7.16 (m, 4H), 6.87 – 6.81 (m, 2H), 5.06 (s, 2H), 4.72 (s, 1H), 2.46 (s, 4H), 2.43 (s, 3H), 2.30 – 2.10 (m, 4H), 1.10 (s, 6H), 1.00 (s, 6H). ¹³C NMR (126 MHz, cdcl₃) δ 196.44, 162.08, 157.06, 138.32, 136.98, 136.86, 129.95, 129.36, 127.06, 126.28, 124.67, 115.77, 114.46, 69.99, 50.78, 40.86, 32.18, 30.97, 29.24, 27.39, 23.35. ESI MS m/z 571.14 (M + Na)⁺

9-(4-((2,4-dibromobenzyl)oxy)phenyl)-3,3,6,6-tetramethyl-3,4,5,6,7,9-hexahydro-1H-xanthene-1,8(2H)-dione (CCG363015) [sz-08-55]

Following the general procedure on a scale of 50mg (0.14mmol) 9-(4-hydroxyphenyl)-3,3,6,6-tetramethyl-3,4,5,6,7,9-hexahydro-1H-xanthene-1,8(2H)-dione (**3**), 2,4-dibromo-1-(bromomethyl)benzene (49 mg, 1.1 Eq, 0.15 mmol) was used and isolated 0.04g (46% yield) of the desired product. ¹H NMR (499 MHz, cdcl₃) δ 7.72 (d, J = 1.9 Hz, 1H), 7.44 (dd, J = 8.3, 1.9 Hz, 1H), 7.39 (d, J = 8.3 Hz, 1H), 7.25 – 7.17 (m, 2H), 6.89 – 6.75 (m, 2H), 4.98 (s, 2H), 4.71 (s, 1H), 2.45 (s, 4H), 2.20 (q, J = 16.3 Hz, 4H), 1.10 (s, 6H), 1.00 (s, 6H). ¹³C NMR (126 MHz, cdcl₃) δ 196.44, 162.10, 156.69, 137.31, 135.77, 134.77, 130.70, 130.02, 129.45, 122.54, 121.74, 115.71, 114.43, 68.84, 50.76, 40.86, 32.19, 31.02, 29.24, 27.37. ESI MS m/z 635.03 (M + Na)⁺

9-(4-((2-bromo-4-methylbenzyl)oxy)phenyl)-3,3,6,6-tetramethyl-3,4,5,6,7,9-hexahydro-1H-xanthene-1,8(2H)-dione (CCG363013) [sz-08-56]

Following the general procedure on a scale of 50mg (0.14mmol) 9-(4-hydroxyphenyl)-3,3,6,6-tetramethyl-3,4,5,6,7,9-hexahydro-1H-xanthene-1,8(2H)-dione (**3**), 2-bromo-1-(bromomethyl)-4-methylbenzene (40 mg, 1.1 Eq, 0.15 mmol) was used and isolated 0.07g (92% yield) of the desired product. ¹H NMR (499 MHz, cdcl₃) δ 7.45 – 7.31 (m, 2H), 7.25 – 7.14 (m, 2H), 7.10 (dt, J = 7.9, 1.1 Hz, 1H), 6.90 – 6.75 (m, 2H), 5.01 (s, 2H), 4.71 (s, 1H), 2.45 (s, 4H), 2.32 (s, 3H), 2.28 – 2.10 (m, 4H), 1.10 (s, 6H), 1.00 (s, 6H). ¹³C NMR (126 MHz, cdcl₃) δ 196.43, 162.07, 157.05, 139.33, 136.94, 133.41, 132.98, 129.35, 128.95, 128.31, 122.18, 115.76, 114.43, 69.27, 50.77, 40.86, 32.18, 30.97, 29.24, 27.39, 20.74. ESI MS m/z 571.14 (M + Na)⁺

9-(4-((5-bromo-2-methylbenzyl)oxy)phenyl)-3,3,6,6-tetramethyl-3,4,5,6,7,9-hexahydro-1H-xanthene-1,8(2H)-dione (CCG363011) [sz-08-57]

Following the general procedure on a scale of 50mg (0.14mmol) 9-(4-hydroxyphenyl)-3,3,6,6-tetramethyl-3,4,5,6,7,9-hexahydro-1H-xanthene-1,8(2H)-dione (**3**), 4-bromo-2-(bromomethyl)-1-methylbenzene (40 mg, 1.1 Eq, 0.15 mmol) was used and isolated 0.07g (92% yield) of the desired product. ¹H NMR (499 MHz, cdcl₃) δ 7.53 (d, J = 2.1 Hz, 1H), 7.33 (dd, J = 8.1, 2.2 Hz, 1H), 7.25 – 7.20 (m, 2H), 7.05 (d, J = 8.1 Hz, 1H), 6.91 – 6.75 (m, 2H), 4.89 (s, 2H), 4.72 (s, 1H), 2.46 (s, 4H), 2.27 (s, 3H), 2.26 – 2.10 (m, 4H), 1.10 (s, 6H), 1.00 (s, 6H). ¹³C NMR (126 MHz, cdcl₃) δ 196.47, 162.11, 157.12, 137.30, 135.28, 131.86, 131.12, 130.87, 129.40, 119.51, 115.73, 114.34, 67.69, 50.77, 40.86, 32.19, 31.02, 29.26, 27.36, 18.39. ESI MS m/z 571.14 (M + Na)⁺

9-(4-((4-bromo-2-methylbenzyl)oxy)phenyl)-3,3,6,6-tetramethyl-3,4,5,6,7,9-hexahydro-1H-xanthene-1,8(2H)-dione (CCG363014) [sz-08-58]

Following the general procedure on a scale of 50mg (0.14mmol) 9-(4-hydroxyphenyl)-3,3,6,6-tetramethyl-3,4,5,6,7,9-hexahydro-1H-xanthene-1,8(2H)-dione (**3**), 4-bromo-1-(bromomethyl)-2-methylbenzene (40 mg, 1.1 Eq, 0.15 mmol) was used and isolated 0.04g (54% yield) of the desired product. ¹H NMR (499 MHz, cdcl₃) δ 7.34 (d, J = 2.0 Hz, 1H), 7.31 (dd, J = 8.1, 2.1 Hz, 1H), 7.25 (d, J = 10.8 Hz, 1H), 7.23 – 7.19 (m, 2H), 6.85 – 6.79 (m, 2H), 4.88 (s, 2H), 4.71 (s, 1H), 2.46 (s, 4H), 2.31 (s, 3H), 2.20 (q, J = 16.3 Hz, 4H), 1.10 (s, 6H), 1.00 (s, 6H). ¹³C NMR (126 MHz, cdcl₃) δ 196.46, 162.08, 157.15, 138.88, 137.00, 134.13, 133.07, 130.22, 129.39, 128.98, 121.91, 115.74, 114.28, 67.81, 50.77, 40.86, 32.19, 31.03, 29.25, 27.37, 18.68. ESI MS m/z 571.14 (M + Na)⁺

9-(4-((3,4-dibromobenzyl)oxy)phenyl)-3,3,6,6-tetramethyl-3,4,5,6,7,9-hexahydro-1H-xanthene-1,8(2H)-dione (CCG363016) [sz-08-59]

Following the general procedure on a scale of 50mg (0.14mmol) 9-(4-hydroxyphenyl)-3,3,6,6-tetramethyl-3,4,5,6,7,9-hexahydro-1H-xanthene-1,8(2H)-dione (**3**), 1,2-dibromo-4-(bromomethyl)benzene (49 mg, 1.1 Eq, 0.15 mmol) was used and isolated 0.06g (68% yield) of the desired product. ¹H NMR (499 MHz, cdcl₃) δ 7.67 (d, J = 2.0 Hz, 1H), 7.59 (d, J = 8.2 Hz, 1H), 7.24 – 7.14 (m, 3H), 6.84 – 6.74 (m, 2H), 4.90 (s, 2H), 4.70 (s, 1H), 2.46 (s, 4H), 2.20 (q, J = 16.3 Hz, 4H), 1.10 (s, 6H), 0.99 (s, 6H). ¹³C NMR (126 MHz, cdcl₃) δ 196.43, 162.10, 156.79, 138.36, 137.27, 133.68, 132.41, 129.45, 127.40, 124.88, 123.92, 115.69, 114.35, 68.42, 50.76, 40.86, 32.19, 31.02, 29.25, 27.34. ESI MS m/z 635.04 (M + Na)⁺

9-(4-((2-chlorobenzyl)oxy)phenyl)-3,3,6,6-tetramethyl-3,4,5,6,7,9-hexahydro-1H-xanthene-1,8(2H)-dione (CCG364641) [sz-09-51]

Following the general procedure on a scale of 50mg (0.14mmol) 9-(4-hydroxyphenyl)-3,3,6,6-tetramethyl-3,4,5,6,7,9-hexahydro-1H-xanthene-1,8(2H)-dione (**3**), 1-(bromomethyl)-2-chlorobenzene (31 mg, 19 μ L, 1.1 Eq, 0.15 mmol) was used and isolated 0.05g (75% yield) of the desired product. ¹H NMR (499 MHz, cdcl₃) δ 7.55 – 7.50 (m, 1H), 7.40 – 7.34 (m, 1H), 7.30 – 7.18 (m, 4H), 6.87 – 6.81 (m, 2H), 5.08 (s, 2H), 4.71 (s, 1H), 2.45 (s, 4H), 2.23 (d, J = 16.3 Hz, 2H), 2.17 (d, J = 16.3 Hz, 2H), 1.10 (s, 6H), 1.00 (s, 6H). ¹³C NMR (126 MHz, cdcl₃) δ 196.44, 162.07, 157.02, 137.03, 134.98, 132.50, 129.38, 129.25, 128.87, 128.80, 126.90, 115.76, 114.42, 67.07, 50.76, 40.87, 32.18, 30.98, 29.23, 27.37. ESI MS m/z 513;18 (M + Na)⁺

9-(4-((4-chlorobenzyl)oxy)phenyl)-3,3,6,6-tetramethyl-3,4,5,6,7,9-hexahydro-1H-xanthene-1,8(2H)-dione (CCG364642) [sz-09-52]

Following the general procedure on a scale of 52mg (0.14mmol) 9-(4-hydroxyphenyl)-3,3,6,6-tetramethyl-3,4,5,6,7,9-hexahydro-1H-xanthene-1,8(2H)-dione (**3**), 1-(bromomethyl)-4-chlorobenzene (32 mg, 1.1 Eq, 0.16 mmol) was used and isolated 0.07g (97% yield) of the desired product. ¹H NMR (499 MHz, cdcl₃) δ 7.32 (d, J = 0.8 Hz, 4H), 7.24 – 7.15 (m, 2H), 6.86 – 6.75 (m, 2H), 4.93 (s, 2H), 4.70 (s, 1H), 2.45 (s, 4H), 2.20 (q, J = 16.3 Hz, 4H), 1.10 (s, 6H), 0.99 (s, 6H). ¹³C NMR (126 MHz, cdcl₃) δ 196.44, 162.08, 157.05, 137.00, 135.75, 133.60, 129.39, 128.81, 128.65, 115.73, 114.33, 69.15, 50.76, 40.86, 32.18, 31.00, 29.24, 27.34. ESI MS m/z 513.18 (M + Na)⁺

9-(4-((4-fluoro-2-methylbenzyl)oxy)phenyl)-3,3,6,6-tetramethyl-3,4,5,6,7,9-hexahydro-1H-xanthene-1,8(2H)-dione (CCG364643) [sz-09-53]

Following the general procedure on a scale of 70mg (0.19mmol) 9-(4-hydroxyphenyl)-3,3,6,6-tetramethyl-3,4,5,6,7,9-hexahydro-1H-xanthene-1,8(2H)-dione (**3**), 1-(bromomethyl)-4-fluoro-2-methylbenzene (43 mg, 29 μ L, 1.1 Eq, 0.21 mmol) was used and isolated 0.07g (75% yield) of the desired product. ¹H NMR (499 MHz, cdcl₃) δ 7.31 (dd, J = 8.4, 5.9 Hz, 1H), 7.24 – 7.18 (m, 2H), 6.93 – 6.85 (m, 2H), 6.85 – 6.80 (m, 2H), 4.89 (s, 2H), 4.71 (s, 1H), 2.46 (s, 4H), 2.33 (s, 3H), 2.21 (q, J = 16.3 Hz, 4H), 1.10 (s, 6H), 1.00 (s, 6H). ¹³C NMR (126 MHz, cdcl₃) δ 196.47, 163.52, 162.05, 157.25, 136.89, 130.65, 130.58, 129.36, 117.17, 117.00, 115.76, 114.27, 112.58, 112.41, 67.86, 50.77, 40.87, 32.18, 31.02, 29.24, 27.36, 18.97. ¹⁹F NMR (470 MHz, cdcl₃) δ -114.88 (td, J = 9.0, 5.8 Hz). ESI MS m/z 511.22 (M + Na)⁺

9-(4-((2-methoxybenzyl)oxy)phenyl)-3,3,6,6-tetramethyl-3,4,5,6,7,9-hexahydro-1H-xanthene-1,8(2H)-dione (CCG364644) [sz-09-54]

Following the general procedure on a scale of 70mg (0.19mmol) 9-(4-hydroxyphenyl)-3,3,6,6-tetramethyl-3,4,5,6,7,9-hexahydro-1H-xanthene-1,8(2H)-dione (**3**), 1-(bromomethyl)-2-methoxybenzene (44 mg, 32 μ L, 1.1 Eq, 0.22 mmol) was used and isolated 0.08g (83% yield) of the desired product. ¹H NMR (499 MHz, cdcl₃) δ 7.42 (dd, J = 7.7, 1.4 Hz, 1H), 7.30 – 7.27 (m, 1H), 7.22 – 7.17 (m, 2H), 6.95 (t, J = 7.5 Hz, 1H), 6.88 (d, J = 8.2 Hz, 1H), 6.87 – 6.83 (m, 2H), 5.02 (s, 2H), 4.71 (s, 1H), 3.83 (d, J = 0.8 Hz, 3H), 2.45 (s, 4H), 2.28 – 2.12 (m, 4H), 1.10 (s, 6H), 1.00 (s, 6H). ¹³C NMR (126 MHz, cdcl₃) δ 196.44, 162.02, 157.51, 156.85, 136.50, 129.25, 128.84, 128.82, 125.60, 120.53, 115.83, 114.40, 110.24, 64.93, 55.35, 50.77, 40.87, 32.18, 30.93, 29.24, 27.38. ESI MS m/z 525.20 (M + K)⁺

9-(4-((2,3-dichlorobenzyl)oxy)phenyl)-3,3,6,6-tetramethyl-3,4,5,6,7,9-hexahydro-1H-xanthene-1,8(2H)-dione (CCG364646) [sz-09-60]

Following the general procedure on a scale of 70mg (0.19mmol) 9-(4-hydroxyphenyl)-3,3,6,6-tetramethyl-3,4,5,6,7,9-hexahydro-1H-xanthene-1,8(2H)-dione (**3**), 1-(bromomethyl)-2,3-dichlorobenzene (50 mg, 30 μ L, 1.1 Eq, 0.21 mmol) was used and isolated 0.08g (83% yield) of the desired product. ¹H NMR (499 MHz, cdcl₃) δ 7.45 (dt, J = 7.7, 1.3 Hz, 1H), 7.40 (dd, J = 8.1, 1.5 Hz, 1H), 7.24 – 7.18 (m, 3H), 6.91 – 6.72 (m, 2H), 5.09 (s, 2H), 4.71 (s, 1H), 2.45 (s, 4H), 2.20 (q, J = 16.4 Hz, 4H), 1.10 (s, 6H), 0.99 (s, 6H). ¹³C NMR (126 MHz, cdcl₃) δ 196.45, 162.11, 156.77, 137.40, 137.29, 132.92, 130.43, 129.45, 129.42, 127.41, 126.68, 115.71, 114.41, 67.39, 50.76, 40.86, 32.18, 31.01, 29.24, 27.36. ESI MS m/z 547.14 (M + Na)⁺

9-(4-((2-chloro-3-fluorobenzyl)oxy)phenyl)-3,3,6,6-tetramethyl-3,4,5,6,7,9-hexahydro-1H-xanthene-1,8(2H)-dione (CCG364647) [sz-09-61]

Following the general procedure on a scale of 70mg (0.19mmol) 9-(4-hydroxyphenyl)-3,3,6,6-tetramethyl-3,4,5,6,7,9-hexahydro-1H-xanthene-1,8(2H)-dione (**3**), 1-(bromomethyl)-2,3-dichlorobenzene (50 mg, 30 μ L, 1.1 Eq, 0.21 mmol) was used and isolated 0.09g (91% yield) of the desired product. ¹H NMR (499 MHz, cdcl₃) δ 7.36 – 7.29 (m, 1H), 7.25 – 7.19 (m, 3H), 7.14 – 7.00 (m, 1H), 6.89 – 6.75 (m, 2H), 5.08 (s, 2H), 4.71 (s, 1H), 2.45 (s, 4H), 2.20 (q, J = 16.3 Hz, 4H), 1.09 (s, 6H), 0.99 (s, 6H). ¹³C NMR (126 MHz, cdcl₃) δ 196.46, 162.14, 159.10, 157.12, 156.81, 137.42, 137.28, 129.44, 127.67, 127.61, 123.89, 123.87, 119.35, 115.70, 115.57, 115.41,

114.39, 66.71, 50.76, 40.85, 32.18, 31.01, 29.24, 27.35. ¹⁹F NMR (470 MHz, cdcl₃) δ -115.17 (dd, J = 8.9, 5.2 Hz). ESI MS m/z 531.17 (M + Na)⁺

9-(4-((4-chloro-2-methylbenzyl)oxy)phenyl)-3,3,6,6-tetramethyl-3,4,5,6,7,9-hexahydro-1H-xanthene-1,8(2H)-dione (CCG364648) [sz-09-62]

Following the general procedure on a scale of 70mg (0.19mmol) 9-(4-hydroxyphenyl)-3,3,6,6-tetramethyl-3,4,5,6,7,9-hexahydro-1H-xanthene-1,8(2H)-dione (**3**), 1-(bromomethyl)-4-chloro-2-methylbenzene (46 mg, 1.1 Eq, 0.21 mmol) was used and isolated 0.08g (80% yield) of the desired product. ¹H NMR (499 MHz, cdcl₃) δ 7.29 (d, J = 8.1 Hz, 1H), 7.23 – 7.19 (m, 2H), 7.19 – 7.13 (m, 2H), 6.89 – 6.71 (m, 2H), 4.89 (s, 2H), 4.71 (s, 1H), 2.46 (s, 4H), 2.31 (s, 3H), 2.20 (q, J = 16.3 Hz, 4H), 1.10 (s, 6H), 1.00 (s, 6H). ¹³C NMR (126 MHz, cdcl₃) δ 196.48, 162.09, 157.17, 138.60, 136.98, 133.67, 133.60, 130.19, 129.99, 129.38, 125.98, 115.73, 114.28, 67.78, 50.77, 40.86, 32.18, 31.03, 29.24, 27.36, 18.74. ESI MS m/z 527.19 (M + Na)⁺

9-(4-((3-chlorobenzyl)oxy)phenyl)-3,3,6,6-tetramethyl-3,4,5,6,7,9-hexahydro-1H-xanthene-1,8(2H)-dione (CCG365668) [sz-09-65]

Following the general procedure on a scale of 70mg (0.19mmol) 9-(4-hydroxyphenyl)-3,3,6,6-tetramethyl-3,4,5,6,7,9-hexahydro-1H-xanthene-1,8(2H)-dione (**3**), 1-(bromomethyl)-3-chlorobenzene (43 mg, 28 μL, 1.1 Eq, 0.21 mmol) was used and isolated 0.08g (80% yield) of the desired product. ¹H NMR (499 MHz, cdcl₃) δ 7.40 (dd, J = 2.0, 1.1 Hz, 1H), 7.29 – 7.26 (m, 3H), 7.23 – 7.18 (m, 2H), 6.92 – 6.73 (m, 2H), 4.94 (s, 2H), 4.70 (s, 1H), 2.45 (s, 4H), 2.20 (q, J = 16.3 Hz, 4H), 1.10 (s, 6H), 0.99 (s, 6H). ¹³C NMR (126 MHz, cdcl₃) δ 196.44, 162.08, 157.01, 139.33, 137.06, 134.40, 129.76, 129.40, 127.94, 127.44, 125.39, 115.73, 114.35, 69.12, 50.76, 40.86, 32.18, 30.99, 29.24, 27.34. ESI MS m/z 491.19 (M + H)⁺

9-(4-((3-methoxybenzyl)oxy)phenyl)-3,3,6,6-tetramethyl-3,4,5,6,7,9-hexahydro-1H-xanthene-1,8(2H)-dione (CCG363237) [sz-09-66]

Following the general procedure on a scale of 70mg (0.19mmol) 9-(4-hydroxyphenyl)-3,3,6,6-tetramethyl-3,4,5,6,7,9-hexahydro-1H-xanthene-1,8(2H)-dione (**3**), 1-(bromomethyl)-3-methoxybenzene (42 mg, 29 μL, 1.1 Eq, 0.21 mmol) was used and isolated 0.07g (73% yield) of the desired product. ¹H NMR (499 MHz, cdcl₃) δ 7.30 – 7.23 (m, 1H), 7.23 – 7.17 (m, 2H), 7.00 – 6.93 (m, 2H), 6.84 (td, J = 6.8, 6.4, 2.3 Hz, 3H), 4.95 (s, 2H), 4.70 (s, 1H), 3.80 (d, J = 0.7 Hz, 3H), 2.45 (s, 4H), 2.23 (d, J = 16.3 Hz, 2H), 2.17 (d, J = 16.3 Hz, 2H), 1.10 (s, 6H), 0.99 (s, 6H). ¹³C NMR (126 MHz, cdcl₃) δ 196.43, 162.05, 159.78, 157.28, 138.83, 136.79, 129.52, 129.33,

119.72, 115.77, 114.36, 113.52, 112.85, 69.84, 55.21, 50.77, 40.86, 32.18, 30.97, 29.23, 27.36.
ESI MS m/z 509.23 (M + Na)⁺

3,3,6,6-tetramethyl-9-(4-((3-methylbenzyl)oxy)phenyl)-3,4,5,6,7,9-hexahydro-1H-xanthene-1,8(2H)-dione (CCG363240) [sz-09-67]

Following the general procedure on a scale of 70mg (0.19mmol) 9-(4-hydroxyphenyl)-3,3,6,6-tetramethyl-3,4,5,6,7,9-hexahydro-1H-xanthene-1,8(2H)-dione (**3**), 1-(bromomethyl)-3-methylbenzene (39 mg, 28 μ L, 1.1 Eq, 0.21 mmol) was used and isolated 0.07g (78% yield) of the desired product. ¹H NMR (499 MHz, $cdCl_3$) δ 7.28 – 7.16 (m, 5H), 7.12 (d, J = 7.4 Hz, 1H), 6.88 – 6.78 (m, 2H), 4.93 (s, 2H), 4.71 (s, 1H), 2.45 (s, 4H), 2.35 (s, 3H), 2.29 – 2.12 (m, 4H), 1.10 (s, 6H), 1.00 (s, 6H). ¹³C NMR (126 MHz, $cdCl_3$) δ 196.44, 162.04, 157.39, 138.17, 137.11, 136.70, 129.32, 128.61, 128.40, 128.32, 124.66, 115.79, 114.33, 70.01, 50.77, 40.87, 32.18, 30.96, 29.24, 27.36, 21.38. ESI MS m/z 493.23 (M + Na)⁺

3,3,6,6-tetramethyl-9-(4-((2-(trifluoromethoxy)benzyl)oxy)phenyl)-3,4,5,6,7,9-hexahydro-1H-xanthene-1,8(2H)-dione (CCG365669) [sz-09-68]

Following the general procedure on a scale of 70mg (0.19mmol) 9-(4-hydroxyphenyl)-3,3,6,6-tetramethyl-3,4,5,6,7,9-hexahydro-1H-xanthene-1,8(2H)-dione (**3**), 1-(bromomethyl)-2-(trifluoromethoxy)benzene (54 mg, 34 μ L, 1.1 Eq, 0.21 mmol) was used and isolated 0.07g (69% yield) of the desired product. ¹H NMR (499 MHz, $cdCl_3$) δ 7.60 – 7.54 (m, 1H), 7.37 – 7.22 (m, 3H), 7.24 – 7.18 (m, 2H), 6.86 – 6.79 (m, 2H), 5.07 (s, 2H), 4.71 (s, 1H), 2.45 (s, 4H), 2.23 (d, J = 16.3 Hz, 2H), 2.17 (d, J = 16.3 Hz, 2H), 1.10 (s, 6H), 0.99 (s, 6H). ¹³C NMR (126 MHz, $cdCl_3$) δ 196.45, 162.08, 156.96, 137.09, 130.13, 129.39, 129.37, 128.94, 127.00, 120.43, 115.75, 114.38, 64.19, 50.76, 40.86, 32.18, 30.98, 29.22, 27.36. ¹⁹F NMR (470 MHz, $cdCl_3$) δ -57.29. ESI MS m/z 563.20 (M + Na)⁺

9-(4-((2-(difluoromethoxy)benzyl)oxy)phenyl)-3,3,6,6-tetramethyl-3,4,5,6,7,9-hexahydro-1H-xanthene-1,8(2H)-dione (CCG365670) [sz-09-69]

Following the general procedure on a scale of 70mg (0.19mmol) 9-(4-hydroxyphenyl)-3,3,6,6-tetramethyl-3,4,5,6,7,9-hexahydro-1H-xanthene-1,8(2H)-dione (**3**), 1-(bromomethyl)-2-(difluoromethoxy)benzene (50 mg, 32 μ L, 1.1 Eq, 0.21 mmol) was used and isolated 0.09g (87% yield) of the desired product. ¹H NMR (499 MHz, $cdCl_3$) δ 7.56 – 7.47 (m, 1H), 7.32 (td, J = 7.8, 7.4, 1.8 Hz, 1H), 7.25 – 7.18 (m, 3H), 7.14 (d, J = 8.1 Hz, 1H), 6.85 – 6.80 (m, 2H), 6.69 – 6.34 (m, 1H), 5.04 (s, 2H), 4.71 (s, 1H), 2.45 (s, 4H), 2.29 – 2.14 (m, 4H), 1.10 (s, 6H), 1.00 (s, 6H).

¹³C NMR (126 MHz, cdcl₃) δ 196.46, 162.10, 157.04, 148.82, 137.03, 129.73, 129.37, 129.18, 129.14, 125.74, 119.24, 118.32, 116.24, 115.75, 114.43, 114.17, 64.72, 50.76, 40.86, 32.18, 30.98, 29.23, 27.36. ¹⁹F NMR (470 MHz, cdcl₃) δ -80.35 (d, J = 74.1 Hz). ESI MS m/z 545.21 (M + Na)⁺

9-(4-((2,6-dimethylbenzyl)oxy)phenyl)-3,3,6,6-tetramethyl-3,4,5,6,7,9-hexahydro-1H-xanthene-1,8(2H)-dione (CCG363137) [sz-09-70]

Following the general procedure on a scale of 75mg (0.2mmol) 9-(4-hydroxyphenyl)-3,3,6,6-tetramethyl-3,4,5,6,7,9-hexahydro-1H-xanthene-1,8(2H)-dione (**3**), 2-(bromomethyl)-1,3-dimethylbenzene (45 mg, 1.1 Eq, 0.23 mmol) was used and isolated 0.1g (98% yield) of the desired product. ¹H NMR (400 MHz, cdcl₃) δ 7.25 – 7.21 (m, 2H), 7.14 (dd, J = 8.3, 6.7 Hz, 1H), 7.06 (d, J = 7.5 Hz, 2H), 6.91 – 6.83 (m, 2H), 4.96 (s, 2H), 4.73 (s, 1H), 2.47 (s, 4H), 2.31 – 2.13 (m, 4H), 1.11 (s, 6H), 1.02 (s, 6H). ¹³C NMR (101 MHz, cdcl₃) δ 196.67, 162.13, 157.72, 138.20, 136.66, 132.94, 129.32, 128.50, 128.29, 115.77, 114.14, 64.36, 50.79, 40.86, 32.23, 31.08, 29.26, 27.45, 19.62. ESI MS m/z 507.25 (M + Na)⁺

9-(4-((2,4-dimethylbenzyl)oxy)phenyl)-3,3,6,6-tetramethyl-3,4,5,6,7,9-hexahydro-1H-xanthene-1,8(2H)-dione (CCG363138) [sz-09-71]

Following the general procedure on a scale of 70mg (0.19mmol) 9-(4-hydroxyphenyl)-3,3,6,6-tetramethyl-3,4,5,6,7,9-hexahydro-1H-xanthene-1,8(2H)-dione (**3**), 1-(bromomethyl)-2,4-dimethylbenzene (42 mg, 32 μL, 1.1 Eq, 0.21 mmol) was used and isolated 0.09g (95% yield) of the desired product. ¹H NMR (400 MHz, cdcl₃) δ 7.23 (dd, J = 9.0, 7.2 Hz, 3H), 7.03 (d, J = 1.7 Hz, 1H), 7.00 (dd, J = 8.1, 1.6 Hz, 1H), 6.91 – 6.79 (m, 2H), 4.90 (s, 2H), 4.72 (s, 1H), 2.46 (s, 4H), 2.32 (d, J = 1.8 Hz, 6H), 2.28 – 2.12 (m, 4H), 1.10 (s, 6H), 1.01 (s, 6H). ¹³C NMR (101 MHz, cdcl₃) δ 196.58, 162.11, 157.50, 138.00, 136.83, 136.82, 136.62, 131.98, 131.22, 129.31, 129.08, 126.58, 115.77, 114.24, 68.34, 50.77, 40.85, 32.21, 30.99, 29.27, 27.40, 21.10, 18.85. ESI MS m/z 507.25 (M + Na)⁺

9-(4-((2,5-dimethylbenzyl)oxy)phenyl)-3,3,6,6-tetramethyl-3,4,5,6,7,9-hexahydro-1H-xanthene-1,8(2H)-dione (CCG363239) [sz-09-72]

Following the general procedure on a scale of 70mg (0.19mmol) 9-(4-hydroxyphenyl)-3,3,6,6-tetramethyl-3,4,5,6,7,9-hexahydro-1H-xanthene-1,8(2H)-dione (**3**), 2-(bromomethyl)-1,4-dimethylbenzene (42 mg, 1.1 Eq, 0.21 mmol) was used and isolated 0.07g (70% yield) of the desired product. ¹H NMR (400 MHz, cdcl₃) δ 7.25 – 7.19 (m, 2H), 7.19 – 7.16 (m, 1H), 7.07 (s,

1H), 7.04 (dd, J = 7.7, 1.8 Hz, 1H), 6.91 – 6.77 (m, 2H), 4.90 (s, 2H), 4.71 (s, 1H), 2.46 (s, 4H), 2.30 (d, J = 6.5 Hz, 6H), 2.27 – 2.12 (m, 4H), 1.10 (s, 6H), 1.00 (s, 6H). 13C NMR (101 MHz, cdcl₃) δ 196.58, 162.10, 157.49, 136.67, 135.46, 134.72, 133.62, 130.26, 129.61, 129.31, 128.85, 115.77, 114.27, 68.51, 50.76, 40.85, 32.21, 30.99, 29.27, 27.37, 20.95, 18.43. ESI MS m/z 507.25 (M + Na)⁺

9-(4-((3,4-dimethylbenzyl)oxy)phenyl)-3,3,6,6-tetramethyl-3,4,5,6,7,9-hexahydro-1H-xanthene-1,8(2H)-dione (CCG363241) [sz-09-73]

Following the general procedure on a scale of 70mg (0.19mmol) 9-(4-hydroxyphenyl)-3,3,6,6-tetramethyl-3,4,5,6,7,9-hexahydro-1H-xanthene-1,8(2H)-dione (**3**), 4-(chloromethyl)-1,2-dimethylbenzene (32 mg, 33 μL, 1.1 Eq, 0.21 mmol) was used and isolated 0.08g (81% yield) of the desired product. 1H NMR (400 MHz, cdcl₃) δ 7.24 – 7.19 (m, 2H), 7.17 (s, 1H), 7.12 (d, J = 1.2 Hz, 2H), 6.92 – 6.73 (m, 2H), 4.90 (s, 2H), 4.71 (s, 1H), 2.46 (s, 4H), 2.26 (d, J = 3.3 Hz, 6H), 2.24 – 2.12 (m, 4H), 1.10 (s, 6H), 1.00 (s, 6H). 13C NMR (101 MHz, cdcl₃) δ 196.54, 162.11, 157.44, 136.75, 136.61, 136.32, 134.53, 129.75, 129.32, 129.13, 125.29, 115.77, 114.29, 69.91, 50.77, 40.84, 32.21, 30.96, 29.28, 27.37, 19.79, 19.54. ESI MS m/z 507.25 (M + Na)⁺

9-(4-((4-methoxybenzyl)oxy)phenyl)-3,3,6,6-tetramethyl-3,4,5,6,7,9-hexahydro-1H-xanthene-1,8(2H)-dione (CCG363238) [sz-09-74]

Following the general procedure on a scale of 70mg (0.19mmol) 9-(4-hydroxyphenyl)-3,3,6,6-tetramethyl-3,4,5,6,7,9-hexahydro-1H-xanthene-1,8(2H)-dione (**3**), 1-(chloromethyl)-4-methoxybenzene (33 mg, 28 μL, 1.1 Eq, 0.21 mmol) was used and isolated 0.08g (89% yield) of the desired product. 1H NMR (400 MHz, cdcl₃) δ 7.34 – 7.28 (m, 2H), 7.23 – 7.17 (m, 2H), 6.92 – 6.86 (m, 2H), 6.85 – 6.79 (m, 2H), 4.89 (s, 2H), 4.70 (s, 1H), 3.80 (s, 3H), 2.45 (s, 4H), 2.27 – 2.11 (m, 4H), 1.09 (s, 6H), 0.99 (s, 6H). 13C NMR (101 MHz, cdcl₃) δ 196.54, 162.09, 159.37, 157.35, 136.65, 129.32, 129.22, 115.76, 114.29, 113.93, 69.66, 55.29, 50.76, 40.84, 32.20, 30.96, 29.27, 27.36. ESI MS m/z 509.22 (M + Na)⁺

9-(4-((3,4-dichlorobenzyl)oxy)phenyl)-3,3,6,6-tetramethyl-3,4,5,6,7,9-hexahydro-1H-xanthene-1,8(2H)-dione (CCG365857) [sz-09-75]

Following the general procedure on a scale of 70mg (0.19mmol) 9-(4-hydroxyphenyl)-3,3,6,6-tetramethyl-3,4,5,6,7,9-hexahydro-1H-xanthene-1,8(2H)-dione (**3**), 4-(bromomethyl)-1,2-dichlorobenzene (50 mg, 31 μL, 1.1 Eq, 0.21 mmol) was used and isolated 0.08g (78% yield) of the desired product. 1H NMR (499 MHz, cdcl₃) δ 7.51 (d, J = 2.0 Hz, 1H), 7.43 (d, J = 8.2 Hz,

1H), 7.23 (dd, J = 9.4, 2.4 Hz, 3H), 6.84 – 6.78 (m, 2H), 4.93 (s, 2H), 4.71 (s, 1H), 2.47 (s, 4H), 2.21 (q, J = 16.3 Hz, 4H), 1.11 (s, 6H), 1.00 (s, 6H). ¹³C NMR (126 MHz, cdcl₃) δ 196.48, 162.13, 156.81, 137.57, 137.26, 132.62, 131.77, 130.49, 129.46, 129.25, 126.57, 115.70, 114.35, 68.50, 50.76, 40.87, 32.20, 31.03, 29.26, 27.34. ESI MS m/z 525.15 (M + H)⁺

9-(4-((4-chloro-2-methoxybenzyl)oxy)phenyl)-3,3,6,6-tetramethyl-3,4,5,6,7,9-hexahydro-1H-xanthene-1,8(2H)-dione (CCG365920) [sz-09-77]

Following the general procedure on a scale of 70mg (0.19mmol) 9-(4-hydroxyphenyl)-3,3,6,6-tetramethyl-3,4,5,6,7,9-hexahydro-1H-xanthene-1,8(2H)-dione (**3**), 1-(bromomethyl)-4-chloro-2-methoxybenzene (46 mg, 1.02 Eq, 0.19 mmol) was used and isolated 0.09g (88% yield) of the desired product. ¹H NMR (499 MHz, cdcl₃) δ 7.34 (d, J = 8.1 Hz, 1H), 7.23 – 7.17 (m, 2H), 6.94 (dt, J = 8.1, 1.5 Hz, 1H), 6.87 (t, J = 1.5 Hz, 1H), 6.86 – 6.79 (m, 2H), 4.97 (s, 2H), 4.71 (s, 1H), 3.83 (d, J = 1.0 Hz, 3H), 2.46 (s, 4H), 2.21 (q, J = 16.3 Hz, 4H), 1.11 (s, 6H), 1.00 (s, 6H). ¹³C NMR (126 MHz, cdcl₃) δ 196.48, 162.07, 157.35, 157.25, 136.74, 134.18, 129.56, 129.32, 124.27, 120.57, 115.79, 114.38, 111.03, 64.44, 55.63, 50.78, 40.87, 32.19, 30.97, 29.25, 27.37. ESI MS m/z 543.19 (M + Na)⁺

9-(4-((2,6-dichlorobenzyl)oxy)phenyl)-3,3,6,6-tetramethyl-3,4,5,6,7,9-hexahydro-1H-xanthene-1,8(2H)-dione (CCG366790) [sz-10-65]

Following the general procedure on a scale of 70mg (0.19mmol) 9-(4-hydroxyphenyl)-3,3,6,6-tetramethyl-3,4,5,6,7,9-hexahydro-1H-xanthene-1,8(2H)-dione (**3**), 1,3-dichloro-2-(chloromethyl)benzene (41 mg, 1.1 Eq, 0.21 mmol) was used and isolated 0.08g (83% yield) of the desired product. ¹H NMR (499 MHz, cdcl₃) δ 7.34 (d, J = 8.0 Hz, 2H), 7.26 – 7.20 (m, 3H), 6.99 – 6.78 (m, 2H), 5.20 (s, 2H), 4.73 (s, 1H), 2.47 (s, 4H), 2.30 – 2.13 (m, 4H), 1.11 (s, 6H), 1.02 (s, 6H). ¹³C NMR (126 MHz, cdcl₃) δ 196.49, 162.07, 157.27, 137.05, 137.05, 132.33, 130.27, 129.34, 128.42, 115.77, 114.42, 64.95, 50.79, 40.88, 32.21, 31.04, 29.23, 27.46. ESI MS m/z 547.14 (M + Na)⁺

9-(4-((2,4-dichlorobenzyl)oxy)phenyl)-3,3,6,6-tetramethyl-3,4,5,6,7,9-hexahydro-1H-xanthene-1,8(2H)-dione (CCG366794) [sz-10-70]

Following the general procedure on a scale of 70mg (0.19mmol) 9-(4-hydroxyphenyl)-3,3,6,6-tetramethyl-3,4,5,6,7,9-hexahydro-1H-xanthene-1,8(2H)-dione (**3**), 2,4-dichloro-1-(chloromethyl)benzene (41 mg, 24 μL, 1.1 Eq, 0.21 mmol) was used and isolated 0.07g (69% yield) of the desired product. ¹H NMR (499 MHz, cdcl₃) δ 7.47 (d, J = 8.3 Hz, 1H), 7.39 (d, J =

2.1 Hz, 1H), 7.25 (dd, J = 8.3, 2.1 Hz, 1H), 7.24 – 7.20 (m, 2H), 6.90 – 6.71 (m, 2H), 5.04 (s, 2H), 4.71 (s, 1H), 2.46 (s, 4H), 2.20 (q, J = 16.3 Hz, 4H), 1.10 (s, 6H), 1.00 (s, 6H). ¹³C NMR (126 MHz, cdcl₃) δ 196.45, 162.12, 156.76, 137.29, 133.92, 133.69, 133.06, 129.70, 129.45, 129.07, 127.24, 115.71, 114.40, 66.54, 50.77, 40.86, 32.19, 31.02, 29.25, 27.36. ESI MS m/z 547.14 (M + Na)⁺

9-(4-((2-(difluoromethyl)benzyl)oxy)phenyl)-3,3,6,6-tetramethyl-3,4,5,6,7,9-hexahydro-1H-xanthene-1,8(2H)-dione (CCG367264) [sz-11-53]

Following the general procedure on a scale of 70mg (0.19mmol) 9-(4-hydroxyphenyl)-3,3,6,6-tetramethyl-3,4,5,6,7,9-hexahydro-1H-xanthene-1,8(2H)-dione (**3**), 1-(bromomethyl)-2-(difluoromethyl)benzene (50 mg, 31 μL, 1.1 Eq, 0.23 mmol) was used and isolated 0.1g (96% yield) of the desired product. ¹H NMR (499 MHz, cdcl₃) δ 7.61 (d, J = 7.5 Hz, 1H), 7.52 (d, J = 7.6 Hz, 1H), 7.47 (t, J = 7.4 Hz, 1H), 7.44 – 7.39 (m, 1H), 7.26 – 7.20 (m, 2H), 7.07 – 6.76 (m, 3H), 5.12 (s, 2H), 4.72 (s, 1H), 2.47 (s, 4H), 2.21 (q, J = 16.3 Hz, 4H), 1.11 (s, 6H), 1.01 (s, 6H). ¹³C NMR (126 MHz, cdcl₃) δ 196.47, 162.13, 156.85, 137.27, 135.19, 132.34, 130.85, 129.45, 129.23, 128.31, 126.08, 115.71, 114.36, 113.81, 111.92, 67.18, 50.78, 40.86, 32.19, 31.04, 29.24, 27.38. ¹⁹F NMR (470 MHz, cdcl₃) δ -112.09, -112.21. ESI MS m/z 529.21 (M + Na)⁺

2-((4-(3,3,6,6-tetramethyl-1,8-dioxo-2,3,4,5,6,7,8,9-octahydro-1H-xanthen-9-yl)phenoxy)methyl)benzotrile (CCG367265) [sz-11-55]

Following the general procedure on a scale of 80mg (0.22 mmol) 9-(4-hydroxyphenyl)-3,3,6,6-tetramethyl-3,4,5,6,7,9-hexahydro-1H-xanthene-1,8(2H)-dione (**3**), 2-(chloromethyl)benzotrile (36 mg, 1.1 Eq, 0.24 mmol) was used and isolated 0.09g (81% yield) of the desired product. ¹H NMR (400 MHz, cdcl₃) δ 7.66 (ddd, J = 7.9, 6.5, 1.5 Hz, 2H), 7.60 (tt, J = 7.8, 1.3 Hz, 1H), 7.40 (ddd, J = 9.0, 6.8, 1.4 Hz, 1H), 7.26 – 7.20 (m, 2H), 6.93 – 6.77 (m, 2H), 5.18 (s, 2H), 4.71 (s, 1H), 2.46 (s, 4H), 2.28 – 2.12 (m, 4H), 1.10 (d, J = 1.2 Hz, 6H), 1.00 (s, 6H). ¹³C NMR (101 MHz, cdcl₃) δ 196.51, 162.19, 156.63, 140.86, 137.52, 133.09, 132.78, 129.49, 128.44, 128.26, 117.07, 115.67, 114.46, 110.89, 67.44, 50.76, 40.84, 32.21, 31.00, 29.28, 27.37. ESI MS m/z 504.21 (M + Na)⁺

9-(4-((2-ethylbenzyl)oxy)phenyl)-3,3,6,6-tetramethyl-3,4,5,6,7,9-hexahydro-1H-xanthene-1,8(2H)-dione (CCG366697) [sz-10-51]

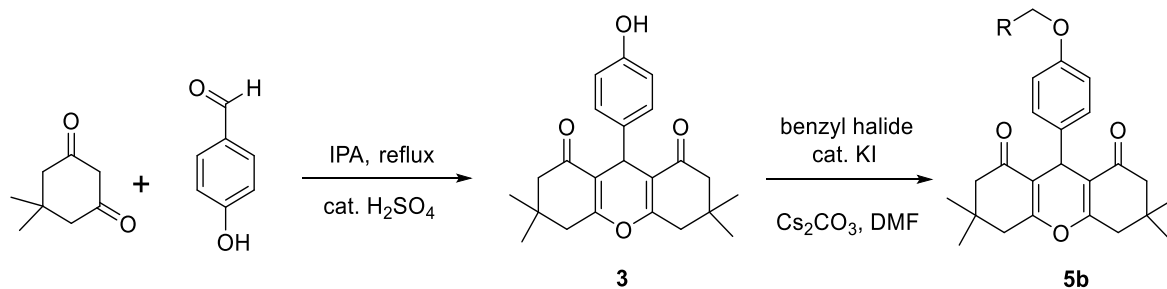
Following the general procedure on a scale of 100mg (0.27 mmol) 9-(4-hydroxyphenyl)-3,3,6,6-tetramethyl-3,4,5,6,7,9-hexahydro-1H-xanthene-1,8(2H)-dione (**3**), 1-(chloromethyl)-2-

ethylbenzene (**16b**) (50.6 mg, 1.2 Eq, 327 μmol) was used and isolated 0.09g (68% yield) of the desired product. ^1H NMR (499 MHz, cdCl_3) δ 7.38 (dd, $J = 7.6, 1.4$ Hz, 1H), 7.32 – 7.27 (m, 1H), 7.27 – 7.18 (m, 4H), 6.94 – 6.77 (m, 2H), 4.98 (s, 2H), 4.73 (s, 1H), 2.70 (q, $J = 7.5$ Hz, 2H), 2.47 (s, 4H), 2.29 – 2.15 (m, 4H), 1.25 (t, $J = 7.5$ Hz, 3H), 1.11 (s, 6H), 1.02 (s, 6H). ^{13}C NMR (126 MHz, cdCl_3) δ 196.52, 162.09, 157.42, 142.89, 136.74, 134.34, 129.35, 129.27, 128.60, 128.46, 125.95, 115.78, 114.28, 68.11, 50.80, 40.87, 32.21, 31.03, 29.26, 27.42, 25.35, 15.27. ESI MS m/z 507.25 ($\text{M} + \text{Na}$)⁺

9-(4-((2-(fluoromethyl)benzyl)oxy)phenyl)-3,3,6,6-tetramethyl-3,4,5,6,7,9-hexahydro-1H-xanthene-1,8(2H)-dione (CCG369551) [sz-11-84]

Following the general procedure on a scale of 250mg (0.68 mmol) 9-(4-hydroxyphenyl)-3,3,6,6-tetramethyl-3,4,5,6,7,9-hexahydro-1H-xanthene-1,8(2H)-dione (**3**), 1-(chloromethyl)-2-(fluoromethyl)benzene (**16c**) (130 mg, 1.2 Eq, 819 μmol) was used and isolated 0.1g (32% yield) of the desired product. ^1H NMR (400 MHz, cdCl_3) δ 7.44 (ddt, $J = 6.1, 4.1, 2.4$ Hz, 2H), 7.40 – 7.32 (m, 2H), 7.25 – 7.18 (m, 2H), 6.88 – 6.79 (m, 2H), 5.49 (d, $J = 47.7$ Hz, 2H), 5.03 (d, $J = 1.1$ Hz, 2H), 4.71 (s, 1H), 2.46 (s, 4H), 2.28 – 2.13 (m, 4H), 1.10 (s, 6H), 1.00 (s, 6H). ^{13}C NMR (101 MHz, cdCl_3) δ 196.52, 162.11, 157.03, 137.08, 135.18, 135.14, 134.80, 134.64, 129.41, 129.13, 129.12, 129.06, 129.03, 128.66, 128.58, 128.42, 128.41, 115.72, 114.27, 83.29, 81.64, 67.67, 50.76, 40.85, 32.20, 31.02, 29.26, 27.38. ^{19}F NMR (376 MHz, cdCl_3) δ 28.07, 27.94, 27.82, -200.50. ESI MS m/z 511.22 ($\text{M} + \text{Na}$)⁺

Scheme 2.2 Synthetic Route and Conditions for **5b**



Compound **5b** General Procedures

To a solution of 9-(4-hydroxyphenyl)-3,3,6,6-tetramethyl-3,4,5,6,7,9-hexahydro-1H-xanthene-1,8(2H)-dione (80 mg, 1 Eq, 0.22 mmol) and benzyl halide (52 mg, 1.2 Eq, 0.26 mmol) in DMF (1mL) was treated with Cs_2CO_3 (0.14 g, 2 Eq, 0.44 mmol) and KI (38 mg, 1.3 Eq, 0.23 mmol). The reaction mixture was stirred at room temperature for 16 h. The reaction was diluted with water,

and the solids were filtered. The crude material was chromatographed over silica gel, eluting with 0-40% EtOAc/Hex. Compounds were isolated above 95% pure.

9-(4-((2-iodobenzyl)oxy)phenyl)-3,3,6,6-tetramethyl-3,4,5,6,7,9-hexahydro-1H-xanthene-1,8(2H)-dione (CCG362939) [sz-08-50]

Following the general procedure on a scale of 65mg (0.18mmol) 9-(4-hydroxyphenyl)-3,3,6,6-tetramethyl-3,4,5,6,7,9-hexahydro-1H-xanthene-1,8(2H)-dione (**3**), 1-bromo-2-(bromomethyl)-3-methylbenzene (48 mg, 1.2 Eq, 0.18 mmol) was used and isolated 0.09g (91% yield) of the desired product. ¹H NMR (499 MHz, cdcl₃) δ 7.83 (dd, J = 7.9, 1.2 Hz, 1H), 7.48 (dd, J = 7.8, 1.6 Hz, 1H), 7.34 (td, J = 7.5, 1.2 Hz, 1H), 7.25 – 7.18 (m, 2H), 7.00 (td, J = 7.6, 1.7 Hz, 1H), 6.89 – 6.78 (m, 2H), 4.96 (s, 2H), 4.72 (s, 1H), 2.45 (d, J = 1.0 Hz, 4H), 2.28 – 2.12 (m, 4H), 1.10 (s, 6H), 1.00 (s, 6H). ¹³C NMR (126 MHz, cdcl₃) δ 196.45, 162.09, 156.92, 139.39, 139.12, 137.08, 129.38, 129.32, 128.66, 128.34, 115.75, 114.50, 97.01, 73.91, 50.77, 40.87, 32.19, 30.98, 29.24, 27.40. ESI MS m/z 605.11 (M + Na)⁺

9-(4-((3-iodobenzyl)oxy)phenyl)-3,3,6,6-tetramethyl-3,4,5,6,7,9-hexahydro-1H-xanthene-1,8(2H)-dione (CCG362974) [sz-08-51]

Following the general procedure on a scale of 55mg (0.15mmol) 9-(4-hydroxyphenyl)-3,3,6,6-tetramethyl-3,4,5,6,7,9-hexahydro-1H-xanthene-1,8(2H)-dione (**3**), 1-(bromomethyl)-3-iodobenzene (50 mg, 1.1 Eq, 0.17 mmol) was used and isolated 0.08g (94% yield) of the desired product. ¹H NMR (499 MHz, cdcl₃) δ 7.75 (t, J = 1.8 Hz, 1H), 7.63 (dt, J = 8.0, 1.4 Hz, 1H), 7.38 – 7.30 (m, 1H), 7.24 – 7.16 (m, 2H), 7.09 (t, J = 7.8 Hz, 1H), 6.86 – 6.75 (m, 2H), 4.91 (s, 2H), 4.71 (s, 1H), 2.46 (s, 4H), 2.20 (q, J = 16.3 Hz, 4H), 1.10 (s, 6H), 1.00 (s, 6H). ¹³C NMR (126 MHz, cdcl₃) δ 196.44, 162.09, 157.01, 139.63, 137.07, 136.85, 136.29, 130.22, 129.40, 126.59, 115.73, 114.35, 94.36, 68.94, 50.77, 40.86, 32.19, 31.00, 29.26, 27.35. ESI MS m/z 605.11 (M + Na)⁺

9-(4-((4-iodobenzyl)oxy)phenyl)-3,3,6,6-tetramethyl-3,4,5,6,7,9-hexahydro-1H-xanthene-1,8(2H)-dione (CCG362934) [sz-08-45]

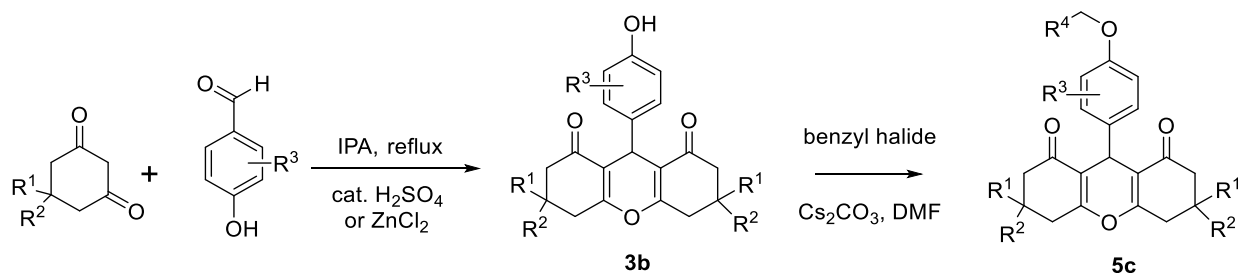
Following the general procedure on a scale of 55mg (0.15mmol) 9-(4-hydroxyphenyl)-3,3,6,6-tetramethyl-3,4,5,6,7,9-hexahydro-1H-xanthene-1,8(2H)-dione (**3**), 1-(bromomethyl)-4-iodobenzene (53 mg, 1.2 Eq, 0.18 mmol) was used and isolated 0.08g (93% yield) of the desired product. ¹H NMR (499 MHz, cdcl₃) δ 7.77 – 7.61 (m, 2H), 7.23 – 7.17 (m, 2H), 7.17 – 7.07 (m, 2H), 6.85 – 6.76 (m, 2H), 4.91 (s, 2H), 4.70 (s, 1H), 2.45 (s, 4H), 2.20 (q, J = 16.3 Hz, 4H), 1.10

(s, 6H), 0.99 (s, 6H). ¹³C NMR (126 MHz, cdcl₃) δ 196.43, 162.07, 157.03, 137.57, 137.02, 136.97, 129.39, 129.32, 115.72, 114.33, 93.29, 69.24, 50.77, 40.86, 32.19, 31.00, 29.25, 27.35. ESI MS m/z 605.12 (M + Na)⁺

3,3,6,6-tetramethyl-9-(4-((2-morpholinobenzyl)oxy)phenyl)-3,4,5,6,7,9-hexahydro-1H-xanthene-1,8(2H)-dione (CCG369832) [sz-13-10]

Following the general procedure on a scale of 50mg (0.14mmol) 9-(4-hydroxyphenyl)-3,3,6,6-tetramethyl-3,4,5,6,7,9-hexahydro-1H-xanthene-1,8(2H)-dione (**3**), 4-(2-(bromomethyl)phenyl)morpholine (**15a**) (35 mg, 1.0 Eq, 0.14 mmol) was used. The reaction mixture was heated in pressure vessel for 16h. Desired compound was isolated 0.002g (3% yield). ¹H NMR (499 MHz, cdcl₃) δ 7.52 – 7.46 (m, 1H), 7.30 (dd, J = 8.7, 7.0 Hz, 1H), 7.22 – 7.17 (m, 2H), 7.12 (dt, J = 7.2, 3.1 Hz, 2H), 6.86 – 6.77 (m, 2H), 5.07 (s, 2H), 4.71 (s, 1H), 3.79 (dd, J = 5.7, 3.4 Hz, 4H), 2.96 – 2.90 (m, 4H), 2.45 (s, 4H), 2.23 (d, J = 16.3 Hz, 2H), 2.18 (d, J = 16.3 Hz, 2H), 1.10 (s, 6H), 1.00 (s, 6H). ¹³C NMR (126 MHz, cdcl₃) δ 196.47, 162.05, 157.41, 151.25, 136.65, 131.98, 130.00, 129.30, 128.89, 124.13, 119.66, 115.80, 114.34, 67.39, 65.91, 53.33, 50.77, 40.87, 32.19, 30.94, 29.23, 27.35. ESI MS m/z 542.28 (M + H)⁺

Scheme 2.3 Synthetic Route and Conditions for **3b** and **5c**



Intermediate **3b** Procedure

9-(4-hydroxy-3-methylphenyl)-3,3,6,6-tetramethyl-3,4,5,6,7,9-hexahydro-1H-xanthene-1,8(2H)-dione (3ba) [sz-08-20]

To a solution of 4-hydroxy-3-methylbenzaldehyde (80 mg, 1 Eq, 0.59 mmol) and 5,5-dimethylcyclohexane-1,3-dione (0.17 g, 2.01 Eq, 1.2 mmol) in 70% IPA (2mL) was treated H₂SO₄ (12 mg, 6.3 μL, 0.2 Eq, 0.12 mmol). The yellow reaction mixture was refluxed at 120°C for 16 h and cooled to room temperature. Precipitates formed overnight. The solids were filtered and washed with cold 70% IPA. White solids formed (0.12g, 54% yield). ¹H NMR (499 MHz, cd₃od) δ 6.92 (d, J = 2.4 Hz, 1H), 6.84 (dd, J = 8.2, 2.3 Hz, 1H), 6.57 (dd, J = 8.2, 3.1 Hz, 1H),

4.50 (s, 1H), 2.55 (d, J = 4.8 Hz, 4H), 2.28 (d, J = 16.3 Hz, 2H), 2.14 (d, J = 16.3 Hz, 2H), 2.10 (d, J = 2.0 Hz, 3H), 1.09 (s, 6H), 0.99 (s, 6H).

9-(3-chloro-4-hydroxyphenyl)-3,3,6,6-tetramethyl-3,4,5,6,7,9-hexahydro-1H-xanthene-1,8(2H)-dione (3bb) [sz-09-78]

To a solution of 3-chloro-4-hydroxybenzaldehyde (300 mg, 1 Eq, 1.92 mmol) and 5,5-dimethylcyclohexane-1,3-dione (540 mg, 2.01 Eq, 3.85 mmol) in 70% IPA (6mL) was treated with H₂SO₄ (37.6 mg, 20.4 μL, 0.2 Eq, 383 μmol). The reaction mixture was refluxed at 120°C for 16 h and cooled to room temperature. Precipitates formed overnight. The solids were filtered and washed with cold 70% IPA. Solids formed (0.6g, 78% yield). ¹H NMR (499 MHz, cdcl₃) δ 7.27 – 7.25 (m, 1H), 7.09 (dd, J = 8.3, 2.1 Hz, 1H), 6.86 (dd, J = 8.4, 1.1 Hz, 1H), 5.43 (d, J = 1.7 Hz, 1H), 4.67 (s, 1H), 2.47 (s, 4H), 2.31 – 2.11 (m, 4H), 1.11 (s, 6H), 1.02 (s, 6H).

9-(4-hydroxy-3-(trifluoromethoxy)phenyl)-3,3,6,6-tetramethyl-3,4,5,6,7,9-hexahydro-1H-xanthene-1,8(2H)-dione (3bc) [sz-09-82]

To a solution of 4-hydroxy-3-(trifluoromethoxy)benzaldehyde (200 mg, 1 Eq, 970 μmol) and 5,5-dimethylcyclohexane-1,3-dione (273 mg, 2.01 Eq, 1.95 mmol) in 70% IPA (3mL) was treated with H₂SO₄ (19.0 mg, 10.3 μL, 0.2 Eq, 194 μmol). The reaction mixture was refluxed at 120°C for 16 h, cooled to room temperature and concentrated under reduced pressure. The crude material was chromatographed over silica gel, eluted with 0-50% EtOAc/Hex. Compound was isolated as solids (0.4g, 96% yield). ¹H NMR (499 MHz, cdcl₃) δ 7.20 (dt, J = 8.4, 1.6 Hz, 1H), 7.04 (p, J = 1.5 Hz, 1H), 6.82 (dd, J = 8.4, 2.3 Hz, 1H), 4.69 (s, 1H), 2.54 – 2.41 (m, 4H), 2.30 – 2.11 (m, 4H), 1.12 (s, 6H), 1.00 (s, 6H). ¹⁹F NMR (470 MHz, cdcl₃) δ -57.89.

9-(3-(difluoromethoxy)-4-hydroxyphenyl)-3,3,6,6-tetramethyl-3,4,5,6,7,9-hexahydro-1H-xanthene-1,8(2H)-dione (3bd) [sz-09-88]

To a solution of 3-(difluoromethoxy)-4-hydroxybenzaldehyde (80 mg, 1 Eq, 0.43 mmol) and 5,5-dimethylcyclohexane-1,3-dione (0.12 g, 2.01 Eq, 0.85 mmol) in 70% IPA (1mL) was treated with H₂SO₄ (8.3 mg, 4.5 μL, 0.2 Eq, 85 μmol). The reaction mixture was refluxed at 120°C for 16 h and cooled to room temperature. Precipitates formed overnight. The solids were filtered and washed with cold 70% IPA. Solids formed (0.1g, 54% yield). ¹H NMR (499 MHz, cdcl₃) δ 7.86 (s, 1H), 7.07 (s, 1H), 7.03 (d, J = 8.2 Hz, 1H), 6.86 (dd, J = 8.4, 1.0 Hz, 1H), 6.49 (t, J = 74.0 Hz, 1H), 4.67 (s, 1H), 2.47 (s, 4H), 2.22 (q, J = 16.3 Hz, 4H), 1.12 (s, 6H), 1.01 (s, 6H). ¹⁹F NMR (470 MHz, cdcl₃) δ -79.74, -79.90 (d, J = 4.7 Hz).

9-(4-hydroxy-3,5-dimethylphenyl)-3,3,6,6-tetramethyl-3,4,5,6,7,9-hexahydro-1H-xanthene-1,8(2H)-dione (3be) [sz-09-98]

To a solution of 4-hydroxy-3,5-dimethylbenzaldehyde (200 mg, 1 Eq, 1.33 mmol) and 5,5-dimethylcyclohexane-1,3-dione (375 mg, 2.01 Eq, 2.68 mmol) in 70% IPA (4mL) was treated with H₂SO₄ (26.1 mg, 14.2 μL, 0.2 Eq, 266 μmol). The reaction mixture was refluxed at 120°C for 16 h and cooled to room temperature. Precipitates formed overnight. The solids were filtered and washed with cold 70% IPA (0.5g, 95% yield). ¹H NMR (499 MHz, cdcl₃) δ 6.86 (s, 2H), 4.62 (s, 1H), 2.54-2.40 (m, 4H), 2.21 (d, J = 7.7 Hz, 4H), 2.14 (s, 6H), 1.10 (s, 6H), 1.02 (s, 6H).

9-(3,5-diethyl-4-hydroxyphenyl)-3,3,6,6-tetramethyl-3,4,5,6,7,9-hexahydro-1H-xanthene-1,8(2H)-dione (3bf) [sz-10-17]

To a solution of 3,5-diethyl-4-hydroxybenzaldehyde (120 mg, 1 Eq, 673 μmol) and 5,5-dimethylcyclohexane-1,3-dione (190 mg, 2.01 Eq, 1.35 mmol) in 70% 2-propanol (3mL) was treated with H₂SO₄ (13.2 mg, 7.18 μL, 0.2 Eq, 135 μmol). The reaction mixture was refluxed at 120°C for 16 h, cooled to room temperature and concentrated under reduced pressure. The crude material was chromatographed over silica gel, eluted with 0-50% EtOAc/Hex. Compound was isolated as solids (0.3g, 97% yield). ¹H NMR (400 MHz, cdcl₃) δ 6.88 (s, 2H), 4.64 (s, 1H), 2.53 (q, J = 7.6 Hz, 4H), 2.45 (s, 4H), 2.20 (d, J = 6.2 Hz, 4H), 1.18 (t, J = 7.6 Hz, 6H), 1.10 (s, 6H), 1.00 (s, 6H).

9-(4-hydroxy-2-methylphenyl)-3,3,6,6-tetramethyl-3,4,5,6,7,9-hexahydro-1H-xanthene-1,8(2H)-dione (3bg)

To a mixture of 2-methyl-4-hydroxybenzaldehyde (0.25 g, 1.8 mmol), 5,5-dimethylcyclohexane-1,3-dione (0.51 g, 3.7 mmol), sulfuric acid (0.05 mL), and water (50 mL) was refluxed for 16 h. The solids dissolved gradually to give a clear green solution which deposited an off-white solid upon heating. The suspension was cooled to r.t. The solids were filtered, washed well with water and a small amount of hexane, and air-dried to give 0.51 g (73% yield). ¹H NMR (400 MHz, DMSO-d₆) δ 9.01 (s, 1H), 6.63 (d, J = 8.2 Hz, 1H), 6.44 – 6.35 (m, 2H), 4.48 (s, 1H), 2.55 – 2.39 (m, 7H plus DMSO), 2.22 (d, J = 16.1 Hz, 2H), 2.01 (d, J = 16.3 Hz, 2H), 1.01 (s, 6H), 0.86 (s, 6H).

9-(3-fluoro-4-hydroxyphenyl)-3,3,6,6-tetramethyl-3,4,5,6,7,9-hexahydro-1H-xanthene-1,8(2H)-dione (3bh)

To a solution of 3-fluoro-4-hydroxybenzaldehyde (0.50 g, 3.6 mmol) in isopropanol (12 mL) was treated sequentially with 5,5-dimethylcyclohexane-1,3-dione (1.0 g, 7.1 mmol) and sulfuric acid (0.05 mL). The resulting yellow solution was refluxed for 16 h. A thick white solid deposited upon cooling. The suspension was chilled in the freezer overnight; the solids were filtered, washed well with cold isopropanol, and air-dried to give 0.92 g (67% yield). ¹H NMR (400 MHz, Chloroform-d) δ 7.00 (dd, J = 11.5, 2.1 Hz, 1H), 6.94 – 6.86 (m, 1H), 6.77 (t, J = 8.6 Hz, 1H), 5.51 (d, J = 3.6 Hz, 1H), 4.65 (s, 1H), 2.46 (s, 4H), 2.32 – 2.08 (m, 4H), 1.10 (s, 6H), 1.00 (s, 6H).

9-(4-hydroxyphenyl)-3,4,5,6,7,9-hexahydro-1H-xanthene-1,8(2H)-dione (3bi)

To a solution of 4-hydroxybenzaldehyde (0.70 g, 5.7 mmol) in isopropanol (18 mL) was treated sequentially with cyclohexane-1,3-dione (1.3 g, 11 mmol) and sulfuric acid (0.05 mL). The resulting yellow solution was refluxed for 5.5 hr. A thick off-white solid began to precipitate after an hour at reflux, and more solids deposited upon cooling. The solid was filtered, washed well with cold isopropanol, and air-dried to give 1.08 g (62% yield). ¹H NMR (400 MHz, DMSO-d₆) δ 9.14 (s, 1H), 7.00 – 6.89 (m, 2H), 6.62 – 6.52 (m, 2H), 4.46 (s, 1H), 2.69 – 2.49 (m, 4H), 2.34 – 2.16 (m, 4H), 2.00 – 1.84 (m, 2H), 1.81 (dt, J = 15.1, 10.7, 4.6 Hz, 2H).

General Procedure for Product 5c

To a solution of **Intermediate 3b** (80 mg, 1 Eq, 0.22 mmol) and benzyl halide (52 mg, 1.2 Eq, 0.26 mmol) in DMF (1mL) was treated with Cs₂CO₃ (0.14 g, 2 Eq, 0.44 mmol). The reaction mixture was stirred at room temperature for 16 h. The reaction was diluted with water, and the solids were filtered. The crude material was chromatographed over silica gel, eluting with 0-40% EtOAc/Hex. Compounds were isolated above 95% pure.

3,3,6,6-tetramethyl-9-(3-methyl-4-((2-methylbenzyl)oxy)phenyl)-3,4,5,6,7,9-hexahydro-1H-xanthene-1,8(2H)-dione (CCG362904) [sz-08-38]

Following the general procedure of **5c** on a scale of 75mg (0.2mmol) 9-(4-hydroxy-3-methylphenyl)-3,3,6,6-tetramethyl-3,4,5,6,7,9-hexahydro-1H-xanthene-1,8(2H)-dione (**3ba**), 1-(bromomethyl)-2-methylbenzene (73 mg, 52 μL, 2 Eq, 0.39 mmol) was used. 0.08g of product was isolated (83% yield). ¹H NMR (499 MHz, cdcl₃) δ 7.41 (dd, J = 7.0, 2.2 Hz, 1H), 7.24 – 7.15 (m, 3H), 7.08 (d, J = 8.3 Hz, 2H), 6.78 (d, J = 8.1 Hz, 1H), 4.95 (s, 2H), 4.69 (s, 1H), 2.47 (s, 4H), 2.34 (s, 3H), 2.27 – 2.14 (m, 7H), 1.10 (s, 6H), 1.02 (s, 6H). ¹³C NMR (126 MHz, cdcl₃) δ 196.50, 162.01, 155.50, 136.39, 136.28, 135.52, 130.75, 130.15, 128.19, 127.84, 126.59, 126.36, 125.88,

115.88, 110.75, 68.30, 50.82, 40.88, 32.22, 30.94, 29.23, 27.43, 18.86, 16.51. ESI MS m/z 485.26 (M + H)⁺

9-(4-((2-methoxybenzyl)oxy)-3-methylphenyl)-3,3,6,6-tetramethyl-3,4,5,6,7,9-hexahydro-1H-xanthene-1,8(2H)-dione (CCG366027) [sz-09-80]

Following the general procedure of **5c** on a scale of 70mg (0.18mmol) 9-(4-hydroxy-3-methylphenyl)-3,3,6,6-tetramethyl-3,4,5,6,7,9-hexahydro-1H-xanthene-1,8(2H)-dione (**3ba**), 1-(bromomethyl)-2-methoxybenzene (41 mg, 29 μ L, 1.1 Eq, 0.20 mmol) was used. 0.08g of product was isolated (84% yield). ¹H NMR (499 MHz, cdcl₃) δ 7.50 (dd, J = 7.5, 1.7 Hz, 1H), 7.28 (td, J = 8.6, 8.1, 1.7 Hz, 1H), 7.09 (d, J = 2.4 Hz, 1H), 7.05 (dd, J = 8.3, 2.4 Hz, 1H), 6.97 (t, J = 7.5 Hz, 1H), 6.89 (d, J = 8.2 Hz, 1H), 6.79 (d, J = 8.4 Hz, 1H), 5.04 (s, 2H), 4.70 (s, 1H), 3.84 (s, 3H), 2.47 (s, 4H), 2.29 – 2.15 (m, 7H). ¹³C NMR (126 MHz, cdcl₃) δ 196.51, 162.00, 156.56, 155.60, 136.12, 130.72, 128.40, 127.99, 126.51, 126.33, 126.21, 120.51, 115.93, 111.13, 110.04, 64.85, 55.32, 50.82, 40.89, 32.22, 30.89, 29.23, 27.44, 16.57. ESI MS m/z 523.24 (M + Na)⁺

9-(4-((2-(difluoromethoxy)benzyl)oxy)-3-methylphenyl)-3,3,6,6-tetramethyl-3,4,5,6,7,9-hexahydro-1H-xanthene-1,8(2H)-dione (CCG366026) [sz-09-81]

Following the general procedure of **5c** on a scale of 70mg (0.18mmol) 9-(4-hydroxy-3-methylphenyl)-3,3,6,6-tetramethyl-3,4,5,6,7,9-hexahydro-1H-xanthene-1,8(2H)-dione (**3ba**), 1-(bromomethyl)-2-(difluoromethoxy)benzene (48 mg, 1.1 Eq, 0.20 mmol) was used. 0.07g of product was isolated (71% yield). ¹H NMR (499 MHz, cdcl₃) δ 7.64 – 7.53 (m, 1H), 7.35 – 7.30 (m, 1H), 7.29 – 7.24 (m, 1H), 7.14 (dt, J = 8.1, 1.1 Hz, 1H), 7.11 (d, J = 2.3 Hz, 1H), 7.05 (dd, J = 8.3, 2.3 Hz, 1H), 6.76 (d, J = 8.4 Hz, 1H), 6.53 (td, J = 74.0, 0.8 Hz, 1H), 5.06 (s, 2H), 4.69 (s, 1H), 2.47 (s, 4H), 2.29 – 2.13 (m, 7H), 1.11 (s, 6H), 1.02 (s, 6H). ¹³C NMR (126 MHz, cdcl₃) δ 196.52, 162.04, 155.18, 148.63, 136.61, 130.96, 129.57, 129.28, 128.87, 126.51, 126.34, 125.70, 118.96, 118.33, 116.26, 115.85, 114.18, 111.13, 64.63, 50.80, 40.88, 32.22, 30.94, 29.22, 27.42, 16.47. ¹⁹F NMR (470 MHz, cdcl₃) δ -80.14, -80.30. ESI MS m/z 559.22 (M + Na)⁺

9-(3-chloro-4-((2-methylbenzyl)oxy)phenyl)-3,3,6,6-tetramethyl-3,4,5,6,7,9-hexahydro-1H-xanthene-1,8(2H)-dione (CCG366047) [sz-09-84]

Following the general procedure of **5c** on a scale of 70mg (0.17mmol) 9-(3-chloro-4-hydroxyphenyl)-3,3,6,6-tetramethyl-3,4,5,6,7,9-hexahydro-1H-xanthene-1,8(2H)-dione (**3bb**), 1-(bromomethyl)-2-methylbenzene (36 mg, 26 μ L, 1.1 Eq, 0.19 mmol) was used. 0.08g of product was isolated (93% yield). ¹H NMR (499 MHz, cdcl₃) δ 7.52 – 7.36 (m, 1H), 7.31 – 7.17 (m, 5H),

6.89 (d, J = 8.5 Hz, 1H), 5.03 (s, 2H), 4.70 (s, 1H), 2.55 – 2.42 (m, 4H), 2.34 (s, 3H), 2.30 – 2.15 (m, 4H), 1.12 (s, 6H), 1.03 (s, 6H). ¹³C NMR (126 MHz, cdcl₃) δ 196.45, 162.38, 152.80, 137.83, 136.50, 134.55, 130.26, 129.58, 128.32, 128.24, 128.13, 125.96, 122.73, 115.27, 113.33, 69.47, 50.75, 40.85, 32.23, 30.97, 29.17, 27.45, 18.92.

9-(3-chloro-4-((2-(difluoromethoxy)benzyl)oxy)phenyl)-3,3,6,6-tetramethyl-3,4,5,6,7,9-hexahydro-1H-xanthene-1,8(2H)-dione (CCG366046) [sz-09-79]

Following the general procedure of **5c** on a scale of 70mg (0.17mmol) 9-(3-chloro-4-hydroxyphenyl)-3,3,6,6-tetramethyl-3,4,5,6,7,9-hexahydro-1H-xanthene-1,8(2H)-dione (**3bb**), 1-(bromomethyl)-2-(difluoromethoxy)benzene (46 mg, 29 μL, 1.1 Eq, 0.19 mmol) was used. 0.08g of product was isolated (85% yield). ¹H NMR (499 MHz, cdcl₃) δ 7.62 (dd, J = 7.8, 1.8 Hz, 1H), 7.33 (td, J = 7.8, 1.8 Hz, 1H), 7.28 – 7.21 (m, 3H), 7.15 (d, J = 8.1 Hz, 1H), 6.96 – 6.80 (m, 1H), 6.56 (t, J = 74.1 Hz, 1H), 5.12 (s, 2H), 4.69 (s, 1H), 2.54 – 2.41 (m, 4H), 2.28 – 2.14 (m, 4H), 1.11 (s, 6H), 1.02 (s, 6H). ¹³C NMR (126 MHz, cdcl₃) δ 196.42, 162.42, 152.45, 148.71, 138.17, 129.75, 129.48, 129.24, 128.69, 128.15, 125.87, 122.69, 119.24, 118.41, 116.34, 115.22, 114.27, 113.48, 65.72, 50.73, 40.84, 32.22, 30.97, 29.17, 27.42. ¹⁹F NMR (470 MHz, cdcl₃) δ -80.24, -80.40. ESI MS m/z 557.18 (M + H)⁺

9-(3-chloro-4-((4-chloro-2-(difluoromethoxy)benzyl)oxy)phenyl)-3,3,6,6-tetramethyl-3,4,5,6,7,9-hexahydro-1H-xanthene-1,8(2H)-dione (CCG366162) [sz-10-02]

Following the general procedure of **5c** on a scale of 70mg (0.17 mmol) 9-(3-chloro-4-hydroxyphenyl)-3,3,6,6-tetramethyl-3,4,5,6,7,9-hexahydro-1H-xanthene-1,8(2H)-dione (**3bb**), 4-chloro-1-(chloromethyl)-2-(difluoromethoxy)benzene (**16a**) (42 mg, 1.05 Eq, 0.18 mmol) was used. 0.04g of product was isolated (36% yield). ¹H NMR (499 MHz, cdcl₃) δ 7.56 (d, J = 8.3 Hz, 1H), 7.26 – 7.23 (m, 2H), 7.22 (d, J = 2.2 Hz, 1H), 7.19 – 7.16 (m, 1H), 6.84 (d, J = 8.3 Hz, 1H), 6.55 (t, J = 73.4 Hz, 1H), 5.07 (s, 2H), 4.69 (s, 1H), 2.53 – 2.41 (m, 4H), 2.28 – 2.14 (m, 4H), 1.11 (s, 6H), 1.02 (s, 6H). ¹³C NMR (126 MHz, cdcl₃) δ 196.40, 162.41, 152.22, 148.75, 138.42, 134.38, 130.30, 129.78, 128.23, 127.35, 126.09, 122.75, 119.80, 117.98, 115.89, 115.18, 113.81, 113.51, 65.27, 50.73, 40.84, 32.22, 31.01, 29.16, 27.41. ¹⁹F NMR (470 MHz, cdcl₃) δ -80.83, -80.99. ESI MS m/z 613.13 (M + Na)⁺

9-(3-chloro-4-((2,6-dichlorobenzyl)oxy)phenyl)-3,3,6,6-tetramethyl-3,4,5,6,7,9-hexahydro-1H-xanthene-1,8(2H)-dione (CCG366791) [sz-10-67]

Following the general procedure of **5c** on a scale of 70mg (0.17 mmol) 9-(3-chloro-4-hydroxyphenyl)-3,3,6,6-tetramethyl-3,4,5,6,7,9-hexahydro-1H-xanthene-1,8(2H)-dione (**3bb**), 1,3-dichloro-2-(chloromethyl)benzene (36 mg, 1.05 Eq, 0.18 mmol) was used. 0.07g of product was isolated (75% yield). ¹H NMR (499 MHz, cdcl₃) δ 7.34 (d, J = 8.5 Hz, 2H), 7.30 (ddd, J = 8.5, 2.3, 0.9 Hz, 1H), 7.23 (ddd, J = 8.5, 7.3, 0.9 Hz, 1H), 7.17 (dd, J = 2.3, 0.9 Hz, 1H), 6.99 (dd, J = 8.4, 0.9 Hz, 1H), 5.26 (s, 2H), 4.71 (s, 1H), 2.48 (d, J = 3.6 Hz, 4H), 2.29 – 2.14 (m, 4H), 1.11 (s, 6H), 1.03 (s, 6H). ¹³C NMR (126 MHz, cdcl₃) δ 196.41, 162.36, 152.76, 138.42, 137.15, 131.86, 130.41, 129.61, 128.44, 128.26, 123.26, 115.25, 114.34, 66.35, 50.75, 40.85, 32.23, 31.01, 29.16, 27.48. ESI MS m/z 581.10 (M + Na)⁺

9-(3-chloro-4-((2,4-dichlorobenzyl)oxy)phenyl)-3,3,6,6-tetramethyl-3,4,5,6,7,9-hexahydro-1H-xanthene-1,8(2H)-dione (CCG366792) [sz-10-68]

Following the general procedure of **5c** on a scale of 70mg (0.17 mmol) 9-(3-chloro-4-hydroxyphenyl)-3,3,6,6-tetramethyl-3,4,5,6,7,9-hexahydro-1H-xanthene-1,8(2H)-dione (**3bb**), 2,4-dichloro-1-(chloromethyl)benzene (36 mg, 1.05 Eq, 0.18 mmol) was used. 0.07g of product was isolated (71% yield). ¹H NMR (499 MHz, cdcl₃) δ 7.59 (dd, J = 8.3, 1.0 Hz, 1H), 7.44 – 7.35 (m, 1H), 7.30 – 7.26 (m, 1H), 7.26 – 7.22 (m, 2H), 6.93 – 6.72 (m, 1H), 5.10 (s, 2H), 4.69 (s, 1H), 2.65 – 2.38 (m, 4H), 2.35 – 2.13 (m, 4H), 1.11 (s, 6H), 1.02 (s, 6H). ¹³C NMR (126 MHz, cdcl₃) δ 196.38, 162.41, 152.18, 138.42, 133.97, 133.20, 132.59, 129.84, 129.37, 128.99, 128.21, 127.39, 122.73, 115.18, 113.40, 67.34, 50.73, 40.84, 32.22, 31.01, 29.18, 27.42. ESI MS m/z 581.10 (M + Na)⁺

3,3,6,6-tetramethyl-9-(2-methyl-4-(2-methylbenzyl)oxy)phenyl)-3,4,5,6,7,9-hexahydro-1H-xanthene-1,8(2H)-dione (CCG363081)

Using intermediate **3bg**, white solids isolated 0.07 g (48% yield). ¹H NMR (400 MHz, DMSO-d₆) δ 7.35 (d, J = 7.2 Hz, 1H), 7.19 (ddd, J = 9.2, 7.5, 4.1 Hz, 3H), 6.77 (d, J = 8.5 Hz, 1H), 6.70 (d, J = 7.2 Hz, 2H), 4.94 (s, 2H), 4.53 (s, 1H), 2.67 (s, 3H), 2.57 – 2.38 (m, 5H plus DMSO), 2.24 (d, J = 26.6 Hz, 5H), 2.03 (d, J = 16.2 Hz, 2H), 1.01 (s, 6H), 0.87 (s, 6H). HPLC: 98.8% (retention time, 8.39 min)

9-{3-fluoro-4-[(2-methylphenyl)methoxy]phenyl}-3,3,6,6-tetramethyl-2,3,4,5,6,7,8,9-octahydro-1H-xanthene-1,8-dione (CCG362897)

Using intermediate **3bh**, white solids isolated 0.08 g (58% yield). ¹H NMR (400 MHz, Chloroform-d) δ 7.53 – 7.46 (m, 1H), 7.40 – 7.25 (m, 3H), 7.23 – 7.15 (m, 1H), 7.10 – 6.97 (m,

2H), 5.13 (s, 2H), 4.81 (s, 1H), 2.57 (s, 4H), 2.47 (s, 3H), 2.41 – 2.25 (m, 4H), 1.22 (s, 6H), 1.12 (s, 6H). HPLC: 96.1% (retention time, 8.03 min)

9-[4-[(2-methylphenyl)methoxy]phenyl]-2,3,4,5,6,7,8,9-octahydro-1H-xanthene-1,8-dione (5be)

Using intermediate **3bi**, white solids isolated 0.05 g (40% yield). ¹H NMR (400 MHz, Chloroform-d) δ 7.40 – 7.33 (m, 1H), 7.33 – 7.15 (m, 5H), 6.91 – 6.81 (m, 2H), 4.95 (s, 2H), 4.77 (s, 1H), 2.71 – 2.49 (m, 4H), 2.45 – 2.25 (m, 7H), 2.01 (qt, J = 13.4, 4.8 Hz, 4H). HPLC: 95.0% (retention time, 7.11 min)

3,3,6,6-tetramethyl-9-(4-((2-methylbenzyl)oxy)-3-(trifluoromethoxy)phenyl)-3,4,5,6,7,9-hexahydro-1H-xanthene-1,8(2H)-dione (CCG366126) [sz-09-85]

Following the general procedure of **5c** on a scale of 75mg (0.17mmol) 9-(4-hydroxy-3-(trifluoromethoxy)phenyl)-3,3,6,6-tetramethyl-3,4,5,6,7,9-hexahydro-1H-xanthene-1,8(2H)-dione (**3bc**), 1-(bromomethyl)-2-methylbenzene (34 mg, 25 μL, 1.1 Eq, 0.18 mmol) was used. 0.09g of product was isolated (95% yield). ¹H NMR (499 MHz, cdcl₃) δ 7.42 – 7.35 (m, 2H), 7.29 – 7.16 (m, 3H), 6.98 (p, J = 1.2 Hz, 1H), 6.96 (d, J = 8.5 Hz, 1H), 5.02 (s, 2H), 4.72 (s, 1H), 2.48 (d, J = 2.7 Hz, 4H), 2.33 (s, 3H), 2.22 (q, J = 16.3 Hz, 4H), 1.12 (s, 6H), 1.00 (s, 6H). ¹³C NMR (126 MHz, cdcl₃) δ 196.47, 162.48, 149.75, 138.13, 137.40, 136.43, 134.43, 130.24, 128.69, 128.26, 128.15, 125.99, 122.14, 115.20, 113.90, 69.41, 50.71, 40.83, 32.15, 31.11, 29.38, 26.97, 18.70. ¹⁹F NMR (470 MHz, cdcl₃) δ -57.99. ESI MS m/z 577.21 (M + Na)⁺

9-(4-((2-(difluoromethoxy)benzyl)oxy)-3-(trifluoromethoxy)phenyl)-3,3,6,6-tetramethyl-3,4,5,6,7,9-hexahydro-1H-xanthene-1,8(2H)-dione (CCG366127) [sz-09-86]

Following the general procedure of **5c** on a scale of 68mg (0.15mmol) 9-(4-hydroxy-3-(trifluoromethoxy)phenyl)-3,3,6,6-tetramethyl-3,4,5,6,7,9-hexahydro-1H-xanthene-1,8(2H)-dione (**3bc**), 1-(bromomethyl)-2-(difluoromethoxy)benzene (39 mg, 25 μL, 1.1 Eq, 0.17 mmol) was used. 0.09g of product was isolated (96% yield). ¹H NMR (499 MHz, cdcl₃) δ 7.55 (dt, J = 7.7, 1.2 Hz, 1H), 7.35 (ddd, J = 13.5, 8.2, 2.0 Hz, 2H), 7.25 (t, J = 7.4 Hz, 1H), 7.15 (d, J = 8.1 Hz, 1H), 7.00 (dt, J = 2.4, 1.2 Hz, 1H), 6.94 (d, J = 8.5 Hz, 1H), 6.53 (t, J = 74.0 Hz, 1H), 5.12 (s, 2H), 4.72 (s, 1H), 2.48 (t, J = 1.4 Hz, 4H), 2.22 (q, J = 16.3 Hz, 4H), 1.12 (s, 6H), 1.00 (s, 6H). ¹³C NMR (126 MHz, cdcl₃) δ 196.42, 162.49, 149.35, 148.65, 137.71, 129.36, 129.27, 128.64, 128.50, 125.84, 122.22, 119.09, 118.31, 116.24, 115.18, 114.17, 113.98, 65.64, 50.69, 40.84, 32.15, 31.10, 29.38, 26.98. ¹⁹F NMR (470 MHz, cdcl₃) δ -58.07, -80.35, -80.51. ESI MS m/z 629.19 (M + Na)⁺

9-(3-(difluoromethoxy)-4-((2-methylbenzyl)oxy)phenyl)-3,3,6,6-tetramethyl-3,4,5,6,7,9-hexahydro-1H-xanthene-1,8(2H)-dione (CCG366128) [sz-09-89]

Following the general procedure of **5c** on a scale of 50mg (0.12mmol) 9-(3-(difluoromethoxy)-4-hydroxyphenyl)-3,3,6,6-tetramethyl-3,4,5,6,7,9-hexahydro-1H-xanthene-1,8(2H)-dione (**3bd**), 1-(bromomethyl)-2-methylbenzene (26 mg, 19 μ L, 1.2 Eq, 0.14 mmol) was used. 0.03g of product was isolated (53% yield). ¹H NMR (499 MHz, cdcl₃) δ 7.41 – 7.36 (m, 1H), 7.33 (dd, J = 8.4, 2.2 Hz, 1H), 7.27 – 7.23 (m, 1H), 7.21 (td, J = 6.1, 5.3, 2.5 Hz, 2H), 6.96 (d, J = 8.4 Hz, 1H), 6.94 (d, J = 2.2 Hz, 1H), 6.46 (t, J = 75.9 Hz, 1H), 5.03 (s, 2H), 4.71 (s, 1H), 2.48 (s, 4H), 2.36 (s, 3H), 2.22 (q, J = 16.3 Hz, 4H), 1.12 (s, 6H), 1.01 (s, 6H). ¹³C NMR (126 MHz, cdcl₃) δ 196.51, 162.42, 148.85, 140.21, 137.86, 136.46, 134.39, 130.32, 128.34, 128.25, 127.58, 126.03, 121.99, 118.38, 116.31, 115.25, 114.25, 113.88, 69.52, 50.74, 40.84, 32.18, 31.15, 29.36, 27.11, 18.79. ¹⁹F NMR (470 MHz, cdcl₃) δ -81.26, -81.42. ESI MS m/z 559.22 (M + Na)⁺

9-(3-(difluoromethoxy)-4-((2-(difluoromethoxy)benzyl)oxy)phenyl)-3,3,6,6-tetramethyl-3,4,5,6,7,9-hexahydro-1H-xanthene-1,8(2H)-dione (CCG366129) [sz-09-90]

Following the general procedure of **5c** on a scale of 50mg (0.12mmol) 9-(3-(difluoromethoxy)-4-hydroxyphenyl)-3,3,6,6-tetramethyl-3,4,5,6,7,9-hexahydro-1H-xanthene-1,8(2H)-dione (**3bd**), 1-(bromomethyl)-2-(difluoromethoxy)benzene (33 mg, 21 μ L, 1.2 Eq, 0.14 mmol) was used. 0.03g of product was isolated (47% yield). ¹H NMR (499 MHz, cdcl₃) δ 7.53 (dd, J = 7.7, 1.7 Hz, 1H), 7.35 (td, J = 7.8, 1.7 Hz, 1H), 7.30 (dd, J = 8.4, 2.3 Hz, 1H), 7.25 (t, J = 7.5 Hz, 1H), 7.16 (d, J = 8.2 Hz, 1H), 6.96 (d, J = 2.2 Hz, 1H), 6.93 (d, J = 8.4 Hz, 1H), 6.50 (td, J = 75.5, 74.7, 38.2 Hz, 2H), 5.11 (s, 2H), 4.71 (s, 1H), 2.48 (s, 4H), 2.22 (q, J = 16.4 Hz, 4H), 1.11 (s, 6H), 1.01 (s, 6H). ¹³C NMR (126 MHz, cdcl₃) δ 196.47, 162.43, 148.88, 148.49, 140.27, 138.13, 129.65, 129.48, 128.36, 127.48, 125.81, 121.95, 119.12, 118.54, 118.29, 116.48, 116.21, 115.22, 114.42, 114.14, 113.95, 65.89, 50.73, 40.83, 32.18, 31.15, 29.34, 27.11. ¹⁹F NMR (470 MHz, cdcl₃) δ -80.37, -80.52, -81.08 (d, J = 3.8 Hz), -81.24. ESI MS m/z 611.20 (M + Na)⁺

9-(3,5-dimethyl-4-((2-methylbenzyl)oxy)phenyl)-3,3,6,6-tetramethyl-3,4,5,6,7,9-hexahydro-1H-xanthene-1,8(2H)-dione (CCG366165) [sz-10-09]

Following the general procedure of **5c** on a scale of 100mg (0.25mmol) 9-(4-hydroxy-3,5-dimethylphenyl)-3,3,6,6-tetramethyl-3,4,5,6,7,9-hexahydro-1H-xanthene-1,8(2H)-dione (**3be**), 1-(bromomethyl)-2-methylbenzene (56.3 mg, 40.8 μ L, 1.2 Eq, 304 μ mol) was used. 0.05g of product was isolated (40% yield). ¹H NMR (400 MHz, cdcl₃) δ 7.54 – 7.48 (m, 1H), 7.25 – 7.20 (m, 2H),

7.18 (q, J = 4.8 Hz, 1H), 6.91 (s, 2H), 4.74 (s, 2H), 4.66 (s, 1H), 2.47 (d, J = 2.0 Hz, 4H), 2.33 (s, 3H), 2.27 – 2.21 (m, 4H), 2.20 (s, 6H), 1.10 (s, 6H), 1.01 (s, 6H). ¹³C NMR (101 MHz, cdcl₃) δ 196.53, 162.11, 154.34, 139.41, 136.26, 135.83, 130.34, 130.03, 128.79, 127.95, 127.63, 125.94, 115.82, 71.63, 50.80, 40.87, 32.26, 31.01, 29.26, 27.34, 18.89, 16.57. ESI MS m/z 521.66 (M + Na)⁺

9-(3,5-diethyl-4-((2-methylbenzyl)oxy)phenyl)-3,3,6,6-tetramethyl-3,4,5,6,7,9-hexahydro-1H-xanthene-1,8(2H)-dione (CCG366204) [sz-10-24]

Following the general procedure of **5c** on a scale of 64mg (0.18mmol) 9-(3,5-diethyl-4-hydroxyphenyl)-3,3,6,6-tetramethyl-3,4,5,6,7,9-hexahydro-1H-xanthene-1,8(2H)-dione (**3bf**), 1-(bromomethyl)-2-methylbenzene (39 mg, 28 μL, 1.2 Eq, 0.21 mmol) was used. 0.09g of product was isolated (95% yield). ¹H NMR (499 MHz, cdcl₃) δ 7.58 (dd, J = 6.6, 2.4 Hz, 1H), 7.25 (ddd, J = 9.6, 7.5, 3.0 Hz, 2H), 7.18 (dd, J = 6.5, 2.4 Hz, 1H), 6.99 (s, 2H), 4.76 (s, 2H), 4.72 (s, 1H), 2.62 (q, J = 7.5 Hz, 4H), 2.48 (d, J = 2.6 Hz, 4H), 2.32 (s, 3H), 2.29 – 2.16 (m, 4H), 1.22 – 1.16 (m, 6H), 1.12 (s, 6H), 1.02 (s, 6H). ¹³C NMR (126 MHz, cdcl₃) δ 196.42, 162.11, 153.44, 139.86, 136.46, 136.31, 135.45, 129.97, 127.49, 127.38, 127.00, 125.99, 115.97, 72.95, 50.79, 40.92, 32.21, 31.27, 29.46, 27.09, 22.91, 18.78, 15.03. ESI MS m/z 549.29 (M + Na)⁺

General Procedure for Intermediate 6

To a solution of desired benzaldehyde (1.0 g, 1 Eq, 8.2 mmol) and DMF (38mL) was treated with Cs₂CO₃ (5 g, 2 Eq, 0.02 mol) and benzyl halide (1500 mg, 1.01 Eq, 8.3 mmol). The reaction was run at room temp for 16h and diluted with water. The precipitates were filtered and rinsed with hexane. Intermediate **6** was isolated.

4-((2-methylbenzyl)oxy)benzaldehyde (6a) [sz-10-30]

Following the general procedure of intermediate **6** on a scale of 1g (9mmol) 4-hydroxybenzaldehyde, Compound **6a** was isolated as white solids (1.8g, 98%). ¹H NMR (499 MHz, cdcl₃) δ 9.91 (s, 1H), 7.92 – 7.81 (m, 2H), 7.48 – 7.35 (m, 1H), 7.34 – 7.20 (m, 3H), 7.14 – 7.05 (m, 2H), 5.14 (s, 2H), 2.40 (s, 3H).

2,5-dimethyl-4-((2-methylbenzyl)oxy)benzaldehyde (6b) [sz-10-44]

Following the general procedure of intermediate **6**, using 4-hydroxy-2,5-dimethylbenzaldehyde (162 mg, 1 Eq, 1.08 mmol), Compound **6b** was isolated as white solids (0.25g, 91%). ¹H NMR

(499 MHz, cdcl₃) δ 10.15 (d, J = 0.7 Hz, 1H), 7.62 (s, 1H), 7.48 – 7.37 (m, 1H), 7.32 – 7.27 (m, 1H), 7.26 – 7.22 (m, 2H), 6.77 (s, 1H), 5.12 (s, 2H), 2.67 (s, 3H), 2.40 (s, 3H), 2.26 (s, 3H).

2,6-dimethyl-4-((2-methylbenzyl)oxy)benzaldehyde (6c) [sz-10-38]

Following the general procedure of intermediate **6**, using 4-hydroxy-2,6-dimethylbenzaldehyde (553 mg, 1.1 Eq, 3.69 mmol), Compound **6c** was isolated as white solids (0.85g, 99%). ¹H NMR (499 MHz, cdcl₃) δ 10.50 (d, J = 0.9 Hz, 1H), 7.39 (d, J = 7.3 Hz, 1H), 7.31 – 7.27 (m, 1H), 7.24 (d, J = 7.3 Hz, 2H), 6.70 (s, 2H), 5.08 (s, 2H), 2.63 (s, 6H), 2.39 (s, 3H).

2-chloro-4-((2-methylbenzyl)oxy)benzaldehyde (6d) [sz-10-91]

Following the general procedure of intermediate **6**, using 2-chloro-4-hydroxybenzaldehyde (100 mg, 1 Eq, 639 μmol), Compound **6d** was isolated as white solids (0.16g, 93%). ¹H NMR (499 MHz, cdcl₃) δ 10.35 (d, J = 0.9 Hz, 1H), 7.91 (dd, J = 8.7, 0.8 Hz, 1H), 7.37 (d, J = 7.4 Hz, 1H), 7.32 – 7.27 (m, 1H), 7.25 (d, J = 7.5 Hz, 2H), 7.04 (dd, J = 2.4, 0.8 Hz, 1H), 6.97 (ddd, J = 8.8, 2.4, 0.9 Hz, 1H), 5.11 (s, 2H), 2.38 (s, 3H).

General Procedure for Compound **7**

To a mixture of Intermediate **6** (0.1g, 1 Eq, 0.44mmol) and desired dione (0.09g, 2.01 Eq, 0.88mmol) in 70% IPA (1.5mL) was treated with Zn₂Cl (12mg, 0.2 Eq, 0.09mmol). The reaction was reflux at 120°C until the reaction was complete. The reaction mixture was then cooled to room temp and concentrated. The crude material was chromatographed over silica gel, eluted with 0-50% EtOAc/Hex. Compound **7** was isolated with a purity above 95%.

9-(2,5-dimethyl-4-((2-methylbenzyl)oxy)phenyl)-3,3,6,6-tetramethyl-3,4,5,6,7,9-hexahydro-1H-xanthene-1,8(2H)-dione (CCG366695) [sz-10-48]

Following the general procedure for **7**, 2,5-dimethyl-4-((2-methylbenzyl)oxy)benzaldehyde (**6b**) (0.15g, 1 Eq, 590 μmol) and 5,5-dimethylcyclohexane-1,3-dione (166 mg, 2.01 Eq, 1.19 mmol) were used. 0.01g of desired pdt was isolated (3% yield). ¹H NMR (499 MHz, cdcl₃) δ 7.46 – 7.40 (m, 1H), 7.26 – 7.17 (m, 3H), 6.67 (s, 1H), 6.63 (s, 1H), 4.95 (s, 2H), 4.77 (s, 1H), 2.81 (s, 3H), 2.48 (d, J = 1.8 Hz, 4H), 2.36 (s, 3H), 2.25 – 2.14 (m, 4H), 2.08 (s, 3H), 1.11 (s, 6H), 1.01 (s, 6H). ¹³C NMR (126 MHz, cdcl₃) δ 196.83, 161.85, 155.00, 136.52, 135.70, 135.65, 134.86, 130.12, 129.97, 128.29, 127.81, 125.86, 123.72, 116.83, 112.85, 68.18, 50.83, 40.92, 32.27, 29.16, 27.28, 27.18, 19.77, 18.90, 15.95. ESI MS m/z 521.26 (M + Na)⁺

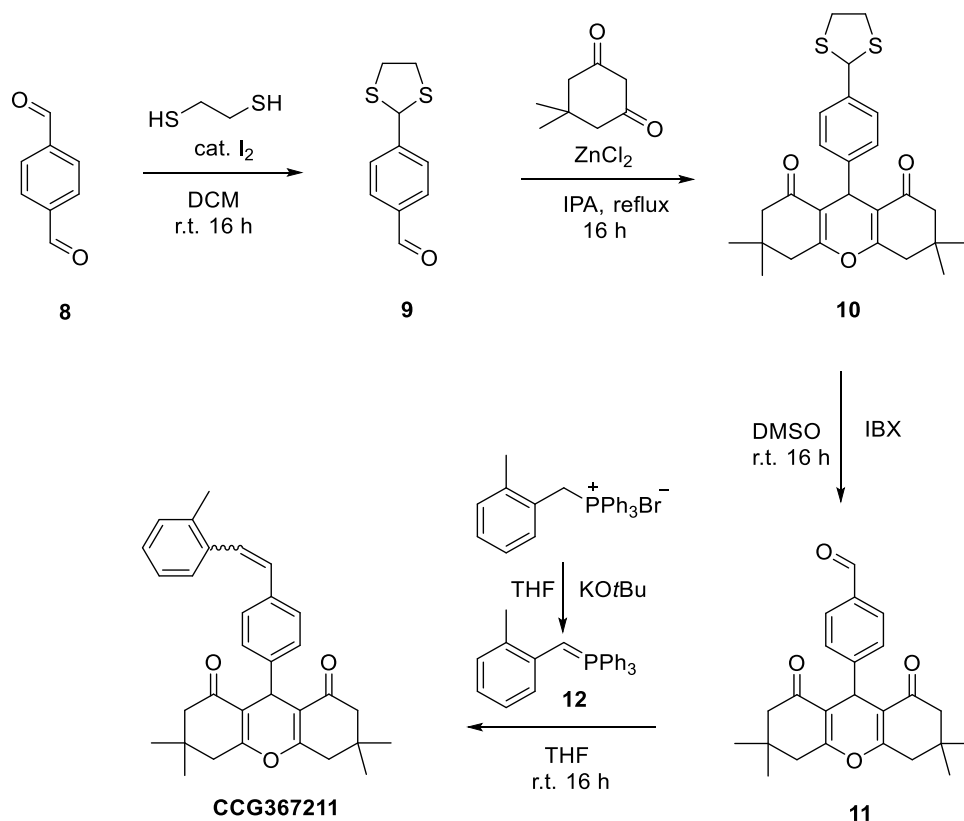
9-(2,6-dimethyl-4-((2-methylbenzyl)oxy)phenyl)-3,3,6,6-tetramethyl-3,4,5,6,7,9-hexahydro-1H-xanthene-1,8(2H)-dione (CCG366696) [sz-10-49]

Following the general procedure for **7**, 2,6-dimethyl-4-((2-methylbenzyl)oxy)benzaldehyde (**6c**) (0.2g, 1 Eq, 786 μ mol) and 5,5-dimethylcyclohexane-1,3-dione (222 mg, 2.01 Eq, 1.58 mmol) were used. 0.09g of desired pdt was isolated (23% yield). ¹H NMR (499 MHz, cdcl₃) δ 7.41 – 7.32 (m, 1H), 7.22 (ddt, J = 11.5, 8.7, 5.9 Hz, 3H), 6.72 (d, J = 2.8 Hz, 1H), 6.47 (d, J = 2.8 Hz, 1H), 5.07 (s, 1H), 4.93 (s, 2H), 2.91 (s, 3H), 2.50 – 2.37 (m, 4H), 2.36 (s, 3H), 2.20 (s, 4H), 2.16 (s, 3H), 1.11 (s, 6H), 1.06 (s, 6H). ¹³C NMR (126 MHz, cdcl₃) δ 196.97, 162.04, 156.80, 141.54, 137.02, 136.83, 135.29, 130.88, 130.25, 128.87, 128.08, 125.96, 115.99, 114.50, 114.41, 68.00, 51.06, 40.85, 31.88, 28.69, 28.22, 27.69, 21.89, 18.92, 18.81. ESI MS m/z 521.26 (M + Na)⁺

9-(2-chloro-4-((2-methylbenzyl)oxy)phenyl)-3,3,6,6-tetramethyl-3,4,5,6,7,9-hexahydro-1H-xanthene-1,8(2H)-dione (CCG367065) [sz-10-100]

Following the general procedure for **7**, 2-chloro-4-((2-methylbenzyl)oxy)benzaldehyde (**6d**) (50 mg, 1 Eq, 0.19 mmol) and 5,5-dimethylcyclohexane-1,3-dione (54 mg, 2.01 Eq, 0.39 mmol) were used. 0.03g of desired pdt was isolated (31% yield). ¹H NMR (400 MHz, cdcl₃) δ 7.40 – 7.31 (m, 2H), 7.21 (pd, J = 6.5, 3.1 Hz, 3H), 6.88 (d, J = 2.6 Hz, 1H), 6.82 (dd, J = 8.6, 2.6 Hz, 1H), 4.94 (s, 1H), 4.93 (s, 2H), 2.39 (s, 4H), 2.34 (s, 3H), 2.28 – 2.13 (m, 4H), 1.10 (s, 6H), 1.03 (s, 6H). ¹³C NMR (101 MHz, cdcl₃) δ 196.68, 162.86, 157.95, 136.91, 134.43, 133.70, 130.39, 128.91, 128.42, 126.04, 115.81, 113.77, 113.47, 68.71, 50.73, 40.79, 32.03, 29.30, 27.40, 18.90. ESI MS m/z 527.19 (M + Na)⁺

Scheme 2.4 Synthesis of CCG367211



4-(1,3-dithiolan-2-yl)benzaldehyde (9) [sz-11-24]

To a solution of terephthalaldehyde (**8**) (1500 mg, 1 Eq, 11.18 mmol) and ethane-1,2-dithiol (1.106 g, 988 μ L, 1.05 Eq, 11.74 mmol) in DCM (50mL) was treated with iodine (283.8 mg, 0.1 Eq, 1.118 mmol), and the resulting reaction mixture was stirred at room temp for 16h. The reaction was quenched with sat. $Na_2S_2O_3$ and extracted with DCM (x3). The organic layer was washed with 1N NaOH, brine, dried over $MgSO_4$ and concentrated. The crude material was chromatographed over silica gel, eluted with 0-4% EtOAc/DCM. Compound **9** was isolated (0.5g, 21% yield). 1H NMR (499 MHz, $cdCl_3$) δ 9.99 (s, 1H), 7.86 – 7.80 (m, 2H), 7.70 – 7.65 (m, 2H), 5.65 (s, 1H), 3.57 – 3.47 (m, 2H), 3.45 – 3.35 (m, 2H).

9-(4-(1,3-dithiolan-2-yl)phenyl)-3,3,6,6-tetramethyl-3,4,5,6,7,9-hexahydro-1H-xanthene-1,8(2H)-dione (10) [sz-10-99]

To a mixture of 4-(1,3-dithiolan-2-yl)benzaldehyde (**9**) (100 mg, 1 Eq, 475 μ mol) in 70% IPA (8mL) were treated with 5,5-dimethylcyclohexane-1,3-dione (167 mg, 2.5 Eq, 1.19 mmol) and zinc chloride (13.0 mg, 0.2 Eq, 95.1 μ mol). The reaction mixture was refluxed at 120°C for 16h.

The reaction mixture was cooled to room temp., precipitates formed. The solids were filtered and washed with water and ethyl ether. Compound **10** was collected as white solids (0.16g, 74% yield). ¹H NMR (499 MHz, cdcl₃) δ 7.42 (d, J = 8.3 Hz, 2H), 7.11 – 6.96 (m, 2H), 5.61 (s, 1H), 5.48 (s, 1H), 3.55 – 3.41 (m, 2H), 3.40 – 3.24 (m, 2H), 2.45 – 2.31 (m, 8H), 1.22 (s, 6H), 1.10 (s, 6H).

4-(3,3,6,6-tetramethyl-1,8-dioxo-2,3,4,5,6,7,8,9-octahydro-1H-xanthen-9-yl)benzaldehyde (**11**)
[sz-11-01]

To a mixture of 9-(4-(1,3-dithiolan-2-yl)phenyl)-3,3,6,6-tetramethyl-3,4,5,6,7,9-hexahydro-1H-xanthene-1,8(2H)-dione (**10**) (150 mg, 1 Eq, 330 μmol) in DMSO (2mL) was treated with IBX (97.0 mg, 1.05 Eq, 346 μmol). The reaction mixture was stirred at room temp. for 16 h. The reaction mixture was quenched with sat. Na₂S₂O₃ and mixed with EtOAc. The mixture was stirred for 10min, and precipitates formed. The mixture was filtered through celite cake. The filtrate was extracted with EtOAc (x3), and the organic layer was washed with brine, dried over MgSO₄. The crude material was chromatographed over silica gel, eluted with 0-40% EtOAc/Hex. Compound **11** was isolated (0.05g, 42% yield). ¹H NMR (499 MHz, cdcl₃) δ 9.92 (s, 1H), 7.81 – 7.68 (m, 2H), 7.47 (d, J = 7.9 Hz, 2H), 4.81 (s, 1H), 2.49 (d, J = 1.7 Hz, 4H), 2.25 (d, J = 16.3 Hz, 2H), 2.16 (d, J = 16.3 Hz, 2H), 1.11 (s, 6H), 0.98 (s, 6H).

(2-methylbenzyl)triphenylphosphonium bromide [sz-10-90]

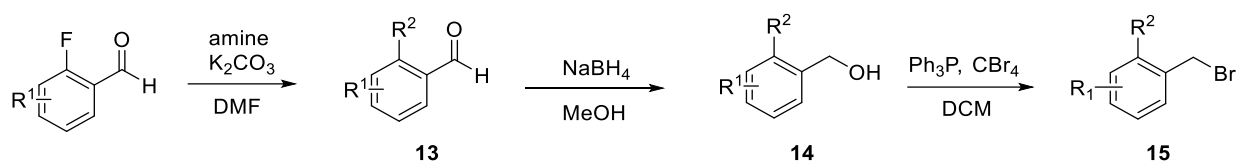
To a mixture of 2-methylbenzylbromide (2000 mg, 1.447 mL, 1 Eq, 10.81 mmol) and triphenylphosphane (2.863 g, 1.01 Eq, 10.92 mmol) was refluxed in DCM (50mL) at 60°C for 5 h. The reaction mixture was cooled to room temp and concentrated. The crude material was triturated from ethyl ether and filtered. Desired pdt was carried to the next step without further purification (4.5g, 93% yield). ¹H NMR (499 MHz, cdcl₃) δ 7.82 – 7.75 (m, 3H), 7.69 (ddd, J = 12.4, 8.1, 1.4 Hz, 6H), 7.66 – 7.58 (m, 6H), 7.15 (t, J = 7.6 Hz, 1H), 7.09 (dd, J = 8.2, 2.6 Hz, 1H), 6.98 (d, J = 7.7 Hz, 2H), 5.39 (d, J = 14.2 Hz, 2H), 1.67 (d, J = 1.4 Hz, 3H), 1.66 (s, 1H).

(E/Z)-3,3,6,6-tetramethyl-9-(4-(2-methylstyryl)phenyl)-3,4,5,6,7,9-hexahydro-1H-xanthene-1,8(2H)-dione (**CCG367211**) [sz-11-47]

(2-methylbenzyl)triphenylphosphonium bromide (500 mg, 1 Eq, 1.23 μmol) was mixed with THF (2mL) in the flask and was treated with potassium tert-butoxide (145 mg, 1.05 Eq, 1.29 mmol). The reaction was stirred at room temp. for 3 h and transferred through cannula into the solution of 4-(3,3,6,6-tetramethyl-1,8-dioxo-2,3,4,5,6,7,8,9-octahydro-1H-xanthen-9-yl)benzaldehyde (**11**)

(200 mg, 1 Eq, 0.53 mmol) in THF (1mL). The reaction mixture was run at room temp for 16 h. The organic layer was washed with brine, dried over MgSO₄, and concentrated. The crude material was chromatographed over silica gel, eluted with 0-70% EtOAc/Hex. Desired pdt was isolated as 1:1.5 isomers (0.16g, 65% yield). ¹H NMR (400 MHz, cdcl₃) δ 7.55 (d, J = 7.0 Hz, 1H), 7.43 – 7.28 (m, 3H), 7.25 (d, J = 16.0 Hz, 1H), 7.22 – 7.14 (m, 3H), 7.14 – 7.06 (m, 1H), 6.99 (ddt, J = 8.5, 6.4, 2.0 Hz, 1H), 6.92 (d, J = 16.1 Hz, 1H), 6.63 – 6.47 (m, 1H), 4.73 (d, J = 32.0 Hz, 1H), 2.49 (d, J = 1.3 Hz, 3H), 2.45 – 2.10 (m, 8H), 1.11 (d, J = 9.9 Hz, 6H), 0.99 (d, J = 24.8 Hz, 6H). ¹³C NMR (101 MHz, cdcl₃) δ 196.42, 196.34, 162.29, 162.29, 162.25, 143.76, 143.00, 136.63, 135.79, 135.71, 130.45, 130.33, 130.01, 129.91, 128.97, 128.78, 128.75, 128.71, 128.04, 127.34, 126.99, 126.42, 126.15, 125.94, 125.56, 125.30, 115.51, 115.48, 50.75, 50.73, 40.88, 40.82, 32.22, 32.19, 31.71, 31.42, 29.35, 29.32, 27.37, 27.15, 19.94, 19.86. ESI MS m/z 489.24 (M + Na)+

Scheme 2.5 Synthetic route of desired bromide



General Procedure for Intermediate 13

To a solution of commercially available benzaldehyde (300 mg, 1 Eq, 2.40 mmol) in DMF (10mL) was treated with K₂CO₃ (1.33 g, 4 Eq, 9.6 mmol) and desired amine (390 mg, 2 Eq, 4.80 mmol). The reaction was run at 90°C in pressure vessel for 16h. The reaction mixture was cooled to room temp and was concentrated. The crude material chromatographed over silica gel, eluted with 0-5% MeOH/DCM. Desired Compound **13** was isolated.

2-morpholinobenzaldehyde (13a) [sz-12-96]

Following the general procedure, commercially available 2-fluorobenzaldehyde (400 mg, 1 Eq, 3.22 mmol) and morpholine (562 mg, 2 Eq, 6.45 mmol) were used. Compound **13a** was isolated 0.67g (99% yield). ¹H NMR (499 MHz, cdcl₃) δ 10.35 (s, 1H), 7.82 (dd, J = 7.7, 1.8 Hz, 1H), 7.57 – 7.51 (m, 1H), 7.18 – 7.09 (m, 2H), 3.94 – 3.87 (m, 4H), 3.13 – 3.05 (m, 4H).

General Procedure for Intermediate 14

To a solution of commercially available aldehyde (200 mg, 1 Eq, 968 μ mol) in alcohol (4mL) was treated with NaBH₄ (44.0 mg, 1.2 Eq, 1.16 mmol). The reaction was run at room temp for 3 h and cooled to 0°C. The reaction mixture was quenched with 2N HCl and extracted with DCM (x3). The extracts were washed with brine and dried over MgSO₄. The crude material was concentrated and carried to next step without further purification.

(2-morpholinophenyl)methanol (14aa) [sz-13-02]

Following the general procedure for Intermediate **14**, 2-morpholinobenzaldehyde (**13a**) (670 mg, 1 Eq, 3.50 mmol) was used. Compound **14aa** was isolated without further purification 0.46g (68% yield). ¹H NMR (499 MHz, cdcl₃) δ 7.34 – 7.27 (m, 1H), 7.23 – 7.19 (m, 2H), 7.17 – 7.10 (m, 1H), 4.81 (s, 2H), 3.91 – 3.82 (m, 4H), 3.04 – 2.96 (m, 4H).

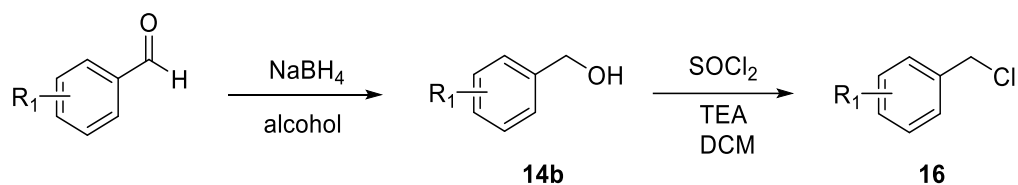
General Procedure for Reagent 15

To a solution of **14** (60 mg, 1 Eq, 0.37 mmol) in DCM (2mL) was treated with carbon tetrabromide (0.15 g, 1.2 Eq, 0.44 mmol). The mixture was cooled to 0°C and treated with triphenylphosphine (0.12 g, 1.2 Eq, 0.44mmol) slowly. The resulted mixture was stirred at room temp until the reaction was complete. The mixture was concentrated and chromatographed over silica gel, eluted with 0-20% EtOAc/DCM. Desired Compound **15** was isolated.

4-(2-(bromomethyl)phenyl)morpholine (15a) [sz-13-05]

Following the general procedure for **15**, (2-morpholinophenyl)methanol (**14aa**) (460 mg, 1 Eq, 2.38 mmol) was used, and Compound **15a** was isolated 0.04g (6% yield). ¹H NMR (499 MHz, cdcl₃) δ 7.44 (dd, J = 7.7, 1.7 Hz, 1H), 7.29 (td, J = 7.6, 1.7 Hz, 1H), 7.11 (q, J = 7.7 Hz, 2H), 4.55 (s, 2H), 3.87 – 3.79 (m, 4H), 2.95 (t, J = 4.4 Hz, 4H).

Scheme 2.6 Synthetic route of desired chloride



(4-chloro-2-(difluoromethoxy)phenyl)methanol (14ba) [sz-09-93]

Following the general procedure for Intermediate **14**, commercially available 4-chloro-2-(difluoromethoxy)benzaldehyde (200 mg, 1 Eq, 968 μ mol) in EtOH (4mL) was used. Compound

14ba was isolated (0.1g, 84% yield). ¹H NMR (400 MHz, cdcl₃) δ 7.42 (d, J = 8.2 Hz, 1H), 7.23 (dd, J = 8.2, 2.0 Hz, 1H), 7.15 (dd, J = 2.1, 1.0 Hz, 1H), 6.55 (t, J = 73.3 Hz, 1H), 4.71 (d, J = 6.0 Hz, 2H), 1.86 (t, J = 6.1 Hz, 1H).

General Procedure for Compound **16**

To a solution of desired alcohol (170 mg, 1 Eq, 815 μmol) in DCM (2mL) at 0°C was treated with TEA (115 mg, 159 μL, 1.4 Eq, 1.14 mmol) and thionyl chloride (145 mg, 89.2 μL, 1.5 Eq, 1.22 mmol) dropwise. The reaction was run at room temperature for 2 h and was quenched with sat. Na₂CO₃. The aqueous layer was extracted with DCM (x3). The extracts were washed with brine, dried over MgSO₄ and concentrated. The crude material was chromatographed over silica gel, eluted with 0-5% EtOAc/Hex to get Compound **16**.

4-chloro-1-(chloromethyl)-2-(difluoromethoxy)benzene (16a) [sz-09-97]

Following general procedure for Compound **16**, (4-chloro-2-(difluoromethoxy)phenyl)methanol (170 mg, 1 Eq, 815 μmol) (**14ba**) was used, and 0.04g of the desired compound was isolated (23% yield). ¹H NMR (499 MHz, cdcl₃) δ 7.42 (d, J = 8.2 Hz, 1H), 7.23 (dt, J = 8.2, 1.3 Hz, 1H), 7.20 (dd, J = 2.1, 1.0 Hz, 1H), 6.57 (td, J = 73.1, 0.8 Hz, 1H), 4.61 (s, 2H). ¹⁹F NMR (470 MHz, cdcl₃) δ -80.86, -81.02.

1-(chloromethyl)-2-ethylbenzene (16b) [sz-10-43]

Following general procedure for Compound **16**, commercially available (2-ethylphenyl)methanol (200 mg, 198 μL, 1 Eq, 1.47 mmol) was used, and 0.2g of the desired compound was isolated (93% yield). ¹H NMR (499 MHz, cdcl₃) δ 7.34 (dd, J = 7.7, 1.4 Hz, 1H), 7.30 (tt, J = 7.4, 1.3 Hz, 1H), 7.25 (d, J = 7.5 Hz, 1H), 7.21 (td, J = 7.4, 1.5 Hz, 1H), 4.65 (s, 2H), 2.80 (q, J = 7.6 Hz, 2H), 1.29 (td, J = 7.6, 1.1 Hz, 3H).

1-(chloromethyl)-2-(fluoromethyl)benzene (16c) [sz-11-81]

Following general procedure for Compound **16**, commercially available (2-Fluoromethyl-phenyl)-methanol (120 mg, 72.7 μL, 1 Eq, 856 μmol) was used, and 0.1g of Compound **16c** was isolated (98% yield). ¹H NMR (499 MHz, cdcl₃) δ 7.45 – 7.41 (m, 2H), 7.41 – 7.37 (m, 2H), 5.63 (s, 1H), 5.53 (s, 1H), 4.71 (s, 2H). ¹⁹F NMR (470 MHz, cdcl₃) δ 23.28, 23.18, 23.08.

2.6 References

- Abuse, N. I. on D. (2021, June 1). *Prescription Opioids DrugFacts*. National Institute on Drug Abuse. <https://nida.nih.gov/publications/drugfacts/prescription-opioids>
- Ahlbeck, K. (2011). Opioids: A two-faced Janus. *Current Medical Research and Opinion*, 27(2), 439–448. <https://doi.org/10.1185/03007995.2010.545379>
- Al-Hasani, R., & Bruchas, M. R. (2011). Molecular Mechanisms of Opioid Receptor-Dependent Signaling and Behavior. *Anesthesiology*, 115(6), 1363–1381. <https://doi.org/10.1097/ALN.0b013e318238bba6>
- Almond, L. M., Yang, J., Jamei, M., Tucker, G. T., & Rostami-Hodjegan, A. (2009). Towards a quantitative framework for the prediction of DDIs arising from cytochrome P450 induction. *Current Drug Metabolism*, 10(4), 420–432. <https://doi.org/10.2174/138920009788498978>
- Baillie, T. A. (2008). Metabolism and Toxicity of Drugs. Two Decades of Progress in Industrial Drug Metabolism. *Chemical Research in Toxicology*, 21(1), 129–137. <https://doi.org/10.1021/tx7002273>
- Banks, W. A. (2009). Characteristics of compounds that cross the blood-brain barrier. *BMC Neurology*, 9(1), S3. <https://doi.org/10.1186/1471-2377-9-S1-S3>
- Bartuzi, D., Kaczor, A. A., & Matosiuk, D. (2015). Activation and Allosteric Modulation of Human μ Opioid Receptor in Molecular Dynamics. *Journal of Chemical Information and Modeling*, 55(11), 2421–2434. <https://doi.org/10.1021/acs.jcim.5b00280>
- Bartuzi, D., Kędzierska, E., Kaczor, A. A., Schmidhammer, H., & Matosiuk, D. (2020). Novel Positive Allosteric Modulators of μ Opioid Receptor—Insight from In Silico and In Vivo Studies. *International Journal of Molecular Sciences*, 21(22), 8463. <https://doi.org/10.3390/ijms21228463>
- Bassoni, D. L., Raab, W. J., Achacoso, P. L., Loh, C. Y., & Wehrman, T. S. (2012). Measurements of β -Arrestin Recruitment to Activated Seven Transmembrane Receptors Using Enzyme Complementation. In A. P. Davenport (Ed.), *Receptor Binding Techniques* (pp. 181–203). Humana Press. https://doi.org/10.1007/978-1-61779-909-9_9
- Bellettato, C. M., & Scarpa, M. (2018). Possible strategies to cross the blood–brain barrier. *Italian Journal of Pediatrics*, 44(2), 131. <https://doi.org/10.1186/s13052-018-0563-0>
- Bioisosteres in Medicinal Chemistry* (1st ed.). (2012). John Wiley & Sons, Ltd. <https://doi.org/10.1002/9783527654307>
- Bohn, L. M., Gainetdinov, R. R., Lin, F.-T., Lefkowitz, R. J., & Caron, M. G. (2000). μ -Opioid receptor desensitization by β -arrestin-2 determines morphine tolerance but not dependence. *Nature*, 408(6813), Article 6813. <https://doi.org/10.1038/35047086>

- Bohn, L. M., Lefkowitz, R. J., Gainetdinov, R. R., Peppel, K., Caron, M. G., & Lin, F.-T. (1999). Enhanced Morphine Analgesia in Mice Lacking β -Arrestin 2. *Science*, 286(5449), 2495–2498. <https://doi.org/10.1126/science.286.5449.2495>
- Bourdonnec, B. L., Windh, R. T., Ajello, C. W., Leister, L. K., Gu, M., Chu, G.-H., Tuthill, P. A., Barker, W. M., Koblish, M., Wiant, D. D., Graczyk, T. M., Belanger, S., Cassel, J. A., Feschenko, M. S., Brogdon, B. L., Smith, S. A., Christ, D. D., Derelanko, M. J., Kutz, S., ... Dolle, R. E. (2008). Potent, Orally Bioavailable Delta Opioid Receptor Agonists for the Treatment of Pain: Discovery of N,N-Diethyl-4-(5-hydroxyspiro[chromene-2,4'-piperidine]-4-yl)benzamide (ADL5859). *Journal of Medicinal Chemistry*, 51(19), 5893–5896. <https://doi.org/10.1021/jm8008986>
- Burford, N. T., Clark, M. J., Wehrman, T. S., Gerritz, S. W., Banks, M., O'Connell, J., Traynor, J. R., & Alt, A. (2013). Discovery of positive allosteric modulators and silent allosteric modulators of the μ -opioid receptor. *Proceedings of the National Academy of Sciences*, 110(26), 10830–10835. <https://doi.org/10.1073/pnas.1300393110>
- Burford, N. T., Livingston, K. E., Canals, M., Ryan, M. R., Budenholzer, L. M. L., Han, Y., Shang, Y., Herbst, J. J., O'Connell, J., Banks, M., Zhang, L., Filizola, M., Bassoni, D. L., Wehrman, T. S., Christopoulos, A., Traynor, J. R., Gerritz, S. W., & Alt, A. (2015). Discovery, Synthesis, and Molecular Pharmacology of Selective Positive Allosteric Modulators of the δ -Opioid Receptor. *Journal of Medicinal Chemistry*, 58(10), 4220–4229. <https://doi.org/10.1021/acs.jmedchem.5b00007>
- Burford, N. T., Traynor, J. R., & Alt, A. (2015). Positive allosteric modulators of the μ -opioid receptor: A novel approach for future pain medications. *British Journal of Pharmacology*, 172(2), 277–286. <https://doi.org/10.1111/bph.12599>
- Cahill, T. J., Thomsen, A. R. B., Tarrasch, J. T., Plouffe, B., Nguyen, A. H., Yang, F., Huang, L.-Y., Kahsai, A. W., Bassoni, D. L., Gavino, B. J., Lamerdin, J. E., Triest, S., Shukla, A. K., Berger, B., Little, J., Antar, A., Blanc, A., Qu, C.-X., Chen, X., ... Lefkowitz, R. J. (2017). Distinct conformations of GPCR- β -arrestin complexes mediate desensitization, signaling, and endocytosis. *Proceedings of the National Academy of Sciences*, 114(10), 2562–2567. <https://doi.org/10.1073/pnas.1701529114>
- Charbogne, P., Kieffer, B. L., & Befort, K. (2014). 15 years of genetic approaches in vivo for addiction research: Opioid receptor and peptide gene knockout in mouse models of drug abuse. *Neuropharmacology*, 76, 204–217. <https://doi.org/10.1016/j.neuropharm.2013.08.028>
- Chen, C.-M., Ding, H., Mabry, K. M., & Ko, M.-C. (2022). Enhanced antidepressant-like effects of a delta opioid receptor agonist, SNC80, in rats under inflammatory pain. *Pharmacology Biochemistry and Behavior*, 214, 173341. <https://doi.org/10.1016/j.pbb.2022.173341>
- Chung, P. C. S., & Kieffer, B. L. (2013). Delta opioid receptors in brain function and diseases. *Pharmacology & Therapeutics*, 140(1), 112–120. <https://doi.org/10.1016/j.pharmthera.2013.06.003>

- Cipriani, A., Furukawa, T. A., Salanti, G., Chaimani, A., Atkinson, L. Z., Ogawa, Y., Leucht, S., Ruhe, H. G., Turner, E. H., Higgins, J. P. T., Egger, M., Takeshima, N., Hayasaka, Y., Imai, H., Shinohara, K., Tajika, A., Ioannidis, J. P. A., & Geddes, J. R. (2018). Comparative efficacy and acceptability of 21 antidepressant drugs for the acute treatment of adults with major depressive disorder: A systematic review and network meta-analysis. *The Lancet*, *391*(10128), 1357–1366. [https://doi.org/10.1016/S0140-6736\(17\)32802-7](https://doi.org/10.1016/S0140-6736(17)32802-7)
- Claff, T., Yu, J., Blais, V., Patel, N., Martin, C., Wu, L., Han, G. W., Holleran, B. J., Van der Poorten, O., White, K. L., Hanson, M. A., Sarret, P., Gendron, L., Cherezov, V., Katritch, V., Ballet, S., Liu, Z.-J., Müller, C. E., & Stevens, R. C. (2019). Elucidating the active δ -opioid receptor crystal structure with peptide and small-molecule agonists. *Science Advances*, *5*(11), eaax9115. <https://doi.org/10.1126/sciadv.aax9115>
- Congreve, M., Carr, R., Murray, C., & Jhoti, H. (2003). A ‘Rule of Three’ for fragment-based lead discovery? *Drug Discovery Today*, *8*(19), 876–877. [https://doi.org/10.1016/S1359-6446\(03\)02831-9](https://doi.org/10.1016/S1359-6446(03)02831-9)
- Conibear, A. E., Asghar, J., Hill, R., Henderson, G., Borbely, E., Tekus, V., Helyes, Z., Palandri, J., Bailey, C., Starke, I., von Mentzer, B., Kendall, D., & Kelly, E. (2020). A Novel G Protein-Biased Agonist at the δ Opioid Receptor with Analgesic Efficacy in Models of Chronic Pain. *The Journal of Pharmacology and Experimental Therapeutics*, *372*(2), 224–236. <https://doi.org/10.1124/jpet.119.258640>
- Conn, P. J., Lindsley, C. W., Meiler, J., & Niswender, C. M. (2014). Opportunities and challenges in the discovery of allosteric modulators of GPCRs for treating CNS disorders. *Nature Reviews. Drug Discovery*, *13*(9), 692–708. <https://doi.org/10.1038/nrd4308>
- Dahal, U. P., Joswig-Jones, C., & Jones, J. P. (2012). Comparative study of the affinity and metabolism of type I and type II binding quinoline carboxamide analogs by cytochrome P450 3A4. *Journal of Medicinal Chemistry*, *55*(1), 280–290. <https://doi.org/10.1021/jm201207h>
- Depression and Other Common Mental Disorders*. (n.d.). Retrieved July 26, 2022, from <https://www.who.int/publications-detail-redirect/depression-global-health-estimates>
- Depressive Disorders. (2022). In *Diagnostic and Statistical Manual of Mental Disorders*. American Psychiatric Association Publishing. https://doi.org/10.1176/appi.books.9780890425787.x04_Depressive_Disorders
- DeWire, S. M., Yamashita, D. S., Rominger, D. H., Liu, G., Cowan, C. L., Graczyk, T. M., Chen, X.-T., Pitis, P. M., Gotchev, D., Yuan, C., Koblish, M., Lark, M. W., & Violin, J. D. (2013). A G Protein-Biased Ligand at the μ -Opioid Receptor Is Potently Analgesic with Reduced Gastrointestinal and Respiratory Dysfunction Compared with Morphine. *Journal of Pharmacology and Experimental Therapeutics*, *344*(3), 708–717. <https://doi.org/10.1124/jpet.112.201616>

- Di, L., Fish, P. V., & Mano, T. (2012). Bridging solubility between drug discovery and development. *Drug Discovery Today*, *17*(9), 486–495. <https://doi.org/10.1016/j.drudis.2011.11.007>
- DiCello, J. J., Carbone, S. E., Saito, A., Pham, V., Szymaszkiwicz, A., Gondin, A. B., Alvi, S., Marique, K., Shenoy, P., Veldhuis, N. A., Fichna, J., Canals, M., Christopoulos, A., Valant, C., & Poole, D. P. (2022). Positive allosteric modulation of endogenous delta opioid receptor signaling in the enteric nervous system is a potential treatment for gastrointestinal motility disorders. *American Journal of Physiology. Gastrointestinal and Liver Physiology*, *322*(1), G66–G78. <https://doi.org/10.1152/ajpgi.00297.2021>
- Drug Bioavailability: Estimation of Solubility, Permeability, Absorption and Bioavailability, Volume 18.* (n.d.). Retrieved November 22, 2022,
- Fava, M. (2003). Diagnosis and definition of treatment-resistant depression. *Biological Psychiatry*, *53*(8), 649–659. [https://doi.org/10.1016/S0006-3223\(03\)00231-2](https://doi.org/10.1016/S0006-3223(03)00231-2)
- Filliol, D., Ghozland, S., Chluba, J., Martin, M., Matthes, H. W. D., Simonin, F., Befort, K., Gavériaux-Ruff, C., Dierich, A., LeMeur, M., Valverde, O., Maldonado, R., & Kieffer, B. L. (2000). Mice deficient for δ - and μ -opioid receptors exhibit opposing alterations of emotional responses. *Nature Genetics*, *25*(2), Article 2. <https://doi.org/10.1038/76061>
- Foster, D. J., & Conn, P. J. (2017). Allosteric modulation of GPCRs: New insights and potential utility for treatment of schizophrenia and other CNS disorders. *Neuron*, *94*(3), 431–446. <https://doi.org/10.1016/j.neuron.2017.03.016>
- Gallantine, E. L., & Meert, T. F. (2005). A Comparison of the Antinociceptive and Adverse Effects of the μ -Opioid Agonist Morphine and the δ -Opioid Agonist SNC80. *Basic & Clinical Pharmacology & Toxicology*, *97*(1), 39–51. https://doi.org/10.1111/j.1742-7843.2005.pto_97107.x
- Ganesan, S. S., Kothandapani, J., & Ganesan, A. (n.d.). Zinc Chloride Catalyzed Collective Synthesis of Arylmethylene Bis(3- hydroxy-2-cyclohexene-1-ones) and 1,8-Dioxo-octahydroxanthene/acridine Derivatives. *Letters in Organic Chemistry*, *11*(9), 682–687.
- Gao, Z.-G., & Jacobson, K. A. (2013). Allosteric modulation and functional selectivity of G protein-coupled receptors. *Drug Discovery Today: Technologies*, *10*(2), e237–e243. <https://doi.org/10.1016/j.ddtec.2012.08.004>
- Gaskin, D. J., & Richard, P. (2012). The Economic Costs of Pain in the United States. *The Journal of Pain*, *13*(8), 715–724. <https://doi.org/10.1016/j.jpain.2012.03.009>
- Guengerich, F. P. (2006). Cytochrome P450s and other enzymes in drug metabolism and toxicity. *The AAPS Journal*, *8*(1), E101–E111. <https://doi.org/10.1208/aapsj080112>
- Guengerich, F. P., & MacDonald, J. S. (2007). Applying Mechanisms of Chemical Toxicity to Predict Drug Safety. *Chemical Research in Toxicology*, *20*(3), 344–369. <https://doi.org/10.1021/tx600260a>

- Hong, S., Yuan, Y., Yang, Q., Chen, L., Deng, J., Chen, W., Lian, H., Mota-Morales, J. D., & Liimatainen, H. (2019). Choline chloride-zinc chloride deep eutectic solvent mediated preparation of partial O-acetylation of chitin nanocrystal in one step reaction. *Carbohydrate Polymers*, 220, 211–218. <https://doi.org/10.1016/j.carbpol.2019.05.075>
- Inturrisi, C. E. (2002). Clinical Pharmacology of Opioids for Pain. *The Clinical Journal of Pain*, 18(4), S3.
- Ippolito, D. L., Temkin, P. A., Rogalski, S. L., & Chavkin, C. (2002). N-terminal Tyrosine Residues within the Potassium Channel Kir3 Modulate GTPase Activity of Gai. *Journal of Biological Chemistry*, 277(36), 32692–32696. <https://doi.org/10.1074/jbc.M204407200>
- Issa, N. T., Wathieu, H., Ojo, A., Byers, S. W., & Dakshnamurthy, S. (2017). Drug Metabolism in Preclinical Drug Development: A Survey of the Discovery Process, Toxicology, and Computational Tools. *Current Drug Metabolism*, 18(6), 556–565. <https://doi.org/10.2174/1389200218666170316093301>
- James, S. L., Abate, D., Abate, K. H., Abay, S. M., Abbafati, C., Abbasi, N., Abbastabar, H., Abd-Allah, F., Abdela, J., Abdelalim, A., Abdollahpour, I., Abdulkader, R. S., Abebe, Z., Abera, S. F., Abil, O. Z., Abraha, H. N., Abu-Raddad, L. J., Abu-Rmeileh, N. M. E., Accrombessi, M. M. K., ... Murray, C. J. L. (2018). Global, regional, and national incidence, prevalence, and years lived with disability for 354 diseases and injuries for 195 countries and territories, 1990–2017: A systematic analysis for the Global Burden of Disease Study 2017. *The Lancet*, 392(10159), 1789–1858. [https://doi.org/10.1016/S0140-6736\(18\)32279-7](https://doi.org/10.1016/S0140-6736(18)32279-7)
- Jones, P. J. H., & Leatherdale, S. T. (1991). Stable isotopes in clinical research: Safety reaffirmed. *Clinical Science*, 80(4), 277–280. <https://doi.org/10.1042/cs0800277>
- Kalgutkar, A. S., & Soglia, J. R. (2005). Minimising the potential for metabolic activation in drug discovery. *Expert Opinion on Drug Metabolism & Toxicology*, 1(1), 91–142. <https://doi.org/10.1517/17425255.1.1.91>
- Kasper, S. (2022). Initiating Antidepressant Medication: What is the Most Important Factor? *Advances in Therapy*, 39(1), 5–12. <https://doi.org/10.1007/s12325-021-02028-7>
- Katz, J. J., & Crespi, H. L. (1966). Deuterated Organisms: Cultivation and Uses. *Science*, 151(3715), 1187–1194. <https://doi.org/10.1126/science.151.3715.1187>
- Kaushik, P., Kumar, A., Kumar, P., Kumar, S., Singh, B. K., & Bahadur, V. (2020). Cu-catalyzed one-pot multicomponent approach for the synthesis of symmetric and asymmetric 1,4-dihydropyridine (1,4-DHP) linked 1,2,3-triazole derivatives. *Synthetic Communications*, 50(13), 2033–2042. <https://doi.org/10.1080/00397911.2020.1762222>
- Kaya, M., Yıldırım, Y., & Çelik, G. Y. (2015). Synthesis, Characterization, and In Vitro Antimicrobial and Antifungal Activity of Novel Acridines. *Pharmaceutical Chemistry Journal*, 48(11), 722–726. <https://doi.org/10.1007/s11094-015-1181-4>

- Kenakin, T. P. (2012). Biased signalling and allosteric machines: New vistas and challenges for drug discovery. *British Journal of Pharmacology*, *165*(6), 1659–1669. <https://doi.org/10.1111/j.1476-5381.2011.01749.x>
- Kenakin, T. P. (Ed.). (2014). Front-matter. In *A Pharmacology Primer (Fourth Edition)* (pp. i–iii). Academic Press. <https://doi.org/10.1016/B978-0-12-407663-1.00015-6>
- Keov, P., Sexton, P. M., & Christopoulos, A. (2011). Allosteric modulation of G protein-coupled receptors: A pharmacological perspective. *Neuropharmacology*, *60*(1), 24–35. <https://doi.org/10.1016/j.neuropharm.2010.07.010>
- Kerns, E. H., & Di, L. (2008). *Drug-like properties: Concepts, structure design and methods: from ADME to toxicity optimization*. Academic Press.
- Khajehali, E., Malone, D., Glass, M., Sexton, P., Christopoulos, A., & Leach, K. (2015). Biased Agonism and Biased Allosteric Modulation at the CB1 Cannabinoid Receptor. *Molecular Pharmacology*, *88*. <https://doi.org/10.1124/mol.115.099192>
- Khoo, Y., Demchenko, I., Frey, B. N., Milev, R. V., Ravindran, A. V., Parikh, S. V., Ho, K., Rotzinger, S., Lou, W., Lam, R. W., Kennedy, S. H., & Bhat, V. (2022). Baseline anxiety, and early anxiety/depression improvement in anxious depression predicts treatment outcomes with escitalopram: A CAN-BIND-1 study report. *Journal of Affective Disorders*, *300*, 50–58. <https://doi.org/10.1016/j.jad.2021.12.027>
- Kirchmair, J., Williamson, M. J., Tyzack, J. D., Tan, L., Bond, P. J., Bender, A., & Glen, R. C. (2012). Computational Prediction of Metabolism: Sites, Products, SAR, P450 Enzyme Dynamics, and Mechanisms. *Journal of Chemical Information and Modeling*, *52*(3), 617–648. <https://doi.org/10.1021/ci200542m>
- Kliwer, A., Schmiedel, F., Sianati, S., Bailey, A., Bateman, J. T., Levitt, E. S., Williams, J. T., Christie, M. J., & Schulz, S. (2019). Phosphorylation-deficient G-protein-biased μ -opioid receptors improve analgesia and diminish tolerance but worsen opioid side effects. *Nature Communications*, *10*, 367. <https://doi.org/10.1038/s41467-018-08162-1>
- Koehl, A., Hu, H., Maeda, S., Zhang, Y., Qu, Q., Paggi, J. M., Latorraca, N. R., Hilger, D., Dawson, R., Matile, H., Schertler, G. F. X., Granier, S., Weis, W. I., Dror, R. O., Manglik, A., Skinotis, G., & Kobilka, B. K. (2018). Structure of the μ -opioid receptor–Gi protein complex. *Nature*, *558*(7711), Article 7711. <https://doi.org/10.1038/s41586-018-0219-7>
- Kola, I., & Landis, J. (2004). Can the pharmaceutical industry reduce attrition rates? *Nature Reviews Drug Discovery*, *3*(8), Article 8. <https://doi.org/10.1038/nrd1470>
- Krapcho, A. P., Weimaster, J. F., Eldridge, J. M., Jahngen, E. G. E., Lovey, A. J., & Stephens, W. P. (1978). Synthetic applications and mechanism studies of the decarboxylations of geminal diesters and related systems effected in dimethyl sulfoxide by water and/or by water with added salts. *The Journal of Organic Chemistry*, *43*(1), 138–147. <https://doi.org/10.1021/jo00395a032>

- Kushner, D. J., Baker, A., & Dunstall, T. G. (1999). Pharmacological uses and perspectives of heavy water and deuterated compounds. *Canadian Journal of Physiology and Pharmacology*, 77(2), 79–88.
- Lambert, D., & Calo, G. (2020). Approval of oliceridine (TRV130) for intravenous use in moderate to severe pain in adults. *BJA: British Journal of Anaesthesia*, 125(6), e473–e474. <https://doi.org/10.1016/j.bja.2020.09.021>
- Le Bourdonnec, B., Windh, R. T., Leister, L. K., Zhou, Q. J., Ajello, C. W., Gu, M., Chu, G.-H., Tuthill, P. A., Barker, W. M., Koblish, M., Wiant, D. D., Graczyk, T. M., Belanger, S., Cassel, J. A., Feschenko, M. S., Brogdon, B. L., Smith, S. A., Derelanko, M. J., Kutz, S., ... Dolle, R. E. (2009). Spirocyclic Delta Opioid Receptor Agonists for the Treatment of Pain: Discovery of N,N-Diethyl-3-hydroxy-4-(spiro[chromene-2,4'-piperidine]-4-yl) Benzamide (ADL5747). *Journal of Medicinal Chemistry*, 52(18), 5685–5702. <https://doi.org/10.1021/jm900773n>
- Lewis, D. F. V., & Dickins, M. (2002). Substrate SARs in human P450s. *Drug Discovery Today*, 7(17), 918–925. [https://doi.org/10.1016/S1359-6446\(02\)02412-1](https://doi.org/10.1016/S1359-6446(02)02412-1)
- Lewis, D. F. V., Jacobs, M. N., & Dickins, M. (2004). Compound lipophilicity for substrate binding to human P450s in drug metabolism. *Drug Discovery Today*, 9(12), 530–537. [https://doi.org/10.1016/S1359-6446\(04\)03115-0](https://doi.org/10.1016/S1359-6446(04)03115-0)
- Li, J.-X. (2015). Pain and depression comorbidity: A preclinical perspective. *Behavioural Brain Research*, 276, 92–98. <https://doi.org/10.1016/j.bbr.2014.04.042>
- Lindsley, C. W., Emmitte, K. A., Hopkins, C. R., Bridges, T. M., Gregory, K. J., Niswender, C. M., & Conn, P. J. (2016). Practical Strategies and Concepts in GPCR Allosteric Modulator Discovery: Recent Advances with Metabotropic Glutamate Receptors. *Chemical Reviews*, 116(11), 6707–6741. <https://doi.org/10.1021/acs.chemrev.5b00656>
- Lipinski, C. A. (2000). Drug-like properties and the causes of poor solubility and poor permeability. *Journal of Pharmacological and Toxicological Methods*, 44(1), 235–249. [https://doi.org/10.1016/S1056-8719\(00\)00107-6](https://doi.org/10.1016/S1056-8719(00)00107-6)
- Lipinski, C., & Hopkins, A. (2004). Navigating chemical space for biology and medicine. *Nature*, 432(7019), Article 7019. <https://doi.org/10.1038/nature03193>
- Livingston, K. E., Stanczyk, M. A., Burford, N. T., Alt, A., Canals, M., & Traynor, J. R. (2018). Pharmacologic Evidence for a Putative Conserved Allosteric Site on Opioid Receptors. *Molecular Pharmacology*, 93(2), 157–167. <https://doi.org/10.1124/mol.117.109561>
- Livingston, K. E., & Traynor, J. R. (2018). Allostery at opioid receptors: Modulation with small molecule ligands. *British Journal of Pharmacology*, 175(14), 2846–2856. <https://doi.org/10.1111/bph.13823>
- Major Depression*. (n.d.). National Institute of Mental Health (NIMH). Retrieved July 10, 2022, from <https://www.nimh.nih.gov/health/statistics/major-depression>

- Manglik, A., Lin, H., Aryal, D. K., McCorvy, J. D., Dengler, D., Corder, G., Levit, A., Kling, R. C., Bernat, V., Hübner, H., Huang, X.-P., Sassano, M. F., Giguère, P. M., Löber, S., Da Duan, Scherrer, G., Kobilka, B. K., Gmeiner, P., Roth, B. L., & Shoichet, B. K. (2016). Structure-based discovery of opioid analgesics with reduced side effects. *Nature*, 537(7619), Article 7619. <https://doi.org/10.1038/nature19112>
- May, L. T., Leach, K., Sexton, P. M., & Christopoulos, A. (2007). Allosteric Modulation of G Protein–Coupled Receptors. *Annual Review of Pharmacology and Toxicology*, 47(1), 1–51. <https://doi.org/10.1146/annurev.pharmtox.47.120505.105159>
- MCKIBBEN, B. P., MEYERS, K. M., Zhang, Y., Marshall, D. R., Cogan, D., Lord, J., Chen, Z., Burke, J., & Balestra, M. (2018). *Bicyclic imidazole derivatives useful for the treatment of renal disease, cardiovascular diseases and fibrotic disorders* (World Intellectual Property Organization Patent WO2018005177A1). <https://patents.google.com/patent/WO2018005177A1/en>
- McPherson, J., Rivero, G., Baptist, M., Llorente, J., Al-Sabah, S., Krasel, C., Dewey, W. L., Bailey, C. P., Rosethorne, E. M., Charlton, S. J., Henderson, G., & Kelly, E. (2010). μ -Opioid Receptors: Correlation of Agonist Efficacy for Signalling with Ability to Activate Internalization. *Molecular Pharmacology*, 78(4), 756–766. <https://doi.org/10.1124/mol.110.066613>
- Meanwell, N. A. (2011). Synopsis of Some Recent Tactical Application of Bioisosteres in Drug Design. *Journal of Medicinal Chemistry*, 54(8), 2529–2591. <https://doi.org/10.1021/jm1013693>
- Meanwell, N. A. (2015). The Influence of Bioisosteres in Drug Design: Tactical Applications to Address Developability Problems. In N. A. Meanwell (Ed.), *Tactics in Contemporary Drug Design* (pp. 283–381). Springer. https://doi.org/10.1007/7355_2013_29
- Melancon, B. J., Hopkins, C. R., Wood, M. R., Emmitte, K. A., Niswender, C. M., Christopoulos, A., Conn, P. J., & Lindsley, C. W. (2012). Allosteric Modulation of Seven Transmembrane Spanning Receptors: Theory, Practice, and Opportunities for Central Nervous System Drug Discovery. *Journal of Medicinal Chemistry*, 55(4), 1445–1464. <https://doi.org/10.1021/jm201139r>
- Moncrieff, J., & Kirsch, I. (2005). Efficacy of antidepressants in adults. *BMJ: British Medical Journal*, 331(7509), 155–157.
- Murray, M. R., & Benitez, H. H. (1967). Deuterium Oxide: Direct Action on Sympathetic Ganglia Isolated in Culture. *Science*, 155(3765), 1021–1024. <https://doi.org/10.1126/science.155.3765.1021>
- Mutlib, A. E., Gerson, R. J., Meunier, P. C., Haley, P. J., Chen, H., Gan, L. S., Davies, M. H., Gemzik, B., Christ, D. D., Krahn, D. F., Markwalder, J. A., Seitz, S. P., Robertson, R. T., & Miwa, G. T. (2000). The Species-Dependent Metabolism of Efavirenz Produces a Nephrotoxic Glutathione Conjugate in Rats. *Toxicology and Applied Pharmacology*, 169(1), 102–113. <https://doi.org/10.1006/taap.2000.9055>

- Nagase, H., & Saitoh, A. (2020). Research and development of κ opioid receptor agonists and δ opioid receptor agonists. *Pharmacology & Therapeutics*, 205, 107427. <https://doi.org/10.1016/j.pharmthera.2019.107427>
- Nebert, D. W., & Russell, D. W. (2002). Clinical importance of the cytochromes P450. *The Lancet*, 360(9340), 1155–1162. [https://doi.org/10.1016/S0140-6736\(02\)11203-7](https://doi.org/10.1016/S0140-6736(02)11203-7)
- Nestler, E. J. (2004). Historical review: Molecular and cellular mechanisms of opiate and cocaine addiction. *Trends in Pharmacological Sciences*, 25(4), 210–218. <https://doi.org/10.1016/j.tips.2004.02.005>
- Olson, K. M., Traynor, J. R., & Alt, A. (2021). Allosteric Modulator Leads Hiding in Plain Site: Developing Peptide and Peptidomimetics as GPCR Allosteric Modulators. *Frontiers in Chemistry*, 9. <https://www.frontiersin.org/articles/10.3389/fchem.2021.671483>
- Pathan, H., & Williams, J. (2012). Basic opioid pharmacology: An update. *British Journal of Pain*, 6(1), 11–16. <https://doi.org/10.1177/2049463712438493>
- Pedersen, M. F., Wróbel, T. M., Märcher-Rørsted, E., Pedersen, D. S., Møller, T. C., Gabriele, F., Pedersen, H., Matusiuk, D., Foster, S. R., Bouvier, M., & Bräuner-Osborne, H. (2020). Biased agonism of clinically approved μ -opioid receptor agonists and TRV130 is not controlled by binding and signaling kinetics. *Neuropharmacology*, 166, 107718. <https://doi.org/10.1016/j.neuropharm.2019.107718>
- Perrine, S. A., Hoshaw, B. A., & Unterwald, E. M. (2006). Delta opioid receptor ligands modulate anxiety-like behaviors in the rat. *British Journal of Pharmacology*, 147(8), 864–872. <https://doi.org/10.1038/sj.bjp.0706686>
- Phang-Lyn, S., & Llerena, V. A. (2021). Biochemistry, Biotransformation. In *StatPearls [Internet]*. StatPearls Publishing. <https://www.ncbi.nlm.nih.gov/books/NBK544353/>
- Pradhan, A. A. A., Becker, J. A. J., Scherrer, G., Tryoen-Toth, P., Filliol, D., Matifas, A., Massotte, D., Gavériaux-Ruff, C., & Kieffer, B. L. (2009). In Vivo Delta Opioid Receptor Internalization Controls Behavioral Effects of Agonists. *PLOS ONE*, 4(5), e5425. <https://doi.org/10.1371/journal.pone.0005425>
- Pradhan, A. A. A., Walwyn, W., Nozaki, C., Filliol, D., Erbs, E., Matifas, A., Evans, C., & Kieffer, B. L. (2010). Ligand-Directed Trafficking of the δ -Opioid Receptor In Vivo: Two Paths Toward Analgesic Tolerance. *Journal of Neuroscience*, 30(49), 16459–16468. <https://doi.org/10.1523/JNEUROSCI.3748-10.2010>
- Pradhan, A. A., Befort, K., Nozaki, C., Gavériaux-Ruff, C., & Kieffer, B. L. (2011). The delta opioid receptor: An evolving target for the treatment of brain disorders. *Trends in Pharmacological Sciences*, 32(10), 581–590. <https://doi.org/10.1016/j.tips.2011.06.008>
- Pradier, M. F., McCoy Jr, T. H., Hughes, M., Perlis, R. H., & Doshi-Velez, F. (2020). Predicting treatment dropout after antidepressant initiation. *Translational Psychiatry*, 10(1), Article 1. <https://doi.org/10.1038/s41398-020-0716-y>

- Prentis, R. A., Lis, Y., & Walker, S. R. (1988). Pharmaceutical innovation by the seven UK-owned pharmaceutical companies (1964-1985). *British Journal of Clinical Pharmacology*, 25(3), 387–396.
- Prueksaritanont, T., & Tang, C. (2012). ADME of Biologics—What Have We Learned from Small Molecules? *The AAPS Journal*, 14(3), 410–419. <https://doi.org/10.1208/s12248-012-9353-6>
- Rasmussen, N. A., & Farr, L. A. (2009). Beta-endorphin response to an acute pain stimulus. *Journal of Neuroscience Methods*, 177(2), 285–288. <https://doi.org/10.1016/j.jneumeth.2008.10.013>
- Remesic, M., Hruby, V. J., Porreca, F., & Lee, Y. S. (2017). Recent Advances in the Realm of Allosteric Modulators for Opioid Receptors for Future Therapeutics. *ACS Chemical Neuroscience*, 8(6), 1147–1158. <https://doi.org/10.1021/acscemneuro.7b00090>
- Research and Development in the Pharmaceutical Industry | Congressional Budget Office*. (2021, April 8). <https://www.cbo.gov/publication/57126>
- Reyes-Alcaraz, A., Garcia-Rojas, E. Y. L., Bond, R. A., & McConnell, B. K. (2020). Allosteric Modulators for GPCRs as a Therapeutic Alternative with High Potential in Drug Discovery. In *Molecular Pharmacology*. IntechOpen. <https://doi.org/10.5772/intechopen.91838>
- Saitoh, A., Kimura, Y., Suzuki, T., Kawai, K., Nagase, H., & Kamei, J. (2004). Potential Anxiolytic and Antidepressant-Like Activities of SNC80, a Selective δ -Opioid Agonist, in Behavioral Models in Rodents. *Journal of Pharmacological Sciences*, 95(3), 374–380. <https://doi.org/10.1254/jphs.FPJ04014X>
- Serafini, G., Adavastro, G., Canepa, G., De Berardis, D., Valchera, A., Pompili, M., Nasrallah, H., & Amore, M. (2018). The Efficacy of Buprenorphine in Major Depression, Treatment-Resistant Depression and Suicidal Behavior: A Systematic Review. *International Journal of Molecular Sciences*, 19(8), 2410. <https://doi.org/10.3390/ijms19082410>
- Shang, Y., Yeatman, H. R., Provasi, D., Alt, A., Christopoulos, A., Canals, M., & Filizola, M. (2016). Proposed Mode of Binding and Action of Positive Allosteric Modulators at Opioid Receptors. *ACS Chemical Biology*, 11(5), 1220–1229. <https://doi.org/10.1021/acscembio.5b00712>
- Sharma, D., Soni, M., Kumar, S., & Gupta, G. (2009). *Solubility Enhancement – Eminent Role in Poorly Soluble Drugs*. 5.
- Smith, J. S., Lefkowitz, R. J., & Rajagopal, S. (2018). Biased Signalling: From Simple Switches to Allosteric Microprocessors. *Nature Reviews. Drug Discovery*, 17(4), 243–260. <https://doi.org/10.1038/nrd.2017.229>

- St. Jean, D. J., & Fotsch, C. (2012). Mitigating Heterocycle Metabolism in Drug Discovery. *Journal of Medicinal Chemistry*, 55(13), 6002–6020. <https://doi.org/10.1021/jm300343m>
- Stanczyk, M. A., Livingston, K. E., Chang, L., Weinberg, Z. Y., Puthenveedu, M. A., & Traynor, J. R. (2019). The δ -opioid receptor positive allosteric modulator BMS 986187 is a G-protein-biased allosteric agonist. *British Journal of Pharmacology*, 176(11), 1649–1663. <https://doi.org/10.1111/bph.14602>
- Stein, C. (2016). Opioid Receptors. *Annual Review of Medicine*, 67(1), 433–451. <https://doi.org/10.1146/annurev-med-062613-093100>
- Stepan, A. F., Karki, K., McDonald, W. S., Dorff, P. H., Dutra, J. K., DiRico, K. J., Won, A., Subramanyam, C., Efremov, I. V., O'Donnell, C. J., Nolan, C. E., Becker, S. L., Pustilnik, L. R., Sneed, B., Sun, H., Lu, Y., Robshaw, A. E., Riddell, D., O'Sullivan, T. J., ... Obach, R. S. (2011). Metabolism-Directed Design of Oxetane-Containing Arylsulfonamide Derivatives as γ -Secretase Inhibitors. *Journal of Medicinal Chemistry*, 54(22), 7772–7783. <https://doi.org/10.1021/jm200893p>
- Stepan, A. F., Mascitti, V., Beaumont, K., & Kalgutkar, A. S. (2013). Metabolism-guided drug design. *MedChemComm*, 4(4), 631. <https://doi.org/10.1039/c2md20317k>
- Stevens, C. W. (2004). Opioid research in amphibians: An alternative pain model yielding insights on the evolution of opioid receptors. *Brain Research. Brain Research Reviews*, 46(2), 204–215. <https://doi.org/10.1016/j.brainresrev.2004.07.003>
- Stevens, C. W., Brasel, C. M., & Mohan, S. (2007). Cloning and bioinformatics of amphibian mu, delta, kappa, and nociceptin opioid receptors expressed in brain tissue: Evidence for opioid receptor divergence in mammals. *Neuroscience Letters*, 419(3), 189–194. <https://doi.org/10.1016/j.neulet.2007.04.014>
- Sun, D., Gao, W., Hu, H., & Zhou, S. (2022). Why 90% of clinical drug development fails and how to improve it? *Acta Pharmaceutica Sinica B*, 12(7), 3049–3062. <https://doi.org/10.1016/j.apsb.2022.02.002>
- Thompson, T. N. (2001). Optimization of metabolic stability as a goal of modern drug design. *Medicinal Research Reviews*, 21(5), 412–449. <https://doi.org/10.1002/med.1017>
- Toll, L., Bruchas, M. R., Calo', G., Cox, B. M., & Zaveri, N. T. (2016). Nociceptin/Orphanin FQ Receptor Structure, Signaling, Ligands, Functions, and Interactions with Opioid Systems. *Pharmacological Reviews*, 68(2), 419–457. <https://doi.org/10.1124/pr.114.009209>
- Trapaidze, N., Keith, D. E., Cvejic, S., Evans, C. J., & Devi, L. A. (1996). Sequestration of the δ Opioid Receptor. *Journal of Biological Chemistry*, 271(46), 29279–29285. <https://doi.org/10.1074/jbc.271.46.29279>
- Wang, C. W., & Chen, J. (2018). *N*-(phenylsulfonyl)benzamides and related compounds as bcl-2 inhibitors (World Intellectual Property Organization Patent WO2018027097A1). <https://patents.google.com/patent/WO2018027097A1/en?q=WO2018027097A1>

- Wang, J., Sánchez-Roselló, M., Aceña, J. L., del Pozo, C., Sorochinsky, A. E., Fustero, S., Soloshonok, V. A., & Liu, H. (2014). Fluorine in Pharmaceutical Industry: Fluorine-Containing Drugs Introduced to the Market in the Last Decade (2001–2011). *Chemical Reviews*, *114*(4), 2432–2506. <https://doi.org/10.1021/cr4002879>
- Waring, M. J. (2010). Lipophilicity in drug discovery. *Expert Opinion on Drug Discovery*, *5*(3), 235–248. <https://doi.org/10.1517/17460441003605098>
- Waterhouse, R. N. (2003). Determination of lipophilicity and its use as a predictor of blood–brain barrier penetration of molecular imaging agents. *Molecular Imaging & Biology*, *5*(6), 376–389. <https://doi.org/10.1016/j.mibio.2003.09.014>
- Wenthur, C. J., Gentry, P. R., Mathews, T. P., & Lindsley, C. W. (2014). Drugs for Allosteric Sites on Receptors. *Annual Review of Pharmacology and Toxicology*, *54*, 165–184. <https://doi.org/10.1146/annurev-pharmtox-010611-134525>
- Wester, M. R., Yano, J. K., Schoch, G. A., Yang, C., Griffin, K. J., Stout, C. D., & Johnson, E. F. (2004). The Structure of Human Cytochrome P450 2C9 Complexed with Flurbiprofen at 2.0-Å Resolution*. *Journal of Biological Chemistry*, *279*(34), 35630–35637. <https://doi.org/10.1074/jbc.M405427200>
- Williams, P. A., Cosme, J., Vinković, D. M., Ward, A., Angove, H. C., Day, P. J., Vonnrhein, C., Tickle, I. J., & Jhoti, H. (2004). Crystal Structures of Human Cytochrome P450 3A4 Bound to Metyrapone and Progesterone. *Science*, *305*(5684), 683–686. <https://doi.org/10.1126/science.1099736>
- Wootten, D., Christopoulos, A., Marti-Solano, M., Babu, M. M., & Sexton, P. M. (2018). Mechanisms of signalling and biased agonism in G protein-coupled receptors. *Nature Reviews Molecular Cell Biology*, *19*(10), Article 10. <https://doi.org/10.1038/s41580-018-0049-3>
- Wootten, D., Christopoulos, A., & Sexton, P. M. (2013). Emerging paradigms in GPCR allostery: Implications for drug discovery. *Nature Reviews Drug Discovery*, *12*(8), Article 8. <https://doi.org/10.1038/nrd4052>
- Wuitschik, G., Carreira, E. M., Wagner, B., Fischer, H., Parrilla, I., Schuler, F., Rogers-Evans, M., & Müller, K. (2010). Oxetanes in Drug Discovery: Structural and Synthetic Insights. *Journal of Medicinal Chemistry*, *53*(8), 3227–3246. <https://doi.org/10.1021/jm9018788>
- Yano, J. K., Wester, M. R., Schoch, G. A., Griffin, K. J., Stout, C. D., & Johnson, E. F. (2004). The Structure of Human Microsomal Cytochrome P450 3A4 Determined by X-ray Crystallography to 2.05-Å Resolution*. *Journal of Biological Chemistry*, *279*(37), 38091–38094. <https://doi.org/10.1074/jbc.C400293200>
- Yeung, C. K., Fujioka, Y., Hachad, H., Levy, R. H., & Isoherranen, N. (2011). Are circulating metabolites important in drug–drug interactions?: Quantitative analysis of risk prediction and inhibitory potency. *Clinical Pharmacology and Therapeutics*, *89*(1), 105–113. <https://doi.org/10.1038/clpt.2010.252>

- Zafrani, Y., Yeffet, D., Sod-Moriah, G., Berliner, A., Amir, D., Marciano, D., Gershonov, E., & Saphier, S. (2017). Difluoromethyl Bioisostere: Examining the “Lipophilic Hydrogen Bond Donor” Concept. *Journal of Medicinal Chemistry*, *60*(2), 797–804. <https://doi.org/10.1021/acs.jmedchem.6b01691>
- Zaretzki, J., Matlock, M., & Swamidass, S. J. (2013). XenoSite: Accurately Predicting CYP-Mediated Sites of Metabolism with Neural Networks. *Journal of Chemical Information and Modeling*, *53*(12), 3373–3383. <https://doi.org/10.1021/ci400518g>
- Zhang, Z., Zhu, M., & Tang, W. (2009). Metabolite Identification and Profiling in Drug Design: Current Practice and Future Directions. *Current Pharmaceutical Design*, *15*(19), 2220–2235. <https://doi.org/10.2174/138161209788682460>

Chapter 3 Improvement of Druggability of the Xanthene-Dione Series—Solubility

3.1 Summary

Compound **1**, a xanthene-dione, is a potent positive allosteric modulator (PAM) of the δ -opioid receptor (DOR). With the addition of a methyl group at the center aromatic ring of **1** to give **CCG363081**, the insertion of extra conformational restriction significantly improves selectivity over the μ -opioid receptor (MOR) without compromising activity at DOR. Although **1** shows remarkable *in vitro* pharmacological activities, its high molecular weight (MW) and high lipophilicity (cLogP = 6.0) (insoluble) reduce its potential as lead candidate for the management of depression. Moreover, the extra lipophilic moiety (methyl group) added to **1** to improve selectivity makes the series even more undruggable. In this chapter, I describe the attempts to improve the druggability of xanthene-dione series by optimizing its solubility profile. Through bringing bioisosteric replacements to both A- and B-rings, removing unnecessary lipophilicity at the C-rings, combining separate modifications of both B- and C-rings, and introducing N-alkyl side chains at C-rings, the solubility profile of the series was significantly improved. This success is demonstrated with analogs, **CCG369831** and **CCG363177**, which maintain some degree of DOR activity.

3.2 Introduction

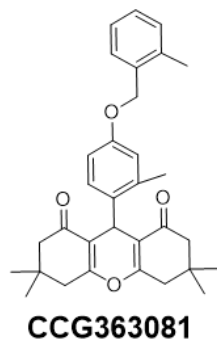


Figure 3.1
Chemical structure
of **CCG363081**

Through the SAR expansion and optimization of our lead compound **1** at both the A- and B-rings, we obtained a selective and potent DOR-PAM with **CCG363081** (**Figure 3.1**) by maintaining a 90 nM potency while having a >1,100-fold selectivity over MOR. However, the physicochemical profile of xanthene-dione compounds is unsatisfactory for further *in vivo* studies and drug development (Kerns & Di, 2008; Prueksaritanont & Tang, 2012). Due to its bulkiness (MW = 471) and high lipophilicity (cLogP = 6.0), **1** has a poor

solubility (<0.1 µg/mL), high protein bound rate (>99%), and high metabolic rate in both mouse and human (hepatic extraction ratio of mouse and human E = 0.90 and 0.81, respectively) (**Figure 3.2**) (Di et al., 2012; Waring, 2010). Furthermore, to optimize the selectivity of xanthene series over MOR, the addition of methyl moiety at the B-ring with analog **CCG363081** worsens the

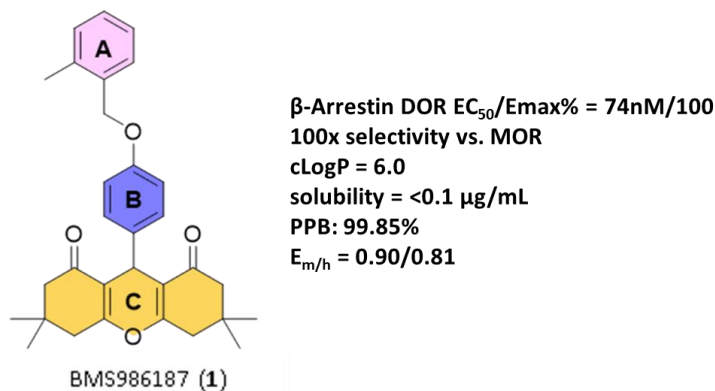


Figure 3.2 *in vitro* pharmacological and DMPK profile of **1**. Data obtained from Pharmaron

lipophilicity and solubility profile. High lipophilicity would lead to low solubility, low absorption, low bioavailability (also results from low solubility), and high metabolic clearance. In addition, high lipophilicity will hinder the permeation of the blood-brain barrier (BBB) (Banks, 2009; Bellettato & Scarpa, 2018; *Drug Bioavailability: Estimation of Solubility, Permeability, Absorption and Bioavailability, Volume 18*, n.d.; Sharma et al., 2009; Waterhouse, 2003).

Compounds with low solubility are not able to penetrate membranes, and this low solubility greatly affects oral absorption of the compound (C. A. Lipinski, 2000). Therefore, although the xanthenedione series has shown competent *in vitro* activities, its unsatisfactory physicochemical profile shows that the low druggability will be a drawback to further development. In this chapter I focus on improving the solubility for this xanthene series without losing its *in vitro* DOR-PAM activity.

3.3 Results and Discussion

3.3.1 Reduction of lipophilicity at the A-ring

3.3.1.1 Pyridine Series

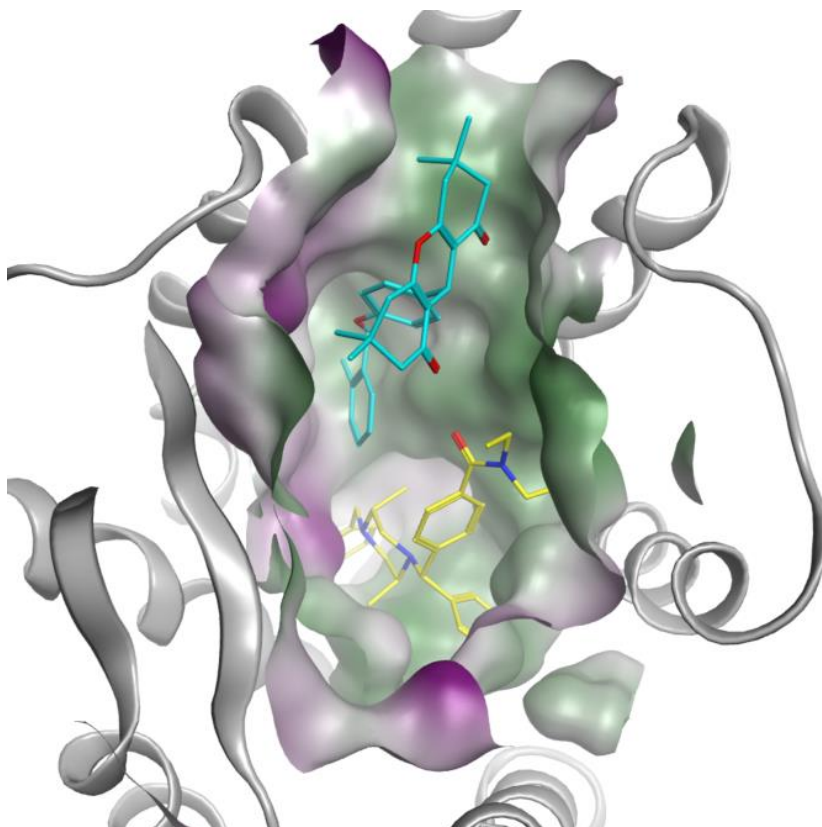


Figure 3.1 Top view of DOR crystal structure (grey) (PDB: 6PT3). **1** (blue with A-ring pointed down to the center of the transmembrane region) was docked in the allosteric site, and orthosteric agonist, DPI-287 (yellow) is bound in orthosteric site. Surface of the binding pockets are shown in green (hydrophobic regions) and purple (hydrophilic regions).

To improve solubility, we endeavored to lower the lipophilicity, initially targeting bioisosteric heteroaromatic ring replacements for the usual alkoxyphenyl subunit (*Bioisosteres in Medicinal*

Chemistry, 2012). We were especially interested in pyridine replacements, as this was predicted to reduce the lipophilicity by 0.6-1.6 log units.

Pyridine bioisosteric replacements for the distal benzyl group (A-ring) were found to lower the LogD_{7.4} by 1.1-2.0 (**Table 3.1**) relative to **1** (**Figure 3.1**). Based on earlier studies of active DOR (**Chapter 2**), the putative allosteric binding pocket is lipophilic, especially around the region where the A-ring binds (**Figure 3.3**) (Shang et al., 2016). Therefore, steric shielding of the pyridine nitrogen (electrostatic effect) was thought to be important for retaining allosteric potency at DOR (Meanwell, 2015). Indeed, the 5-chloropyridin-2-yl (**CCG369591**) and 2-methylpyridin-3-yl (**CCG367266**) which have a more exposed pyridine nitrogen than other compounds, greatly lose DOR PAM potency ($EC_{50} = 8.10 \mu\text{M}$ and $EC_{50} = 1.82 \mu\text{M}$ respectively) versus their phenyl progenitor **CCG364642** ($EC_{50} = 0.60 \mu\text{M}$) and **1** ($EC_{50} = 0.074 \mu\text{M}$) (**Table 2.1, Figure 3.4**).

The SAR of allosteric modulators has been shown to be steep, such that similar moiety changes and combinations can exhibit drastic results (Conn et al., 2014; Lindsley et al., 2016). Thus, different combinations and moieties were tried and tested. The 2-chloro derivative (**CCG364641**) ($EC_{50} = 0.047 \mu\text{M}$),

the phenyl progenitor of **CCG369575**, exhibits the

same DOR PAM potency as **1** ($EC_{50} = 0.074 \mu\text{M}$). Compared to their phenyl progenitors, the pyridine compounds **CCG367310** loses a 10-fold potency ($EC_{50} = 0.68 \mu\text{M}$), and **CCG369575**, completely loses DOR PAM potency (**Table 3.1**). A similar trend is also seen with **CCG369653**, which does not exhibit any DOR PAM activity, while **CCG369590** shows moderate activity ($EC_{50} = 1.37 \mu\text{M}$). Furthermore, the 2,6-dimethylpyridin-3-yl (**CCG369656**) has low DOR PAM

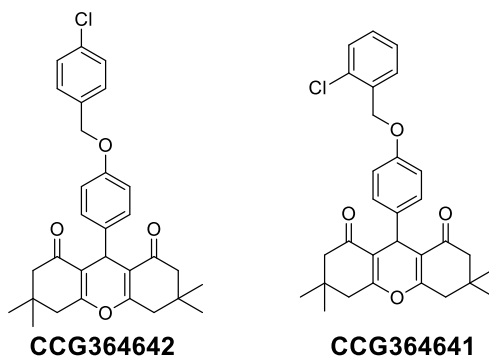
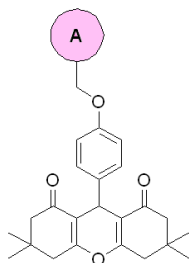


Figure 3.2 Chemical structures of **CCG364642** and **CCG364641**

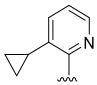
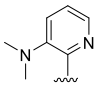
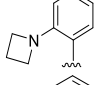
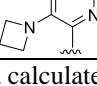
potency with an EC₅₀ of 4.91 μM, although solubility is improved to 2.8 μg/mL. In comparison replacing the 2-methyl for a 2-methoxy provides **CCG369731** that has no measurable DOR PAM activity.

Table 3.1: 6-membered heterocycle replacements for A-ring



β-Arrestin Recruitment^a

Compound	A	DOR EC ₅₀ (μM)/E _{max}	MOR EC ₅₀ (μM)/E _{max}	LogD _{7.4} ^b	Solubility ^c (μg/mL)
369591		8.10/104	>10/ N/A	4.9	
369575		>10/ N/A	>10/ N/A	4.9	<0.1
367266		1.82/105	>10/ N/A	4.4	
367310		0.68/110	>10/ N/A	4.8	0.1
369653		>10/ N/A	>10/ N/A	5.4	<0.1
369656		4.91/98	>10/ N/A	4.5	2.8
369577		>10/ N/A	>10/ N/A	4.2	
369590		1.37/89	>10/ N/A	4.8	0.03
369731		>10/ N/A	>10/ N/A	4.8	

369654		0.44/104	>10/ N/A	5.1	
369831		2.16/75	>10/ N/A	4.4	76.9
369795		>10/ N/A	>10/ N/A	5.5	
369853		>10/ N/A	>10/ N/A	4.3	

a. Same as **Table 2.1**. b. Data calculated from Chemicalize. c. Data obtained from Analiza

The solubility data indicate that a bioisosteric replacement of the benzyl A-ring to pyridyl is not sufficient to improve the solubility profile of the xanthene-dione series. Therefore, we added an additional basic nitrogen in place of the 2-methyl group. Adding a 3-(dimethylamino)pyridin-2-yl replacement (**CCG369831**), greatly improved the solubility to 76.9 $\mu\text{g/mL}$, but this compound

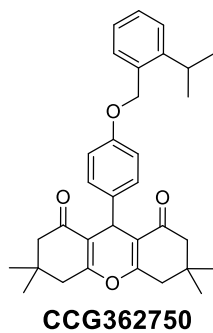


Figure 3.3
Chemical structure
of **CCG362750**

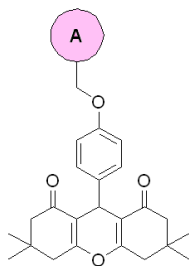
lost >10-fold DOR PAM potency ($\text{EC}_{50} = 2.16 \mu\text{M}$) relative to the parent 2-isopropyl benzyl compound (**CCG362750**) ($\text{EC}_{50} = 0.14 \mu\text{M}$) (**Table 2.2** and **Figure 3.3**) and its pyridyl analog, **CCG367310** ($\text{EC}_{50} = 0.68 \mu\text{M}$). Attachment of an azetidine-ring also led to loss of activity (**CCG369853**), but this substitution also caused a complete loss of DOR PAM activity in **1** (**CCG369795**). Overall, juggling between the solubility and DOR activity with the pyridine bioisosteres led to analogs exhibiting weaker or no DOR PAM potency, being at least 10-fold less active than the corresponding phenyl ring

benchmark compounds.

3.3.1.2 5-membered heterocycles

Because there was generally a 10-fold loss of DOR PAM activity and little improvement in solubility provided by the pyridine analogs, even within the electrostatic nitrogen sterically shielded with adjacent alkyl groups, I decided to investigate 5-membered heterocyclic bioisosteres.

Table 3.2: 5-membered heterocycle replacements for A-ring



β-Arrestin Recruitment^a

Compound	A	DOR EC ₅₀ (μM)/Emax	MOR EC ₅₀ (μM)/Emax	LogD _{7.4} ^b	Solubility ^c (μg/mL)
366164		1.05/105	4.1/70	6.2	
366168		2.86/113	3.93/75	5.2	
369576		0.40/111	>10/ N/A	6.0	
366163		>10/ N/A	>10/ N/A	3.5	
366167		>10/ N/A	>10/ N/A	4.9	
366161		2.59/104	>10/ N/A	4.2	
369578		2.28/96	>10/ N/A	4.9	15.3
369579		>10/ N/A	>10/ N/A	3.5	55.7
369751		>10/ N/A	>10/ N/A	3.6	

a. Same as **Table 2.1**. *b.* Data calculated from Chemicalize. *c.* Data obtained from Analiza

Since both 5-chlorothiophen-2-yl (**CCG366164**) and 3-chlorothiophen-2-yl moieties (**CCG369576**) maintain some activity as DOR PAMs (approximately 0.8 μM), the oxazol-2-yl (**CCG366163**) and 3-isopropyl-1,2,4-oxadiazol-5-yl (**CCG366167**) derivatives were prepared and evaluated (**Table 3.2**). However, due to presumably exposed electrostatic effects of the nitrogen and steric clash of the isopropyl group with the receptor side chains, no DOR PAM activity was measurable with these analogs. Furthermore, I observed that both **CCG366164** and **CCG366168** lost selectivity over MOR (MOR EC_{50} = 4.1 μM , 3.93 μM respectively) presumably because the position of chloro-group is more favored by MOR. Thus, mimicking the 2- and 2,6-disubstitutions of the benzyl group at the 5-membered heterocycle became essential for maintaining the DOR selectivity of xanthene-dione series over MOR.

Therefore, we prepared the 3,5-dimethyl-1,2-oxazol (**CCG366161**) and 5-methyl-1,3-thiazole (**CCG369578**) moieties, hoping the extra methyl groups would shield the electrostatic effect of the nitrogen. While these analogs were calculated to have lower $\text{LogD}_{7.4}$ values (by 1.1-1.8) and have improved solubility profile, for example the solubility of **CCG369578** was determined as 15.3 $\mu\text{g/mL}$, only modest DOR PAM activity was observed ($> 2 \mu\text{M}$). Further SAR expansion introduced imidazole to give **CCG369579** and **CCG369751**, which have lower $\text{LogD}_{7.4}$ values by 2.4 units and **CCG369579** which has good solubility (55.7 $\mu\text{g/mL}$). Unfortunately, these compounds had no measurable DOR PAM activity.

3.3.2 Reduction of lipophilicity in the B-ring

Since bioisosteric replacements at the A-ring improved solubility but did not maintain the DOR PAM activity level of **1**, I decided to reduce unnecessary lipophilicity at the B-ring by first replacing the phenyl ring with pyridines (**Table 3.3**). The 6-((2-methylbenzyl)oxy)pyridin-3-yl analog (**CCG362908**) shows improved in solubility (4.9 $\mu\text{g/mL}$) relative to **1** ($< 0.1 \mu\text{g/mL}$) but

loses activity as a DOR PAM ($EC_{50} > 10 \mu\text{M}$), presumably due to a more exposed basic nitrogen ring atom. While the 5-((2-methylbenzyl)oxy)pyridin-2-yl congener (**CCG363177**) has a somewhat more shielded ring nitrogen, it is better tolerated as a DOR PAM, with more improved solubility profile (DOR PAM $EC_{50} = 2.96 \mu\text{M}$; sol.= $10.9 \mu\text{g/mL}$). However, both analogs lost >80 -fold potency relative to **1**.

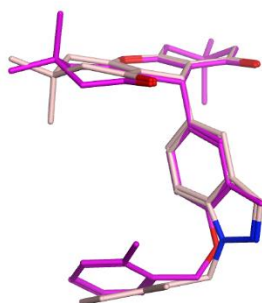
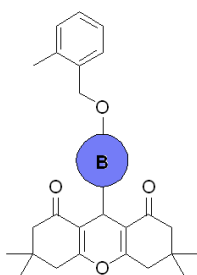


Figure 3.4 Flexalignment and overlay of **CCG362904** (purple) and **CCG366793** (pink)

From prior SAR studies (**Table 2.3**) **CCG362904** not only maintains a decent level of DOR PAM activity at just 3-times less than the parent **1** (DOR PAM $EC_{50} = 0.24 \mu\text{M}$) but also shows improved selectivity over MOR. Therefore, elaboration of **CCG362904** was examined. From the flexalignment of **CCG362904** and a benzo-fused heterocycle, both compounds align well with one another (**Figure 3.4**). Thus, we predicted that bioisosteric replacements of **CCG362904** with benzo-fused nitrogen heterocycles could potentially maintain decent DOR PAM activity and selectivity while improving the solubility profile.

Unfortunately, the indole derivative (**CCG366795**) had no measurable DOR PAM activity. Indazole (**CCG366793** and **CCG367104**) and benzimidazole (**CCG367064** and **CCG367107**) derivatives and their isomers were also investigated. These analogs were found to have lower $\text{LogD}_{7.4}$ values (by 0.1-0.4) with solubilities of $8.8 \mu\text{g/mL}$ and $2.6 \mu\text{g/mL}$ respectively, but only **CCG366793** exhibited weak DOR activity ($EC_{50} = 4.8 \mu\text{M}$). The remainder of the analogs were inactive up to $10 \mu\text{M}$. These data indicated that the attempt of bioisosteric replacement of the B-ring of **CCG362904** was not applicable presumably due to more exposed electrostatic effects of the extra nitrogen.

Table 3.3: Bioisosteric replacements of phenyl B-ring

Compound	B	<u>β-Arrestin Recruitment</u> ^a			
		DOR EC ₅₀ (μM)/E _{max}	MOR EC ₅₀ (μM)/E _{max}	LogD _{7.4} ^b	Solubility ^c (μg/mL)
362908		>10/ N/A	>10/ N/A	5.4	4.9
363177		2.96/76	>10/ N/A	4.9	10.9
366795		>10/ N/A	>10/ N/A	6.5	
366793		4.79/ 88	>10/ N/A	5.6	8.8
367104		>10/ N/A	>10/ N/A	5.9	
367064		>10/ N/A	>10/ N/A	5.6	2.6
367107		>10/ N/A	>10/ N/A	5.6	

a. Same as **Table 2.1**. b-c. Same as **Table 3.1**.

3.3.3 Reduction of lipophilicity/molecular weight at the C-rings

While we were able to successfully modify the benzyl group and central appended phenyl ring of the parent xanthene-dione system with a variety of more polar bioisosteres and indeed lower the

lipophilicity and improve the solubility, we were unable to preserve adequate DOR-PAM activity. To address this, I next turned attention to the C-rings, the 3,4,5,6,7,9-Hexahydro-3,3,6,6-tetramethyl-1H-xanthene-1,8(2H)-dione scaffold, as a substrate for further modification (**Table 3.4**). I started by reducing the number of appended methyl substituents and extending the chain length to explore the size of the binding pockets. Although this exploration gives no lipophilicity reduction, it could provide a better understanding of the differences between the DOR and MOR allosteric binding pockets. Removal of one methyl group on either side of the molecule resulted in (**CCG366672**), which had a lowered $\text{LogD}_{7.4}$ value by 0.6 unit but resulted in a 10-fold loss in potency. Ethyl substitution (**CCG366166**) did not lower the lipophilicity but lost even more potency and gained some activity at MOR. These findings highlight the importance of the methyl groups in the xanthene-dione rings. To further improve the solubility, I tried switching the methyl moiety into trifluoro moieties (**CCG366180**) (**Table 3.4**). However, this resulted in a 10-fold loss in DOR PAM activity relative to **CG366672**, which indicates that the DOR allosteric site disfavored electrostatic effects in the side chains of the C-rings.

Although the removal of appended methyl substituents of the tetramethyl parent to corresponding dimethyl analog (**CG366672**) indicates loss in selectivity for DOR, activity in the primary DOR PAM assay was evident. Therefore, I removed all the methyl groups of the parent (**1**) to furnish **CCG362898**. This provided a further lowering of the $\text{LogD}_{7.4}$ value (by 1.2 units) with only a 10-fold loss of DOR PAM potency ($\text{EC}_{50} = 0.72 \mu\text{M}$) and without loss of selectivity. This persistence of DOR PAM activity after removal of tetramethyl moiety allowed us to move one step forward by reducing the size of the flanking rings from 6-membered to 5-membered provided (**CCG366673**), which further lowered the $\text{LogD}_{7.4}$ by 2.1 units. Unfortunately, no DOR PAM activity was observed for this analog.

Taken together, data with these synthesized analogs show that dimethyl groups and the 6-membered ring size are essential for good potency at DOR. Nevertheless, we were not sure if both of the geminal dimethyl moieties and all three rings of the 3,4,5,6,7,9-Hexahydro-3,3,6,6-tetramethyl-1H-xanthene-1,8(2H)-dione scaffold are necessary for DOR PAM activity. In the event, we found that the bicyclic analog (**CCG363244**), but not (**CCG363621** and **CCG364645**) showed tolerable activity in DOR ($EC_{50} = 0.71 \mu\text{M}$) and lowered the $\text{LogD}_{7.4}$ by 0.9 unit. However, when both fused dione rings were removed, leaving just the central pyran ring (**CCG363622**), the $\text{LogD}_{7.4}$ was reduced by 1.8, but there was a complete loss of all DOR PAM activity (**Table 3.4**). In addition, an attempt to replace one of the three rings with methyl-pyrazole moiety (**CCG367106**) leads to a complete loss of DOR PAM activity. Overall, the exercise of modifying the C-rings shows us that the dimethyl moiety and tetramethyl substitution and the diones of the C-rings are essential for potent DOR-PAM activity and selectivity over MOR, but modifications can be made, e.g. **CCG362898** and **CCG363244** with a 10-fold loss in potency.

Table 3.4: Modifications at C-rings

Compound	C	<u>β-Arrestin Recruitment</u> ^a			
		DOR EC_{50} (μM)/ E_{max}	MOR EC_{50} (μM)/ E_{max}	Selectivity ^b	$\text{LogD}_{7.4}$ ^c
366181		1.05/77	>10/ N/A	N/A	7.7
366166		1.13/122	2.71/70		6.3

366672		0.39/101	2.46/111	5	5.4
366180		4.72/63	>10/ N/A	>2	5.9
362898		0.72/76	>10/ N/A	>10	4.8
366673		>10/ N/A	>10/ N/A	N/A	3.9
363244		0.71/66	>10/ N/A	>11	5.1
363621		>10/ N/A	>10/ N/A	N/A	N/A
364645		>10/ N/A	>10/ N/A	N/A	N/A
363622		>10/ N/A	>10/ N/A	N/A	4.2
367106		>10/ N/A	>10/ N/A	N/A	4.8

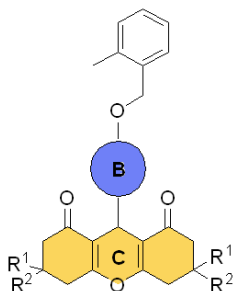
a-b. Same as **Table 2.1**. *c.* LogD_{7.4} calculated and predicted by Chemicalize.

3.3.4 Combined modifications of B- and C-rings to reduce lipophilicity

As separate modifications have been made to both the B- and C-rings, a combination of the modifications was used to explore potential synergistic effects. From the bioisosteric expansion of SAR at both A- and B-rings, pyridine was found to improve the solubility profile while maintaining some of the DOR PAM activity. While **CCG362898** has reduced lipophilicity (LogD_{7.4} = 4.8) from changes in the C-ring substitutions, it also maintained some degree of DOR PAM activity. Therefore, combinations of **CCG362898** and the pyridines in the B-ring were prepared and examined to give **CCG362905** and **CCG362907**. The LogD_{7.4} of the analogs were reduced by 1.8-2.3 units; unfortunately, no measurable DOR PAM activity was observed with

either derivative (**Table 3.5**). Thus, a new strategy of reducing lipophilicity/improving solubility profile is needed to maintain DOR PAM activity with xanthene-dione series.

Table 3.5: Combined modifications of B- and C-rings



β-Arrestin Recruitment^a

Compound	B & C	DOR EC ₅₀ (μM)/E _{max}	MOR EC ₅₀ (μM)/E _{max}	LogD _{7.4} ^b
362905		>10/ N/A	>10/ N/A	3.7
362907		>10/ N/A	>10/ N/A	4.2

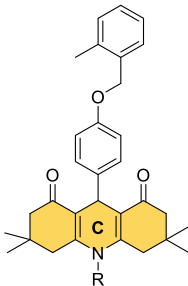
a. Same as **Table 2.1**. b. LogD_{7.4} calculated and predicted by Chemicalize.

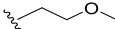
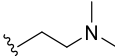
3.3.5 Attempts to improve solubility by addition of N-alkyl side chains

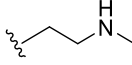
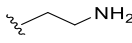
Since methyl groups and the xanthene rings are important for DOR PAM potency, I decided to introduce one last structural component by replacing the central ring oxygen atom of the C-rings with a nitrogen atom bearing basic N-alkyl side chains (**Table 3.6**). I postulated that the C-rings are pointing towards the outside of the cell membrane while binding to DOR, (**Figure 3.3** and **Chapter 2**) and are therefore mostly solvent-exposed (**Figure 3.3**). By introducing N-alkyl side chains, I hoped to improve the solubility while maintaining activity as DOR PAMs. I started with

the unsubstituted parent hexahydroacridine (**CCG366670**) and found that the solubility profile was significantly improved (14.0 $\mu\text{g/mL}$), but the compound was devoid of any DOR PAM activity. Simple methylation of the hexahydroacridine nitrogen, to give **CCG366671**, provided a low degree of DOR PAM activity ($\text{EC}_{50} = 5.41 \mu\text{M}$) and a 3-fold reduction in solubility (4.7 $\mu\text{g/mL}$) relative to **CCG366670**. Thus, I hoped to see further restoration of DOR PAM activity and solubility by extending the chain length of the nitrogen side chain. Both 2-(dimethylamino)ethyl (**CCG367088**) and 2-(methylamino)ethyl (**CCG369574**) hexahydroacridine derivatives were synthesized in an attempt to improve the solubility, especially **CCG369574**, which had $\text{LogD}_{7.4}$ of 3.2 and high solubility profile (197.7 $\mu\text{g/mL}$). However, no potency in the DOR PAM assay was gained compared to the N-Me analog. Further attempts with 2-(aminoethyl) (**CCG367212**) appendages provide no DOR PAM activity at the highest level tested, confirming that proton donors are strongly disfavored.

Table 3.6: N-Alkyl substitutions at C-rings to improve aqueous solubility



Compound	R	<u>β-Arrestin Recruitment</u> ^a		$\text{LogD}_{7.4}$ ^b	Solubility ^c ($\mu\text{g/mL}$)
		DOR EC_{50} (μM)/ E_{max}			
366670	H	>10/ N/A		5.7	14.0
366671	Me	5.41/73		6.0	4.7
367087		>10/ N/A		6.0	N/A
367088		>10/ N/A		4.8	9.1

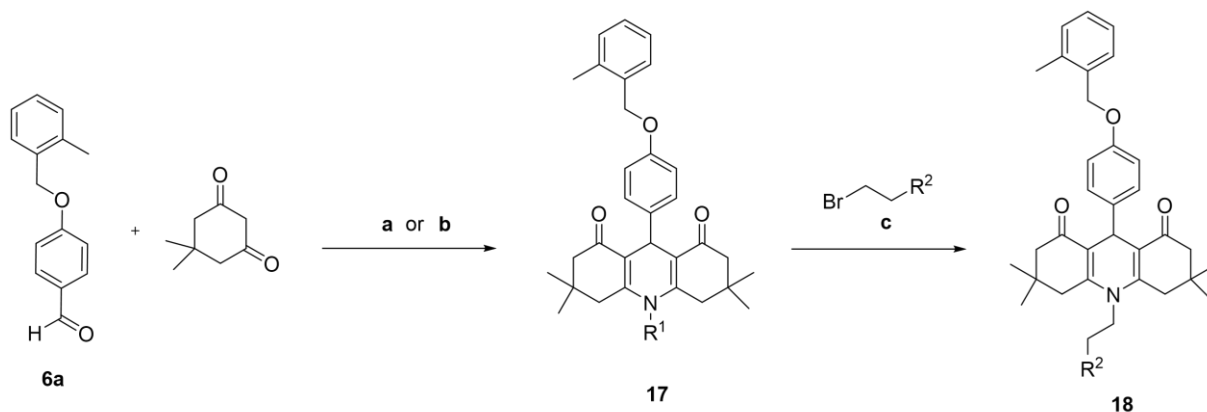
369574		>10/ N/A	3.2	197.7
367212		>10/ N/A	3.4	24.3

a. Same as **Table 2.1**. b-c. LogD_{7.4} are calculated and predicted by Chemicalize, and solubility data was obtained from Analiza

3.4 Synthesis of 1,8-dioxo-decahydroacridine derivatives

The synthesis of 1,8-dioxo-decahydroacridine derivatives on **Table 3.5** started with condensation of **6a** and dimedone in the presence of ammonium acetate or methyl amine hydrochloride to form

Scheme 3.1 Synthetic Routes for 1,8-dioxo-decahydroacridine derivatives



Reagents and Condition: (a) **3a**, NH₄OAc, TEA, 70% IPA, reflux, 16h (80%); (b) **3a**, AcOK, MeNH₂-HCl, IPA, reflux, 16h (49%); (c) **3a**, alkyl bromide, Cs₂CO₃, cat. KI, DMF, 90-150°C, 16h (4-50%).

Compound **17a** and **17b**, respectively (Kaushik et al., 2020; Kaya et al., 2015). **17a** was further substituted with desired bromides to form desired N-alkyl 1,8-dioxo-decahydroacridine derivatives **18** (**Scheme 3.1**).

3.5 Conclusion

Attempts to lower the lipophilicity of xanthene-dione series of DOR PAMs were carried out by incorporating bioisosteres, removing unnecessary lipophilicity, combining alterations to B- and C-rings, and adding N-alkyl side chains. While some success was realized in improving the solubility of targeted analogs, such as **CCG369831** and **CCG363177**, these changes were accompanied by

reduction or loss of DOR PAM activity. Further optimization aimed at reducing the lipophilicity and optimizing the metabolic stability of the xanthene series is required to obtain a compound with an adequate solubility profile for eventual *in vivo* studies. Overall, it is clearly very challenging to improve solubility and maintain potency as DOR PAMs at the same time, suggesting the allosteric site is highly lipophilic (Figure 3.3).

3.6 Experimentals

3.6.1 Cell culture and biological assays

As described in **Chapter 2**

3.6.2 Modeling

As described in **Chapter 2**

3.6.3 Solubility measurements

All the solubility data was obtained from Analiza, Inc.

3.6.4 Synthesis

9-(4-((3,5-dimethylisoxazol-4-yl)methoxy)phenyl)-3,3,6,6-tetramethyl-3,4,5,6,7,9-hexahydro-1H-xanthene-1,8(2H)-dione (CCG366161) [sz-09-96]

Following the general procedure on a scale of 70mg (0.19mmol) 9-(4-hydroxyphenyl)-3,3,6,6-tetramethyl-3,4,5,6,7,9-hexahydro-1H-xanthene-1,8(2H)-dione (**3**), 4-(chloromethyl)-3,5-dimethylisoxazole (33 mg, 29 μ L, 1.2 Eq, 0.23 mmol) was used and isolated 0.06g (61% yield) of the desired product. ¹H NMR (499 MHz, cdcl₃) δ 7.26 – 7.20 (m, 2H), 6.85 – 6.71 (m, 2H), 4.70 (d, J = 2.5 Hz, 3H), 2.47 (d, J = 1.7 Hz, 4H), 2.35 (s, 3H), 2.27 – 2.14 (m, 7H), 1.11 (s, 6H), 1.00 (s, 6H). ¹³C NMR (126 MHz, cdcl₃) δ 196.51, 167.46, 162.12, 159.81, 156.81, 137.36, 129.49, 115.66, 114.39, 110.39, 59.32, 50.77, 40.86, 32.20, 31.13, 29.26, 27.34, 11.06, 10.09. ESI MS m/z 498.22 (M + Na)⁺

3,3,6,6-tetramethyl-9-(4-(oxazol-2-ylmethoxy)phenyl)-3,4,5,6,7,9-hexahydro-1H-xanthene-1,8(2H)-dione (CCG366163) [sz-10-04]

Following the general procedure on a scale of 70mg (0.19mmol) 9-(4-hydroxyphenyl)-3,3,6,6-tetramethyl-3,4,5,6,7,9-hexahydro-1H-xanthene-1,8(2H)-dione (**3**), 2-(chloromethyl)-1,3-oxazole (22 mg, 17 μ L, 1 Eq, 0.19 mmol) was used and isolated 0.06g (69% yield) of the desired product. ¹H NMR (499 MHz, cdcl₃) δ 7.65 (d, J = 1.0 Hz, 1H), 7.23 – 7.15 (m, 2H), 7.11 (d, J = 0.9 Hz, 1H), 6.93 – 6.75 (m, 2H), 5.06 (s, 2H), 4.70 (s, 1H), 2.45 (s, 4H), 2.19 (q, J = 16.3 Hz, 4H), 1.09

(s, 6H), 0.98 (s, 6H). ¹³C NMR (126 MHz, cdcl₃) δ 196.43, 162.16, 159.87, 156.46, 139.64, 137.61, 129.45, 127.42, 115.65, 114.35, 62.23, 50.75, 40.84, 32.18, 30.98, 29.23, 27.34. ESI MS m/z 479.19 (M + Na)⁺

9-(4-((5-chlorothiophen-2-yl)methoxy)phenyl)-3,3,6,6-tetramethyl-3,4,5,6,7,9-hexahydro-1H-xanthene-1,8(2H)-dione (CCG366164) [sz-10-05]

Following the general procedure on a scale of 70mg (0.19mmol) 9-(4-hydroxyphenyl)-3,3,6,6-tetramethyl-3,4,5,6,7,9-hexahydro-1H-xanthene-1,8(2H)-dione (**3**), thiophene, 2-chloro-5-(chloromethyl)- (38 mg, 28 μL, 1.2 Eq, 0.23 mmol) was used and isolated 0.05g (57% yield) of the desired product. ¹H NMR (499 MHz, cdcl₃) δ 7.25 – 7.19 (m, 2H), 6.83 (d, J = 3.7 Hz, 1H), 6.82 – 6.80 (m, 2H), 6.79 (d, J = 3.7 Hz, 1H), 5.02 (s, 2H), 4.71 (s, 1H), 2.46 (s, 4H), 2.21 (q, J = 16.3 Hz, 4H), 1.11 (s, 6H), 1.00 (s, 6H). ¹³C NMR (126 MHz, cdcl₃) δ 196.42, 162.09, 156.60, 138.41, 137.34, 130.53, 129.42, 125.91, 125.68, 115.71, 114.47, 65.09, 50.76, 40.87, 32.20, 31.02, 29.26, 27.34. ESI MS m/z 519.13 (M + Na)⁺

9-(4-((3-isopropyl-1,2,4-oxadiazol-5-yl)methoxy)phenyl)-3,3,6,6-tetramethyl-3,4,5,6,7,9-hexahydro-1H-xanthene-1,8(2H)-dione (CCG366167) [msf-01-05-01]

Following the general procedure on a scale of 70mg (0.19mmol) 9-(4-hydroxyphenyl)-3,3,6,6-tetramethyl-3,4,5,6,7,9-hexahydro-1H-xanthene-1,8(2H)-dione (**3**), 5-(Chloromethyl)-3-(propan-2-yl)-1,2,4-oxadiazole (46 mg, 1.5 Eq, 0.29 mmol) was used and isolated 0.04g (43% yield) of the desired product. ¹H NMR (499 MHz, cdcl₃) δ 7.26 – 7.20 (m, 2H), 6.88-6.81 (m, 2H), 5.17 (d, J = 1.1Hz, 2H), 4.71 (s, 1H), 3.12 (pd, J = 6.9, 1.0 Hz, 1H), 2.46 (s, 4H), 2.23 (d, J = 16.3 Hz, 2H), 2.17 (d, J = 16.3 Hz, 2H), 1.34 (dd, J = 7.0, 1.0 Hz, 6H), 1.10 (s, 6H), 0.99 (s, 6H). ¹³C NMR (126 MHz, cdcl₃) δ 196.45, 175.17, 174.42, 162.22, 156.11, 138.17, 129.55, 115.60, 114.47, 61.22, 50.73, 40.85, 32.20, 31.03, 29.26, 27.30, 26.72, 20.39. ESI MS m/z 513.23 (M + Na)⁺

9-(4-((2-chlorothiazol-5-yl)methoxy)phenyl)-3,3,6,6-tetramethyl-3,4,5,6,7,9-hexahydro-1H-xanthene-1,8(2H)-dione (CCG366168) [msf-01-06-01]

Following the general procedure on a scale of 70mg (0.19mmol) 9-(4-hydroxyphenyl)-3,3,6,6-tetramethyl-3,4,5,6,7,9-hexahydro-1H-xanthene-1,8(2H)-dione (**3**), 2-chloro-5-(chloromethyl)thiazole (48 mg, 1.5 Eq, 0.29 mmol) was used and isolated 0.03g (32% yield) of the desired product. ¹H NMR (499 MHz, cdcl₃) δ 7.48 (d, J = 1.1 Hz, 2H), 7.26-7.19 (m, 2H), 6.82-6.76 (m, 2H), 5.07 (s, 2H), 4.70 (s, 1H), 2.51-2.44 (m, 4H), 2.32-2.07 (m, 4H), 1.10 (s, 6H), 0.99 (s, 6H). ¹³C NMR (126 MHz, cdcl₃) δ 196.46, 162.21, 156.19, 152.54, 139.77, 137.82,

136.72, 129.55, 115.60, 114.46, 62.55, 50.75, 40.84, 32.19, 31.07, 29.26, 27.31. ESI MS m/z 520.13 (M + Na)+

3,3,6,6-tetramethyl-9-(4-((2-methylpyridin-3-yl)methoxy)phenyl)-3,4,5,6,7,9-hexahydro-1H-xanthene-1,8(2H)-dione (CCG367266) [sz-11-60]

Following the general procedure on a scale of 90mg (0.25 mmol) 9-(4-hydroxyphenyl)-3,3,6,6-tetramethyl-3,4,5,6,7,9-hexahydro-1H-xanthene-1,8(2H)-dione (**3**), 3-(chloromethyl)-2-methylpyridine (38 mg, 1.1 Eq, 0.27 mmol) was used and isolated 0.1g (88% yield) of the desired product. ¹H NMR (499 MHz, cdcl₃) δ 8.42 (dd, J = 5.0, 1.7 Hz, 1H), 7.66 (dd, J = 7.7, 1.7 Hz, 1H), 7.25 – 7.16 (m, 2H), 7.11 (dd, J = 7.7, 4.9 Hz, 1H), 6.90 – 6.76 (m, 2H), 4.93 (s, 2H), 4.70 (s, 1H), 2.54 (s, 3H), 2.45 (s, 4H), 2.28 – 2.07 (m, 4H), 1.08 (s, 6H), 0.98 (s, 6H). ¹³C NMR (126 MHz, cdcl₃) δ 196.45, 162.14, 156.97, 156.71, 148.42, 137.25, 135.85, 130.53, 129.45, 121.22, 115.67, 114.30, 67.38, 50.76, 40.83, 32.17, 31.04, 29.25, 27.33, 21.96. ESI MS m/z 472.24 (M + H)+

3,3,6,6-tetramethyl-9-(4-((3-methylpyridin-2-yl)methoxy)phenyl)-3,4,5,6,7,9-hexahydro-1H-xanthene-1,8(2H)-dione (CCG367310) [sz-11-63]

Following the general procedure on a scale of 250mg (0.68 mmol) 9-(4-hydroxyphenyl)-3,3,6,6-tetramethyl-3,4,5,6,7,9-hexahydro-1H-xanthene-1,8(2H)-dione (**3**), 2-(chloromethyl)-3-methylpyridine (100 mg, 1.04 Eq, 706 μmol) was used and isolated 0.1g (43% yield) of the desired product. ¹H NMR (499 MHz, cdcl₃) δ 8.41 (dd, J = 4.8, 1.6 Hz, 1H), 7.48 (dd, J = 7.8, 1.7 Hz, 1H), 7.22 – 7.17 (m, 2H), 7.15 (dd, J = 7.6, 4.8 Hz, 1H), 6.99 – 6.75 (m, 2H), 5.11 (s, 2H), 4.70 (s, 1H), 2.45 (s, 4H), 2.38 (s, 3H), 2.26 – 2.13 (m, 4H), 1.09 (s, 6H), 0.99 (s, 6H). ¹³C NMR (126 MHz, cdcl₃) δ 196.45, 162.08, 157.27, 154.53, 146.51, 138.32, 136.81, 133.32, 129.26, 123.32, 115.79, 114.40, 70.87, 50.77, 40.86, 32.18, 30.91, 29.24, 27.36, 18.20. ESI MS m/z 472.24 (M + H)+

9-(4-((3-chloropyridin-2-yl)methoxy)phenyl)-3,3,6,6-tetramethyl-3,4,5,6,7,9-hexahydro-1H-xanthene-1,8(2H)-dione (CCG369575) [sz-11-96]

Following the general procedure on a scale of 140mg (0.38 mmol) 9-(4-hydroxyphenyl)-3,3,6,6-tetramethyl-3,4,5,6,7,9-hexahydro-1H-xanthene-1,8(2H)-dione (**3**), 3-chloro-2-(chloromethyl)pyridine (74.3 mg, 1.2 Eq, 458 μmol) was used and isolated 0.1g (43% yield) of the desired product. ¹H NMR (400 MHz, cdcl₃) δ 8.52 (d, J = 4.8 Hz, 1H), 7.75 – 7.67 (m, 1H), 7.25 – 7.22 (m, 1H), 7.20 (d, J = 8.9 Hz, 2H), 6.88 (d, J = 8.6 Hz, 2H), 5.21 (s, 2H), 4.70 (s, 1H), 2.45

(s, 4H), 2.27 – 2.13 (m, 4H), 1.09 (s, 6H), 0.99 (s, 6H). ¹³C NMR (101 MHz, cdcl₃) δ 196.50, 162.11, 157.13, 153.34, 147.48, 137.37, 136.99, 131.67, 129.26, 124.18, 115.74, 114.53, 68.82, 50.74, 40.83, 32.20, 30.90, 29.26, 27.33. ESI MS m/z 514.17 (M + Na)⁺

9-(4-((3-methoxy)pyridin-2-yl)methoxy)phenyl)-3,3,6,6-tetramethyl-3,4,5,6,7,9-hexahydro-1H-xanthene-1,8(2H)-dione (CCG369577) [sz-12-01]

Following the general procedure on a scale of 140mg (0.38 mmol) 9-(4-hydroxyphenyl)-3,3,6,6-tetramethyl-3,4,5,6,7,9-hexahydro-1H-xanthene-1,8(2H)-dione (**3**), 2-(chloromethyl)-3-methoxy-pyridine (72.3 mg, 1.2 Eq, 458 μmol) was used and isolated 0.03g (16% yield) of the desired product. ¹H NMR (499 MHz, cdcl₃) δ 8.21 (dd, J = 4.5, 1.4 Hz, 1H), 7.22 (dd, J = 8.3, 4.5 Hz, 1H), 7.19 (d, J = 1.5 Hz, 1H), 7.19 – 7.15 (m, 2H), 6.96 – 6.83 (m, 2H), 5.13 (s, 2H), 4.69 (s, 1H), 3.84 (s, 3H), 2.44 (s, 4H), 2.27 – 2.11 (m, 4H), 1.09 (s, 6H), 0.98 (s, 6H). ¹³C NMR (126 MHz, cdcl₃) δ 196.42, 162.01, 157.56, 154.19, 145.88, 141.03, 136.51, 129.12, 123.94, 117.72, 115.84, 114.58, 66.75, 55.46, 50.77, 40.86, 32.18, 30.85, 29.24, 27.33. ESI MS m/z 510.22 (M + Na)⁺

9-(4-((3-chlorothiophen-2-yl)methoxy)phenyl)-3,3,6,6-tetramethyl-3,4,5,6,7,9-hexahydro-1H-xanthene-1,8(2H)-dione (CCG369576) [sz-11-97]

Following the general procedure on a scale of 140mg (0.38 mmol) 9-(4-hydroxyphenyl)-3,3,6,6-tetramethyl-3,4,5,6,7,9-hexahydro-1H-xanthene-1,8(2H)-dione (**3**), 3-chloro-2-(chloromethyl)thiophene (76.6 mg, 1.2 Eq, 458 μmol) (**16h**) was used and isolated 0.09g (43% yield) of the desired product. ¹H NMR (400 MHz, cdcl₃) δ 7.29 – 7.25 (m, 1H), 7.22 (dd, J = 8.0, 1.3 Hz, 2H), 6.90 (dd, J = 5.4, 0.9 Hz, 1H), 6.84 (dd, J = 8.3, 1.3 Hz, 2H), 5.10 (d, J = 0.8 Hz, 2H), 4.70 (s, 1H), 2.45 (s, 4H), 2.28 – 2.09 (m, 4H), 1.10 (s, 6H), 0.99 (s, 6H). ¹³C NMR (101 MHz, cdcl₃) δ 196.49, 162.11, 156.61, 137.29, 132.31, 129.41, 127.51, 125.30, 123.90, 115.70, 114.43, 62.65, 50.74, 40.84, 32.20, 31.01, 29.27, 27.35. ESI MS m/z 519.13 (M + Na)⁺

3,3,6,6-tetramethyl-9-(4-((5-methylthiazol-4-yl)methoxy)phenyl)-3,4,5,6,7,9-hexahydro-1H-xanthene-1,8(2H)-dione (CCG369578) [sz-12-03]

Following the general procedure on a scale of 100mg (0.27mmol) 9-(4-hydroxyphenyl)-3,3,6,6-tetramethyl-3,4,5,6,7,9-hexahydro-1H-xanthene-1,8(2H)-dione (**3**), 4-(Chloromethyl)-5-methylthiazole hydrochloride (60.3 mg, 1.2 Eq, 327 μmol) was used and isolated 0.1g (77% yield) of the desired product. ¹H NMR (400 MHz, cdcl₃) δ 8.56 (s, 1H), 6.94 – 6.72 (m, 2H), 5.06 (s, 2H), 4.69 (s, 1H), 2.47 (s, 3H), 2.44 (s, 4H), 2.26 – 2.09 (m, 4H), 1.08 (s, 6H), 0.98 (s, 6H). ¹³C

NMR (101 MHz, cdcl₃) δ 196.50, 162.10, 157.09, 149.54, 148.11, 136.88, 132.39, 129.32, 115.74, 114.38, 63.87, 50.75, 40.83, 32.20, 30.97, 29.27, 27.33, 11.18. ESI MS m/z 500.18 (M + Na)⁺
3,3,6,6-tetramethyl-9-(4-((1-methyl-1H-imidazol-5-yl)methoxy)phenyl)-3,4,5,6,7,9-hexahydro-1H-xanthene-1,8(2H)-dione (CCG369579) [sz-12-04]

Following the general procedure on a scale of 100mg (0.27mmol) 9-(4-hydroxyphenyl)-3,3,6,6-tetramethyl-3,4,5,6,7,9-hexahydro-1H-xanthene-1,8(2H)-dione (**3**), 5-(Chloromethyl)-1-methyl-1H-imidazole HCl (54.7 mg, 1.2 Eq, 327 μ mol) was used and isolated 0.08g (60% yield) of the desired product. 1H NMR (400 MHz, cdcl₃) δ 7.42 (s, 1H), 7.24 – 7.16 (m, 2H), 7.03 (d, J = 1.1 Hz, 1H), 6.84 – 6.73 (m, 2H), 4.88 (s, 2H), 4.67 (s, 1H), 3.61 (s, 3H), 2.44 (s, 4H), 2.27 – 2.07 (m, 4H), 1.07 (s, 6H), 0.97 (s, 6H). 13C NMR (101 MHz, cdcl₃) δ 196.54, 162.17, 156.54, 139.42, 137.35, 130.17, 129.46, 127.12, 115.61, 114.23, 59.43, 50.74, 40.80, 32.18, 31.68, 31.06, 29.24, 27.33. ESI MS m/z 483.22 (M + Na)⁺

3,3,6,6-tetramethyl-9-(4-((1-methyl-1H-imidazol-2-yl)methoxy)phenyl)-3,4,5,6,7,9-hexahydro-1H-xanthene-1,8(2H)-dione (CCG369751) [sz-12-76]

Following the general procedure on a scale of 100mg (0.27mmol) 9-(4-hydroxyphenyl)-3,3,6,6-tetramethyl-3,4,5,6,7,9-hexahydro-1H-xanthene-1,8(2H)-dione (**3**), 2-Chloromethyl-1-methyl-1H-imidazole HCl (54.7 mg, 1.2 Eq, 327 μ mol) was used and isolated 0.01g (10% yield) of the desired product. 1H NMR (400 MHz, cdcl₃) δ 7.23 – 7.17 (m, 2H), 6.98 (s, 1H), 6.90 – 6.84 (m, 3H), 5.06 (s, 2H), 4.69 (s, 1H), 3.68 (s, 3H), 2.45 (s, 4H), 2.34 – 2.08 (m, 4H), 1.09 (s, 6H), 0.99 (s, 6H). 13C NMR (101 MHz, cdcl₃) δ 196.55, 162.12, 156.56, 143.48, 137.31, 129.43, 127.59, 122.29, 115.69, 114.33, 62.45, 50.75, 40.84, 32.20, 31.03, 29.22, 27.40.

9-(4-((5-chloro-3-methoxypyridin-2-yl)methoxy)phenyl)-3,3,6,6-tetramethyl-3,4,5,6,7,9-hexahydro-1H-xanthene-1,8(2H)-dione (CCG369590) [sz-12-15]

Following the general procedure on a scale of 70mg (0.19mmol) 9-(4-hydroxyphenyl)-3,3,6,6-tetramethyl-3,4,5,6,7,9-hexahydro-1H-xanthene-1,8(2H)-dione (**3**), 5-chloro-2-(chloromethyl)-3-methoxypyridine (40 mg, 1.1 Eq, 0.21 mmol) (**16i**) was used and isolated 0.04g (42% yield) of the desired product. 1H NMR (499 MHz, cdcl₃) δ 8.28 (s, 1H), 8.20 (s, 1H), 7.21 (d, J = 8.4 Hz, 2H), 6.84 (d, J = 8.2 Hz, 2H), 5.07 (s, 2H), 4.70 (s, 1H), 3.91 (s, 3H), 2.45 (s, 4H), 2.19 (q, J = 16.3 Hz, 4H), 1.09 (s, 6H), 0.99 (s, 6H). 13C NMR (126 MHz, cdcl₃) δ 196.50, 162.09, 157.15, 154.64,

142.40, 137.12, 133.25, 132.05, 130.69, 129.34, 115.70, 114.37, 60.56, 56.83, 50.77, 40.85, 32.19, 31.07, 29.22, 27.39. ESI MS m/z 544.18 (M + Na)⁺

9-(4-((5-chloropyridin-2-yl)methoxy)phenyl)-3,3,6,6-tetramethyl-3,4,5,6,7,9-hexahydro-1H-xanthene-1,8(2H)-dione (CCG369591) [sz-12-17]

Following the general procedure on a scale of 100mg (0.27mmol) 9-(4-hydroxyphenyl)-3,3,6,6-tetramethyl-3,4,5,6,7,9-hexahydro-1H-xanthene-1,8(2H)-dione (**3**), 5-chloro-2-(chloromethyl)pyridine (53.1 mg, 1.2 Eq, 327 μ mol) was used and isolated 0.11g (83% yield) of the desired product. ¹H NMR (499 MHz, $cdCl_3$) δ 8.52 (d, J = 2.4 Hz, 1H), 7.66 (dd, J = 8.4, 2.5 Hz, 1H), 7.45 (d, J = 8.4 Hz, 1H), 7.23 – 7.13 (m, 2H), 6.88 – 6.73 (m, 2H), 5.09 (s, 2H), 4.69 (s, 1H), 2.45 (s, 4H), 2.19 (q, J = 16.3 Hz, 4H), 1.09 (s, 6H), 0.98 (s, 6H). ¹³C NMR (126 MHz, $cdCl_3$) δ 196.42, 162.09, 156.62, 155.77, 147.95, 137.25, 136.48, 130.73, 129.45, 122.08, 115.71, 114.32, 69.91, 50.75, 40.85, 32.18, 30.98, 29.23, 27.34. ESI MS m/z 514.17 (M + Na)⁺

9-(4-((3,5-dimethylpyridin-2-yl)methoxy)phenyl)-3,3,6,6-tetramethyl-3,4,5,6,7,9-hexahydro-1H-xanthene-1,8(2H)-dione (CCG369653) [sz-12-36]

Following the general procedure on a scale of 70mg (0.19mmol) 9-(4-hydroxyphenyl)-3,3,6,6-tetramethyl-3,4,5,6,7,9-hexahydro-1H-xanthene-1,8(2H)-dione (**3**), 2-(chloromethyl)-3,5-dimethylpyridine HCl (40 mg, 1.1 Eq, 0.21 mmol) was used and isolated 0.05g (54% yield) of the desired product. ¹H NMR (499 MHz, $cdCl_3$) δ 8.22 (d, J = 2.1 Hz, 1H), 7.28 (d, J = 2.1 Hz, 1H), 7.21 – 7.12 (m, 2H), 6.89 – 6.78 (m, 2H), 5.06 (s, 2H), 4.69 (s, 1H), 2.44 (s, 4H), 2.28 (s, 3H), 2.25 – 2.11 (m, 4H), 1.08 (s, 6H), 0.98 (s, 6H). ¹³C NMR (126 MHz, $cdCl_3$) δ 196.44, 162.05, 157.31, 151.62, 146.83, 139.02, 136.67, 132.88, 132.71, 129.21, 115.79, 114.39, 70.59, 50.76, 40.85, 32.17, 30.88, 29.22, 27.35, 18.04, 17.99. ESI MS m/z 508.24 (M + Na)⁺

9-(4-((2,6-dimethylpyridin-3-yl)methoxy)phenyl)-3,3,6,6-tetramethyl-3,4,5,6,7,9-hexahydro-1H-xanthene-1,8(2H)-dione (CCG369656) [sz-12-52]

Following the general procedure on a scale of 70mg (0.19mmol) 9-(4-hydroxyphenyl)-3,3,6,6-tetramethyl-3,4,5,6,7,9-hexahydro-1H-xanthene-1,8(2H)-dione (**3**), 3-(chloromethyl)-2,6-dimethylpyridine (36 mg, 1.2 Eq, 0.23 mmol) (**16j**) was used and isolated 0.04g (43% yield) of the desired product. ¹H NMR (400 MHz, $cdCl_3$) δ 7.54 (d, J = 7.8 Hz, 1H), 7.24 – 7.18 (m, 2H), 6.98 (d, J = 7.8 Hz, 1H), 6.85 – 6.77 (m, 2H), 4.91 (s, 2H), 4.70 (s, 1H), 2.51 (d, J = 1.8 Hz, 6H), 2.45 (s, 4H), 2.28 – 2.11 (m, 4H), 1.09 (s, 6H), 0.99 (s, 6H). ¹³C NMR (101 MHz, $cdCl_3$) δ 196.54,

162.12, 157.19, 157.06, 156.16, 137.07, 136.64, 129.41, 127.29, 120.69, 115.69, 114.27, 67.39, 50.75, 40.84, 32.20, 31.03, 29.27, 27.35, 24.22, 21.90. ESI MS m/z 508.24 (M + Na)⁺

9-(4-((2-methoxy-6-methylpyridin-3-yl)methoxy)phenyl)-3,3,6,6-tetramethyl-3,4,5,6,7,9-hexahydro-1H-xanthene-1,8(2H)-dione (CCG369731) [sz-12-64]

Following the general procedure on a scale of 70mg (0.19mmol) 9-(4-hydroxyphenyl)-3,3,6,6-tetramethyl-3,4,5,6,7,9-hexahydro-1H-xanthene-1,8(2H)-dione (**3**), 3-(chloromethyl)-2-methoxy-6-methylpyridine (39 mg, 1.2 Eq, 0.23 mmol) (**16k**) was used and isolated 0.04g (42% yield) of the desired product. ¹H NMR (499 MHz, cdcl₃) δ 7.54 (d, J = 7.3 Hz, 1H), 7.22 – 7.15 (m, 2H), 6.85 – 6.79 (m, 2H), 6.70 (d, J = 7.4 Hz, 1H), 4.93 (s, 2H), 4.70 (s, 1H), 3.94 (s, 3H), 2.45 (s, 4H), 2.43 (s, 3H), 2.19 (q, J = 16.3 Hz, 4H), 1.09 (s, 6H), 0.99 (s, 6H). ¹³C NMR (126 MHz, cdcl₃) δ 196.41, 162.03, 160.36, 157.20, 155.24, 137.22, 136.72, 129.31, 116.40, 115.78, 115.68, 114.34, 64.38, 53.14, 50.76, 40.86, 32.18, 30.95, 29.24, 27.35, 23.90.

9-(4-((3-cyclopropylpyridin-2-yl)methoxy)phenyl)-3,3,6,6-tetramethyl-3,4,5,6,7,9-hexahydro-1H-xanthene-1,8(2H)-dione (CCG369654) [sz-12-45]

Following the general procedure on a scale of 70mg (0.19mmol) 9-(4-hydroxyphenyl)-3,3,6,6-tetramethyl-3,4,5,6,7,9-hexahydro-1H-xanthene-1,8(2H)-dione (**3**), 2-(chloromethyl)-3-cyclopropylpyridine (38 mg, 1.2 Eq, 0.23 mmol) (**16l**) was used and isolated 0.04g (45% yield) of the desired product. ¹H NMR (499 MHz, cdcl₃) δ 8.39 (dt, J = 4.8, 1.3 Hz, 1H), 7.28 (dd, J = 8.0, 1.6 Hz, 1H), 7.21 – 7.17 (m, 2H), 7.15 (dd, J = 7.9, 4.8 Hz, 1H), 6.94 – 6.82 (m, 2H), 5.25 (s, 2H), 4.70 (s, 1H), 2.44 (s, 4H), 2.26 – 2.14 (m, 4H), 1.09 (s, 6H), 0.99 (s, 6H). ¹³C NMR (126 MHz, cdcl₃) δ 196.45, 162.05, 157.41, 155.39, 146.12, 138.48, 136.72, 133.24, 129.22, 123.29, 115.81, 114.45, 70.39, 50.77, 40.86, 32.18, 30.89, 29.23, 27.35, 11.46, 7.58. ESI MS m/z 520.24 (M + Na)⁺

9-(4-((2-(azetidin-1-yl)benzyl)oxy)phenyl)-3,3,6,6-tetramethyl-3,4,5,6,7,9-hexahydro-1H-xanthene-1,8(2H)-dione (CCG369795) [sz-12-89]

Following the general procedure on a scale of 40mg (0.11mmol) 9-(4-hydroxyphenyl)-3,3,6,6-tetramethyl-3,4,5,6,7,9-hexahydro-1H-xanthene-1,8(2H)-dione (**3**), 1-(2-(bromomethyl)phenyl)azetidine (27 mg, 1.1 Eq, 0.12 mmol) (**15c**) was used. The reaction mixture was heated in pressure vessel for 16h. Desired compound was isolated 0.004g (7% yield). ¹H NMR (400 MHz, cdcl₃) δ 7.13 (d, J = 8.5 Hz, 2H), 7.05 (t, J = 7.1 Hz, 2H), 6.83 (d, J = 8.3 Hz, 1H), 6.64 (t, J = 7.3 Hz, 1H), 6.57 (d, J = 8.6 Hz, 2H), 4.68 (s, 1H), 4.32 (s, 2H), 3.58 (t, J = 6.0 Hz, 2H),

3.29 (s, 2H), 2.44 (s, 4H), 2.22 (d, J = 16.3 Hz, 2H), 2.15 (d, J = 16.3 Hz, 2H), 1.83 (q, J = 6.5 Hz, 2H), 1.09 (s, 6H), 0.98 (s, 6H). ¹³C NMR (126 MHz, cdcl₃) δ 196.33, 161.95, 157.26, 155.06, 136.23, 131.71, 129.13, 127.99, 118.10, 115.93, 115.85, 113.96, 65.06, 50.76, 48.09, 40.85, 32.16, 30.86, 29.27, 27.44, 27.30, 14.18. ESI MS m/z 512.27 (M + H)⁺

9-(4-((3-(dimethylamino)pyridin-2-yl)methoxy)phenyl)-3,3,6,6-tetramethyl-3,4,5,6,7,9-hexahydro-1H-xanthene-1,8(2H)-dione (CCG369831) [sz-13-07]

Following the general procedure on a scale of 150mg (0.41mmol) 9-(4-hydroxyphenyl)-3,3,6,6-tetramethyl-3,4,5,6,7,9-hexahydro-1H-xanthene-1,8(2H)-dione (**3**), 2-(bromomethyl)-N,N-dimethylpyridin-3-amine (97 mg, 1.1 Eq, 0.45 mmol) (**15b**) was used. The reaction mixture was heated in pressure vessel for 16h. Desired compound was isolated 0.02g (10% yield). ¹H NMR (499 MHz, cdcl₃) δ 8.31 (dt, J = 4.5, 1.2 Hz, 1H), 7.38 (dt, J = 8.2, 1.2 Hz, 1H), 7.21 – 7.11 (m, 3H), 6.95 – 6.80 (m, 2H), 5.14 (s, 2H), 4.70 (s, 1H), 2.74 (d, J = 0.9 Hz, 6H), 2.44 (s, 4H), 2.27 – 2.11 (m, 4H), 1.09 (s, 6H), 0.98 (s, 6H). ¹³C NMR (126 MHz, cdcl₃) δ 196.45, 162.04, 157.48, 150.54, 149.34, 143.45, 136.50, 129.10, 126.38, 123.42, 115.85, 114.48, 67.50, 50.76, 44.87, 40.86, 32.19, 30.81, 29.27, 27.29. ESI MS m/z 501.27 (M + H)⁺

9-(4-((3-(azetidin-1-yl)pyridin-2-yl)methoxy)phenyl)-3,3,6,6-tetramethyl-3,4,5,6,7,9-hexahydro-1H-xanthene-1,8(2H)-dione (CCG369853) [sz-13-08]

Following the general procedure on a scale of 75mg (0.2mmol) 9-(4-hydroxyphenyl)-3,3,6,6-tetramethyl-3,4,5,6,7,9-hexahydro-1H-xanthene-1,8(2H)-dione (**3**), 3-(azetidin-1-yl)-2-(bromomethyl)pyridine (51 mg, 1.1 Eq, 0.23 mmol) (**15d**) was used. The reaction mixture was heated in pressure vessel for 16h. Desired compound was isolated 0.003g (3% yield). ¹H NMR (400 MHz, cdcl₃) δ 7.87 – 7.81 (m, 1H), 7.24 – 7.17 (m, 2H), 7.03 (dd, J = 8.1, 4.8 Hz, 1H), 6.84 (d, J = 8.1 Hz, 1H), 6.76 (d, J = 8.6 Hz, 2H), 4.69 (s, 1H), 4.06 (t, J = 5.5 Hz, 2H), 3.32 (s, 2H), 2.45 (s, 4H), 2.38 (s, 2H), 2.23 (d, J = 16.3 Hz, 2H), 2.18 (s, 2H), 2.12 (dd, J = 10.7, 4.9 Hz, 2H), 1.10 (s, 6H), 0.99 (s, 6H). ¹³C NMR (126 MHz, cdcl₃) δ 196.45, 162.07, 156.95, 143.63, 142.27, 136.90, 136.69, 129.45, 122.08, 115.71, 115.33, 113.89, 66.45, 50.75, 41.58, 40.85, 32.18, 31.02, 29.26, 28.66, 27.30, 20.33. ESI MS m/z 535.26 (M + Na)⁺

9-(6-hydroxypyridin-3-yl)-3,3,6,6-tetramethyl-3,4,5,6,7,9-hexahydro-1H-xanthene-1,8(2H)-dione (3bg) [sz-08-21]

To a solution of 6-hydroxynicotinaldehyde (80 mg, 1 Eq, 0.65 mmol) and 5,5-dimethylcyclohexane-1,3-dione (0.18 g, 2.01 Eq, 1.3 mmol) in 70% IPA (2mL) was treated with

H₂SO₄ (13 mg, 6.9 μL, 0.2 Eq, 0.13 mmol). The reaction mixture was refluxed at 120°C for 16 h and cooled to room temperature. Precipitates formed overnight. The solids were filtered and washed with cold 70% IPA. Solids formed (0.12g, 61% yield). ¹H NMR (499 MHz, dmsO) δ 11.35 (s, 1H), 7.17 (dd, J = 9.5, 2.7 Hz, 1H), 7.03 (d, J = 2.8 Hz, 1H), 6.20 (d, J = 9.4 Hz, 1H), 4.23 (s, 1H), 2.51 (d, J = 2.9 Hz, 4H), 2.25 (d, J = 16.1 Hz, 2H), 2.12 (d, J = 16.1 Hz, 2H), 1.02 (s, 6H), 0.92 (s, 6H).

9-(6-hydroxypyridin-3-yl)-3,4,5,6,7,9-hexahydro-1H-xanthene-1,8(2H)-dione (3bh) [sz-08-22]

To a solution of 6-hydroxynicotinaldehyde (80 mg, 1 Eq, 0.65 mmol) and cyclohexane-1,3-dione (0.15 g, 2.00 Eq, 1.3 mmol) in 70% IPA (2mL) was treated with H₂SO₄ (13 mg, 6.9 μL, 0.2 Eq, 0.13 mmol). The reaction mixture was refluxed at 120°C for 16 h and cooled to room temperature. Precipitates formed overnight. The solids were filtered and washed with cold 70% IPA. Solids formed (0.16g, 77% yield). ¹H NMR (499 MHz, dmsO) δ 7.23 (dd, J = 9.4, 2.7 Hz, 1H), 7.04 (s, 1H), 6.19 (d, J = 9.5 Hz, 1H), 4.28 (s, 1H), 2.68 – 2.51 (m, 4H), 2.28 (dd, J = 8.2, 5.3 Hz, 4H), 2.04 – 1.71 (m, 4H).

9-(5-hydroxypyridin-2-yl)-3,4,5,6,7,9-hexahydro-1H-xanthene-1,8(2H)-dione (3bi) [sz-08-23]

To a solution of 5-hydroxypicolinaldehyde (80 mg, 1 Eq, 0.65 mmol) and cyclohexane-1,3-dione (0.15 g, 2.01 Eq, 1.3 mmol) in 70% IPA (2mL) was treated with H₂SO₄ (13 mg, 6.9 μL, 0.2 Eq, 0.13 mmol). The reaction mixture was refluxed at 120°C for 16 h and cooled to room temperature. Precipitates formed overnight. The solids were filtered and washed with cold 70% IPA. Solids formed (0.08g, 41% yield). ¹H NMR (499 MHz, cd₃od) δ 7.96 – 7.84 (m, 1H), 7.38 (dt, J = 8.4, 2.0 Hz, 1H), 7.15 – 7.01 (m, 1H), 4.52 (s, 1H), 2.70 – 2.58 (m, 4H), 2.42 – 2.24 (m, 4H), 2.11 – 1.90 (m, 4H).

3,6-diethyl-9-(4-hydroxyphenyl)-3,4,5,6,7,9-hexahydro-1H-xanthene-1,8(2H)-dione (3bj) [sz-09-99]

To a solution of 4-hydroxybenzaldehyde (100 mg, 1 Eq, 819 μmol) and 5,5-dimethylcyclohexane-1,3-dione (375 mg, 2.01 Eq, 2.68 mmol) in 70% IPA (4mL) was treated with H₂SO₄ (16.1 mg, 8.73 μL, 0.2 Eq, 164 μmol). The reaction mixture was refluxed at 120°C for 16 h and cooled to room temperature. Precipitates formed overnight. The solids were filtered and washed with cold 70% IPA (0.25g, 83% yield). ¹H NMR (499 MHz, cdCl₃) δ 7.12 – 7.04 (m, 2H), 6.60 (ddd, J = 11.0, 5.4, 3.1 Hz, 2H), 4.70 (t, J = 8.0 Hz, 1H), 2.68 (dd, J = 17.4, 3.8 Hz, 1H), 2.60 (dd, J = 17.4,

3.5 Hz, 1H), 2.53 – 2.23 (m, 4H), 2.08 (dd, J = 9.3, 5.9 Hz, 2H), 2.02 (dd, J = 9.7, 5.9 Hz, 2H), 1.42 (dq, J = 10.0, 5.3, 3.5 Hz, 4H), 0.96 – 0.89 (m, 6H).

9-(4-hydroxyphenyl)-3,6-bis(trifluoromethyl)-3,4,5,6,7,9-hexahydro-1H-xanthene-1,8(2H)-dione (3bk) [sz-10-06]

To a solution of 4-hydroxybenzaldehyde (85 mg, 1 Eq, 0.70 mmol) and 5-(trifluoromethyl)cyclohexane-1,3-dione (0.25 g, 2.01 Eq, 1.4 mmol) in 70% IPA (3mL) was treated with H₂SO₄ (14 mg, 7.4 μL, 0.2 Eq, 0.14 mmol). The reaction mixture was refluxed at 120°C for 16 h, cooled to room temperature and concentrated under reduced pressure. The crude material was chromatographed over silica gel, eluted with 0-50% EtOAc/Hex. Compound was isolated as solids (0.3g, 97% yield). ¹H NMR (400 MHz, cdcl₃) δ 7.10 (d, J = 8.2 Hz, 2H), 6.68 (dd, J = 8.5, 2.6 Hz, 2H), 4.72 (t, J = 11.3 Hz, 1H), 2.87 (dd, J = 17.1, 6.2 Hz, 4H), 2.81 – 2.57 (m, 4H), 2.41 (dd, J = 16.5, 13.3 Hz, 2H). ¹⁹F NMR (376 MHz, cdcl₃) δ -73.56 – -73.71 (m).

9-(4-hydroxyphenyl)-3,6-diisobutyl-3,4,5,6,7,9-hexahydro-1H-xanthene-1,8(2H)-dione (3bl) [sz-10-07]

To a solution of 4-hydroxybenzaldehyde (100 mg, 1 Eq, 819 μmol) and 1,3-Dioxo-5-isobutylcyclohexane (277 mg, 2.01 Eq, 1.65 mmol) in 70% IPA (2mL) was treated with H₂SO₄ (16.1 mg, 8.73 μL, 0.2 Eq, 164 μmol). The reaction mixture was refluxed at 120°C for 16 h and cooled to room temperature. Precipitates formed overnight. The solids were filtered and washed with cold 70% IPA (0.2g, 61% yield). ¹H NMR (400 MHz, cdcl₃) δ 9.58 (s, 1H), 7.18 – 7.00 (m, 2H), 6.61 (td, J = 7.3, 6.5, 2.1 Hz, 2H), 4.69 (t, J = 5.3 Hz, 1H), 2.60 (ddd, J = 28.7, 16.9, 4.3 Hz, 2H), 2.50 – 2.33 (m, 3H), 2.33 – 2.09 (m, 3H), 2.08 – 1.93 (m, 2H), 1.64 (dp, J = 13.5, 6.8 Hz, 2H), 1.26 – 1.20 (m, 4H), 0.90 – 0.85 (m, 12H).

9-(4-hydroxyphenyl)-3,6-dimethyl-3,4,5,6,7,9-hexahydro-1H-xanthene-1,8(2H)-dione (3bm) [sz-10-33]

To a solution of 4-hydroxybenzaldehyde (220 mg, 1 Eq, 1.80 mmol) and 5-methylcyclohexane-1,3-dione (457 mg, 2.01 Eq, 3.62 mmol) in 70% 2-propanol (7mL) was treated with H₂SO₄ (35.3 mg, 19.2 μL, 0.2 Eq, 360 μmol). The reaction mixture was refluxed at 120°C for 16 h and cooled to room temperature. Precipitates formed overnight. The solids were filtered and washed with cold 70% IPA (0.3g, 51% yield). ¹H NMR (499 MHz, cdcl₃) δ 7.17 – 7.07 (m, 2H), 6.62 (d, J = 8.0

Hz, 2H), 4.71 (t, J = 7.3 Hz, 1H), 2.73 – 2.51 (m, 2H), 2.43 (tdd, J = 16.8, 10.4, 6.6 Hz, 3H), 2.37 – 2.15 (m, 3H), 2.12 – 1.99 (m, 2H), 1.15 – 1.02 (m, 6H).

3-acetyl-4-(4-hydroxyphenyl)-2,7,7-trimethyl-4,6,7,8-tetrahydro-5H-chromen-5-one (3bn) [sz-08-85]

To a solution of 4-hydroxybenzaldehyde (500 mg, 1 Eq, 4.09 mmol) in 70% 2-propanol (16mL) was treated with 5,5-dimethylcyclohexane-1,3-dione (603 mg, 1.05 Eq, 4.30 mmol) and pentane-2,4-dione (430 mg, 441 μ L, 1.05 Eq, 4.30 mmol) and sulfuric acid (80.3 mg, 43.6 μ L, 0.2 Eq, 819 μ mol). The reaction mixture was heated to 120°C in pressure vessel for 16h. The reaction mixture was cooled room temp and concentrated. The crude material was chromatographed over silica gel, eluted 0-80% EtOAc/Hex. Solids were isolated (0.2g, 12% yield). ¹H NMR (499 MHz, cdcl₃) δ 7.12 – 7.04 (m, 2H), 6.66 – 6.61 (m, 2H), 4.69 (s, 1H), 2.38 (s, 2H), 2.33 (s, 3H), 2.21 (d, J = 14.7 Hz, 2H), 2.14 (s, 3H), 1.07 (s, 3H), 0.90 (s, 3H). ¹³C NMR (126 MHz, cdcl₃) δ 200.45, 197.88, 162.82, 156.33, 155.04, 135.29, 129.52, 116.47, 115.51, 115.04, 50.75, 40.80, 34.89, 32.30, 29.55, 29.00, 27.26, 18.94.

3,3,6,6-tetramethyl-9-(6-((2-methylbenzyl)oxy)pyridin-3-yl)-3,4,5,6,7,9-hexahydro-1H-xanthene-1,8(2H)-dione (CCG362908) [sz-08-30]

Following the general procedure of **5c** on a scale of 50mg (0.14mmol) 9-(6-hydroxypyridin-3-yl)-3,3,6,6-tetramethyl-3,4,5,6,7,9-hexahydro-1H-xanthene-1,8(2H)-dione (**3bg**), 1-(bromomethyl)-2-methylbenzene (50 mg, 36 μ L, 2 Eq, 0.27 mmol) was used. 0.04g of product was isolated (62% yield). ¹H NMR (400 MHz, cdcl₃) δ 7.27 – 7.12 (m, 4H), 7.06 (d, J = 2.6 Hz, 1H), 7.01 – 6.96 (m, 1H), 6.47 (d, J = 9.3 Hz, 1H), 5.04 (s, 2H), 4.40 (s, 1H), 2.48 – 2.30 (m, 4H), 2.23 (s, 3H), 2.18 (s, 2H), 2.15 (s, 2H), 1.06 (s, 6H), 0.95 (s, 6H). ¹³C NMR (101 MHz, cdcl₃) δ 196.27, 162.89, 161.98, 139.73, 136.76, 136.09, 133.72, 130.59, 128.72, 128.09, 126.36, 121.87, 120.12, 114.09, 50.60, 50.09, 40.79, 40.69, 40.59, 32.21, 32.14, 29.16, 28.22, 27.37, 19.13. ESI MS m/z 472.24 (M + H)⁺ *9-(6-((2-methylbenzyl)oxy)pyridin-3-yl)-3,4,5,6,7,9-hexahydro-1H-xanthene-1,8(2H)-dione (CCG362907)* [sz-08-31]

Following the general procedure of **5c** on a scale of 50mg (0.16mmol) 9-(6-hydroxypyridin-3-yl)-3,4,5,6,7,9-hexahydro-1H-xanthene-1,8(2H)-dione (**3bh**), 1-(bromomethyl)-2-methylbenzene (59 mg, 42 μ L, 2 Eq, 0.32 mmol) was used. 0.04g of product was isolated (52% yield). ¹H NMR (400 MHz, cdcl₃) δ 7.29 – 7.14 (m, 4H), 7.02 (dd, J = 7.4, 4.7 Hz, 2H), 6.47 (d, J = 9.4 Hz, 1H), 5.05 (s, 2H), 4.45 (s, 1H), 2.60 – 2.41 (m, 4H), 2.30 (dt, J = 9.9, 5.4 Hz, 4H), 2.23 (s, 3H), 2.05 – 1.94

(m, 2H), 1.87 (dddd, J = 21.7, 11.4, 8.7, 5.9 Hz, 2H). ¹³C NMR (101 MHz, cdcl₃) δ 196.43, 164.53, 161.99, 139.95, 136.90, 135.94, 133.80, 130.56, 128.94, 128.13, 126.34, 122.09, 120.03, 115.35, 50.06, 36.79, 28.01, 27.00, 20.20, 19.12. ESI MS m/z 416.18 (M + H)⁺

9-(5-((2-methylbenzyl)oxy)pyridin-2-yl)-3,4,5,6,7,9-hexahydro-1H-xanthene-1,8(2H)-dione (CCG362905) [sz-08-34]

Following the general procedure of **5c** on a scale of 30mg (0.1mmol) 9-(5-hydroxypyridin-2-yl)-3,4,5,6,7,9-hexahydro-1H-xanthene-1,8(2H)-dione (**3bi**), 1-(bromomethyl)-2-methylbenzene (36 mg, 25 μL, 2 Eq, 0.19 mmol) was used. 0.009g of product was isolated (22% yield). ¹H NMR (499 MHz, cdcl₃) δ 8.18 (d, J = 2.9 Hz, 1H), 7.57 (d, J = 8.5 Hz, 1H), 7.40 – 7.29 (m, 1H), 7.25 – 7.23 (m, 1H), 7.22 – 7.14 (m, 3H), 4.98 (s, 2H), 4.86 (s, 1H), 2.70 (dt, J = 17.7, 5.3 Hz, 2H), 2.54 (dddd, J = 17.9, 8.2, 6.3, 1.5 Hz, 2H), 2.43 – 2.25 (m, 7H), 2.09 – 1.93 (m, 4H). ¹³C NMR (126 MHz, cdcl₃) δ 197.14, 164.58, 154.43, 153.44, 137.28, 136.81, 134.29, 130.45, 128.80, 128.49, 126.07, 125.27, 121.14, 115.64, 68.90, 36.90, 33.65, 27.18, 20.32, 18.86. ESI MS m/z 416.18 (M + H)⁺

3,6-diethyl-9-(4-((2-methylbenzyl)oxy)phenyl)-3,4,5,6,7,9-hexahydro-1H-xanthene-1,8(2H)-dione (CCG366166) [sz-10-10]

Following the general procedure of **5c** on a scale of 90mg (0.25mmol) 3,6-diethyl-9-(4-hydroxyphenyl)-3,4,5,6,7,9-hexahydro-1H-xanthene-1,8(2H)-dione (**3bj**), 1-(bromomethyl)-2-methylbenzene (73 mg, 53 μL, 1.6 Eq, 0.39 mmol) was used. 0.09g of product was isolated (81% yield). ¹H NMR (400 MHz, cdcl₃) δ 7.43 – 7.31 (m, 1H), 7.25 – 7.17 (m, 5H), 6.85 (dq, J = 8.6, 3.1 Hz, 2H), 5.03 – 4.88 (m, 2H), 4.74 (t, J = 6.2 Hz, 1H), 2.74 – 2.63 (m, 1H), 2.63 – 2.55 (m, 1H), 2.54 – 2.38 (m, 3H), 2.32 – 2.20 (m, 1H), 2.12 – 1.93 (m, 4H), 1.42 (q, J = 7.1 Hz, 4H), 0.94 (ddt, J = 7.7, 6.2, 2.6 Hz, 6H). ¹³C NMR (101 MHz, cdcl₃) δ 196.75, 163.75, 157.45, 137.01, 136.79, 134.99, 130.35, 129.34, 128.79, 128.22, 126.00, 116.79, 116.54, 114.25, 68.48, 43.24, 35.19, 34.28, 33.27, 32.94, 31.03, 28.29, 18.90, 10.98. ESI MS m/z 493.23 (M + Na)⁺

9-(4-((2-methylbenzyl)oxy)phenyl)-3,6-bis(trifluoromethyl)-3,4,5,6,7,9-hexahydro-1H-xanthene-1,8(2H)-dione (CCG366180) [sz-10-13]

Following the general procedure of **5c** on a scale of 65mg (0.15mmol) 9-(4-hydroxyphenyl)-3,6-bis(trifluoromethyl)-3,4,5,6,7,9-hexahydro-1H-xanthene-1,8(2H)-dione (**3bk**), 1-(bromomethyl)-2-methylbenzene (32 mg, 23 μL, 1.2 Eq, 0.17 mmol) was used. 0.03g of product was isolated (39% yield). ¹H NMR (499 MHz, cdcl₃) δ 7.40 – 7.32 (m, 1H), 7.26 – 7.23 (m, 1H), 7.21 (d, J = 6.7 Hz,

2H), 7.18 (d, J = 8.4 Hz, 2H), 6.91 – 6.84 (m, 2H), 4.97 (s, 2H), 4.78 (s, 1H), 2.91 – 2.84 (m, 4H), 2.80 – 2.73 (m, 2H), 2.68 (ddd, J = 16.9, 3.9, 1.6 Hz, 2H), 2.42 (d, J = 3.8 Hz, 1H), 2.38 (d, J = 6.4 Hz, 1H), 2.35 (s, 3H). ¹³C NMR (126 MHz, cdcl₃) δ 192.03, 160.54, 157.94, 136.76, 135.58, 134.76, 130.40, 129.23, 128.74, 128.31, 126.03, 117.34, 114.66, 68.58, 37.12, 36.89, 35.43, 30.85, 26.12, 26.10, 18.86. ¹⁹F NMR (470 MHz, cdcl₃) δ -73.58 (d, J = 7.4 Hz). ESI MS m/z 573.14 (M + Na)⁺

3,6-diisobutyl-9-(4-((2-methylbenzyl)oxy)phenyl)-3,4,5,6,7,9-hexahydro-1H-xanthene-1,8(2H)-dione (CCG366181) [sz-10-14]

Following the general procedure of **5c** on a scale of 58mg (0.14mmol) 9-(4-hydroxyphenyl)-3,6-diisobutyl-3,4,5,6,7,9-hexahydro-1H-xanthene-1,8(2H)-dione (**3bl**), 1-(bromomethyl)-2-methylbenzene (30 mg, 22 μL, 1.2 Eq, 0.16 mmol) was used. 0.04g of product was isolated (58% yield). ¹H NMR (499 MHz, cdcl₃) δ 7.40 – 7.33 (m, 1H), 7.26 – 7.17 (m, 5H), 6.86 (q, J = 8.5 Hz, 2H), 4.96 (t, J = 3.1 Hz, 2H), 4.74 (t, J = 6.1 Hz, 1H), 2.61 (ddd, J = 34.2, 17.0, 4.3 Hz, 2H), 2.43 (ddt, J = 30.4, 16.9, 4.3 Hz, 3H), 2.35 (d, J = 2.3 Hz, 3H), 2.32 – 2.20 (m, 2H), 2.20 – 2.11 (m, 1H), 2.09 – 1.95 (m, 2H), 1.72 – 1.63 (m, 2H), 1.24 (dtdd, J = 13.8, 11.2, 8.5, 5.6 Hz, 4H), 0.89 (ddd, J = 9.3, 6.6, 2.4 Hz, 12H). ¹³C NMR (126 MHz, cdcl₃) δ 196.70, 196.62, 163.60, 162.85, 157.50, 136.78, 136.62, 135.01, 130.34, 129.39, 129.38, 128.78, 128.20, 125.99, 116.82, 116.53, 114.27, 114.21, 68.49, 45.03, 44.55, 43.84, 43.67, 33.86, 33.47, 31.21, 31.04, 30.35, 24.74, 22.65, 22.43, 18.87. ESI MS m/z 549.29 (M + Na)⁺

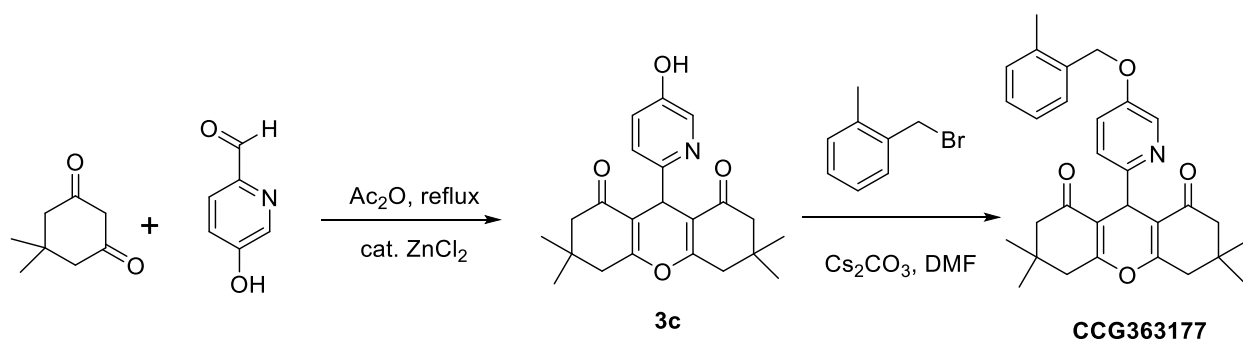
3,6-dimethyl-9-(4-((2-methylbenzyl)oxy)phenyl)-3,4,5,6,7,9-hexahydro-1H-xanthene-1,8(2H)-dione (CCG366672) [sz-10-40]

Following the general procedure of **5c** on a scale of 70mg (0.21mmol) 9-(4-hydroxyphenyl)-3,6-dimethyl-3,4,5,6,7,9-hexahydro-1H-xanthene-1,8(2H)-dione (**3bm**), 1-(bromomethyl)-2-methylbenzene (46 mg, 33 μL, 1.2 Eq, 0.25 mmol) was used. 0.03g of product was isolated (35% yield). ¹H NMR (499 MHz, cdcl₃) δ 7.44 – 7.31 (m, 1H), 7.26 – 7.17 (m, 5H), 6.91 – 6.77 (m, 2H), 4.95 (s, 2H), 4.75 (t, J = 7.4 Hz, 1H), 2.72 – 2.54 (m, 2H), 2.43 (dtd, J = 19.2, 9.5, 8.9, 3.4 Hz, 3H), 2.35 (s, 3H), 2.33 – 2.24 (m, 2H), 2.24 – 2.16 (m, 1H), 2.13 – 1.97 (m, 2H), 1.16 – 0.98 (m, 6H). ¹³C NMR (126 MHz, cdcl₃) δ 196.61, 163.50, 162.73, 157.48, 137.03, 136.76, 135.02, 130.34, 129.34, 128.77, 128.19, 125.99, 116.70, 116.49, 114.34, 114.29, 68.51, 45.28, 35.29, 34.94, 30.98, 28.48, 27.89, 20.83, 18.87. ESI MS m/z 465.20 (M + Na)⁺

3-acetyl-2,7,7-trimethyl-4-(4-((2-methylbenzyl)oxy)phenyl)-4,6,7,8-tetrahydro-5H-chromen-5-one (CCG363244) [sz-08-94]

Following the general procedure of **5c** on a scale of 40mg (0.12mmol) 3-acetyl-4-(4-hydroxyphenyl)-2,7,7-trimethyl-4,6,7,8-tetrahydro-5H-chromen-5-one (**3bn**), 1-(bromomethyl)-2-methylbenzene (27 mg, 20 μ L, 1.2 Eq, 0.15 mmol) was used. 0.04g of product was isolated (66% yield). ¹H NMR (499 MHz, cdcl₃) δ 7.37 (dd, J = 7.0, 2.2 Hz, 1H), 7.25 – 7.22 (m, 1H), 7.21 (d, J = 2.2 Hz, 2H), 7.19 (d, J = 2.2 Hz, 2H), 6.93 – 6.79 (m, 2H), 4.97 (s, 2H), 4.73 (s, 1H), 2.38 (s, 2H), 2.35 (d, J = 0.9 Hz, 6H), 2.27 – 2.17 (m, 2H), 2.15 (s, 3H), 1.09 (s, 3H), 0.92 (s, 3H). ¹³C NMR (126 MHz, cdcl₃) δ 199.67, 196.84, 162.20, 157.74, 156.47, 136.72, 136.30, 134.81, 130.36, 129.42, 128.70, 128.25, 126.00, 116.28, 115.05, 114.67, 68.55, 50.80, 40.80, 34.89, 32.24, 29.62, 29.06, 27.38, 18.96, 18.86. ESI MS m/z 453.20 (M + Na)⁺

Scheme 3.2 Synthesis for **CCG363177**



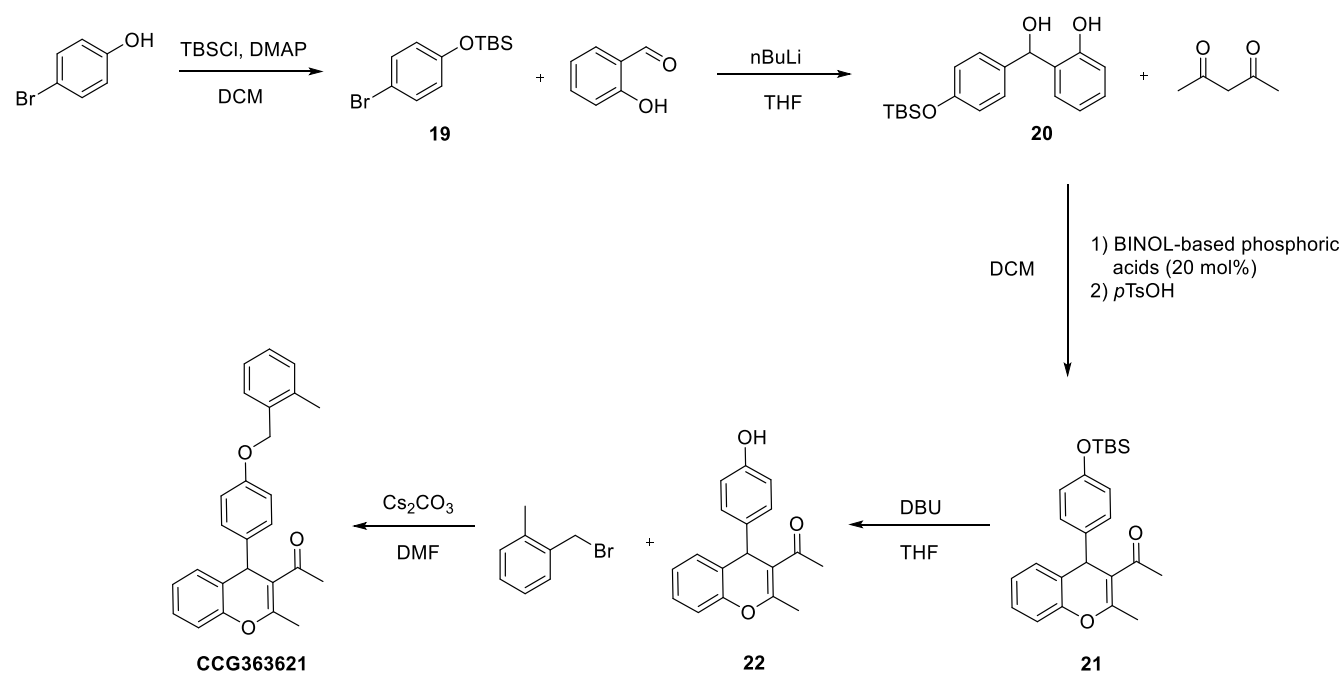
9-(5-hydroxypyridin-2-yl)-3,3,6,6-tetramethyl-3,4,5,6,7,9-hexahydro-1H-xanthene-1,8(2H)-dione (3c) [sz-08-73]

To a mixture of 5-hydroxypicolinaldehyde (80 mg, 1 Eq, 0.65 mmol) and 5,5-dimethylcyclohexane-1,3-dione (0.18 g, 2.01 Eq, 1.3 mmol) in acetic anhydride (0.14 g, 0.13 mL, 2.1 Eq, 1.4 mmol) were added acetic anhydride (0.14 g, 0.13 mL, 2.1 Eq, 1.4 mmol). The reaction mixture was refluxed at 70°C for 16h. The reaction mixture was cooled to room temp. and concentrated. The crude material was chromatographed over silica gel, eluted with 0-5% MeOH/DCM. The compound was isolated as solids (0.22g, 92%). ¹H NMR (499 MHz, dms_o) δ 8.00 (s, 1H), 7.31 (s, 2H), 4.60 (s, 1H), 2.56 (d, J = 17.6 Hz, 2H), 2.45 (d, J = 17.3 Hz, 2H), 2.26 (d, J = 16.2 Hz, 2H), 2.04 (d, J = 16.1 Hz, 2H), 1.02 (s, 6H), 0.89 (s, 6H).

3,3,6,6-tetramethyl-9-(5-((2-methylbenzyl)oxy)pyridin-2-yl)-3,4,5,6,7,9-hexahydro-1H-xanthene-1,8(2H)-dione (**CCG363177**) [sz-08-78]

Following the general procedure of **5** on a scale of 130mg (0.35mmol) 9-(5-hydroxypyridin-2-yl)-3,3,6,6-tetramethyl-3,4,5,6,7,9-hexahydro-1H-xanthene-1,8(2H)-dione (**3c**), 1-(bromomethyl)-2-methylbenzene (72.0 mg, 52.2 μ L, 1.1 Eq, 389 μ mol) was used and isolated 0.05g (27% yield) of the desired product. ¹H NMR (499 MHz, cdcl₃) δ 8.14 (d, J = 2.9 Hz, 1H), 7.54 (d, J = 8.5 Hz, 1H), 7.37 – 7.32 (m, 1H), 7.26 – 7.15 (m, 4H), 4.97 (s, 2H), 4.83 (s, 1H), 2.57 – 2.40 (m, 4H), 2.34 (s, 3H), 2.27 – 2.12 (m, 4H), 1.10 (s, 6H), 1.01 (s, 6H). ¹³C NMR (126 MHz, cdcl₃) δ 197.00, 163.15, 154.30, 153.40, 137.25, 136.78, 134.29, 130.42, 128.79, 128.45, 126.03, 124.94, 121.06, 114.46, 68.89, 50.80, 40.86, 33.43, 32.28, 29.29, 27.21, 18.85. ESI MS m/z 472.24 (M + H)⁺

Scheme 3.3 Synthetic route for **CCG363621** (El-Sepelgy et al., 2014)



(4-bromophenoxy)(tert-butyl)dimethylsilane (**19**)

To a solution of 4-bromophenol (1500 mg, 1 Eq, 8.670 mmol) in DCM (36mL) was treated with DMAP (52.96 mg, 0.05 Eq, 433.5 μ mol), TEA (1.316 g, 1.81 mL, 1.5 Eq, 13.01 mmol), and TBS-Cl (1.437 g, 1.1 Eq, 9.537 mmol) under room temp. The reaction was run for 16h and was quenched with sat. NaHCO₃ and extracted with DCM (x3). The extracts were washed with brine, dried over MgSO₄, and concentrated. The crude material was chromatographed over silica gel, eluted with 0-

10%EtOAc/Hex. Compound **10** was isolated as clear oil (2.16g, 87% yield). ¹H NMR (499 MHz, cdcl₃) δ 7.35 – 7.29 (m, 2H), 6.74 – 6.69 (m, 2H), 0.97 (d, J = 0.7 Hz, 9H), 0.18 (d, J = 0.7 Hz, 6H). ¹³C NMR (126 MHz, cdcl₃) δ 154.84, 132.27, 121.88, 113.58, 25.60, 18.17, -4.52.

2-((4-((tert-butyldimethylsilyl)oxy)phenyl)(hydroxy)methyl)phenol (20)

To a mixture of (4-bromophenoxy)(tert-butyl)dimethylsilane (**19**) (420 mg, 1 Eq, 1.46 mmol) in THF (7mL) was cooled to -70°C and treated with nBuLi (93.7 mg, 585 μL, 2.5 molar, 1 Eq, 1.46 mmol) dropwise. The reaction was run in the ice bath for 1.5h and treated with 2-hydroxybenzaldehyde (71.4 mg, 61.0 μL, 0.4 Eq, 585 μmol) dropwise. The reaction continued to run in room temp continue the reaction was complete. The mixture was quenched by sat. NH₄Cl and extracted with EtOAc (x3). The extracts were washed with brine, dried over MgSO₄, and concentrated. The crude material was chromatographed over silica gel, and the compound **20** was isolated (0.1g, 20% yield). ¹H NMR (499 MHz, cdcl₃) δ 8.05 (s, 1H), 7.25 – 7.22 (m, 2H), 7.19 (ddd, J = 8.6, 6.8, 2.2 Hz, 1H), 6.90 (dd, J = 8.1, 1.1 Hz, 1H), 6.85 – 6.79 (m, 4H), 5.96 (d, J = 2.5 Hz, 1H), 0.99 (s, 9H), 0.20 (s, 6H).

1-(4-(4-((tert-butyldimethylsilyl)oxy)phenyl)-2-methyl-4H-chromen-3-yl)ethan-1-one (21)

To a mixture of 2-((4-((tert-butyldimethylsilyl)oxy)phenyl)(hydroxy)methyl)phenol (**20**) (40 mg, 1 Eq, 0.12 mmol) and 1,1'-binaphthyl-2,2'-diyl hydrogenphosphate (2.1 mg, 0.05 Eq, 6.1 μmol) in DCM (3mL) at room temp. The reaction mixture was treated with pentane-2,4-dione (18 mg, 19 μL, 1.5 Eq, 0.18 mmol) in one portion, whereupon the reaction mixture was stirred for 16h at room temp. Then, 4-methylbenzenesulfonic acid hydrate (4.6 mg, 0.2 Eq, 24 μmol) was added to the mixture and heated to 40°C for 2h. The reaction mixture was cooled to room temp and concentrated. The crude material was chromatographed over silica gel, eluted with 0-50% EtOAc/Hexane. Compound **21** was isolated as clear gum (0.03, 65% yield) ¹H NMR (499 MHz, cdcl₃) δ 7.19 – 7.04 (m, 4H), 7.02 – 6.92 (m, 2H), 6.78 – 6.64 (m, 2H), 4.95 (s, 1H), 2.44 (d, J = 0.9 Hz, 3H), 2.16 (s, 3H), 0.95 (s, 9H), 0.15 (s, 6H). ¹³C NMR (126 MHz, cdcl₃) δ 199.21, 158.72, 154.45, 148.99, 138.63, 128.92, 128.52, 127.47, 125.15, 124.37, 120.22, 116.24, 114.26, 41.49, 29.99, 25.61, 25.61, 20.01, 18.10, -4.45.

1-(4-(4-hydroxyphenyl)-2-methyl-4H-chromen-3-yl)ethan-1-one (22)

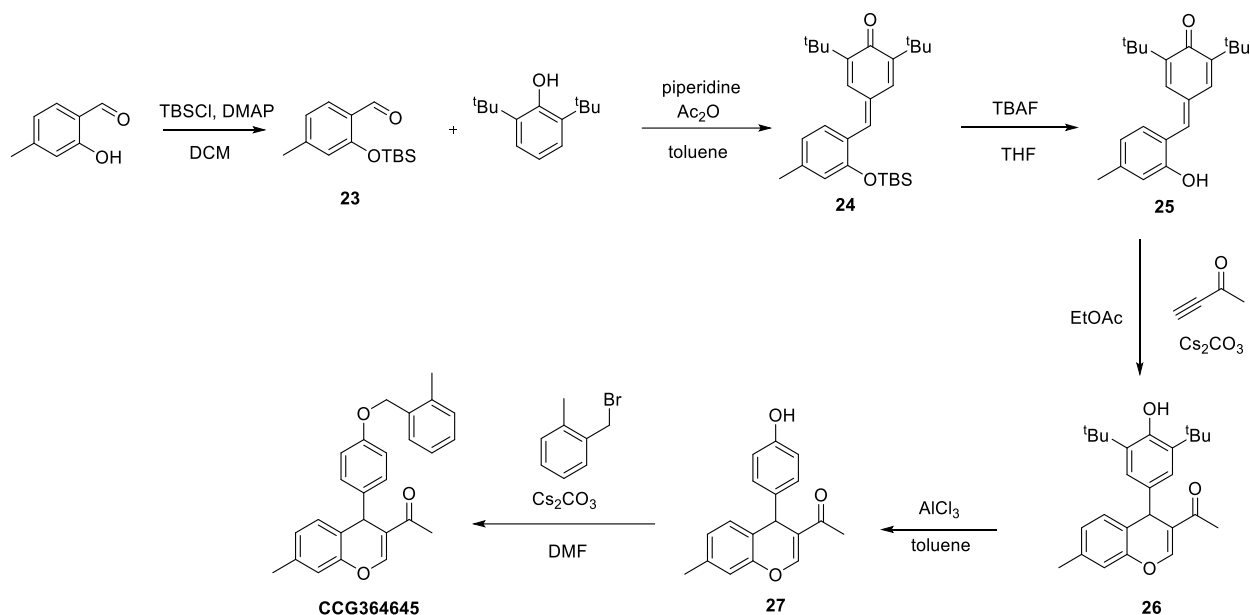
To a solution of 1-(4-(4-((tert-butyldimethylsilyl)oxy)phenyl)-2-methyl-4H-chromen-3-yl)ethan-1-one (**21**) (30 mg, 1 Eq, 76 μmol) in acetonitrile (0.3mL) and water (5.5 μL) was treated with DBU (12 mg, 11 μL, 1 Eq, 76 μmol). The reaction mixture was stirred at room temp for 4h. The

reaction was quenched with sat. NH_4Cl , and the aqueous layer was extracted with DCM (x3). The extracts were combined, washed with brine, dried over MgSO_4 , and concentrated under reduced pressure. The compound was carried to the next step without further purification. Compound **22** was isolated as clear oil (0.02g, 89% yield). ^1H NMR (499 MHz, cdCl_3) δ 7.15 – 7.08 (m, 2H), 7.08 – 7.05 (m, 2H), 7.01 – 6.96 (m, 2H), 6.72 – 6.61 (m, 2H), 6.03 (s, 1H), 4.95 (s, 1H), 2.44 (s, 3H), 2.19 (s, 3H). ^{13}C NMR (126 MHz, cdCl_3) δ 200.39, 159.02, 154.84, 148.84, 137.80, 128.93, 128.74, 127.55, 124.95, 124.50, 116.26, 115.75, 114.47, 41.24, 29.98, 20.09.

1-(2-methyl-4-(4-((2-methylbenzyl)oxy)phenyl)-4H-chromen-3-yl)ethan-1-one (CCG363621) [sz-08-100]

To a solution of 1-(4-(4-hydroxyphenyl)-2-methyl-4H-chromen-3-yl)ethan-1-one (**22**) (19 mg, 1 Eq, 68 μmol) in DMF (1mL) was treated with 1-(bromomethyl)-2-methylbenzene (15 mg, 11 μL , 1.2 Eq, 81 μmol) and Cs_2CO_3 (44 mg, 2 Eq, 0.14 mmol). The reaction mixture was stirred at room temp for 16h. The reaction mixture was diluted with water and extracted with DCM (x3). The extracts were washed with sat. LiCl and brine, dried over MgSO_4 , and concentrated. The crude material was chromatographed over silica gel, eluted with 0-50% EtOAc/Hex. Desired compound was isolated as white solids (0.02g, 86% yield). ^1H NMR (499 MHz, cdCl_3) δ 7.36 (dd, $J = 7.0$, 2.2 Hz, 1H), 7.25 – 7.22 (m, 1H), 7.22 – 7.16 (m, 4H), 7.16 – 7.10 (m, 2H), 7.02 – 6.97 (m, 2H), 6.91 – 6.87 (m, 2H), 4.98 (s, 1H), 4.96 (s, 2H), 2.45 (d, $J = 0.8$ Hz, 3H), 2.34 (s, 3H), 2.19 (s, 3H). ^{13}C NMR (126 MHz, cdCl_3) δ 199.05, 158.84, 157.82, 149.02, 138.42, 136.72, 134.73, 130.38, 128.87, 128.69, 128.56, 128.29, 127.52, 126.02, 125.16, 124.45, 116.28, 115.04, 114.38, 68.60, 41.41, 30.08, 20.05, 18.85. ESI MS m/z 407.16 ($\text{M} + \text{Na}$) $^+$

Scheme 3.4 Synthetic route for **CCG364645** (Mei et al., 2018)



2-((tert-butyldimethylsilyl)oxy)-4-methylbenzaldehyde (23)

To a solution of 2-hydroxy-4-methylbenzaldehyde (390 mg, 1 Eq, 2.86 mmol) in DCM (12mL) at room temp was treated with DMAP (17.5 mg, 0.05 Eq, 143 μ mol), TEA (580 mg, 799 μ L, 2 Eq, 5.73 mmol), and TBS-Cl (475 mg, 1.1 Eq, 3.15 mmol). The reaction was run for 16h and diluted with sat. NaHCO₃. The aqueous layer was extracted with DCM (x3). The extracts were washed with brine, dried over MgSO₄ and concentrated. The crude material was chromatographed over silica gel, eluted with 0-10% EtOAc/Hex. Compound **23** was isolated as semisolids (0.6g, 85% yield). ¹H NMR (400 MHz, cdcl₃) δ 10.39 (d, J = 0.8 Hz, 1H), 7.70 (d, J = 7.9 Hz, 1H), 6.91 – 6.78 (m, 1H), 6.67 (s, 1H), 2.35 (s, 3H), 1.02 (d, J = 0.6 Hz, 9H), 0.27 (d, J = 0.6 Hz, 6H).

2,6-di-tert-butyl-4-(2-((tert-butyldimethylsilyl)oxy)-4-methylbenzylidene)cyclohexa-2,5-dien-1-ol (24)

To a solution of 2,6-di-tert-butylphenol (0.28 g, 1.1 Eq, 1.4 mmol) and protected 2-((tert-butyldimethylsilyl)oxy)-4-methylbenzaldehyde (**23**) (0.31 g, 1 Eq, 1.2 mmol) in toluene (4mL) was heated to reflux in Dean-Stark apparatus. Piperidine (0.21 g, 0.24 mL, 2 Eq, 2.5 mmol) in toluene (2mL) was added dropwise. Then, the temperature was elevated to 150°C and stirred for 16h. The reaction mixture was then cooled to 120°C and acetic anhydride (0.25 g, 0.23 mL, 2 Eq, 2.5 mmol) was added dropwise. The reaction mixture continued to run for 0.5h and quenched with ice water. The aqueous layer was extracted with EtOAc (x3). The extracts were washed with brine,

dried over MgSO₄, and concentrated. The crude material was chromatographed over silica gel, eluted with 0-10% EtOAc/Hex. Compound **24** was isolated (0.4g, 81% yield). ¹H NMR (499 MHz, cdcl₃) δ 7.49 (d, J = 2.4 Hz, 1H), 7.34 (s, 1H), 7.29 (d, J = 7.8 Hz, 1H), 6.99 (d, J = 2.4 Hz, 1H), 6.89 – 6.83 (m, 1H), 6.73 – 6.69 (m, 1H), 2.35 (s, 3H), 1.34 (s, 9H), 1.31 (s, 9H), 1.02 (d, J = 0.8 Hz, 9H), 0.21 (d, J = 0.8 Hz, 6H).

2,6-di-tert-butyl-4-(2-hydroxy-4-methylbenzylidene)cyclohexa-2,5-dien-1-one (25)

To a mixture of 2,6-di-tert-butyl-4-(2-((tert-butyldimethylsilyl)oxy)-4-methylbenzylidene)cyclohexa-2,5-dien-1-one (**24**) (0.2380 g, 1 Eq, 542.5 μmol) in THF (3mL) was cooled to 0°C. TBAF (156.0 mg, 596.7 μL, 1 molar, 1.1 Eq, 596.7 μmol) was added dropwise, and the reaction was run at 0°C for 10min and quenched with sat. NH₄Cl. The aqueous layer was extracted with DCM (x3), and the organic layer was washed with brine, dried over MgSO₄, and concentrated. The crude material was chromatographed over silica gel, eluted with 0-30% EtOAc/Hex. Compound **25** was isolated (0.16g, 92% yield). ¹H NMR (499 MHz, cdcl₃) δ 7.43 (d, J = 2.4 Hz, 1H), 7.28 (s, 1H), 7.24 (d, J = 7.8 Hz, 1H), 7.06 (d, J = 2.4 Hz, 1H), 6.84 (d, J = 7.9 Hz, 1H), 6.71 (d, J = 1.4 Hz, 1H), 4.99 (d, J = 1.4 Hz, 1H), 2.36 (s, 3H), 1.33 (s, 9H), 1.29 (s, 9H).

1-(4-(3,5-di-tert-butyl-4-hydroxyphenyl)-7-methyl-4H-chromen-3-yl)ethan-1-one (26)

To a mixture of 2,6-di-tert-butyl-4-(2-hydroxy-4-methylbenzylidene)cyclohexa-2,5-dien-1-one (**25**) (0.160 g, 1 Eq, 493 μmol) in dry EtOAc (6mL) was treated with but-3-yn-2-one (40.3 mg, 46 μL, 1.2 Eq, 592 μmol), Cs₂CO₃ (161 mg, 1 Eq, 493 μmol), and 4 Å MS (0.5g). The reaction was run at room temp for 16h. The mixture was then filtered and concentrated. The crude material was chromatographed over silica gel, eluted with 0-30% EtOAc/Hex. Compound **26** was isolated (0.07g, 36% yield) ¹H NMR (499 MHz, cdcl₃) δ 7.76 (s, 1H), 7.01 (d, J = 7.7 Hz, 1H), 6.98 (s, 2H), 6.88 (s, 1H), 6.86 (dd, J = 7.8, 1.7 Hz, 1H), 5.00 (s, 1H), 4.97 (s, 1H), 2.31 (s, 3H), 2.24 (s, 3H), 1.36 (s, 18H).

1-(4-(4-hydroxyphenyl)-7-methyl-4H-chromen-3-yl)ethan-1-one (27)

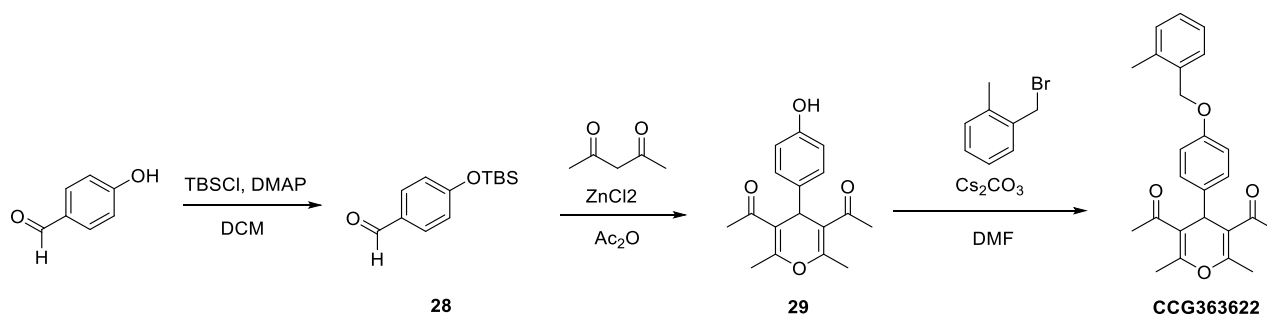
To a mixture of 1-(4-(3,5-di-tert-butyl-4-hydroxyphenyl)-7-methyl-4H-chromen-3-yl)ethan-1-one (**26**) (69 mg, 1 Eq, 0.18 mmol) and 4 Å MS (0.2g) in dry toluene (7mL) was treated with aluminum chloride (0.23 g, 10 Eq, 1.8 mmol). The reaction was heated to 35°C and run for 16h. The mixture was cooled to room temp and quenched with water. The aqueous layer was extracted with DCM (x3), and the organic layer was washed with brine, dried over MgSO₄, and concentrated. The crude material was chromatographed over silica gel, eluted with 0-50% EtOAc/Hex. Compound **27** was

isolated (0.004g, 8% yield). ¹H NMR (499 MHz, cd₃od) δ 7.97 (s, 1H), 7.80 (s, 1H), 7.02 – 6.97 (m, 2H), 6.94 (d, J = 7.8 Hz, 1H), 6.88 (s, 1H), 6.84 (d, J = 8.1 Hz, 1H), 6.66 – 6.57 (m, 2H), 4.88 (s, 1H), 2.28 (s, 3H), 2.22 (s, 3H).

1-(7-methyl-4-(4-((2-methylbenzyl)oxy)phenyl)-4H-chromen-3-yl)ethan-1-one (CCG364645) [sz-09-57]

To a solution of 1-(4-(4-hydroxyphenyl)-7-methyl-4H-chromen-3-yl)ethan-1-one (4 mg, 1 Eq, 0.01 mmol) (**27**) in DMF (0.2mL) was treated with 1-(bromomethyl)-2-methylbenzene (3 mg, 2 μL, 1.1 Eq, 0.02 mmol) and Cs₂CO₃ (9 mg, 2 Eq, 0.03 mmol). The reaction mixture was stirred at room temp for 16h. The reaction mixture was diluted with water and extracted with DCM (x3). The extracts were washed with sat. LiCl and brine, dried over MgSO₄, and concentrated. The crude material was chromatographed over silica gel, eluted with 0-30% EtOAc/Hex. Compound **28** was isolated as white solids (0.004g, 80% yield). ¹H NMR (499 MHz, cdcl₃) δ 7.75 (d, J = 0.8 Hz, 1H), 7.37 – 7.32 (m, 1H), 7.25 – 7.21 (m, 1H), 7.21 – 7.17 (m, 2H), 7.17 – 7.12 (m, 2H), 6.96 (d, J = 7.9 Hz, 1H), 6.89 (d, J = 1.5 Hz, 1H), 6.87 – 6.83 (m, 3H), 5.00 (s, 1H), 4.94 (s, 2H), 2.33 (s, 3H), 2.30 (s, 3H), 2.23 (d, J = 0.8 Hz, 3H). ¹³C NMR (126 MHz, cdcl₃) δ 195.42, 157.50, 151.39, 148.91, 138.71, 137.76, 136.72, 134.87, 130.35, 129.84, 128.92, 128.70, 128.22, 126.12, 125.99, 121.82, 120.62, 116.79, 114.61, 68.53, 37.58, 25.44, 20.96, 18.83. ESI MS m/z 407.16 (M + Na)⁺

Scheme 3.5 Synthesis of CCG363622



4-((tert-butyldimethylsilyl)oxy)benzaldehyde (28)

To a solution of 4-hydroxybenzaldehyde (500 mg, 1 Eq, 4.09 mmol) in DCM (17mL) at room temp was treated with TEA (497 mg, 685 μL, 1.2 Eq, 4.91 mmol), DMAP (25.0 mg, 0.05 Eq, 205 μmol), and TBS-Cl (741 mg, 1.2 Eq, 4.91 mmol). The reaction was run for 16h and diluted with sat. NaHCO₃. The aqueous layer was extracted with DCM (x3). The extracts were washed with

brine, dried over MgSO₄ and concentrated. The crude material was chromatographed over silica gel, eluted with 0-30% EtOAc/Hex. Compound **28** was isolated as semisolids (0.9g, 98% yield). ¹H NMR (499 MHz, cdcl₃) δ 9.89 (s, 1H), 7.90 – 7.69 (m, 2H), 7.00 – 6.88 (m, 2H), 0.99 (d, J = 0.6 Hz, 9H), 0.25 (d, J = 0.6 Hz, 6H). ¹³C NMR (126 MHz, cdcl₃) δ 190.85, 161.49, 131.88, 130.41, 120.46, 25.54, 18.23, -4.38.

1,1'-(4-(4-hydroxyphenyl)-2,6-dimethyl-4H-pyran-3,5-diyl)bis(ethan-1-one) (**29**)

To a mixture of 4-((tert-butyldimethylsilyl)oxy)benzaldehyde (**28**) (280 mg, 1 Eq, 1.18 mmol) and pentane-2,4-dione (285 mg, 292 μL, 2.4 Eq, 2.84 mmol) in acetic anhydride (0.3μL) was treated with zinc chloride (161 mg, 1 Eq, 1.18 mmol). The reaction was heated to 120°C in pressure vessel for 16h. The reaction was diluted with water, and the precipitates were filtered and washed with water. Solids formed (0.2g, 49% yield). ¹H NMR (400 MHz, cdcl₃) δ 7.02 (d, J = 8.2 Hz, 2H), 6.71 – 6.61 (m, 2H), 4.74 (s, 1H), 2.28 (d, J = 0.9 Hz, 6H), 2.21 (d, J = 0.8 Hz, 6H).

1,1'-(2,6-dimethyl-4-(4-((2-methylbenzyl)oxy)phenyl)-4H-pyran-3,5-diyl)bis(ethan-1-one)
(**CCG363622**) [sz-08-83]

To a solution of 1,1'-(4-(4-hydroxyphenyl)-2,6-dimethyl-4H-pyran-3,5-diyl)bis(ethan-1-one) (170 mg, 1 Eq, 594 μmol) (**29**) in DMF (4mL) was treated with 1-(bromomethyl)-2-methylbenzene (165 mg, 119 μL, 1.5 Eq, 891 μmol) and Cs₂CO₃ (387 mg, 2 Eq, 1.19 mmol). The reaction mixture was stirred at room temp for 16h. The reaction mixture was diluted with water and extracted with DCM (x3). The extracts were washed with sat. LiCl and brine, dried over MgSO₄, and concentrated. The crude material was chromatographed over silica gel, eluted with 0-30% EtOAc/Hex. Desired compound was isolated as white solids (0.004g, 80% yield). ¹H NMR (499 MHz, cdcl₃) δ 7.38 (dd, J = 7.0, 2.3 Hz, 1H), 7.28 – 7.23 (m, 2H), 7.20 (dd, J = 7.0, 1.8 Hz, 1H), 7.18 – 7.13 (m, 2H), 6.91 – 6.86 (m, 2H), 4.98 (s, 2H), 4.80 (s, 1H), 2.36 (s, 3H), 2.31 (d, J = 0.6 Hz, 6H), 2.23 (s, 6H). ¹³C NMR (126 MHz, cdcl₃) δ 198.61, 157.89, 156.49, 136.84, 136.72, 134.74, 130.39, 129.24, 128.69, 128.30, 126.03, 117.19, 114.84, 68.59, 38.19, 30.36, 19.32, 18.86. ESI MS m/z 389.17 (M - H)-

1-(2-methylbenzyl)-1H-indole-4-carbaldehyde (**6g**) [sz-10-61]

Following the general procedure of intermediate **6**, using 4-Formyl-1H-indole (100 mg, 1 Eq, 689 μmol), Compound **6g** was isolated (0.15g, 89%). ¹H NMR (499 MHz, cdcl₃) δ 10.28 (d, J = 0.7 Hz, 1H), 7.66 (dt, J = 7.2, 0.8 Hz, 1H), 7.57 (dd, J = 8.2, 0.9 Hz, 1H), 7.36 – 7.30 (m, 2H), 7.24

(dd, J = 5.3, 3.6 Hz, 3H), 7.11 (dt, J = 8.5, 4.3 Hz, 1H), 6.73 (d, J = 7.6 Hz, 1H), 5.37 (s, 2H), 2.32 (s, 3H).

1-(2-methylbenzyl)-1H-benzo[d]imidazole-5-carbaldehyde (6h) [sz-10-88-02-02]

Following the general procedure of intermediate **6**, 1H-benzo[d]imidazole-6-carbaldehyde (100 mg, 1.0 Eq, 684 μ mol) was used. The crude material was chromatographed over silica gel, eluting with 0-30% EtOAc/DCM. Regioisomers were separated. Compound **6h** was isolated (0.07g, 38%). ¹H NMR (499 MHz, cdcl₃) δ 10.08 (s, 1H), 8.36 – 8.28 (m, 1H), 7.93 (s, 1H), 7.86 (dd, J = 8.4, 1.5 Hz, 1H), 7.41 (d, J = 8.5 Hz, 1H), 7.31 – 7.23 (m, 2H), 7.17 (td, J = 7.4, 1.7 Hz, 1H), 6.94 (dd, J = 7.7, 1.3 Hz, 1H), 5.36 (s, 2H), 2.30 (s, 3H).

1-(2-methylbenzyl)-1H-benzo[d]imidazole-6-carbaldehyde (6i) [sz-10-88-02-01]

Following the general procedure of intermediate **6**, 1H-benzo[d]imidazole-6-carbaldehyde (100 mg, 1.0 Eq, 684 μ mol) was used. The crude material was chromatographed over silica gel, eluting with 0-30% EtOAc/DCM. Regioisomers were separated. Compound **6i** was isolated (0.06g, 35%). ¹H NMR (499 MHz, cdcl₃) δ 10.05 (s, 1H), 7.96 (s, 1H), 7.95 – 7.89 (m, 2H), 7.83 (dd, J = 8.3, 1.5 Hz, 1H), 7.31 – 7.23 (m, 2H), 7.18 (td, J = 7.3, 1.8 Hz, 1H), 6.95 (d, J = 7.6 Hz, 1H), 5.39 (s, 2H), 2.32 (s, 3H).

1-(2-methylbenzyl)-1H-indazole-5-carbaldehyde (6j) [sz-10-60-01]

Following the general procedure of intermediate **6**, Indazole-5-carbaldehyde (100 mg, 1 Eq, 684 μ mol) was used. The crude material was chromatographed over silica gel, eluting with 0-30% EtOAc/Hex. Regioisomers were separated. Compound **6j** was isolated (0.1, 57%). ¹H NMR (499 MHz, cdcl₃) δ 10.05 (s, 1H), 8.29 (s, 1H), 8.23 (d, J = 1.1 Hz, 1H), 7.90 (dd, J = 8.7, 1.3 Hz, 1H), 7.39 (d, J = 8.9 Hz, 1H), 7.25 – 7.19 (m, 2H), 7.13 (t, J = 7.3 Hz, 1H), 6.87 (d, J = 7.6 Hz, 1H), 5.64 (s, 2H), 2.35 (s, 3H). ¹³C NMR (126 MHz, cdcl₃) δ 191.43, 142.13, 135.97, 135.54, 133.97, 130.72, 130.59, 128.20, 127.75, 127.52, 126.37, 125.49, 124.07, 110.14, 51.62, 51.52, 19.31.

2-(2-methylbenzyl)-2H-indazole-5-carbaldehyde (6k) [sz-10-60-02]

Following the general procedure of intermediate **6**, Indazole-5-carbaldehyde (100 mg, 1 Eq, 684 μ mol) was used. The crude material was chromatographed over silica gel, eluting with 0-30% EtOAc/Hex. Regioisomers were separated. Compound **6k** was isolated (0.07, 43%).

8-(4-((2-methylbenzyl)oxy)phenyl)-3,5,6,8-tetrahydro-1H-dicyclopenta[b,e]pyran-1,7(2H)-dione (CCG366673) [sz-10-41]

Following the general procedure for **7**, 4-((2-methylbenzyl)oxy)benzaldehyde (**6a**) (0.1g, 1 Eq, 442 μ mol) and cyclopentane-1,3-dione (87.1 mg, 2.01 Eq, 888 μ mol) were used. 0.08g of desired compound was isolated (47% yield). ¹H NMR (499 MHz, cdcl₃) δ 7.37 (d, J = 7.1 Hz, 1H), 7.26 – 7.22 (m, 1H), 7.22 – 7.19 (m, 2H), 7.08 – 7.04 (m, 2H), 6.86 – 6.81 (m, 2H), 5.30 (s, 1H), 4.97 (s, 2H), 2.62 (s, 8H), 2.35 (s, 3H). ¹³C NMR (126 MHz, cdcl₃) δ 200.36, 157.49, 136.70, 134.85, 132.15, 130.37, 128.67, 128.24, 128.11, 126.01, 118.82, 114.62, 68.58, 30.61, 29.45, 18.86. ESI MS m/z 387.15 (M + H)⁺

1,6,6-trimethyl-9-(4-((2-methylbenzyl)oxy)phenyl)-5,6,7,9-tetrahydrochromeno[3,2-c]pyrazol-8(1H)-one (CCG367106) [sz-11-23]

To a solution of 4-((2-methylbenzyl)oxy)benzaldehyde (**6a**) (100 mg, 1 Eq, 442 μ mol), 4-Hydroxy-1-methyl-1H-pyrazole (44.2 mg, 1.02 Eq, 451 μ mol) and 5,5-dimethylcyclohexane-1,3-dione (61.9 mg, 1 Eq, 442 μ mol) in 70% 2-propanol (3.38 mL) was treated with H₂SO₄ (4.33 mg, 2.36 μ L, .1 Eq, 44.2 μ mol). The reaction was refluxed at 120°C for 16 h. The reaction mixture was cooled to room temp and concentrated. The crude material was first rinsed with water and dried under reduced pressure. Then, it was chromatographed over silica gel, eluting with 0-40% EtOAc/Hex. Desired compound was isolated as a clear gum (0.006g, 3% yield). ¹H NMR (400 MHz, cdcl₃) δ 7.37 (d, J = 7.0 Hz, 1H), 7.31 (s, 1H), 7.25 – 7.17 (m, 3H), 7.17 – 7.12 (m, 2H), 6.91 – 6.84 (m, 2H), 5.08 (s, 1H), 4.96 (s, 2H), 3.49 (s, 3H), 2.53 (s, 2H), 2.35 (s, 3H), 2.30 – 2.14 (m, 2H), 1.10 (s, 3H), 1.01 (s, 3H). ¹³C NMR (126 MHz, cdcl₃) δ 196.94, 164.59, 157.80, 136.73, 135.78, 134.75, 134.38, 130.37, 129.50, 128.71, 128.28, 127.32, 126.00, 123.98, 114.65, 112.52, 68.57, 50.91, 41.87, 36.84, 34.58, 32.11, 28.79, 27.48, 18.87. ESI MS m/z 429.21 (M + H)⁺

3,3,6,6-tetramethyl-9-(1-(2-methylbenzyl)-1H-indol-4-yl)-3,4,5,6,7,9-hexahydro-1H-xanthene-1,8(2H)-dione (CCG366795) [sz-10-78]

Following the general procedure for **7**, 1-(2-methylbenzyl)-1H-indole-4-carbaldehyde (**6g**) (75mg, 1 Eq, 0.30mmol) and 5,5-dimethylcyclohexane-1,3-dione (85 mg, 2.01 Eq, 0.60 mmol) were used. 0.01g of desired compound was isolated (8% yield). ¹H NMR (499 MHz, cdcl₃) δ 7.18 (dt, J = 4.1, 1.2 Hz, 2H), 7.12 – 7.02 (m, 4H), 6.97 (dd, J = 3.3, 0.9 Hz, 1H), 6.78 (d, J = 7.6 Hz, 1H), 6.73 (d, J = 3.3 Hz, 1H), 5.19 (s, 2H), 5.18 – 5.13 (m, 1H), 2.49 (s, 4H), 2.28 (s, 3H), 2.25 – 2.07 (m, 4H), 1.10 (s, 6H), 0.94 (s, 6H). ¹³C NMR (126 MHz, cdcl₃) δ 196.46, 161.65, 136.85, 136.21, 135.79, 135.27, 130.29, 127.79, 127.59, 127.47, 126.28, 121.36, 120.46, 115.67, 107.92, 100.59, 50.74, 48.15, 40.89, 32.10, 30.18, 29.26, 27.40, 19.09. ESI MS m/z 516.25 (M + Na)⁺

3,3,6,6-tetramethyl-9-(1-(2-methylbenzyl)-1H-benzo[d]imidazol-5-yl)-3,4,5,6,7,9-hexahydro-1H-xanthene-1,8(2H)-dione (CCG367064) [sz-10-84]

Following the general procedure for **7**, 1-(2-methylbenzyl)-1H-benzo[d]imidazole-5-carbaldehyde (**6h**) (60 mg, 1 Eq, 0.24 mmol) and 5,5-dimethylcyclohexane-1,3-dione (68 mg, 2.01 Eq, 0.48 mmol) were used. 0.03g of desired compound was isolated (28% yield). ¹H NMR (499 MHz, cdcl₃) δ 7.65 (s, 1H), 7.56 – 7.47 (m, 2H), 7.24 (dd, J = 7.3, 1.4 Hz, 1H), 7.22 (d, J = 1.5 Hz, 1H), 7.20 (d, J = 8.3 Hz, 1H), 7.16 (td, J = 7.4, 1.7 Hz, 1H), 7.00 (dd, J = 7.6, 1.3 Hz, 1H), 5.21 (s, 2H), 4.85 (s, 1H), 2.55 – 2.39 (m, 4H), 2.28 (s, 3H), 2.25 – 2.10 (m, 4H), 1.09 (s, 6H), 0.98 (s, 6H). ¹³C NMR (126 MHz, cdcl₃) δ 196.66, 162.05, 144.11, 142.81, 139.42, 136.20, 132.96, 130.79, 128.53, 128.51, 126.61, 125.51, 118.72, 116.09, 109.00, 50.82, 47.06, 40.87, 32.18, 31.76, 29.07, 27.71, 19.12. ESI MS m/z 495.26 (M + H)⁺

3,3,6,6-tetramethyl-9-(1-(2-methylbenzyl)-1H-benzo[d]imidazol-6-yl)-3,4,5,6,7,9-hexahydro-1H-xanthene-1,8(2H)-dione (CCG367107) [sz-10-96]

Following the general procedure for **7**, 1-(2-methylbenzyl)-1H-benzo[d]imidazole-6-carbaldehyde (**6i**) (40 mg, 1 Eq, 0.16 mmol) and 5,5-dimethylcyclohexane-1,3-dione (45 mg, 2.01 Eq, 0.32 mmol) were used. 0.02g of desired compound was isolated (22% yield). ¹H NMR (499 MHz, cd₃od) δ 7.71 (s, 1H), 7.54 (d, J = 8.4 Hz, 1H), 7.33 (d, J = 1.6 Hz, 1H), 7.28 – 7.18 (m, 2H), 7.18 – 7.10 (m, 2H), 6.99 (d, J = 7.5 Hz, 1H), 5.31 (s, 2H), 4.78 (s, 1H), 2.54 – 2.42 (m, 4H), 2.28 (s, 3H), 2.21 (d, J = 16.3 Hz, 2H), 2.09 (d, J = 16.3 Hz, 2H), 1.08 (s, 6H), 0.92 (s, 6H). ¹³C NMR (126 MHz, cd₃od) δ 197.69, 163.09, 142.82, 141.54, 139.59, 132.83, 130.75, 128.53, 128.40, 126.50, 122.95, 118.86, 115.54, 110.44, 77.61, 77.35, 77.10, 50.50, 46.98, 40.60, 32.06, 31.98, 28.80, 26.87, 18.67. ESI MS m/z 495.26 (M + H)⁺

3,3,6,6-tetramethyl-9-(1-(2-methylbenzyl)-1H-indazol-5-yl)-3,4,5,6,7,9-hexahydro-1H-xanthene-1,8(2H)-dione (CCG366793) [sz-10-69]

Following the general procedure for **7**, 1-(2-methylbenzyl)-1H-indazole-5-carbaldehyde (**6j**) (55 mg, 1 Eq, 0.22 mmol) and 5,5-dimethylcyclohexane-1,3-dione (62 mg, 2.01 Eq, 0.44 mmol) were used. 0.03g of desired compound was isolated (25% yield). ¹H NMR (499 MHz, cdcl₃) δ 7.93 (d, J = 1.0 Hz, 1H), 7.60 (d, J = 1.6 Hz, 1H), 7.37 – 7.30 (m, 1H), 7.21 – 7.13 (m, 3H), 7.09 (td, J = 6.7, 5.6, 3.1 Hz, 1H), 6.87 (d, J = 7.6 Hz, 1H), 5.49 (s, 2H), 4.86 (s, 1H), 2.49 (s, 4H), 2.34 (s, 3H), 2.27 – 2.12 (m, 4H), 1.11 (s, 6H), 0.99 (s, 6H). ¹³C NMR (126 MHz, cdcl₃) δ 196.51, 162.12,

138.99, 137.04, 135.89, 134.83, 133.29, 130.42, 127.97, 127.72, 126.21, 124.38, 120.28, 115.91, 108.76, 51.18, 50.76, 40.88, 32.22, 31.60, 29.16, 27.50, 19.34. ESI MS m/z 517.24 (M + Na)⁺
3,3,6,6-tetramethyl-9-(2-(2-methylbenzyl)-2H-indazol-5-yl)-3,4,5,6,7,9-hexahydro-1H-xanthene-1,8(2H)-dione (CCG367104) [sz-11-27]

Following the general procedure for **7**, 2-(2-methylbenzyl)-2H-indazole-5-carbaldehyde (**6k**) (74 mg, 1 Eq, 0.30 mmol) and 5,5-dimethylcyclohexane-1,3-dione (91 mg, 2.2 Eq, 0.65 mmol) were used. 0.07g of desired compound was isolated (49% yield). ¹H NMR (499 MHz, cdcl₃) δ 7.63 (s, 1H), 7.61 (d, J = 1.7 Hz, 1H), 7.56 (dd, J = 9.0, 1.0 Hz, 1H), 7.26 – 7.23 (m, 1H), 7.22 – 7.16 (m, 2H), 7.10 (dd, J = 9.0, 1.7 Hz, 1H), 7.08 – 7.04 (m, 1H), 5.53 (s, 2H), 4.82 (s, 1H), 2.46 (s, 4H), 2.28 (s, 3H), 2.25 – 2.10 (m, 4H), 1.09 (s, 6H), 0.98 (s, 6H). ¹³C NMR (126 MHz, cdcl₃) δ 196.46, 162.27, 148.14, 136.78, 136.60, 133.63, 130.66, 129.31, 128.64, 126.49, 126.44, 122.91, 121.91, 119.83, 117.21, 115.54, 55.45, 50.78, 40.88, 32.18, 31.91, 29.24, 27.37, 19.06. ESI MS m/z 495.26 (M + H)⁺

3,3,6,6-tetramethyl-9-(4-((2-methylbenzyl)oxy)phenyl)-3,4,6,7,9,10-hexahydroacridine-1,8(2H,5H)-dione (17a) (CCG366670) [sz-11-03]

To a solution of 4-((2-methylbenzyl)oxy)benzaldehyde (**6a**) (500 mg, 1 Eq, 2.21 mmol) and 5,5-dimethylcyclohexane-1,3-dione (626 mg, 2.02 Eq, 4.46 mmol) in 70% 2-propanol (7mL) was treated with ammonium acetate (511 mg, 3 Eq, 6.63 mmol) and TEA (447 mg, 616 μL, 2 Eq, 4.42 mmol). The reaction was refluxed at 120°C for 16h. The reaction mixture was cooled to room temp and concentrated. The solids were diluted with water. The mixture was extracted with DCM (x3), and the organic layer was washed with brine, dried over MgSO₄, and dried under reduced pressure. Desired compound was isolated as yellow solids (0.8g, 80% yield). ¹H NMR (499 MHz, cdcl₃) δ 7.40 – 7.32 (m, 1H), 7.28 (s, 1H), 7.26 (d, J = 2.0 Hz, 1H), 7.24 – 7.21 (m, 1H), 7.18 (dd, J = 7.8, 6.0 Hz, 2H), 6.85 – 6.78 (m, 2H), 6.27 (s, 1H), 5.05 (s, 1H), 4.92 (s, 2H), 2.35 (d, J = 17.6 Hz, 5H), 2.27 – 2.15 (m, 6H), 1.09 (s, 6H), 0.99 (s, 6H). ¹³C NMR (126 MHz, cdcl₃) δ 195.34, 157.16, 147.14, 139.18, 136.78, 135.10, 130.28, 128.99, 128.80, 128.14, 125.96, 114.17, 113.99, 68.45, 50.76, 41.24, 32.79, 32.70, 29.46, 27.27, 18.88. ESI MS m/z 470.26 (M + H)⁺

General Procedure for Compound 18

To a solution 3,3,6,6-tetramethyl-9-(4-((2-methylbenzyl)oxy)phenyl)-3,4,6,7,9,10-hexahydroacridine-1,8(2H,5H)-dione (**17a**) (0.1g, 1 Eq, 0.21 mmol) and alkyl bromide (90 mg,

3.0 Eq, 0.64 mmol) in DMF (1mL) was treated with Cs₂CO₃ (0.14 g, 2 Eq, 0.43 mmol) and sodium iodide (3.19 mg, 0.1 Eq, 21.3 μmol). The reaction mixture heated to 90-150°C in pressure vessel until the reaction was complete. The mixture was cooled to room temp and was diluted with water. The solids were filtered. The crude material was chromatographed over silica gel, eluting with 0-90% EtOAc/Hex. Compounds were isolated above 95% pure.

10-(2-methoxyethyl)-3,3,6,6-tetramethyl-9-(4-((2-methylbenzyl)oxy)phenyl)-3,4,6,7,9,10-hexahydroacridine-1,8(2H,5H)-dione (CCG367087) [sz-11-16]

Following the general procedure for **18**, 1-bromo-2-methoxyethane (88.8 mg, 60.0 μL, 3 Eq, 639 μmol) was used. 0.08g of desired compound was isolated (67% yield). ¹H NMR (400 MHz, cdcl₃) δ 7.35 (dd, J = 6.9, 2.3 Hz, 1H), 7.26 (d, J = 1.9 Hz, 1H), 7.25 – 7.22 (m, 1H), 7.22 – 7.13 (m, 3H), 6.85 – 6.76 (m, 2H), 5.19 (s, 1H), 4.92 (s, 2H), 3.92 (t, J = 5.0 Hz, 2H), 3.49 (t, J = 4.9 Hz, 2H), 3.36 (s, 3H), 2.64 (d, J = 16.6 Hz, 2H), 2.32 (s, 3H), 2.30 (d, J = 16.5 Hz, 2H), 2.20 (s, 4H), 2.16 (s, 4H), 1.07 (s, 6H), 0.98 (s, 6H). ¹³C NMR (101 MHz, cdcl₃) δ 195.92, 156.97, 150.27, 138.81, 136.76, 135.13, 130.29, 128.80, 128.75, 128.12, 125.93, 115.84, 114.12, 72.28, 68.46, 59.06, 49.96, 44.09, 40.56, 32.54, 31.22, 31.17, 29.24, 27.97, 18.88. ESI MS m/z 528.31 (M + H)⁺

10-(2-(dimethylamino)ethyl)-3,3,6,6-tetramethyl-9-(4-((2-methylbenzyl)oxy)phenyl)-3,4,6,7,9,10-hexahydroacridine-1,8(2H,5H)-dione (CCG367088) [sz-11-18]

Following the general procedure for **18**, 2-Bromo-N,N-dimethylethylamine Hydrobromide (124 mg, 2.5 Eq, 532 μmol) was used. The crude material was chromatographed over silica gel, eluted with 0-20% MeOH/DCM. 0.005g of desired compound was isolated (4% yield). ¹H NMR (400 MHz, cdcl₃) δ 7.36 (dd, J = 6.9, 2.5 Hz, 1H), 7.19 (dq, J = 7.0, 5.1, 4.6 Hz, 5H), 6.83 – 6.76 (m, 2H), 5.19 (s, 1H), 4.93 (s, 2H), 3.78 (t, J = 7.1 Hz, 2H), 2.55 (d, J = 16.6 Hz, 2H), 2.47 (t, J = 7.1 Hz, 2H), 2.38 (d, J = 16.6 Hz, 2H), 2.33 (d, J = 1.4 Hz, 9H), 2.22 (s, 4H), 1.08 (s, 6H), 1.00 (s, 6H). ¹³C NMR (101 MHz, cdcl₃) δ 195.66, 157.04, 149.71, 138.65, 136.75, 135.14, 130.28, 128.72, 128.11, 125.94, 115.91, 114.18, 68.47, 59.90, 49.91, 45.94, 42.97, 40.44, 32.55, 31.24, 29.25, 27.97, 18.88. ESI MS m/z 541.34 (M + H)⁺

10-(2-aminoethyl)-3,3,6,6-tetramethyl-9-(4-((2-methylbenzyl)oxy)phenyl)-3,4,6,7,9,10-hexahydroacridine-1,8(2H,5H)-dione (CCG367212) [sz-11-38]

Following the general procedure for **18**, tert-butyl (2-bromoethyl)carbamate (95.4 mg, 2 Eq, 426 μmol) was used. 0.03g of desired compound was isolated (24% yield). ¹H NMR (499 MHz, cdcl₃) δ 7.35 (dd, J = 7.1, 2.1 Hz, 1H), 7.24 – 7.20 (m, 1H), 7.19 – 7.14 (m, 4H), 6.82 – 6.76 (m, 2H),

5.26 (s, 1H), 4.92 (s, 2H), 3.74 (t, J = 6.6 Hz, 2H), 2.88 (t, J = 6.5 Hz, 2H), 2.62 (d, J = 16.7 Hz, 2H), 2.36 (d, J = 16.6 Hz, 2H), 2.32 (s, 3H), 2.24 (d, J = 1.4 Hz, 4H), 1.25 – 1.11 (m, 2H), 1.08 (s, 6H), 1.02 (s, 6H). ¹³C NMR (126 MHz, cdcl₃) δ 195.74, 157.10, 150.39, 138.23, 136.67, 135.10, 130.27, 128.63, 128.28, 128.08, 125.92, 115.82, 114.37, 68.49, 50.02, 47.22, 42.81, 40.65, 32.62, 30.57, 29.10, 28.16, 18.85. ESI MS m/z 513.30 (M + H)⁺

3,3,6,6-tetramethyl-10-(2-(methylamino)ethyl)-9-(4-((2-methylbenzyl)oxy)phenyl)-3,4,6,7,9,10-hexahydroacridine-1,8(2H,5H)-dione (CCG369574) [sz-11-86]

Following the general procedure for **18**, tert-butyl (2-chloroethyl)(methyl)carbamate (82.5 mg, 2 Eq, 426 μmol) was used. 0.05g of desired compound was isolated (48% yield). ¹H NMR (400 MHz, cdcl₃) δ 8.13 (s, 1H), 7.31 (dd, J = 6.8, 2.3 Hz, 1H), 7.28 (s, 1H), 7.26 (s, 1H), 7.23 – 7.18 (m, 1H), 7.17 – 7.13 (m, 2H), 6.83 – 6.78 (m, 2H), 5.06 (s, 1H), 4.84 (s, 2H), 4.39 – 4.22 (m, 2H), 3.65 – 3.51 (m, 2H), 2.90 (s, 3H), 2.29 (s, 3H), 2.25 (s, 2H), 2.22 (d, J = 5.7 Hz, 3H), 2.20 – 2.10 (m, 3H), 1.05 (s, 6H), 0.95 (s, 6H). ¹³C NMR (101 MHz, cdcl₃) δ 196.04, 157.10, 149.16, 139.50, 136.81, 134.93, 130.29, 128.95, 128.87, 128.21, 125.97, 114.07, 113.27, 68.39, 61.56, 50.91, 46.82, 40.57, 32.81, 32.58, 31.14, 29.54, 27.18, 18.89. ESI MS m/z 544.35 (M + NH₄)⁺

3,3,6,6,10-pentamethyl-9-(4-((2-methylbenzyl)oxy)phenyl)-3,4,6,7,9,10-hexahydroacridine-1,8(2H,5H)-dione (17b) (CCG366672) [sz-10-37]

To a mixture of 4-((2-methylbenzyl)oxy)benzaldehyde (100 mg, 1 Eq, 442 μmol), 5,5-dimethylcyclohexane-1,3-dione (125 mg, 2.02 Eq, 893 μmol) in 2-propanol (3mL), was treated with potassium acetate (65.1 mg, 1.5 Eq, 663 μmol) and methylamine hydrochloride (44.8 mg, 1.5 Eq, 663 μmol). The reaction was refluxed at 120°C for 16h. The reaction mixture was cooled to room temp and concentrated. The solids were diluted with water. The mixture was extracted with DCM (x3), and the organic layer was washed with brine, dried over MgSO₄, and dried under reduced pressure. Compound **17b** was isolated as yellow solids (0.1g, 49% yield). ¹H NMR (499 MHz, cdcl₃) δ 7.39 – 7.33 (m, 1H), 7.26 – 7.13 (m, 5H), 6.86 – 6.75 (m, 2H), 5.23 (s, 1H), 4.94 (d, J = 1.2 Hz, 2H), 3.27 (d, J = 1.2 Hz, 3H), 2.59 (dd, J = 16.7, 1.3 Hz, 2H), 2.36 (d, J = 16.7 Hz, 2H), 2.34 (s, 3H), 2.23 (d, J = 1.3 Hz, 4H), 1.09 (d, J = 1.3 Hz, 6H), 1.05 (d, J = 1.3 Hz, 6H). ¹³C NMR (126 MHz, cdcl₃) δ 195.36, 157.12, 150.75, 138.49, 136.72, 135.16, 130.29, 128.71, 128.55, 128.11, 125.95, 115.27, 114.28, 68.48, 49.97, 40.58, 33.40, 32.72, 31.04, 28.83, 28.58, 18.86. ESI MS m/z 484.28 (M + H)⁺

3-(dimethylamino)picolinaldehyde (13b) [sz-12-84]

Following the general procedure, commercially available 3-fluoropicolinaldehyde (300 mg, 1 Eq, 2.40 mmol) and dimethylamine HCl (391 mg, 2 Eq, 4.80 mmol) were used. Compound **13b** was isolated 0.32g (89% yield). ¹H NMR (499 MHz, cdcl₃) δ 10.09 (s, 1H), 8.25 (dd, J = 3.9, 1.5 Hz, 1H), 7.36 – 7.29 (m, 2H), 2.98 (s, 6H).

2-(azetidin-1-yl)benzaldehyde (13c) [sz-12-28]

Following the general procedure, commercially available 2-fluorobenzaldehyde (200 mg, 1 Eq, 1.61 mmol) and azetidine (138 mg, 1.5 Eq, 2.42 mmol) were used. Compound **13c** was isolated 0.16g (62% yield). ¹H NMR (499 MHz, cdcl₃) δ 10.00 (s, 1H), 7.68 (dd, J = 8.0, 1.6 Hz, 1H), 7.39 (td, J = 8.1, 7.5, 1.6 Hz, 1H), 6.80 (t, J = 7.4 Hz, 1H), 6.50 (d, J = 8.4 Hz, 1H), 4.08 (t, J = 7.5 Hz, 4H), 2.46 – 2.36 (m, 2H).

3-(azetidin-1-yl)picolinaldehyde (13d) [sz-12-77]

Following the general procedure, commercially available 3-fluoropicolinaldehyde (100 mg, 1 Eq, 0.8 mmol) and azetidine (69 mg, 1.5 Eq, 1.2 mmol) were used. Compound **13d** was isolated 0.1g (77% yield). ¹H NMR (499 MHz, cdcl₃) δ 10.02 (s, 1H), 8.16 (dd, J = 4.4, 1.2 Hz, 1H), 7.28 (dd, J = 8.6, 4.2 Hz, 1H), 6.90 (d, J = 8.6 Hz, 1H), 4.06 (t, J = 7.5 Hz, 4H), 2.41 (p, J = 7.6 Hz, 2H).

(3-(dimethylamino)pyridin-2-yl)methanol (14ab) [sz-12-90]

Following the general procedure for Intermediate **14**, 3-(dimethylamino)picolinaldehyde (**13b**) (320 mg, 1 Eq, 2.13 mmol) was used. Compound **14ab** was isolated without further purification 0.32g (98% yield). ¹H NMR (400 MHz, cdcl₃) δ 8.24 (d, J = 5.1 Hz, 1H), 7.36 (d, J = 7.9 Hz, 1H), 7.18 (dd, J = 8.1, 4.7 Hz, 1H), 4.78 (s, 2H), 2.71 (d, J = 0.6 Hz, 6H).

(2-(azetidin-1-yl)phenyl)methanol (14ac) [sz-12-31]

Following the general procedure for Intermediate **14**, 2-(azetidin-1-yl)benzaldehyde (**13c**) (160 mg, 1 Eq, 0.99 mmol) was used, and Compound **61c** was isolated without further purification 0.09g (56% yield). ¹H NMR (499 MHz, cdcl₃) δ 7.25 – 7.18 (m, 2H), 6.86 (t, J = 7.4 Hz, 1H), 6.65 (d, J = 8.1 Hz, 1H), 4.64 (s, 2H), 3.99 (t, J = 7.2 Hz, 4H), 2.35 (q, J = 7.3 Hz, 2H).

(3-(azetidin-1-yl)pyridin-2-yl)methanol (14ad) [sz-12-81]

Following the general procedure for Intermediate **14**, 3-(azetidin-1-yl)picolinaldehyde (**13d**) (90 mg, 1 Eq, 0.55 mmol) was used, and Compound **14ad** was isolated without further purification 0.05g (55% yield). ¹H NMR (400 MHz, cdcl₃) δ 8.02 (d, J = 4.6 Hz, 1H), 7.12 (dd, J = 8.1, 4.8 Hz, 1H), 6.75 (d, J = 8.1 Hz, 1H), 4.62 (s, 2H), 3.93 (t, J = 7.2 Hz, 4H), 2.36 (q, J = 7.2 Hz, 2H).

2-(bromomethyl)-N,N-dimethylpyridin-3-amine (15b) [sz-13-01]

Following the general procedure for **15**, (3-(dimethylamino)pyridin-2-yl)methanol (**14ab**) (340 mg, 1 Eq, 0.37 mmol) was used, and Compound **15b** was isolated 0.22g (46% yield). ¹H NMR (499 MHz, cdcl₃) δ 8.28 – 8.21 (m, 1H), 7.88 (s, 1H), 7.66 (s, 1H), 5.11 (s, 2H), 3.10 (s, 6H).

1-(2-(bromomethyl)phenyl)azetidine (15c) [sz-12-86]

Following the general procedure for **15**, (2-(azetidin-1-yl)phenyl)methanol (**14ac**) (60 mg, 1 Eq, 0.37 mmol) was used, and Compound **15c** was isolated 0.03g (32% yield). ¹H NMR (499 MHz, cdcl₃) δ 7.20 (t, J = 7.6 Hz, 1H), 7.14 (d, J = 7.4 Hz, 1H), 6.93 (d, J = 8.1 Hz, 1H), 6.80 (t, J = 7.4 Hz, 1H), 4.34 (s, 2H), 3.35 (s, 2H), 3.15 (t, J = 6.4 Hz, 2H), 1.98 (p, J = 6.4 Hz, 2H).

3-(azetidin-1-yl)-2-(bromomethyl)pyridine (15d) [sz-12-92]

Following the general procedure for **15**, (3-(azetidin-1-yl)pyridin-2-yl)methanol (**14ad**) (65 mg, 1 Eq, 0.4 mmol) was used, and Compound **15d** was isolated 0.01g (11% yield). ¹H NMR (400 MHz, cdcl₃) δ 8.04 (dd, J = 4.5, 1.2 Hz, 1H), 7.26 (d, J = 1.2 Hz, 1H), 7.15 (dd, J = 8.2, 4.6 Hz, 1H), 4.59 (s, 2H), 3.40 (t, J = 6.8 Hz, 2H), 3.14 (t, J = 6.2 Hz, 2H), 1.97 (p, J = 6.5 Hz, 2H).

(4-chloro-2-(difluoromethoxy)phenyl)methanol (14bb) [sz-09-93]

Following the general procedure for Intermediate **14**, commercially available 4-chloro-2-(difluoromethoxy)benzaldehyde (200 mg, 1 Eq, 968 μmol) in EtOH (4mL) was used. Compound **14bb** was isolated (0.1g, 84% yield). ¹H NMR (400 MHz, cdcl₃) δ 7.42 (d, J = 8.2 Hz, 1H), 7.23 (dd, J = 8.2, 2.0 Hz, 1H), 7.15 (dd, J = 2.1, 1.0 Hz, 1H), 6.55 (t, J = 73.3 Hz, 1H), 4.71 (d, J = 6.0 Hz, 2H), 1.86 (t, J = 6.1 Hz, 1H).

(5-chloro-3-methoxypyridin-2-yl)methanol (14bc) [sz-12-06]

Following the general procedure for Intermediate **14**, commercially available 5-chloro-3-methoxypicolinaldehyde (70 mg, 1 Eq, 0.41 mmol) in EtOH (2mL) was used, and 0.04g of Compound **14bc** was isolated (59% yield). ¹H NMR (499 MHz, cdcl₃) δ 8.28 (s, 1H), 8.19 (s, 1H), 4.85 (d, J = 6.4 Hz, 2H), 3.99 (s, 3H).

(3-cyclopropylpyridin-2-yl)methanol (14bd) [sz-12-40]

Following the general procedure for Intermediate **14**, commercially available 3-cyclopropylpicolinaldehyde (70 mg, 1 Eq, 0.48 mmol) in MeOH (3mL) was used. Compound **14bd** was isolated (0.07g, 97% yield). ¹H NMR (499 MHz, cdcl₃) δ 8.39 (d, J = 4.9 Hz, 1H), 7.34 (d, J = 7.7 Hz, 1H), 7.21 – 7.11 (m, 1H), 4.90 (s, 2H), 1.75 (td, J = 8.5, 4.3 Hz, 1H), 1.06 – 0.92 (m, 2H), 0.75 – 0.57 (m, 2H).

4-chloro-1-(chloromethyl)-2-(difluoromethoxy)benzene (16e) [sz-09-97]

Following general procedure for Compound **16**, (4-chloro-2-(difluoromethoxy)phenyl)methanol (170 mg, 1 Eq, 815 μmol) (**14bb**) was used, and 0.04g of the desired compound was isolated (23% yield). ^1H NMR (499 MHz, cdCl_3) δ 7.42 (d, $J = 8.2$ Hz, 1H), 7.23 (dt, $J = 8.2, 1.3$ Hz, 1H), 7.20 (dd, $J = 2.1, 1.0$ Hz, 1H), 6.57 (td, $J = 73.1, 0.8$ Hz, 1H), 4.61 (s, 2H). ^{19}F NMR (470 MHz, cdCl_3) δ -80.86, -81.02.

1-(chloromethyl)-2-ethylbenzene (16f) [sz-10-43]

Following general procedure for Compound **16**, commercially available (2-ethylphenyl)methanol (200 mg, 198 μL , 1 Eq, 1.47 mmol) was used, and 0.2g of the desired compound was isolated (93% yield). ^1H NMR (499 MHz, cdCl_3) δ 7.34 (dd, $J = 7.7, 1.4$ Hz, 1H), 7.30 (tt, $J = 7.4, 1.3$ Hz, 1H), 7.25 (d, $J = 7.5$ Hz, 1H), 7.21 (td, $J = 7.4, 1.5$ Hz, 1H), 4.65 (s, 2H), 2.80 (q, $J = 7.6$ Hz, 2H), 1.29 (td, $J = 7.6, 1.1$ Hz, 3H).

1-(chloromethyl)-2-(fluoromethyl)benzene (16g) [sz-11-81]

Following general procedure for Compound **16**, commercially available (2-Fluoromethyl-phenyl)-methanol (120 mg, 72.7 μL , 1 Eq, 856 μmol) was used, and 0.1g of Compound **16g** was isolated (98% yield). ^1H NMR (499 MHz, cdCl_3) δ 7.45 – 7.41 (m, 2H), 7.41 – 7.37 (m, 2H), 5.63 (s, 1H), 5.53 (s, 1H), 4.71 (s, 2H). ^{19}F NMR (470 MHz, cdCl_3) δ 23.28, 23.18, 23.08.

3-chloro-2-(chloromethyl)thiophene (16h) [sz-11-92]

Following general procedure for Compound **16**, commercially available (3-chlorothiophen-2-yl)methanol (200 mg, 1 Eq, 1.35 mmol) was used, and 0.2g of Compound **16h** was isolated (89% yield). ^1H NMR (400 MHz, cdCl_3) δ 7.32 – 7.29 (m, 1H), 6.91 (d, $J = 5.4$ Hz, 1H), 4.77 (d, $J = 0.7$ Hz, 2H).

5-chloro-2-(chloromethyl)-3-methoxypyridine (16i) [sz-12-12]

Following general procedure for Compound **16**, (5-chloro-3-methoxypyridin-2-yl)methanol (**14bc**) (40 mg, 1 Eq, 0.23 mmol) was used, and 0.04g of Compound **16i** was isolated (90% yield). ^1H NMR (499 MHz, cdCl_3) δ 8.30 (s, 1H), 8.21 (s, 1H), 4.71 (s, 2H), 4.01 (d, $J = 0.8$ Hz, 3H).

3-(chloromethyl)-2,6-dimethylpyridine (16j) [sz-12-51]

Following general procedure for Compound **16**, commercially available (2,6-dimethylpyridin-3-yl)methanol (67 mg, 1 Eq, 0.49 mmol) was used, and 0.05g of Compound **16j** was isolated (72% yield). ^1H NMR (499 MHz, cdCl_3) δ 7.49 (d, $J = 7.7$ Hz, 1H), 6.99 (d, $J = 8.3$ Hz, 1H), 4.58 (s, 2H), 2.53 (s, 6H).

3-(chloromethyl)-2-methoxy-6-methylpyridine (16k) [sz-12-63]

Following general procedure for Compound **16**, commercially available (2-methoxy-6-methylpyridin-3-yl)methanol (70 mg, 1 Eq, 0.46 mmol) was used, and 0.04g of Compound **16k** was isolated (54% yield). ¹H NMR (499 MHz, cdcl₃) δ 7.50 (d, J = 7.3 Hz, 1H), 7.42 (d, J = 7.3 Hz, 1H), 4.57 (s, 2H), 3.98 (s, 3H), 2.44 (s, 3H).

2-(chloromethyl)-3-cyclopropylpyridine (16l) [sz-12-43]

Following general procedure for Compound **16**, (3-cyclopropylpyridin-2-yl)methanol (**14bd**) (70 mg, 1 Eq, 0.47 mmol) was used, and 0.07g of Compound **16l** was isolated (89% yield). ¹H NMR (499 MHz, cdcl₃) δ 8.51 – 8.31 (m, 1H), 7.37 (d, J = 7.8 Hz, 1H), 7.21 (t, J = 6.5 Hz, 1H), 4.92 (s, 2H), 2.18 – 2.06 (m, 1H), 1.14 – 1.02 (m, 2H), 0.74 (dt, J = 6.7, 4.7 Hz, 2H).

3.7 References

- Banks, W. A. (2009). Characteristics of compounds that cross the blood-brain barrier. *BMC Neurology*, 9(1), S3. <https://doi.org/10.1186/1471-2377-9-S1-S3>
- Bellettato, C. M., & Scarpa, M. (2018). Possible strategies to cross the blood–brain barrier. *Italian Journal of Pediatrics*, 44(2), 131. <https://doi.org/10.1186/s13052-018-0563-0>
- Bioisosteres in Medicinal Chemistry* (1st ed.). (2012). John Wiley & Sons, Ltd. <https://doi.org/10.1002/9783527654307>
- Burford, N. T., Livingston, K. E., Canals, M., Ryan, M. R., Budenholzer, L. M. L., Han, Y., Shang, Y., Herbst, J. J., O’Connell, J., Banks, M., Zhang, L., Filizola, M., Bassoni, D. L., Wehrman, T. S., Christopoulos, A., Traynor, J. R., Gerritz, S. W., & Alt, A. (2015). Discovery, Synthesis, and Molecular Pharmacology of Selective Positive Allosteric Modulators of the δ -Opioid Receptor. *Journal of Medicinal Chemistry*, 58(10), 4220–4229. <https://doi.org/10.1021/acs.jmedchem.5b00007>
- Conn, P. J., Lindsley, C. W., Meiler, J., & Niswender, C. M. (2014). Opportunities and challenges in the discovery of allosteric modulators of GPCRs for treating CNS disorders. *Nature Reviews. Drug Discovery*, 13(9), 692–708. <https://doi.org/10.1038/nrd4308>
- Di, L., Fish, P. V., & Mano, T. (2012). Bridging solubility between drug discovery and development. *Drug Discovery Today*, 17(9), 486–495. <https://doi.org/10.1016/j.drudis.2011.11.007>
- Drug Bioavailability: Estimation of Solubility, Permeability, Absorption and Bioavailability, Volume 18*. (n.d.). Retrieved November 22, 2022
- El-Sepelgy, O., Haseloff, S., Alamsetti, S. K., & Schneider, C. (2014). Brønsted Acid Catalyzed, Conjugate Addition of β -Dicarbonyls to In Situ Generated ortho-Quinone Methides—Enantioselective Synthesis of 4-Aryl-4H-Chromenes. *Angewandte Chemie International Edition*, 53(30), 7923–7927. <https://doi.org/10.1002/anie.201403573>
- Kaushik, P., Kumar, A., Kumar, P., Kumar, S., Singh, B. K., & Bahadur, V. (2020). Cu-catalyzed one-pot multicomponent approach for the synthesis of symmetric and asymmetric 1,4-dihydropyridine (1,4-DHP) linked 1,2,3-triazole derivatives. *Synthetic Communications*, 50(13), 2033–2042. <https://doi.org/10.1080/00397911.2020.1762222>
- Kaya, M., Yıldırım, Y., & Çelik, G. Y. (2015). Synthesis, Characterization, and In Vitro Antimicrobial and Antifungal Activity of Novel Acridines. *Pharmaceutical Chemistry Journal*, 48(11), 722–726. <https://doi.org/10.1007/s11094-015-1181-4>
- Kerns, E. H., & Di, L. (2008). *Drug-like properties: Concepts, structure design and methods: from ADME to toxicity optimization*. Academic Press.

- Lindsley, C. W., Emmitte, K. A., Hopkins, C. R., Bridges, T. M., Gregory, K. J., Niswender, C. M., & Conn, P. J. (2016). Practical Strategies and Concepts in GPCR Allosteric Modulator Discovery: Recent Advances with Metabotropic Glutamate Receptors. *Chemical Reviews*, *116*(11), 6707–6741. <https://doi.org/10.1021/acs.chemrev.5b00656>
- Livingston, K. E., Stanczyk, M. A., Burford, N. T., Alt, A., Canals, M., & Traynor, J. R. (2018). Pharmacologic Evidence for a Putative Conserved Allosteric Site on Opioid Receptors. *Molecular Pharmacology*, *93*(2), 157–167. <https://doi.org/10.1124/mol.117.109561>
- Meanwell, N. A. (2015). The Influence of Bioisosteres in Drug Design: Tactical Applications to Address Developability Problems. In N. A. Meanwell (Ed.), *Tactics in Contemporary Drug Design* (pp. 283–381). Springer. https://doi.org/10.1007/7355_2013_29
- Mei, G.-J., Xu, S.-L., Zheng, W.-Q., Bian, C.-Y., & Shi, F. (2018). [4 + 2] Cyclization of para-Quinone Methide Derivatives with Alkynes. *The Journal of Organic Chemistry*, *83*(3), 1414–1421. <https://doi.org/10.1021/acs.joc.7b02942>
- Prueksaritanont, T., & Tang, C. (2012). ADME of Biologics—What Have We Learned from Small Molecules? *The AAPS Journal*, *14*(3), 410–419. <https://doi.org/10.1208/s12248-012-9353-6>
- Shang, Y., Yeatman, H. R., Provasi, D., Alt, A., Christopoulos, A., Canals, M., & Filizola, M. (2016). Proposed Mode of Binding and Action of Positive Allosteric Modulators at Opioid Receptors. *ACS Chemical Biology*, *11*(5), 1220–1229. <https://doi.org/10.1021/acscchembio.5b00712>
- Sharma, D., Soni, M., Kumar, S., & Gupta, G. (2009). *Solubility Enhancement – Eminent Role in Poorly Soluble Drugs*. 5.
- Waring, M. J. (2010). Lipophilicity in drug discovery. *Expert Opinion on Drug Discovery*, *5*(3), 235–248. <https://doi.org/10.1517/17460441003605098>
- Waterhouse, R. N. (2003). Determination of lipophilicity and its use as a predictor of blood–brain barrier penetration of molecular imaging agents. *Molecular Imaging & Biology*, *5*(6), 376–389. <https://doi.org/10.1016/j.mibio.2003.09.014>

Chapter 4 Improvement in the Metabolic Stability of Xanthene-dione Series of DOR PAMs

4.1 Summary

Metabolic stability is one of the most important considerations in the process of drug discovery. Metabolically stable substrates can reduce clearance from the body and lower the dosage requirements. In addition, this would reduce the potential of forming toxic metabolites during the process of metabolism and lower the toxicity of the drug. Since drugs are generally metabolized by liver microsomes, which is often mediated through cytochrome P450s, identification of the metabolic interspecies and sites of metabolism has been essential for drug development in order to improve metabolic stability. Throughout the years, computational modeling has been developed to predict the sites of metabolism and lower the cost and has shown to be successful. From the prediction of our benchmark compound **1** and the exhibition of its in vitro DMPK (distribution, metabolism, pharmacokinetics) profile, multiple potential sites of metabolism were identified. Further optimization of the xanthene-dione series to reduce metabolic stability is necessary to yield druggable substrates. In this chapter, I describe our strategies for improving the metabolic stability of the xanthene series of DOR PAMs.

4.2 Introduction

4.2.1 The problem of metabolism

About 90% of the drugs in clinical development fail to make it to market. Among the reasons for failure, 10-15% is due to poor pharmacokinetics and 30% due to toxicity (Prentis et al., 1988; *Research and Development in the Pharmaceutical Industry | Congressional Budget Office, 2021*;

Sun et al., 2022). Most compounds are made to target therapeutic efficacy, with less focus on their drug metabolism and pharmacokinetic properties until late stages (Baillie, 2008; Thompson, 2001). To improve the success rate and reduce the inefficiency of drug development, DMPK (distribution, metabolism, pharmacokinetics) of the drug candidates becomes a major component that should be addressed early in the development process (Kola & Landis, 2004). As one crucial component of DMPK properties, metabolic stability controls a drug's duration of action (clearance) and drug-induced toxicity (e.g. intermediate metabolites) (Guengerich & MacDonald, 2007; C. Lipinski & Hopkins, 2004). Furthermore, the exposure of the drug in the body is partially governed by the metabolic stability of the drug. Therefore, drug metabolism has played an increasing important role not only in identifying drug exposure, but also identifying safe drug candidates that are orally available with low dosage requirements (St. Jean & Fotsch, 2012; Stepan et al., 2013).

Metabolic instability in liver microsomes is one of the problems arising in early drug design, often mediated through cytochrome P450s (CYPs). This instability is characterized by short half-life and high clearance. Additionally, metabolically unstable compounds have low pharmaceutical efficacy and are often less safe, due to the potential formation of more toxic metabolites (Almond et al., 2009; St. Jean & Fotsch, 2012; Yeung et al., 2011; Zhang et al., 2009). Moreover, these new metabolites can lead to drug-drug interactions, enzyme inhibition, and therapeutic failure.(Almond et al., 2009; Yeung et al., 2011). Therefore, a balance of acceptable DMPK properties and pharmacological efficacy is necessary for the identification of a lead compound.

Lipinski's rule of five ($c\text{LogP} \leq 5$, $\text{MW} < 500$, no more than 5 H-donors and 10 H-acceptors) has become the rule of thumb for evaluating the drug-likeness including metabolic

stability. and application of these rules are more likely to result more druggable compounds (C. A. Lipinski, 2000). As an extension of Lipinski's rule of five, the rules for the development of lead-like substrates include $c\text{LogP} < 3$, $\text{MW} < 300$, no more than 3 H-donors, 3 H-acceptors, and 3 rotatable bonds has been used (Congreve et al., 2003). This is due to the difficulties in maintaining drug-likeness during the lead optimization while improving both selectivity and efficacy. Therefore, a reduction of the lipophilicity, the identification of the potential metabolic soft-spots, and blockage of metabolism without losing *in vitro* activity are important in the discovery process.

From the previous chapter, our benchmark compound **1** and the rest of xanthene-dione series suffer from low solubility. Due to the size of the compound ($\text{MW} \geq 470$) and greasiness

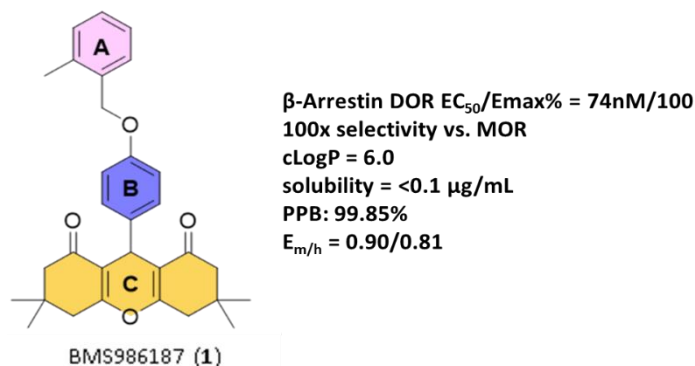


Figure 4.1 Chemical structure of **1**, and its receptor activities together with the DMPK profile

(high $c\text{LogP} = 6.0$) (**Figure 4.1**), these properties of the xanthene-diones significantly lower its metabolic stability ($E_{\text{m/h}} = 0.90/0.81$) and druggability. Thus, in this chapter, I describe attempts to improve the metabolic stability by lowering the $c\text{LogP}$ and identifying and blocking potential sites of metabolism (**Figure 4.1**).

4.3 Results

4.3.1 Computational prediction of potential sites of metabolism for **1**

CYPs are ubiquitous, but only three families (CYP1, CYP2 and CYP3) are involved in xenobiotic metabolism and metabolize >90% of the known drugs (Guengerich, 2006; Nebert & Russell, 2002). CYPs catalyze number of Phase I metabolic reactions, including hydroxylation, epoxidation, S/N-oxidation, alcohol/aldehyde oxidation, and dealkylation (Lewis et al., 2004; Lewis & Dickins, 2002; Phang-Lyn & Llerena, 2021; Zhang et al., 2009). After Phase I metabolic reactions, drugs become more hydrophilic and form active metabolites with the addition of the functional groups. These metabolites are then conjugated by Phase II enzymes and excreted from the body. Therefore, knowing which atoms of a drug lead will be oxidized or hydrolyzed by the CYP enzymes is important for remodeling the compound to reduce its rate of metabolism rate without losing activity (Kalgutkar & Soglia, 2005). However, it is too costly to identify all the interspecies or CYP-mediated sites of metabolism for all the interested drug candidates through experiments.

Based on experimental data gathered over years, computational CYP prediction models have been trained and developed to predict the potential sites of metabolism of a compound. A database of metabolic sites of 680 compounds has been made publicly available by Xenosite (Kirchmair et al., 2012; Zaretski et al., 2013). Usage of a computational predictor not only significantly reduces the cost, but also increases the speed of receiving the results (Issa et al., 2017). In addition, as a newer predictor model that was developed based on the developments of previous models, Xenosite has shown higher accuracy than other metabolic predictors. Herein, we used XenoSite to predict the *in vivo* metabolism of **1** (**Figure 4.2**) (Zaretski et al., 2013).

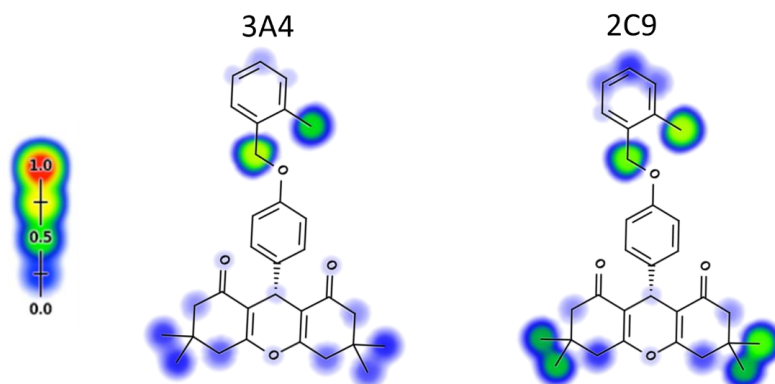


Figure 4.2 Predicted potential metabolic soft-spots of **1** with CYP isoforms 3A4 and 2C9 by XenoSite

Since the xanthene-dione PAMs are large in size and highly lipophilic, we chose CYP3A4 and CYP2C9 which are known to metabolize bulky and greasy compounds, to identify potential metabolic sites (Wester et al., 2004; Williams et al., 2004; Yano et al., 2004). Examples of the predicted xenobiotic metabolism of **1** by 3A4 and 2C6 are shown in **Figure 4.2** and the probabilities of each atom being metabolized are indicated by colors. Overall, due to the properties

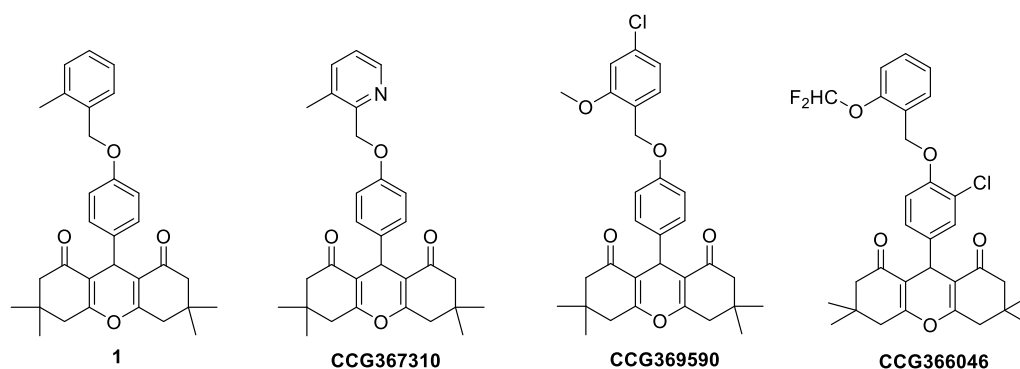


Figure 4.3 Chemical structures of compounds listed in **Table 4.1**

of xanthene-dione series, most of the atoms of **1** can be easily metabolized by the CYPs.

In vitro DMPK data (obtained from Pharmaron) **Table 4.1** confirms the prediction that **1** suffers from a poor *in vitro* DMPK profile. **1** exhibits a high metabolic rate in both mouse and human ($E_{m/h} = 0.90/0.81$). The compound is highly protein bound and has solubility at <0.1

µg/mL. Due to this low solubility, the Caco-2 permeability data cannot be interpreted with confidence. This DMPK profile of our benchmark analog **1** indicates that optimization of DMPK properties of the xanthene-dione series is required for *in vivo* studies.

Table 4.1 *in vitro* DMPK profiles of selected analogs ^a

Cpd	Species	PPB (%)	<i>In vitro</i> T _{1/2} (min)	Cl _{int} (mL/min/kg)	Hepatic Extraction Ratio (E)	Solubility (µg/mL)	Caco-2 P _{app} (A-B)/ P _{app} (B-A) (10 ⁻⁶ , cm/s)
1	Mouse	>99.85	20.68	791.68	0.90	<0.1	<0.15/ n/a
	Human		38.82	90.85	0.81		
367310	Mouse	>99.62	<2.26	>7253.14	>0.99	0.1	<0.81/ n/a
	Human		12.27	287.48	0.93		
369590	Mouse	>99.81	7.26	2256.56	0.96	0.03	<0.07/ n/a
	Human		33.13	106.45	0.84		
366046	Mouse	>99.88	42.04	389.41	0.81	<0.01	<0.14/ n/a
	Human		136.19	25.89	0.56		

a. Data obtained from Pharmaron

4.3.2 Strategies to reduce metabolism

4.3.2.1 Reduction of lipophilicity

Reduction of lipophilicity is one of the most important tactics to improve metabolic stability by reducing either the molecular weight or the cLogP of the substrates. CYP3A4 and CYP2C9 are mainly responsible for oxidizing lipophilic substrates through hydrophobic interactions (e.g. π -interactions) involved between the CYP enzymes and their substrates in the binding sites (Wester et al., 2004; Yano et al., 2004). Therefore, **1** suffers from potential extensive oxidation on A- and C-rings motifs by both CYP3A4 and CYP2C9. This is due to the fact that **1** has a high lipophilicity profile (cLogP = 6.0) and size (MW = 470). However, since all components of the molecule are needed for the activity of **1** as a DOR PAM (**Chapters 2 and 3**) I decided not to reduce the molecular size but instead try to reduce cLogP by replacing the A- and B-rings with pyridines (**CCG367310** and **CCG363177**) (**Figure 4.2**) which is predicted to reduce the LogD_{7.4} by 1.1-1.2 log units. However, as mentioned in **Chapter 3 (Table 3.2)**, this leads to a significant loss in DOR PAM activity (EC₅₀ = 2.96 μ M). Additionally, bioisosteric replacement of phenyl B-ring with indazole (**CCG366793**) did not help with restoring DOR PAM potency relative to **CCG363177** (**Figure 4.2**). Thus, I decided not to start with **CCG363177** but instead **CCG367310** (**Table 4.1**).

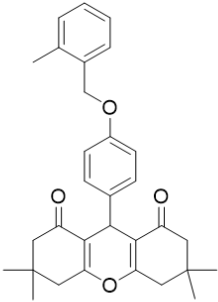
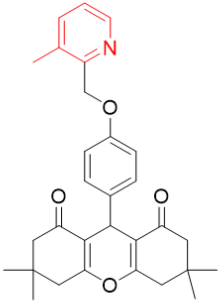
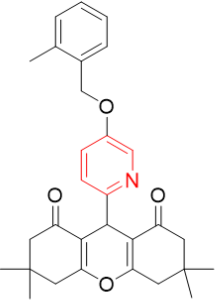
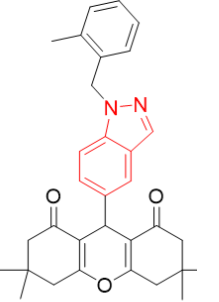
				
	1	CCG367310	CCG363177	CCG366793
DOR EC ₅₀	0.072 μ M	0.68 μ M	2.96 μ M	4.79 μ M
MOR EC ₅₀	2.68 μ M	>10 μ M	>10 μ M	>10 μ M
LogD _{7.4}	6.0	4.8	4.9	5.6

Figure 4.4 DOR and MOR activities and LogD_{7.4} values of modified xanthene analogs at A- and B-rings relative to **1**

However, without blocking the sites of metabolism (methyl groups), simply lowering LogD_{7.4} by 1.2 log unit did not bring any improvement to the *in vitro* DMPK profile relative to **1**. A similar trend was observed with analog **CCG369590** (**Figure 4.3**). These phenomena indicate that a greater reduction in lipophilicity is necessary, potentially cLogP should be lowered to < 3 to reduce the metabolic rate.

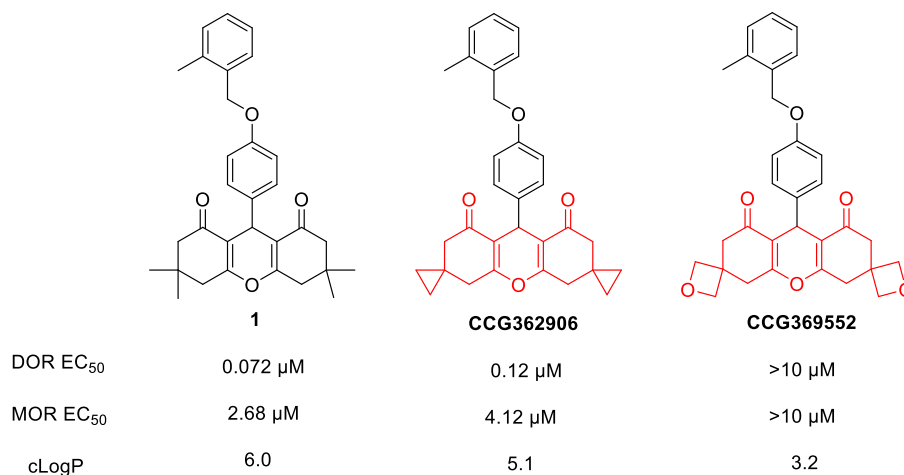


Figure 4.5 DOR and MOR activities and cLogP values of modified xanthene analogs at C-rings relative to **1**

Therefore, I tried to reduce the lipophilicity by modulating the C-rings. Relative to **1**, the spirocyclic cyclopropyl derivative **CCG362906** maintains a similar level of DOR PAM activity and selectivity over MOR (**Figure 4.5**). However, this modification only lowers the cLogP by 0.9 units. Thus, I decided to go a step further by introducing polarity to the side chains through changing the spirocyclic cyclopropyl into spirocyclic oxetane moiety (**CCG369552**) (**Figure 4.5**). The oxetane moiety is known to reduce rates of metabolism due to significant reduction in lipophilicity and reduction of CYP binding affinity due to unfavorable interactions between the oxygen and the enzyme active site (Stepan et al., 2011; Wuitschik et al., 2010). The calculated lipophilicity of **CCG369552** was halved relative to **1** (**Figure 4.5**). However, there was a complete loss of DOR activity with this modification.

4.3.2.2 Modification of predicted metabolic sites

Since the reduction of lipophilicity and introduction of polarity of xanthene-dione series suffers from a large loss of DOR PAM activity, I attempted to modify the sites of metabolism. As shown above, **1** can be metabolized across most of the molecule. I decided to first block the center proton of **1**

(highlight in **Figure 4.6**) by incorporating a trifluoro moiety (**CCG367105**). However,

no DOR PAM activity was observed for this molecule, potentially due to a conformational change and unfavorable electronic effects.

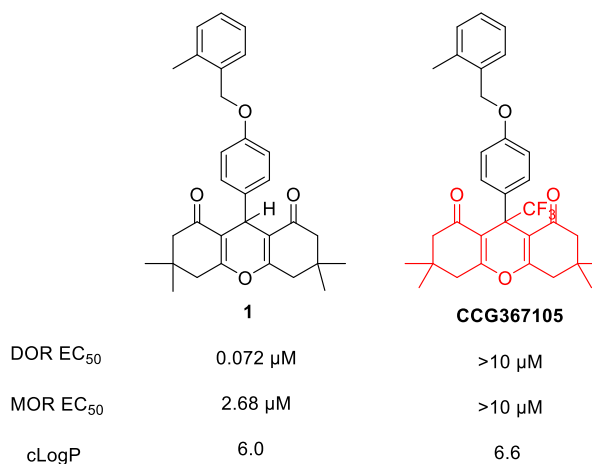


Figure 4.6 DOR and MOR activities and cLogP values of **CCG367105** relative to **1**

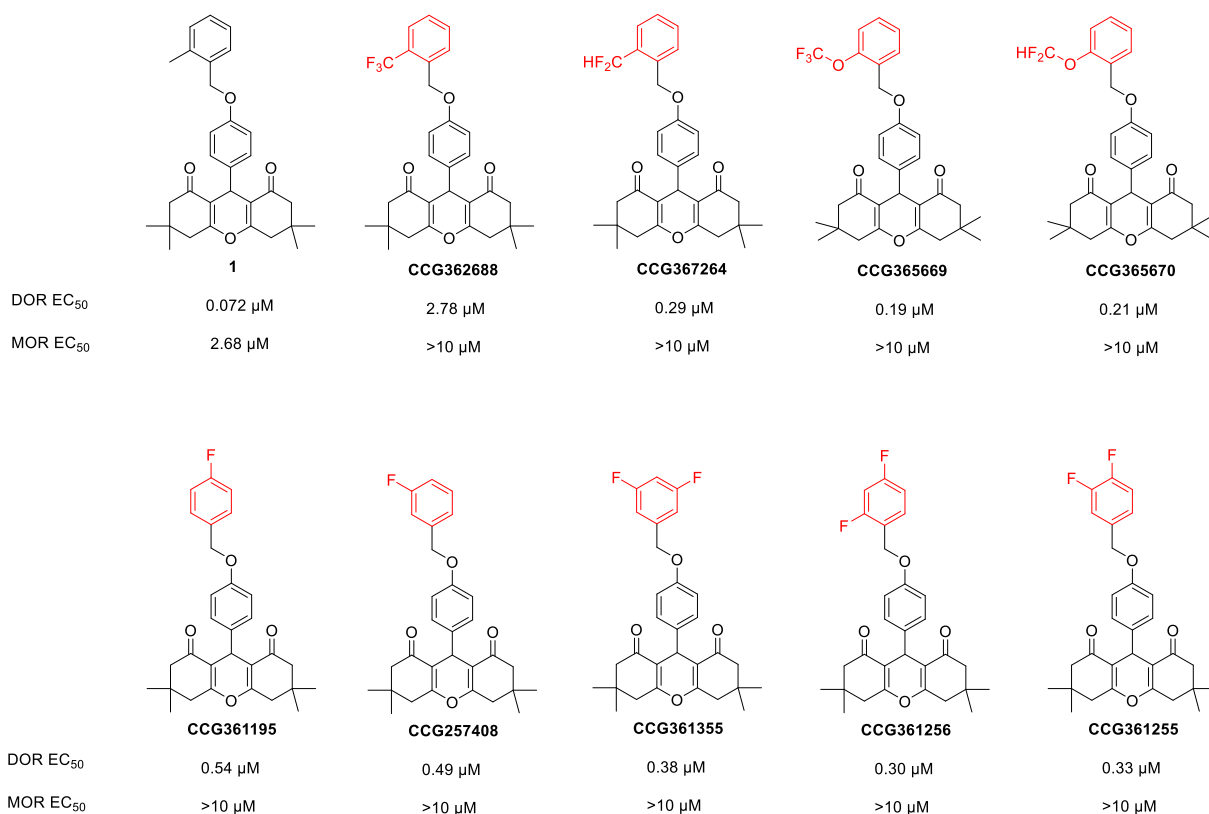


Figure 4.7 Examples of chemical structures, DOR, and MOR activities of analogs designed to block metabolic sites at A-ring.

I next tried to modulate the sites of metabolism in the A- and B-rings by incorporating the halogen atoms, fluorine and chlorine (Stepan et al., 2013). First the 2-methyl of A-ring was replaced with the trifluoro moiety (**CCG362688**). However, this compound suffered from a 15-fold potency loss in DOR relative to **1** (**Chapter 2 and Figure 4.7**). I also found that replacing the 2-methyl with difluoro (**CCG367264**), trifluoromethoxy (**CCG365669**), or difluoromethoxy (**CCG365670**) moieties restored most of the DOR PAM activity and maintain the potency level around 0.2 μM with **CCG367264** being the most potent DOR PAM in the cAMP accumulation assay (EC₅₀ = 0.0076 μM); **Chapter 2**). I also worked on replacing the protons of A-ring with halogens at the 4- or 3,5-positions of A-ring which is a known metabolic site of CYP3A4 (Dahal et al., 2012). I was glad to see both fluorine analogs, 4-fluoro (**CCG361195**) and 3,5-difluoro moiety (**CCG361355**)

maintain a decent level of DOR activity ($EC_{50} \approx 0.4 \mu\text{M}$). To further improve the potency, we also tried 2,4-disubstitutions, and found that 2,4-difluoro moiety (**CCG361256**) has DOR-PAM activity maintained at $0.3 \mu\text{M}$ (**Figure 4.7**).

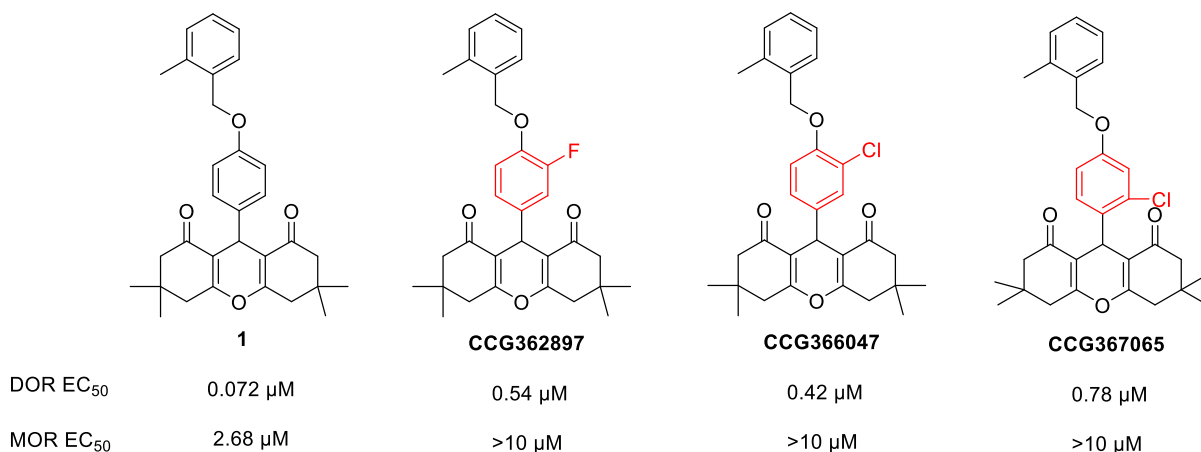


Figure 4.8 Examples of chemical structures, DOR, and MOR activities of analogs designed to block metabolic sites at B-ring.

Since the incorporation of fluorine worked well in the A-ring, we also applied the strategy to the B-ring, as we know that methyl substitutions at B-ring lock the conformation of the xanthene-dione series and improve selectivity for DOR over MOR. Additionally, this extra conformational restriction should reduce the metabolic rate (Meanwell, 2011). Unfortunately, neither fluorine (**CCG362897**) nor chlorine (**CCG366047** and **CCG367065**) substitutions maintained high DOR PAM activity (**Figure 4.8**).

Next, I attempted to combine features that might make a more druggable xanthene-dione. As shown in **Figure 4.9**, **CCG366046** exhibited a 6-fold loss of DOR PAM activity compared to **1** and maintained selectivity over MOR. The metabolic rate of dropped from high for **1** ($E_h = 0.81$) to medium ($E_h = 0.56$) for **CCG366046**. Metabolic rate was improved by blocking the site of metabolism at A-ring and incorporation of conformational restriction at ring B with chlorine.

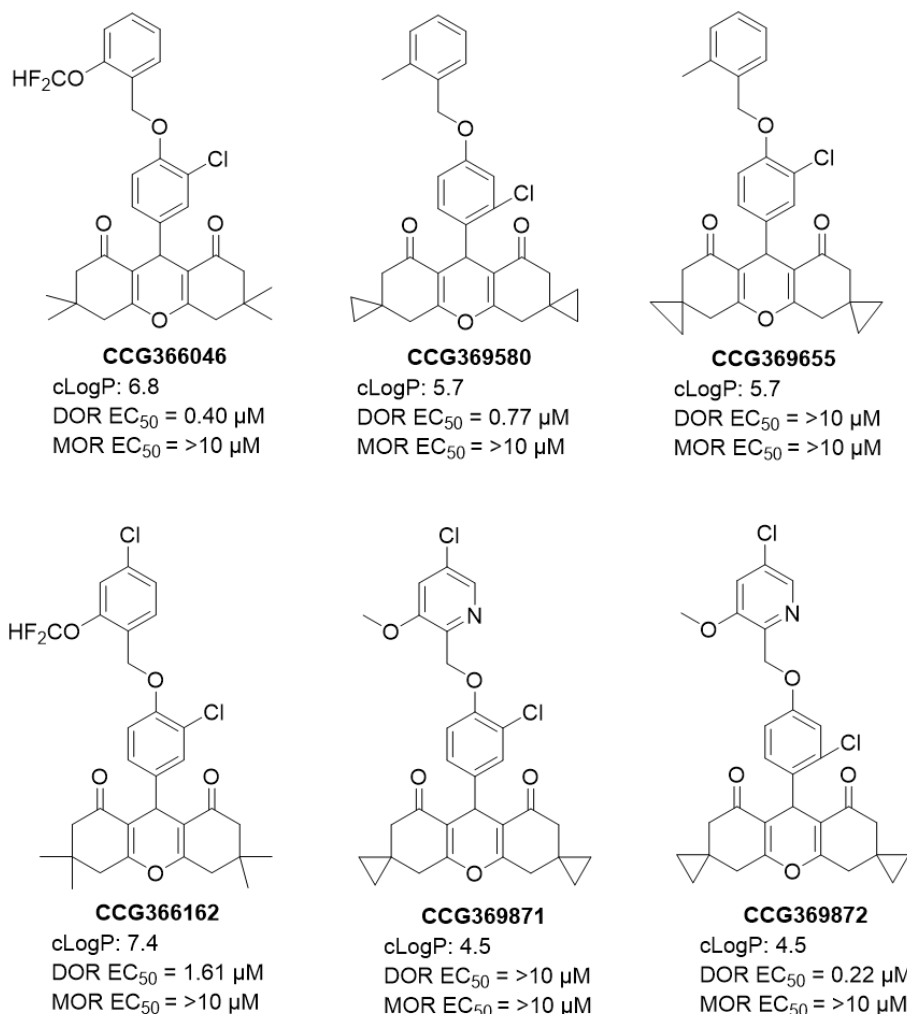


Figure 4.9 Analogs with combined modifications for reduction of metabolism are listed together with their cLogP and the in vitro data in both DOR and MOR.

Therefore, we tried to go a step further with **CCG366162** with an additional Cl atom in ring A. However, this resulted in a severe loss of potency and a high cLogP value. Thus, we decided to go back and work with compounds with spirocyclopropyl moieties in the C-rings in combination

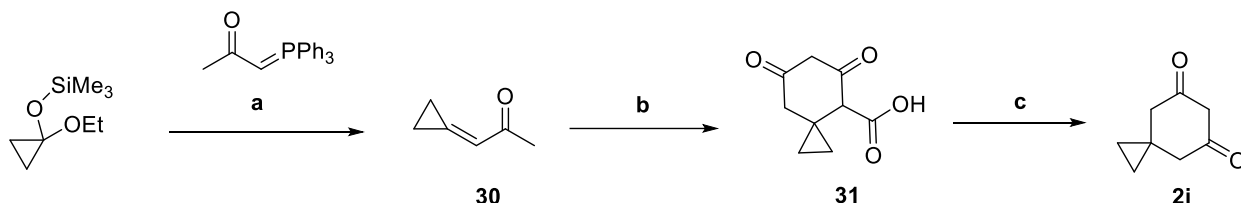
with a chlorine in the B-ring (**CCG369580** and **CCG369655**) (**Figure 4.9**). Although the chloro-moiety will increase lipophilicity, it is important for selectivity over MOR by creating an additional conformation restriction. We were surprised to see that different chlorine positions at B-ring gave drastically different results. **CCG369580** showed a tolerable 10-fold loss of potency as a DOR PAM ($EC_{50} = 0.77 \mu\text{M}$), while **CCG369655** was inactive. In contrast, compounds with other chloro substitutions in the B-ring (e.g. **CCG366046**, **CCG366162**, and **CCG366792**), which all shared a 2-chloro in the B-ring, retained a decent to tolerable range of potency as DOR PAMs. This phenomenon again indicates that the SAR of xanthene-dione series of DOR PAMs is very steep, and it is necessary to identify various feature combinations to avoid missing out the possibility of forming good analogs. Therefore, to further lower the cLogP while improving the metabolic stability, both **CCG369871** and **CCG369872** were synthesized. Again, the 2-chloro substitution in ring B was inactive. However, we are glad to see that **CCG369872** exhibits a 0.2 μM potency against DOR (just 2-3-fold lower than the parent compound **1**) and maintains selectivity over MOR while lowering the clogP by 1.5 log unit (**Figure 4.9**).

4.4 Synthesis of spiro[2.5]octane and 2-oxaspiro[3.5]nonane xanthene analogs

Synthesis of spiro-cyclopropyl and spiro-oxetane xanthene analogs started with formation of the spiro-diones **2i** and **2j**, followed by the general procedures for the synthesis of xanthene series shown in **Scheme 2.1** from **Chapter 2**. Synthesis of spiro[2.5]octane-5,7-dione is shown in **Scheme 4.1**, starting with the Wittig reaction with the commercially available (1-ethoxycyclopropoxy)-trimethyl-silane treated with 1-(triphenyl-1 λ -phosphaneylidene)propan-2-one and cat. *p*TsOH to form intermediate **30**. Then **30** was cyclized with the treatment dimethyl malonate and sodium ethoxide to yield cyclized carboxylate. With the addition of HCl, the cyclized

carboxylate was saponified and generated carboxylic acid **31**. The carboxylic acid of **31** was decarboxylated with the treatment of HCl and yield product **2i** (MCKIBBEN et al., 2018).

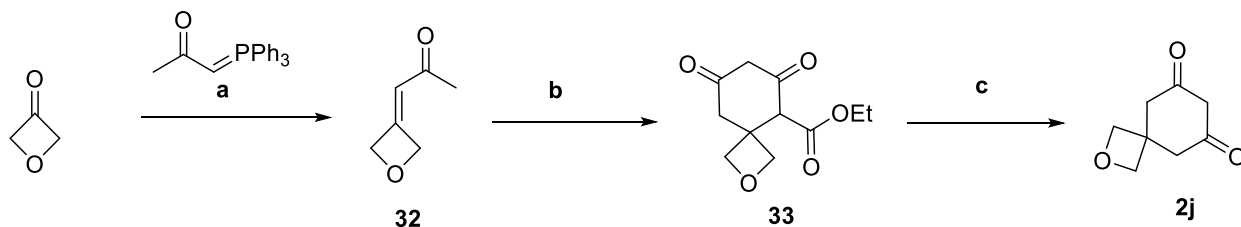
Scheme 4.1 Synthesis of spiro[2.5]octane-5,7-dione **2i**



Reagents and Conditions: a) Wittig reagent, cat. *p*TsOH, 1,2-dichlorobenzene, 100 °C; b) dimethyl malonate, NaOEt, KOH, EtOH; c) HCl, water, 60 °C.

Synthesis of 2-oxaspiro[3.5]nonane-6,8-dione is shown in **Scheme 4.2** (Krapcho et al., 1978; C. W. Wang & Chen, 2018). The synthetic route started with Wittig reaction of commercially available oxetan-3-one and treatment with 1-(triphenyl-15-phosphaneylidene)propan-2-one under room temp. to form intermediate **32**. With the addition of dimethyl malonate and base, **32** was cyclized to form carboxylate **33**. Using Krapcho decarboxylation, 2-oxaspiro[3.5]nonane-6,8-dione **2j** was formed.

Scheme 4.2 Synthesis of 2-oxaspiro[3.5]nonane-6,8-dione **2j**



Reagents and Conditions: a) Wittig reagent, DCM, r.t.; b) dimethyl malonate, NaOEt, 65 °C; c) NaCN, DMSO, 160 °C.

4.5 Conclusion

In this chapter, exercises and attempts to improve the metabolic stability of the xanthene series were performed. As a high lipophilic and bulky analog, **1** showed a poor *in vitro* DMPK profile and multiple potential sites of metabolism. Strategies for improving the DMPK profile while maintaining the *in vitro* activity of **1** in DOR and selectivity over MOR include blocking sites of metabolism by adding trifluoro moiety, incorporating halogens (fluorine and methyl replacement with chlorine), and replacement of dimethyl side chains of C-rings with spiro-oxetane moiety. Additionally, strategies included lowering the lipophilicity by incorporating pyridine moieties and exchanging the dimethyl side chains of C-rings with spiro-cyclopropyl groups. From all the attempts, an improvement was in metabolic stability with **CCG366046**, which lowered the human hepatic extraction ration from the high to the medium range ($E_h = 0.56$). This compound only lost 6-fold activity at DOR and was inactive up to 10 μ M at MOR but did have a high LogP value (6.8). However, CCG369872 with spirocyclopropyl moieties in the C-rings and a 2-Cl in ring B showed a much improved cLogP (4.7) and only a 3-fold loss of DOR PAM potency ($EC_{50} = 0.2\mu$ M) with no activity as a MOR PAM. It will be important to examine the *in vitro* stability of this compound.

4.6 Experimental

4.6.1 Biological evaluation

These were as described in **Chapter 2**

4.6.2 Prediction of metabolic sites

Metabolic sites of **1** were obtained from XenoSite (<https://xenosite.org/>)

The Metabolic Rainbow: Deep Learning Phase I Metabolism in Five Colors. Na Le Dang, Matthew K. Matlock, Tyler B. Hughes, and S. Joshua Swamidass *Journal of Chemical Information and Modeling* 2020 60 (3), 1146-1164. <https://doi.org/10.1021/acs.jcim.9b00836>

4.6.3 Synthesis

1-cyclopropylidenepropan-2-one (30) [sz-12-19]

To a solution of (1-Ethoxycyclopropoxy)-trimethyl-silane (1.08 g, 1.25 mL, 1 Eq, 6.21 mmol) in 1,2-dichlorobenzene (6.39 g, 4.89 mL, 7 Eq, 43.5 mmol) was treated with 1-(triphenyl-15-phosphaneylidene)propan-2-one (2.37 g, 1.2 Eq, 7.45 mmol) and PTSOH (118 mg, 0.1 Eq, 621 μ mol). The mixture was heated to 100°C in pressure vessel for 4 h. The reaction mixture was cooled to room temp and chromatographed over silica gel, eluted with 100% hexane and 100% DCM. Compound was isolated as oil (0.5g, 84% yield). ¹H NMR (499 MHz, cdcl₃) δ 6.45 (t, J = 2.0 Hz, 1H), 2.34 (d, J = 0.9 Hz, 3H), 1.53 – 1.47 (m, 2H), 1.38 – 1.31 (m, 2H).

5,7-dioxospiro[2.5]octane-6-carboxylic acid (31) [sz-12-21&23]

To a solution of 1-cyclopropylidenepropan-2-one (**30**) (500 mg, 1 Eq, 5.20 mmol) in ethanol (10.6 mL) was treated with dimethyl malonate (756 mg, 654 μ L, 1.1 Eq, 5.72 mmol) and sodium ethoxide (3.37 g, 3.88 mL, 21% Wt, 2 Eq, 10.4 mmol). The reaction was heated to 65°C in pressure vessel for 4 h. The reaction mixture was quenched with 1N HCl and concentrated. The aqueous layer was extracted with DCM (x3) and washed with brine, dried over MgSO₄. The crude material was concentrated and further dried under reduced pressure. The dried material was treated with KOH (8 g, 4 mL, 20% Wt, 7 Eq, 0.03 mol). The reaction was heated to 95°C for 4 h. The reaction was concentrated and was subjected to the next reaction without further purification. ¹H NMR (400 MHz, d₂o) δ 5.01 (s, 1H), 2.95 (s, 1H), 2.76 (d, J = 17.1 Hz, 1H), 1.28 (d, J = 17.2 Hz, 1H), 0.66 – 0.54 (m, 1H), 0.38 – 0.29 (m, 1H), 0.25 (d, J = 6.9 Hz, 2H).

spiro[2.5]octane-5,7-dione (2i) [sz-12-25]

To a solution of 5,7-dioxospiro[2.5]octane-6-carboxylic acid (**31**) (0.9 g, 1 Eq, 4 mmol) in 2N HCl until pH is at 3, was heated at 65°C for 1 h. The reaction mixture was cooled to room temp and extracted with DCM (x4). The organic layer was dried over MgSO₄ and concentrated. The crude material was chromatographed over silica gel, packed with hexane. Eluting with 0-50% EtOAc/Hexane. The compound was isolated and dried under reduced pressure (0.25g, 40% yield). ¹H NMR (499 MHz, dmsO) δ 11.07 (s, 1H), 5.24 (s, 1H), 2.11 (s, 4H), 0.35 (s, 4H).

1-(oxetan-3-ylidene)propan-2-one (32) [sz-11-87]

To a solution of commercially available oxetan-3-one (3000 mg, 2.437 mL, 1 Eq, 41.63 mmol) in DCM (70 mL) was treated with 1-(triphenyl-15-phosphaneylidene)propan-2-one (13.92 g, 1.05 Eq, 43.71 mmol). The resulted reaction mixture was stirred at room temp for 5 h. The aqueous layer was extracted with DCM (x3) and washed with brine, dried over MgSO₄, and concentrated. The crude material chromatographed over silica gel, eluted with 20-60% ethyl ether/pentane. The compound was isolated as clear oil (3.9g, 84% yield). ¹H NMR (499 MHz, cdcl₃) δ 6.03 (dd, J = 4.9, 2.5 Hz, 1H), 5.61 – 5.49 (m, 2H), 5.36 – 5.31 (m, 2H), 2.20 (s, 3H).

ethyl 6,8-dioxo-2-oxaspiro[3.5]nonane-7-carboxylate (33) [sz-11-88]

To a solution of 1-(oxetan-3-ylidene)propan-2-one (**32**) (1.00 g, 1 Eq, 8.03 mmol) in EtOH (20 mL) was treated with dimethyl malonate (1.76 g, 1.5 Eq, 12.0 mmol) and sodium ethoxide (5.20 g, 6.0 mL, 21% Wt, 2 Eq, 16.1 mmol). The resulted reaction mixture was heated to 65 °C in pressure vessel for 3 h. The reaction mixture was quenched with 1N HCl. The aqueous layer was extracted with DCM (x3) and washed with brine, dried over MgSO₄, and concentrated. The reaction mixture was concentrated and chromatographed over silica gel, eluted with 0-65% EtOAc/Hex, then switched to 0-30% MeOH/DCM. Compound was isolated as clear gum (1.3g, 74% yield). ¹H NMR (400 MHz, cdcl₃) δ 5.41 (d, J = 1.1 Hz, 1H), 4.77 (d, J = 6.9 Hz, 1H), 4.49 – 4.44 (m, 2H), 4.37 (s, 1H), 4.35 (s, 1H), 4.19 – 4.15 (m, 1H), 3.76 (s, 1H), 3.06 – 2.79 (m, 2H), 1.24 (t, J = 7.1 Hz, 3H).

2-oxaspiro[3.5]nonane-6,8-dione (2j) [sz-11-88]

To a mixture of ethyl 6,8-dioxo-2-oxaspiro[3.5]nonane-5-carboxylate (**33**) (300 mg, 1 Eq, 1.33 mmol) in DMSO (7mL) was treated with sodium cyanide (130 mg, 2 Eq, 2.65 mmol). The reaction mixture was refluxed at 160°C for 4 h. The reaction mixture was cooled to room temp and diluted with water. The aqueous layer was extracted with DCM (x4). The organic layer was dried over MgSO₄ and concentrated. The crude material was chromatographed over silica gel, eluted with 0-

20% MeOH/DCM. The compound was isolated as solids (0.06g, 30% yield). ¹H NMR (499 MHz, cd₃od) δ 4.46 (s, 4H), 3.36 (s, 2H), 2.70 (d, J = 1.7 Hz, 4H).

9'-(3-chloro-4-hydroxyphenyl)-5',9'-dihydro-2'H-dispiro[cyclopropane-1,3'-xanthene-6',1''-cyclopropane]-1',8'(4'H,7'H)-dione (3bj) [sz-12-35]

To a solution of 3-chloro-4-hydroxybenzaldehyde (80 mg, 1 Eq, 0.51 mmol) and spiro[2.5]octane-5,7-dione (**2i**) (0.14 g, 2.01 Eq, 1.0 mmol) in 70% 2-propanol (2mL) was treated with zinc chloride (14 mg, 0.2 Eq, 0.10 mmol). The reaction mixture was refluxed at 120°C for 16 h and cooled to room temperature. Precipitates formed overnight. The solids were filtered and washed with cold 70% IPA (0.1g, 49% yield). ¹H NMR (499 MHz, cd₃od) δ 8.54 (s, 1H), 7.17 (d, J = 2.2 Hz, 1H), 7.04 – 6.99 (m, 1H), 6.74 (d, J = 8.3 Hz, 1H), 4.65 (s, 1H), 2.71 (d, J = 18.3 Hz, 2H), 2.45 (d, J = 16.9 Hz, 2H), 2.43 – 2.37 (m, 2H), 2.03 (d, J = 16.8 Hz, 2H), 0.54 (dd, J = 9.6, 4.4 Hz, 2H), 0.52 – 0.49 (m, 2H), 0.47 – 0.44 (m, 2H), 0.39 (t, J = 5.1 Hz, 2H).

(5-chloro-3-methoxy-pyridin-2-yl)methanol (14bb) [sz-12-06]

Following the general procedure for Intermediate **14**, commercially available 5-chloro-3-methoxypicolinaldehyde (70 mg, 1 Eq, 0.41 mmol) in EtOH (2mL) was used, and 0.04g of Compound **14bb** was isolated (59% yield). ¹H NMR (499 MHz, cdcl₃) δ 8.28 (s, 1H), 8.19 (s, 1H), 4.85 (d, J = 6.4 Hz, 2H), 3.99 (s, 3H).

5-chloro-2-(chloromethyl)-3-methoxypyridine (16d) [sz-12-12]

Following general procedure for Compound **16**, (5-chloro-3-methoxy-pyridin-2-yl)methanol (**15b**) (40 mg, 1 Eq, 0.23 mmol) was used, and 0.04g of Compound **16d** was isolated (90% yield). ¹H NMR (499 MHz, cdcl₃) δ 8.30 (s, 1H), 8.21 (s, 1H), 4.71 (s, 2H), 4.01 (d, J = 0.8 Hz, 3H).

3-chloro-4-((5-chloro-3-methoxy-pyridin-2-yl)methoxy)benzaldehyde (6l) [sz-13-14]

Following the general procedure of intermediate **7**, using 2-chloro-4-hydroxybenzaldehyde (50 mg, 1 Eq, 0.32 mmol) and 5-chloro-2-(chloromethyl)-3-methoxypyridine (**16d**) (61 mg, 1 Eq, 0.32 mmol), Compound **6l** was isolated (0.02g, 15%). ¹H NMR (400 MHz, cdcl₃) δ 9.87 (s, 1H), 8.35 (s, 1H), 8.28 (s, 1H), 7.91 (d, J = 2.0 Hz, 1H), 7.84 – 7.75 (m, 1H), 7.23 (d, J = 8.5 Hz, 1H), 5.33 (s, 2H), 3.99 (d, J = 0.7 Hz, 3H).

2-chloro-4-((5-chloro-3-methoxy-pyridin-2-yl)methoxy)benzaldehyde (6m) [sz-13-15]

Following the general procedure of intermediate **7**, using 2-chloro-4-hydroxybenzaldehyde (80 mg, 1 Eq, 0.42 mmol) and 5-chloro-2-(chloromethyl)-3-methoxypyridine (**16d**) (65 mg, 1 Eq, 0.42 mmol), Compound **6m** was isolated (0.02g, 15%). ¹H NMR (400 MHz, cdcl₃) δ 10.35 (d, J = 0.9

Hz, 1H), 8.35 (s, 1H), 8.27 (s, 1H), 7.92 (d, J = 8.8 Hz, 1H), 7.07 (d, J = 2.4 Hz, 1H), 6.98 (ddd, J = 8.8, 2.4, 0.8 Hz, 1H), 5.24 (s, 2H), 3.99 (s, 3H).

9'-(4-((2-methylbenzyl)oxy)phenyl)-5',9'-dihydro-2'H-dispiro[cyclopropane-1,3'-xanthene-6',1''-cyclopropane]-1',8'(4'H,7'H)-dione (CCG362906) [sz-08-33]

Following the general procedure of **5a** on a scale of 30mg (0.1mmol) 9'-(4-hydroxyphenyl)-5',9'-dihydro-2'H-dispiro[cyclopropane-1,3'-xanthene-6',1''-cyclopropane]-1',8'(4'H,7'H)-dione (**8e**), 1-(bromomethyl)-2-methylbenzene (31 mg, 22 μ L, 2 Eq, 0.17 mmol) was used. 0.03g of product was isolated (64% yield). ¹H NMR (499 MHz, cdcl₃) δ 7.44 – 7.34 (m, 1H), 7.30 – 7.14 (m, 5H), 6.93 – 6.78 (m, 2H), 4.96 (s, 2H), 4.84 (s, 1H), 2.55 (dd, J = 17.9, 1.4 Hz, 2H), 2.43 – 2.28 (m, 7H), 2.09 (d, J = 16.7 Hz, 2H), 0.56 – 0.33 (m, 8H). ¹³C NMR (126 MHz, cdcl₃) δ 196.25, 163.10, 157.48, 136.86, 136.77, 135.03, 130.32, 129.36, 128.78, 128.18, 125.98, 117.08, 114.28, 68.47, 46.15, 36.75, 31.25, 18.88, 14.39, 14.39, 14.39, 11.71, 10.99. ESI MS m/z 467.21 (M + H)+

9'-(3-chloro-4-((2-methylbenzyl)oxy)phenyl)-5',9'-dihydro-2'H-dispiro[cyclopropane-1,3'-xanthene-6',1''-cyclopropane]-1',8'(4'H,7'H)-dione (CCG3639655) [sz-12-46]

Following the general procedure of **5c** on a scale of 44mg (0.11mmol) 9'-(3-chloro-4-hydroxyphenyl)-5',9'-dihydro-2'H-dispiro[cyclopropane-1,3'-xanthene-6',1''-cyclopropane]-1',8'(4'H,7'H)-dione (**3bj**), 1-(bromomethyl)-2-methylbenzene 41mg, 30 μ L, 2.0 Eq, 0.22 mmol) was used. 0.02g of product was isolated (40% yield). ¹H NMR (499 MHz, cdcl₃) δ 7.44 (d, J = 7.2 Hz, 1H), 7.31 (dd, J = 8.5, 2.3 Hz, 1H), 7.21 (qd, J = 8.5, 4.3 Hz, 4H), 6.89 (d, J = 8.5 Hz, 1H), 5.03 (s, 2H), 4.81 (s, 1H), 2.56 (d, J = 17.8 Hz, 2H), 2.44 – 2.30 (m, 7H), 2.10 (d, J = 16.8 Hz, 2H), 0.56 – 0.37 (m, 8H). ¹³C NMR (126 MHz, cdcl₃) δ 196.19, 163.44, 152.83, 137.90, 136.48, 134.56, 130.26, 129.58, 128.30, 128.12, 125.96, 122.72, 116.55, 113.27, 69.44, 46.12, 36.73, 31.14, 18.92, 14.38, 11.65, 10.98. ESI MS m/z 523.16 (M + Na)+

9'-(2-chloro-4-((2-methylbenzyl)oxy)phenyl)-5',9'-dihydro-2'H-dispiro[cyclopropane-1,3'-xanthene-6',1''-cyclopropane]-1',8'(4'H,7'H)-dione (33e) (CCG369580) [sz-12-05]

Following the general procedure for **7**, 2-chloro-4-((2-methylbenzyl)oxy)benzaldehyde (**6m**) (50 mg, 1 Eq, 0.19 mmol) and spiro[2.5]octane-5,7-dione (**2i**) (54 mg, 2.05 Eq, 0.39 mmol) were used. 0.07g of desired product was isolated (68% yield). ¹H NMR (400 MHz, cdcl₃) δ 7.42 (d, J = 8.6 Hz, 1H), 7.38 – 7.33 (m, 1H), 7.26 – 7.17 (m, 3H), 6.89 (d, J = 2.6 Hz, 1H), 6.84 (dd, J = 8.6, 2.6 Hz, 1H), 5.02 (s, 1H), 4.94 (s, 2H), 2.53 (dd, J = 17.8, 1.6 Hz, 2H), 2.38 – 2.29 (m, 7H), 2.08 (d, J = 16.7 Hz, 2H), 0.55 – 0.35 (m, 8H). ¹³C NMR (101 MHz, cdcl₃) δ 196.42, 163.82, 157.98,

136.91, 134.45, 133.94 (d, J = 16.5 Hz), 132.24, 130.40, 128.91, 128.42, 126.05, 115.88, 114.85, 113.33, 68.70, 46.07, 36.67, 31.84, 18.91, 14.31, 11.64, 10.97. ESI MS m/z 523.16 (M + Na)+
9'-(4-((2-methylbenzyl)oxy)phenyl)-5',9'-dihydro-2'H-dispiro[oxetane-3,3'-xanthene-6',3''-oxetane]-1',8'(4'H,7'H)-dione (CCG369552) [sz-11-93]

Following the general procedure for **7**, 4-((2-methylbenzyl)oxy)benzaldehyde (**6a**) (50 mg, 1 Eq, 0.22 mmol) and 2-oxaspiro[3.5]nonane-6,8-dione (**2j**) (68 mg, 2 Eq, 0.44 mmol) were used. 0.01g of product was isolated (8% yield). ¹H NMR (400 MHz, cdcl₃) δ 7.35 (d, J = 7.4 Hz, 1H), 7.21 (q, J = 6.5, 6.0 Hz, 3H), 7.10 (d, J = 8.6 Hz, 2H), 6.79 (d, J = 8.6 Hz, 2H), 5.00 (s, 1H), 4.93 (s, 2H), 4.55 – 4.40 (m, 4H), 4.36 (s, 4H), 2.94 (d, J = 16.5 Hz, 2H), 2.86 – 2.72 (m, 4H), 2.59 (d, J = 16.5 Hz, 2H), 2.33 (s, 3H). ¹³C NMR (126 MHz, cdcl₃) δ 193.39, 157.47, 146.69, 138.65, 136.76, 134.82, 130.36, 128.76, 128.53, 128.27, 125.99, 115.52, 114.43, 81.26, 80.55, 68.52, 46.20, 39.46, 36.94, 32.68, 18.86. ESI MS m/z 537.16 (M + K)+

9'-(3-chloro-4-((5-chloro-3-methoxypyridin-2-yl)methoxy)phenyl)-5',9'-dihydro-2'H-dispiro[cyclopropane-1,3'-xanthene-6',1''-cyclopropane]-1',8'(4'H,7'H)-dione (CCG369871) [sz-13-16]

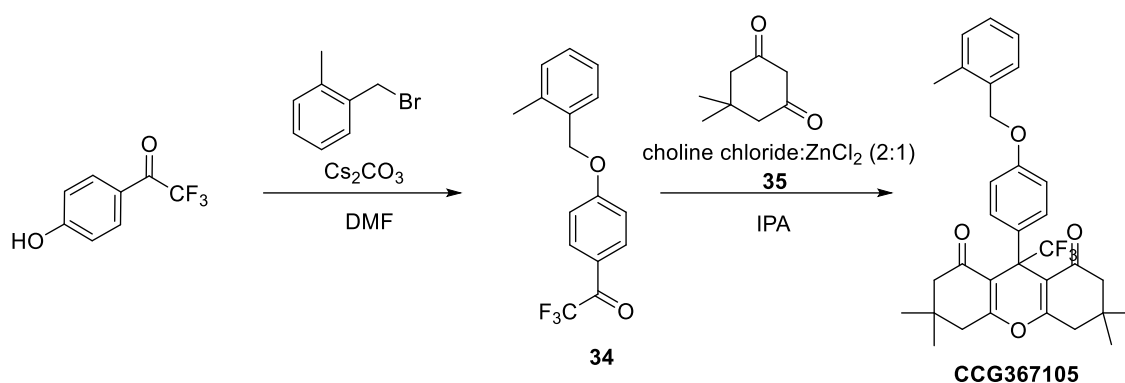
Following the general procedure for **7**, 3-chloro-4-((5-chloro-3-methoxypyridin-2-yl)methoxy)benzaldehyde (**6l**) (13.5 mg, 1 Eq, 0.04 mmol) and spiro[2.5]octane-5,7-dione (**2i**) (12 mg, 2.0 Eq, 0.09 mmol) were used. 0.02g of desired product was isolated (63% yield). ¹H NMR (499 MHz, cdcl₃) δ 8.30 (s, 1H), 8.21 (s, 1H), 7.40 – 7.28 (m, 1H), 7.18 (dd, J = 2.3, 0.9 Hz, 1H), 6.96 (dd, J = 8.5, 0.9 Hz, 1H), 5.16 (d, J = 0.8 Hz, 2H), 4.81 (s, 1H), 3.92 (d, J = 0.9 Hz, 3H), 2.56 (d, J = 17.8 Hz, 2H), 2.39 (d, J = 8.0 Hz, 2H), 2.35 (d, J = 6.9 Hz, 2H), 2.10 (d, J = 16.8 Hz, 2H), 0.49 (dq, J = 10.0, 6.3, 5.4 Hz, 6H), 0.43 (dq, J = 9.4, 4.2 Hz, 2H). ¹³C NMR (126 MHz, cdcl₃) δ 196.21, 163.47, 154.69, 152.69, 142.48, 138.50, 133.28, 132.18, 130.24, 129.58, 128.37, 123.08, 116.49, 114.04, 61.87, 56.90, 46.12, 36.73, 31.22, 14.37, 11.65, 10.98. ESI MS m/z 552.13 (M + H)+

9'-(2-chloro-4-((5-chloro-3-methoxypyridin-2-yl)methoxy)phenyl)-5',9'-dihydro-2'H-dispiro[cyclopropane-1,3'-xanthene-6',1''-cyclopropane]-1',8'(4'H,7'H)-dione (CCG369872) [sz-13-17]

Following the general procedure for **7**, 2-chloro-4-((5-chloro-3-methoxypyridin-2-yl)methoxy)benzaldehyde (**6m**) (16 mg, 1 Eq, 0.05 mmol) and spiro[2.5]octane-5,7-dione (**2i**) (14 mg, 2.0 Eq, 0.1 mmol) were used. 0.02g of desired product was isolated (60% yield). ¹H NMR

(499 MHz, cdcl₃) δ 8.31 (s, 1H), 8.22 (s, 1H), 7.44 (d, J = 8.6 Hz, 1H), 6.90 (d, J = 2.6 Hz, 1H), 6.87 – 6.77 (m, 1H), 5.08 (s, 2H), 5.01 (s, 1H), 3.94 (d, J = 0.7 Hz, 3H), 2.62 – 2.44 (m, 2H), 2.35 (d, J = 6.1 Hz, 2H), 2.31 (d, J = 5.0 Hz, 2H), 2.07 (d, J = 16.7 Hz, 2H), 0.47 (tt, J = 9.2, 4.4 Hz, 6H), 0.42 – 0.38 (m, 2H). ¹³C NMR (126 MHz, cdcl₃) δ 196.42, 163.86, 157.63, 154.57, 142.44, 134.03, 133.92, 133.27, 132.51, 132.04, 130.16, 115.99, 114.78, 113.23, 60.57, 56.82, 46.06, 36.67, 31.94, 14.29, 11.65, 10.96. ESI MS *m/z* 574.11 (M + Na)⁺

Scheme 4.3 Synthesis of **CCG367105**



Choline chloride:ZnCl₂ (35) [sz-11-06] (Hong et al., 2019)

ZnCl₂ (1.9g, 2.0 Eq, 14.32 mmol) was heated until melted and treated with choline chloride (1g, 1 Eq, 7.16 mmol). The mixture was continue heated until two reagents formed clear glue. The catalyst was used without purification.

2,2,2-trifluoro-1-(4-((2-methylbenzyl)oxy)phenyl)ethan-1-one (34) [sz-10-32]

Following the general procedure of intermediate **32** on a scale of 0.2g 2,2,2-trifluoro-1-(4-hydroxyphenyl)ethan-1-one (1.19mmol), Compound **34** was isolated as white gum (0.28g, 89%). ¹H NMR (499 MHz, cdcl₃) δ 8.08 (dq, J = 8.0, 1.0 Hz, 2H), 7.41 – 7.36 (m, 1H), 7.33 – 7.28 (m, 1H), 7.26 – 7.16 (m, 2H), 7.13 – 7.07 (m, 2H), 5.16 (s, 2H), 2.39 (s, 3H).

3,3,6,6-tetramethyl-9-(4-((2-methylbenzyl)oxy)phenyl)-9-(trifluoromethyl)-3,4,5,6,7,9-hexahydro-1H-xanthene-1,8(2H)-dione (CCG367105) [sz-11-07]

Following the general procedure for **33**, 2,2,2-trifluoro-1-(4-((2-methylbenzyl)oxy)phenyl)ethan-1-one (**34**) (0.44g, 1 Eq, 2.50 mmol), cyclopentane-1,3-dione (440 mg, 2.1 Eq, 3.14 mmol), and

one drop of catalyst choline chloride/ZnCl₂ (**35**) were used. The reaction was stirred until completion. 0.008g of product was isolated (1% yield). ¹H NMR (499 MHz, cdcl₃) δ 7.37 (t, J = 7.9 Hz, 3H), 7.25 (d, J = 1.6 Hz, 1H), 7.24 – 7.18 (m, 2H), 6.99 – 6.93 (m, 2H), 5.02 (s, 2H), 3.08 – 2.88 (m, 2H), 2.48 (d, J = 2.3 Hz, 2H), 2.37 (s, 3H), 2.35 – 2.17 (m, 4H), 1.10 (s, 3H), 1.07 (d, J = 2.4 Hz, 6H), 1.05 (s, 3H). ¹³C NMR (126 MHz, cdcl₃) δ 194.96, 194.58, 173.59, 159.19, 149.38, 136.78, 134.43, 130.44, 129.38, 128.78, 128.42, 128.33, 126.07, 119.03, 114.14, 111.27, 68.59, 52.49, 51.72, 43.03, 41.63, 32.37, 31.69, 28.38, 28.30, 27.83, 27.76, 18.88. ¹⁹F NMR (470 MHz, cdcl₃) δ -73.27. ESI MS m/z 539.23 (M + H)⁺

4.7 References

- Almond, L. M., Yang, J., Jamei, M., Tucker, G. T., & Rostami-Hodjegan, A. (2009). Towards a quantitative framework for the prediction of DDIs arising from cytochrome P450 induction. *Current Drug Metabolism*, *10*(4), 420–432. <https://doi.org/10.2174/138920009788498978>
- Baillie, T. A. (2008). Metabolism and Toxicity of Drugs. Two Decades of Progress in Industrial Drug Metabolism. *Chemical Research in Toxicology*, *21*(1), 129–137. <https://doi.org/10.1021/tx7002273>
- Congreve, M., Carr, R., Murray, C., & Jhoti, H. (2003). A ‘Rule of Three’ for fragment-based lead discovery? *Drug Discovery Today*, *8*(19), 876–877. [https://doi.org/10.1016/S1359-6446\(03\)02831-9](https://doi.org/10.1016/S1359-6446(03)02831-9)
- Dahal, U. P., Joswig-Jones, C., & Jones, J. P. (2012). Comparative study of the affinity and metabolism of type I and type II binding quinoline carboxamide analogs by cytochrome P450 3A4. *Journal of Medicinal Chemistry*, *55*(1), 280–290. <https://doi.org/10.1021/jm201207h>
- Guengerich, F. P. (2006). Cytochrome P450s and other enzymes in drug metabolism and toxicity. *The AAPS Journal*, *8*(1), E101–E111. <https://doi.org/10.1208/aapsj080112>
- Guengerich, F. P., & MacDonald, J. S. (2007). Applying Mechanisms of Chemical Toxicity to Predict Drug Safety. *Chemical Research in Toxicology*, *20*(3), 344–369. <https://doi.org/10.1021/tx600260a>
- Hong, S., Yuan, Y., Yang, Q., Chen, L., Deng, J., Chen, W., Lian, H., Mota-Morales, J. D., & Liimatainen, H. (2019). Choline chloride-zinc chloride deep eutectic solvent mediated preparation of partial O-acetylation of chitin nanocrystal in one step reaction. *Carbohydrate Polymers*, *220*, 211–218. <https://doi.org/10.1016/j.carbpol.2019.05.075>
- Issa, N. T., Wathieu, H., Ojo, A., Byers, S. W., & Dakshanamurthy, S. (2017). Drug Metabolism in Preclinical Drug Development: A Survey of the Discovery Process, Toxicology, and Computational Tools. *Current Drug Metabolism*, *18*(6), 556–565. <https://doi.org/10.2174/1389200218666170316093301>
- Kalgutkar, A. S., & Soglia, J. R. (2005). Minimising the potential for metabolic activation in drug discovery. *Expert Opinion on Drug Metabolism & Toxicology*, *1*(1), 91–142. <https://doi.org/10.1517/17425255.1.1.91>
- Kirchmair, J., Williamson, M. J., Tyzack, J. D., Tan, L., Bond, P. J., Bender, A., & Glen, R. C. (2012). Computational Prediction of Metabolism: Sites, Products, SAR, P450 Enzyme Dynamics, and Mechanisms. *Journal of Chemical Information and Modeling*, *52*(3), 617–648. <https://doi.org/10.1021/ci200542m>

- Kola, I., & Landis, J. (2004). Can the pharmaceutical industry reduce attrition rates? *Nature Reviews Drug Discovery*, 3(8), Article 8. <https://doi.org/10.1038/nrd1470>
- Krapcho, A. P., Weimaster, J. F., Eldridge, J. M., Jahngen, E. G. E., Lovey, A. J., & Stephens, W. P. (1978). Synthetic applications and mechanism studies of the decarbalkoxylations of geminal diesters and related systems effected in dimethyl sulfoxide by water and/or by water with added salts. *The Journal of Organic Chemistry*, 43(1), 138–147. <https://doi.org/10.1021/jo00395a032>
- Lewis, D. F. V., & Dickins, M. (2002). Substrate SARs in human P450s. *Drug Discovery Today*, 7(17), 918–925. [https://doi.org/10.1016/S1359-6446\(02\)02412-1](https://doi.org/10.1016/S1359-6446(02)02412-1)
- Lewis, D. F. V., Jacobs, M. N., & Dickins, M. (2004). Compound lipophilicity for substrate binding to human P450s in drug metabolism. *Drug Discovery Today*, 9(12), 530–537. [https://doi.org/10.1016/S1359-6446\(04\)03115-0](https://doi.org/10.1016/S1359-6446(04)03115-0)
- Lipinski, C. A. (2000). Drug-like properties and the causes of poor solubility and poor permeability. *Journal of Pharmacological and Toxicological Methods*, 44(1), 235–249. [https://doi.org/10.1016/S1056-8719\(00\)00107-6](https://doi.org/10.1016/S1056-8719(00)00107-6)
- Lipinski, C., & Hopkins, A. (2004). Navigating chemical space for biology and medicine. *Nature*, 432(7019), Article 7019. <https://doi.org/10.1038/nature03193>
- MCKIBBEN, B. P., MEYERS, K. M., Zhang, Y., Marshall, D. R., Cogan, D., Lord, J., Chen, Z., Burke, J., & Balestra, M. (2018). *Bicyclic imidazole derivatives useful for the treatment of renal disease, cardiovascular diseases and fibrotic disorders* (World Intellectual Property Organization Patent No. WO2018005177A1). <https://patents.google.com/patent/WO2018005177A1/en>
- Meanwell, N. A. (2011). Synopsis of Some Recent Tactical Application of Bioisosteres in Drug Design. *Journal of Medicinal Chemistry*, 54(8), 2529–2591. <https://doi.org/10.1021/jm1013693>
- Nebert, D. W., & Russell, D. W. (2002). Clinical importance of the cytochromes P450. *The Lancet*, 360(9340), 1155–1162. [https://doi.org/10.1016/S0140-6736\(02\)11203-7](https://doi.org/10.1016/S0140-6736(02)11203-7)
- Phang-Lyn, S., & Llerena, V. A. (2021). Biochemistry, Biotransformation. In *StatPearls [Internet]*. StatPearls Publishing. <https://www.ncbi.nlm.nih.gov/books/NBK544353/>
- Prentis, R. A., Lis, Y., & Walker, S. R. (1988). Pharmaceutical innovation by the seven UK-owned pharmaceutical companies (1964-1985). *British Journal of Clinical Pharmacology*, 25(3), 387–396.
- Research and Development in the Pharmaceutical Industry | Congressional Budget Office*. (2021, April 8). <https://www.cbo.gov/publication/57126>
- St. Jean, D. J., & Fotsch, C. (2012). Mitigating Heterocycle Metabolism in Drug Discovery. *Journal of Medicinal Chemistry*, 55(13), 6002–6020. <https://doi.org/10.1021/jm300343m>

- Stepan, A. F., Karki, K., McDonald, W. S., Dorff, P. H., Dutra, J. K., DiRico, K. J., Won, A., Subramanyam, C., Efremov, I. V., O'Donnell, C. J., Nolan, C. E., Becker, S. L., Pustilnik, L. R., Sneed, B., Sun, H., Lu, Y., Robshaw, A. E., Riddell, D., O'Sullivan, T. J., ... Obach, R. S. (2011). Metabolism-Directed Design of Oxetane-Containing Arylsulfonamide Derivatives as γ -Secretase Inhibitors. *Journal of Medicinal Chemistry*, 54(22), 7772–7783. <https://doi.org/10.1021/jm200893p>
- Stepan, A. F., Mascitti, V., Beaumont, K., & Kalgutkar, A. S. (2013). Metabolism-guided drug design. *MedChemComm*, 4(4), 631. <https://doi.org/10.1039/c2md20317k>
- Sun, D., Gao, W., Hu, H., Zhou, S. (2022). Why 90% of clinical drug development fails and how to improve it? *Acta Pharmaceutica Sinica B*, 12(7), 3049-3062. <https://doi.org/10.1016/j.apsb.2022.02.002>
- Thompson, T. N. (2001). Optimization of metabolic stability as a goal of modern drug design. *Medicinal Research Reviews*, 21(5), 412–449. <https://doi.org/10.1002/med.1017>
- Wang, C. W., & Chen, J. (2018). *N*-(phenylsulfonyl)benzamides and related compounds as bcl-2 inhibitors (World Intellectual Property Organization Patent No. WO2018027097A1). <https://patents.google.com/patent/WO2018027097A1/en?q=WO2018027097A1>
- Wester, M. R., Yano, J. K., Schoch, G. A., Yang, C., Griffin, K. J., Stout, C. D., & Johnson, E. F. (2004). The Structure of Human Cytochrome P450 2C9 Complexed with Flurbiprofen at 2.0-Å Resolution*. *Journal of Biological Chemistry*, 279(34), 35630–35637. <https://doi.org/10.1074/jbc.M405427200>
- Williams, P. A., Cosme, J., Vinković, D. M., Ward, A., Angove, H. C., Day, P. J., Vonnrhein, C., Tickle, I. J., & Jhoti, H. (2004). Crystal Structures of Human Cytochrome P450 3A4 Bound to Metyrapone and Progesterone. *Science*, 305(5684), 683–686. <https://doi.org/10.1126/science.1099736>
- Wuitschik, G., Carreira, E. M., Wagner, B., Fischer, H., Parrilla, I., Schuler, F., Rogers-Evans, M., & Müller, K. (2010). Oxetanes in Drug Discovery: Structural and Synthetic Insights. *Journal of Medicinal Chemistry*, 53(8), 3227–3246. <https://doi.org/10.1021/jm9018788>
- Yano, J. K., Wester, M. R., Schoch, G. A., Griffin, K. J., Stout, C. D., & Johnson, E. F. (2004). The Structure of Human Microsomal Cytochrome P450 3A4 Determined by X-ray Crystallography to 2.05-Å Resolution*. *Journal of Biological Chemistry*, 279(37), 38091–38094. <https://doi.org/10.1074/jbc.C400293200>
- Yeung, C. K., Fujioka, Y., Hachad, H., Levy, R. H., & Isoherranen, N. (2011). Are circulating metabolites important in drug-drug interactions?: Quantitative analysis of risk prediction and inhibitory potency. *Clinical Pharmacology and Therapeutics*, 89(1), 105–113. <https://doi.org/10.1038/clpt.2010.252>
- Zaretzki, J., Matlock, M., & Swamidass, S. J. (2013). XenoSite: Accurately Predicting CYP-Mediated Sites of Metabolism with Neural Networks. *Journal of Chemical Information and Modeling*, 53(12), 3373–3383. <https://doi.org/10.1021/ci400518g>

Zhang, Z., Zhu, M., & Tang, W. (2009). Metabolite Identification and Profiling in Drug Design: Current Practice and Future Directions. *Current Pharmaceutical Design*, 15(19), 2220–2235. <https://doi.org/10.2174/138161209788682460>

Chapter 5 Future Directions to Optimize the Xanthene-dione Series of DOR-PAMs

5.1 Further optimization of the metabolic stability and solubility of the xanthene-diones

From the studies reported in this thesis, I was able to enhance selectivity for DOR over MOR. I was also able to slowly and gradually improve either the lipophilicity or the metabolic stability of xanthene-dione series while in some cases retaining activity as a DOR PAM. Thus, further improvement on the metabolic stability and solubility can be attempted strategically and systematically.

5.1.1 Incorporation of deuterium

One of the major sites of metabolism of **1** is at the protons of the benzyl group (A-ring; Figure

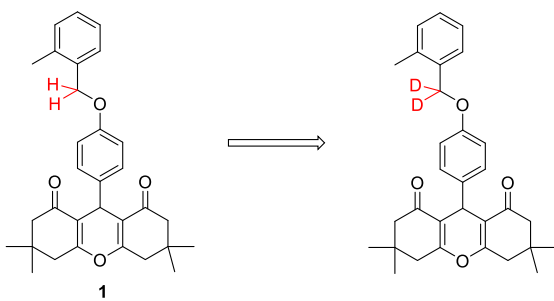


Figure 5.1 Blocking site of metabolism of **1** (red) with deuteration

5.1). To lower the rate of metabolism, deuterium has been found to be a good strategy. Deuteration shows low systemic toxicity and can alter both the rate of metabolism and the ratio of metabolite formation. Drugs incorporating of deuterium are known (Jones & Leatherdale, 1991; Katz & Crespi, 1966; Kushner et

al., 1999; Murray & Benitez, 1967; Mutlib et al., 2000). Since deuteration can reduce the toxicity of reactive metabolites and reduce drug clearance, which results in increased half-life it is a good strategy to improve the metabolic stability of the xanthene-dione series without changing its molecular conformation of electronics.

5.1.2 Expansion and combination of xanthene-dione modifications at the A-ring to further improve metabolic stability and lipophilicity

As SAR has been performed separately on the A-rings for different purposes such as potency as a DOR PAM, selectivity over MOR, reduction of lipophilicity, and improvement of metabolic stability, a combination of the modifications can be addressed. This is shown in **Figure 5.2**. Examples such as, **CCG361256**, **CCG369832**, and **CCG367310** are analogues that retain a decent level of DOR PAM activity provide attempts to reduce the lipophilicity and/or address metabolic liability. We observed that from the halogen “walks” around A-ring, that 2,4-disubstitutions can be well accepted by DOR and maintain a decent level of potency as DOR PAMs while blocking a

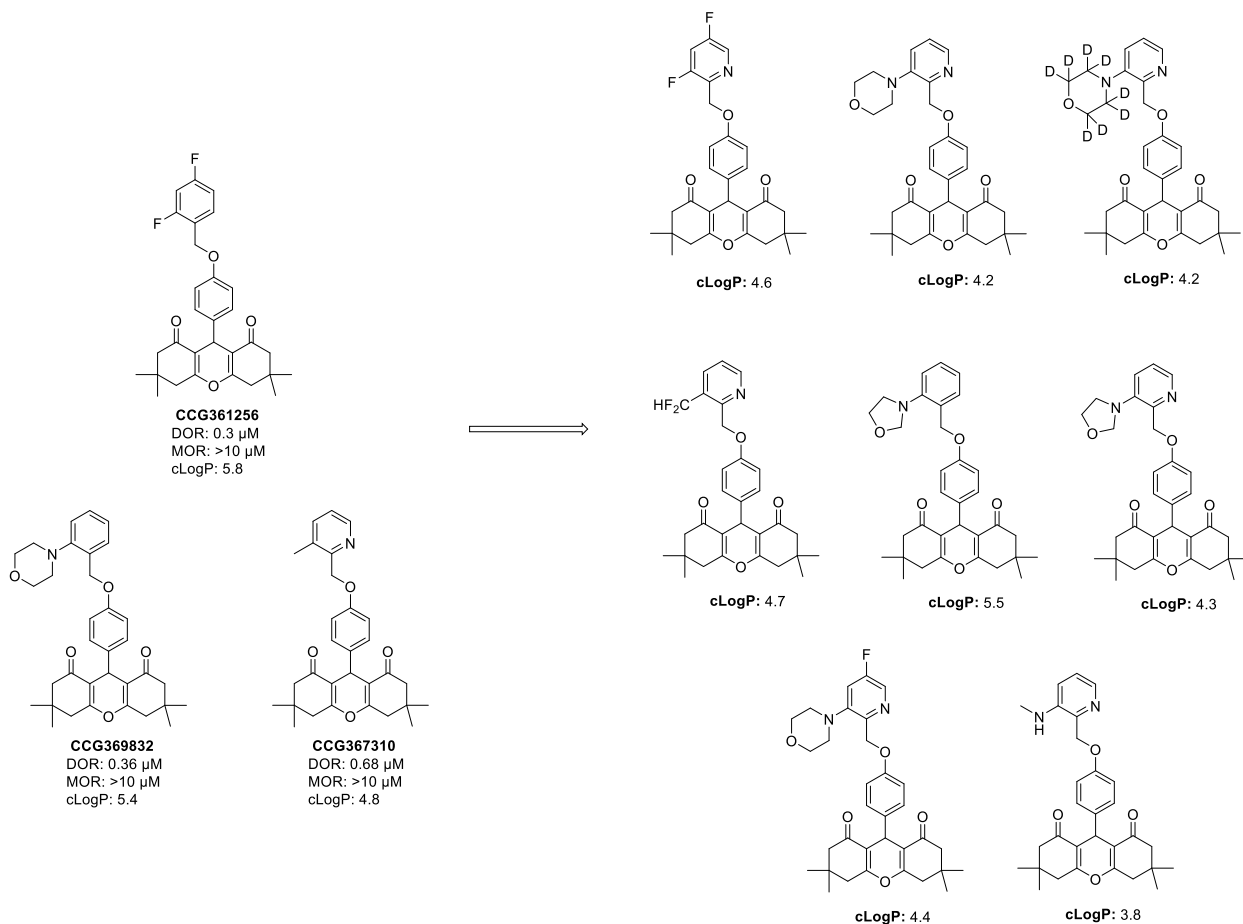


Figure 5.2 Examples of designed analogues with combined modifications at A-ring to block sites of metabolism and lower lipophilicity while maintain potency against DOR.

potential site of metabolism at the 2-position of the A-ring (**Figure 4.1**). Furthermore, as the allosteric binding pocket of DOR is big and flexible, large moieties such as 2- morpholin-4-yle can bind well to DOR. In addition, to address the issue of lipophilicity through modification at A-ring with heteroatoms it is important to shield the electronic effect of nitrogen. With all the information in hand, a combination of the changes to provide potential new leads is given in **Figure 5.2**.

5.1.3 Expansion and combination of xanthene-dione modifications in the B-ring to further improve metabolic stability and lipophilicity while maintaining potency as a DOR and selectivity over MOR

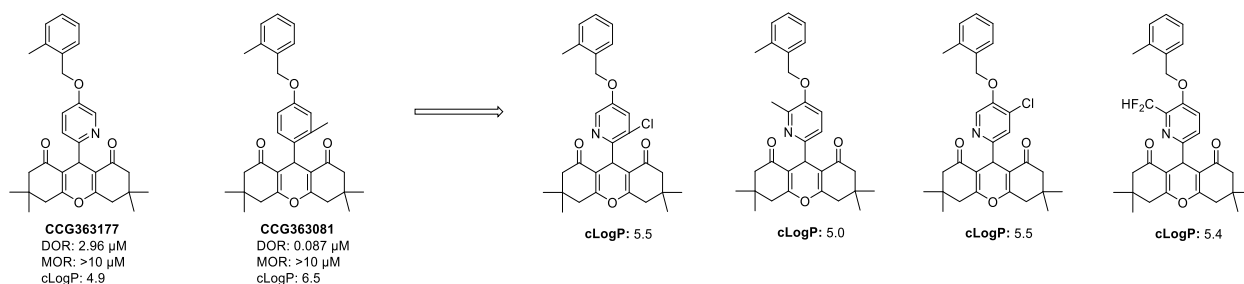


Figure 5.3 Examples of designed analogues with combined moieties at the B-ring to address lipophilicity while maintaining potency against DOR and selectivity over MOR.

From the SAR expansion on the B-ring, I have observed that methyl or chloro-substitutions are essential to provide enhanced selectivity over MOR. The extra conformation restrictions created and potentially extra steric clashes with MOR allowed us to gain a 1,000-fold selectivity over MOR. However, the extra incorporation of lipophilic substitutions into the xanthene-dione series worsened the DMPK profile of the series. To address this issue, we found that a pyridyl B-ring with a shielded nitrogen could improve solubility. Herein, I have designed the combined moieties of **CCG363177** and **CCG363081** to maintain the activity of xanthene-dione as a DOR-PAM with selectivity over MOR while retaining its lipophilicity profile of xanthene-dione series by shielding the electronic effect of nitrogen with the lipophilic substitutions (**Figure 5.3**).

5.1.4 Combined modifications in B- and C-rings

Based on the studies of **Chapter 4**, the spirocyclopropyl moiety (**CCG362906**) is the only replacement of the dimethyl moiety of (**1**) that retains the potency as a DOR PAM while lowering lipophilicity. Therefore, it makes sense to keep this as a new standard moiety in the C-rings. Examples of analogues with the combination of modified B-ring and C-rings were designed and are shown in **Figure 5.4**. With the individual modification on either B- (**CCG363177**) or C-rings (**CCG362906**), the $\text{LogD}_{7.4}$ of the analog is lowered by around 1 log unit. However, after combining both moieties together, the $\text{LogD}_{7.4}$ of the xanthene analogues can be lowered by around 1.5-2.0 log units without losing DOR PAM activity and selectivity over MOR.

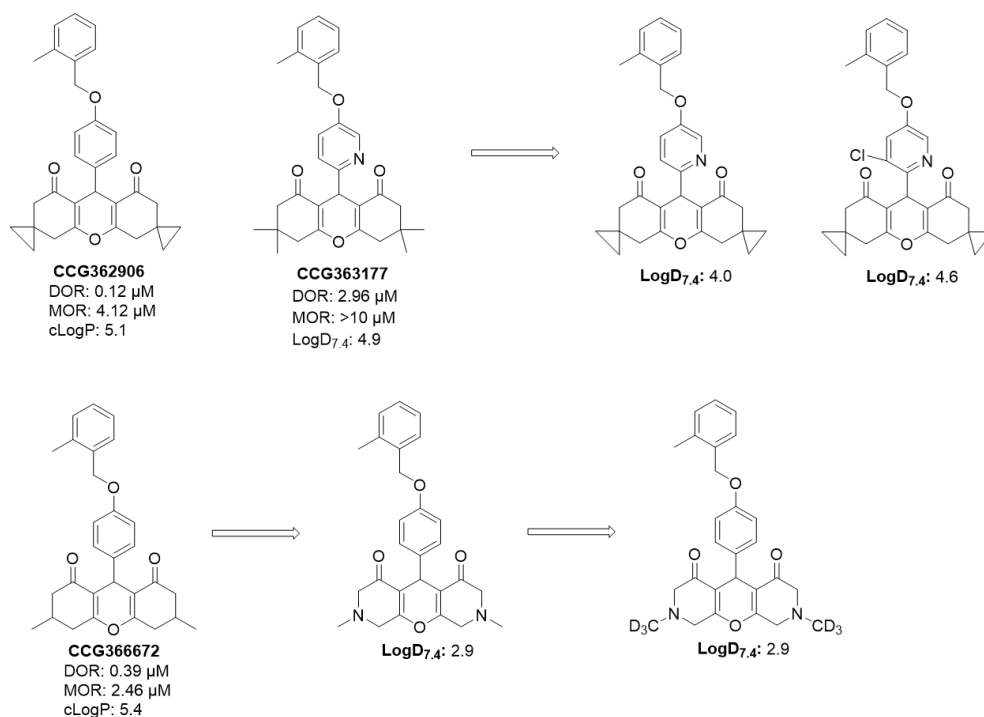


Figure 5.4 Examples of combined modifications of both B- and C-rings. Examples of combined modifications of both B- and C-rings.

5.1.5 Combined modifications of A-, B-, and C-rings

Additionally, modified moieties in the A-ring and the deuterated benzyl linker can be added with the rest of the modifications. Examples of combined moieties are shown in **Figure 5.5**. The newly

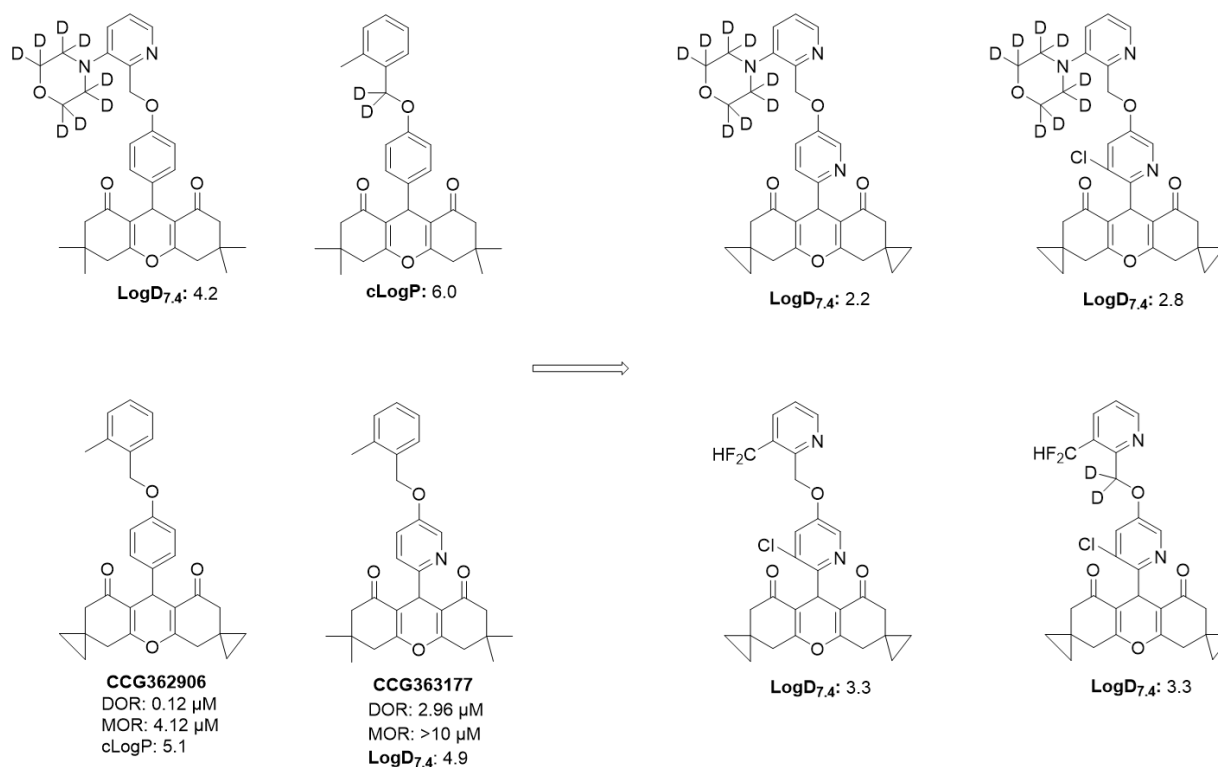


Figure 5.5 Examples of combined moieties on all the parts of the xanthene series.

designed analogues would lower the cLogP of our benchmark compound **1** from 6.0 to approximately 3.0 which allows the xanthene-dione series to fall into a reasonable range of lipophilicity. By doing this, we can greatly improve the solubility and membrane permeability of the series. Additionally, we block most of the sites of metabolism by deuteration and fluorination without losing the conformation of the compounds, activity as a DOR PAM, or selectivity over MOR.

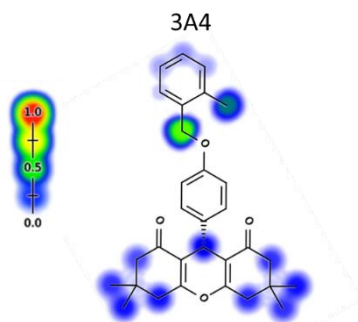


Figure 5.6 Predicted sites of metabolism by CYP3A4 with Xenosite

Other approaches to further improve the metabolic stability include compounds that have proved synthetically difficult. During the prediction of the sites of metabolism, it is seen that the proton at the center C-rings can easily be dehydrogenated by CYP 3A4 (**Figure 5.6**). Substitution of this proton with CF_3 (**CCG367105**) led to a complete loss of DOR PAM activity. Thus, to block the site of metabolism without changing its conformation,

fluorination or deuteration of the proton may be necessary to further improve the metabolic stability of the xanthene series (**Figure 5.7**).

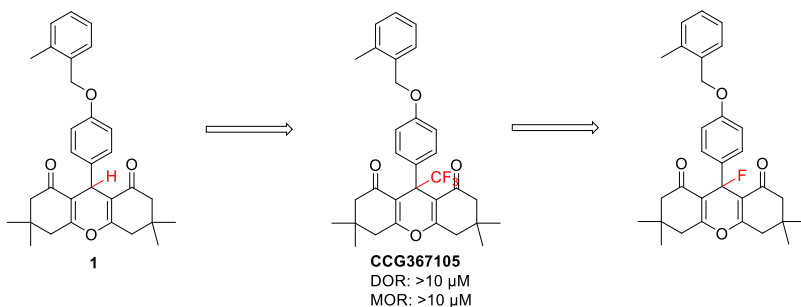


Figure 5.7 Blockage of the site of metabolism with CF_3 moiety (**CCG367105**) and new fluorination moiety

5.2 Conclusions

In this project, my goal was to optimize the selectivity and druggability of the xanthene-dione series of DOR PAMs as potential treatments for major depressive disorders. I started with optimizing the selectivity of the xanthene-dione series over MOR, and successfully increased selectivity to 1,000-fold by introducing the extra conformation restriction and creating steric clashes with the MOR side chains by incorporating methyl groups on the B-ring. However, optimization of the drug-likeness of this series while retaining this activity and selectivity has proved challenging. Attempts to improve individual properties, such as solubility and metabolic stability, have been effective. However, combination of improved properties without losing the pharmacological properties has remained difficult. Our attempts and exercises to optimize the drug-likeness of xanthene-dione compounds show that optimization can be achieved by blocking the predicted sites of metabolism and lowering the lipophilicity while maintaining the current conformation of the compounds. The next challenge is to do this while retaining the level of activity and selectivity of **1**.

5.3 References

- Jones, P. J. H., & Leatherdale, S. T. (1991). Stable isotopes in clinical research: Safety reaffirmed. *Clinical Science*, 80(4), 277–280. <https://doi.org/10.1042/cs0800277>
- Katz, J. J., & Crespi, H. L. (1966). Deuterated Organisms: Cultivation and Uses. *Science*, 151(3715), 1187–1194. <https://doi.org/10.1126/science.151.3715.1187>
- Kushner, D. J., Baker, A., & Dunstall, T. G. (1999). Pharmacological uses and perspectives of heavy water and deuterated compounds. *Canadian Journal of Physiology and Pharmacology*, 77(2), 79–88.
- Murray, M. R., & Benitez, H. H. (1967). Deuterium Oxide: Direct Action on Sympathetic Ganglia Isolated in Culture. *Science*, 155(3765), 1021–1024. <https://doi.org/10.1126/science.155.3765.1021>
- Mutlib, A. E., Gerson, R. J., Meunier, P. C., Haley, P. J., Chen, H., Gan, L. S., Davies, M. H., Gemzik, B., Christ, D. D., Krahn, D. F., Markwalder, J. A., Seitz, S. P., Robertson, R. T., & Miwa, G. T. (2000). The Species-Dependent Metabolism of Efavirenz Produces a Nephrotoxic Glutathione Conjugate in Rats. *Toxicology and Applied Pharmacology*, 169(1), 102–113. <https://doi.org/10.1006/taap.2000.9055>